The Expeditions ANT-XXIII/1

of the Research Vessel Polarstern in 2005

Edited by
Dr. Michiel Rutgers v. d. Loeff
with contributions of the participants

ANT-XXIII/1

13 October - 17 November 2005

Bremerhaven - Cape Town

Fahrtleiter / Chief Scientist:
Dr. Michiel Rutgers v. d. Loeff

Koordinator / Coordinator:
Prof. Dr. W. Arntz

1. ZUSAMMENFASSUNG UND FAHRTVERLAUF

Michiel Rutgers van der Loeff
Alfred-Wegener-Institut

Die Expedition ANT-XXIII/1 begann am 13. Oktober 2005 in Bremerhaven. Es nahmen 42 Wissenschaftler aus verschiedenen Disziplinen teil. Die Expedition stellte ein Pilotprojekt für das internationale Forschungsprogramm GEOTRACES dar. Die diesbezügliche Forschung konzentrierte sich auf die gemeinschaftliche Analyse einer großen Bandbreite an Tracern in Wasserproben. Fünfzehn Geochemiker verglichen die Eigenschaften unterschiedlicher Arten der Probennahme von Oberflächenwasser (die Schiffsseewasserleitung, ein neben dem Schiff geschleppter "Fisch" und ein Teflon-Schnorchelsystem unter dem Schiffsrumpf). Auf sechs umfassenden Tiefenstationen (6 - 10 Stunden) wurden große Volumina von Tiefenwasser im Rahmen mehrerer Einsätze des CTD-Kranzwasserschöpfers gewonnen. Hiervon wurden auch Proben zur Interkalibration von Messungen innerhalb der GEOTRACES-Forschergemeinschaft genommen. Die meisten Proben wurden für die Messung im Heimatlabor gesammelt, aber die Analysen, die bereits an Bord vorgenommen werden konnten, zeigten den erwarteten Trend zu höheren Eisen-, Aluminium- und Titangehalten in Gebieten von Staubeinträgen. Die Erfahrungen mit der Probennahme fließen in die Methodenentwicklung der an GEOTRACES beteiligten Gruppen ein.

Während des ersten Teils der Expedition (vor Vigo) wurden bathymetrische Arbeiten in der Biscaya durchgeführt, die zeigen sollten, wie stark die Intensität der Schallquellen des Hydrosweep- und des Parasound-Systems vermindert werden kann, ohne Qualitätseinbußen am Messergebnis in Kauf zu nehmen. Ein Sonarsystem zur Walbeobachtung in der Umgebung des Schiffs wurde getestet.

Während des Besuchs in Vigo (23. und 24. Oktober) wurde ein Treffen der spanischen SCAR-Delegierten an Bord abgehalten. Zu Ehren ehemaliger spanischer Mitglieder der Schiffscrew fand eine Grillparty statt. Eine Pressekonferenz sowie ein Seminar zur deutsch-spanischen Zusammenarbeit in der Polarforschung wurden an Bord abgehalten und von einem Empfang auf der Brücke abgerundet. Die Veranstaltung fand ein breites Echo in den örtlichen Medien. Die Arbeitsgruppe der Bathymetrie verließ in Vigo das Schiff, während andere Gruppen eine Verstärkung erfuhren. Am 25. Oktober verließ FS *Polarstern* die Stadt mit 37 Wissenschaftlern an Bord. Technische Probleme mit einem Kühlcontainer zwangen uns zu einem kurzen Besuch in Las Palmas.

Messungen unterwegs
Insgesamt zehn Wissenschaftler nahmen an verschiedenen Untersuchungen der Atmosphäre mit optischen Methoden sowie mit Wetterballons teil. Viele dieser Studien dienen zur Validierung von Satellitendaten von ENVISAT. Diese Messungen benötigen zwar keine Schiffszeit, erfordern aber oft einen klaren Himmel. Diese Voraussetzung war insbesondere während des letzten Teils der Fahrt oft nicht gegeben.

Trotzdem konnten alle Gruppen ausreichende Daten für ihre Untersuchungen gewinnen.

Schwer abbaubare organische Schadstoffe (POPs) wurden im Wasser wie in der Luft gemessen, um ihre Transportwege in Ozean und Atmosphäre aufzudecken. Durch einen so genannten "Fisch" aus Edelstahl, der neben dem Schiff geschleppt wurde, konnte neben dem Schiff kontinuierlich Wasser unter reinen Bedingungen gesammelt werden. Alle drei bis zwölf Stunden (Tabelle 1.1) wurden großvolumige Proben genommen und für die Messung einer Reihe von Spurenstoffen aufgeteilt. Alternativ wurden ähnliche Proben über einen so genannten Schnorchel mit einem komplett aus Teflon gefertigten Schlauch- und Pumpsystem unter dem Schiff (11 m Tiefe) genommen.

Tägliche Stationen
Im Rahmen von 19 kurzen Stationen (Tabelle 1.2) jeweils zur örtlichen Mittagszeit wurden optische Untersuchungen in den oberen 200 Metern der Wassersäule durchgeführt. Hierzu wurden auch Wasserschöpferproben genommen. Ein Multisensorsystem zur Messung inhärenter optischer Eigenschaften des Meerwassers wurde dabei ebenfalls eingesetzt. Weiterhin wurde ein im Wasser frei absinkendes Gerät benutzt, welches die in der Tiefe eintreffende optische Einstrahlung sowie die zurückgeworfene Strahlung aufnahm. Ziel dieser Messungen war die Entwicklung von Algorithmen, die es erlauben, neben Chlorophyllkonzentrationen auch organische Kohlenstoffgehalte aus Satellitendaten abzuleiten.

Umfassende Stationen
Ein wichtiger Ansatz von GEOTRACES ist die parallele Messung einer großen Zahl von Tracern. Analytische Fortschritte haben zwar die Anforderungen an die Probengröße für viele Traceruntersuchungen reduziert, aber durch die gleichen Fortschritte sind weitere Elemente und Isotope erst in analytische Reichweite gekommen. Durch diese Entwicklung besteht nach wie vor die Anforderung, große Probenvolumina zu gewinnen. Im Verlauf von sechs besonders umfassenden Stationen (fett gedruckt in Tabelle 1.2) wurden Proben zur Bestimmung der Tiefenverteilung einer großen Bandbreite von Tracern gewonnen. Die erste dieser Stationen fand in der Biscaya statt, wo das typische Salzgehaltsmaximum ausströmenden Mittelmeerwassers gefunden wurde. Zwei weitere Stationen liegen vor Westafrika, wo Küstenauftrieb, aber insbesondere auch Staubeinträge zu erwarten sind. Eine vierte Station wurde direkt südlich des Äquators im äquatorialen Auftrieb durchgeführt. Die fünfte Station fand mitten im Angolabecken statt, wo die typischen Bedingungen des Wirbelsystems des südlichen Atlantik erwartet wurden. Die letzte dieser Stationen fand knapp südlich des Walfischrückens statt, wo die Möglichkeit bestand, Antarktisches Bodenwasser zu beproben.

Wetter
Die Wetterbedingungen waren günstig, und das gesamte geplante Messprogramm konnte wie vorgesehen stattfinden. Die Expedition brachte Wissenschaftler vieler Disziplinen zusammen, und eine Reihe neuer Kooperationen entwickelte sich. Der Austausch zwischen optischen Untersuchungen am Meerwasser und atmosphärischen Untersuchungen sowie zwischen Optik und Ultrafiltration war besonders produktiv.

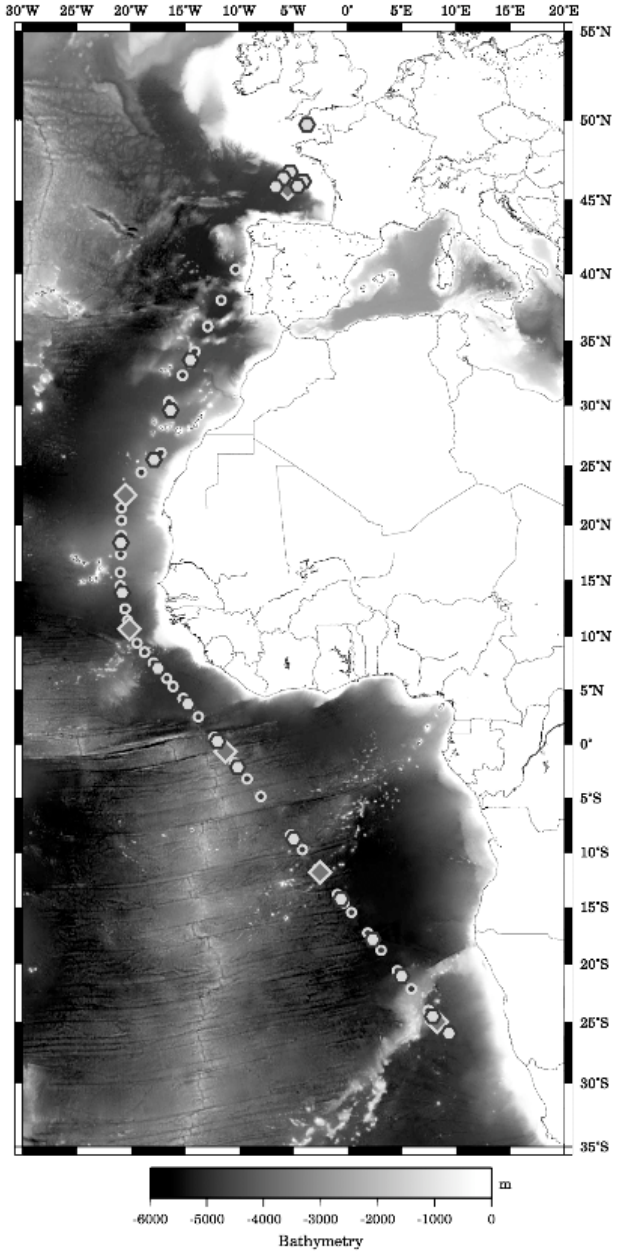

Fig. 1.1: Bathymetrical map of the Eastern Atlantic showing the location of major stations (diamonds), bio-optical stations (light hexagons) and surface samples obtained by the towed fish (dark circles).

Abb. 1.1: Bathymetrische Karte des östlichen Atlantiks mit Lokation der großen Stationen (Rauten), biooptische Stationen (helle Hexagone) und oberflächenproben mit dem Schleppfisch (dunkle Kreise)

SUMMARY AND ITINERARY

The expedition ANT-XXIII/1 started in Bremerhaven on 13 October with 42 scientists from a range of disciplines. The expedition served as pilot project for the emerging new international research programme GEOTRACES. This research focussed on the joint analysis of water samples for a wide range of tracers. A team of 15 geochemists compared the quality of several ways to collect underway surface water (ship's seawater supplies, a fish towed to the side of the ship and a snorkel below the ship). On six major deep stations (6 - 10 hours) large water samples were collected with several CTD/rosette casts. Samples were also taken for intercalibration and will be distributed within the GEOTRACES community. Most samples were taken home, but the analyses that could already be done on board showed the expected higher concentrations of iron, aluminium and titanium in the area of dust inputs. The sampling experience will be communicated to the GEOTRACES community.

During the first part of the expedition, until the visit to Vigo, bathymetric studies were made in the Bay of Biscay to investigate to what extent the sound levels used for hydrosweep and parasound could be reduced without too much loss of quality. A Sonar system was tested that might serve to observe whales around the ship.

During the visit to Vigo on 23 and 24 October a meeting of the Spanish SCAR delegates was held on board and a grill party was organized for the former Spanish crew members. A press conference and a seminar on Spanish-German cooperation in polar research were organized, and the visit was completed with a reception on the bridge. There was ample coverage of the visit in the local media. In Vigo the bathymetric group left while the other groups obtained some reinforcement, and on 25 October RV *Polarstern* left Vigo with 37 scientists. Technical problems with a refrigerated reefer with food for *Neumayer* station forced us to pay a short visit to Las Palmas.

Underway measurements
A total of 10 scientists made atmospheric studies with optical measurements and with weather balloons. Many of these studies served as ground validation for data collected with instruments on board the ENVISAT satellite. These measurements did not require ship time, but many required a clear sky, a condition that was often not given, especially in the last part of the expedition. Nevertheless, all groups could collect adequate data.

Persistent organic pollutants were measured in water and air to study how these components are transported through seawater and atmosphere.

Clean surface water was collected continuously using a stainless steel fish towed beside the ship. Every 3 to 12 hours (Table 1.1) large samples were collected and distributed for a range of parallel trace element studies. Alternatively, a snorkel was

mounted in the moonpool of the ship to collect seawater from below the hull (11 m depth) through an all-teflon tubing system and teflon membrane pump.

Daily stations
On 19 short stations (Table 1.2), performed around local noon, optical measurements were made in the surface 200 m. On these stations, a rosette cast was taken and a multisensor device was lowered to measure inherent optical properties in the water column. Then an instrument was lowered in free fall beside the ship to measure downwelling irradiance and upwelling radiance. The objective was to develop algorithms to derive not only the chlorophyll content but also the amount of organic carbon from satellite observations.

Major stations
An essential characteristic of the GEOTRACES approach is that many tracers should be analysed in parallel. The advancement of analytical techniques has reduced the sample volumes required for many tracer studies, but at the same time it enabled us to analyse elements and isotopes that used to be beyond our reach with conventional methods. As a result, there are still many analyses requiring large volumes of seawater. At 6 major stations (bold in Table 1.2) we have collected samples to determine the depth distribution of a wide spectrum of tracers. The first station was in the Bay of Biscay and included the typical salinity maximum of Mediterranean outflow water. Two more stations were positioned off West Africa to represent the regime of coastal upwelling, but especially of atmospheric dust inputs. A fourth station was just south of the equator, selected in the equatorial upwelling regime. The fifth station was in the middle of the Angola Basin to represent the conditions of the South Atlantic Gyre and the last station was just south of the Walvis Ridge, selected to allow the sampling of Antarctic Bottom Water.

Weather
Weather conditions were favourable and the planned programme could be performed entirely. The cruise brought scientists of many disciplines together, which yielded new cooperations. The exchange of ideas between marine optics and atmospheric research, and between optics and ultrafiltration studies was most productive.

Tab. 1.1: Samples collected with towed fish and with snorkel, with time and position at start, and salinity and temperature from ship's thermosalinometer (bow)

Name	Date	Time (UTC)	Latitude		Longitude		Salinity	Temperature [°C]
fish1	18/10/05	17:00	45.850	°N	6.166	°W	35.69	17.73
fish2	19/10/05	6:44	45.925	°N	4.643	°W	35.54	18.44
snorkel1	25/10/05	18:53	40.292	°N	10.327	°W	36.10	19.25
snorkel2	26/10/05	7:50	38.083	°N	11.656	°W	36.43	20.22
snorkel3	26/10/05	19:55	36.151	°N	12.885	°W	36.65	21.53
snorkel4	27/10/05	08:55	34.201	°N	14.108	°W	36.50	21.70
fish3	27/10/05	15:00	33.387	°N	14.609	°W	36.82	22.12
fish4	27/10/05	21:00	32.383	°N	15.222	°W	36.83	22.90
snorkel5	27/10/05	21:00	32.383	°N	15.222	°W	36.83	22.90
fish5	28/10/05	09:00	30.311	°N	16.464	°W	36.92	23.05
snorkel6	28/10/05	09:16	30.268	°N	16.489	°W	36.91	23.07
fish6	29/10/05	09:01	26.157	°N	17.163	°W	36.96	24.39
fish7	29/10/05	14:58	25.380	°N	18.029	°W	37.06	24.97
fish8	29/10/05	20:58	24.528	°N	18.975	°W	36.95	24.69
fish9	30/10/05	06:57	22.840	°N	20.248	°W	36.67	24.29
fish10	30/10/05	21:00	21.518	°N	20.860	°W	36.54	25.12
fish11	31/10/05	02:54	20.344	°N	20.884	°W	36.40	25.07
fish12	31/10/05	09:02	19.118	°N	20.910	°W	36.31	25.11
fish13	31/10/05	14:51	18.198	°N	20.929	°W	36.24	26.20
fish14	31/10/05	18:35	17.439	°N	20.945	°W	36.49	26.93
fish15	01/11/05	03:09	15.757	°N	20.979	°W	35.88	28.61
fish16	01/11/05	09:00	14.626	°N	20.973	°W	35.75	28.30
fish17	01/11/05	14:56	13.716	°N	20.781	°W	35.59	27.78
fish18	01/11/05	21:05	12.546	°N	20.534	°W	35.71	28.88
fish19	02/11/05	02:59	11.417	°N	20.296	°W	35.57	29.08
fish20	02/11/05	13:59	10.580	°N	20.121	°W	35.62	29.60
fish21	02/11/05	21:04	9.396	°N	19.490	°W	35.32	29.45
fish22	03/11/05	02:51	8.521	°N	18.754	°W	35.05	29.10
fish23	03/11/05	09:07	7.580	°N	17.964	°W	34.75	29.17
fish24	03/11/05	15:33	6.999	°N	17.447	°W	34.54	29.63
fish25	03/11/05	21:00	6.143	°N	16.760	°W	34.46	29.62
fish26	04/11/05	02:05	5.356	°N	16.103	°W	34.05	29.01
fish27	04/11/05	09:02	4.296	°N	15.219	°W	34.37	28.48
fish28	04/11/05	15:00	3.522	°N	14.574	°W	34.73	28.42
fish29	04/11/05	21:02	2.586	°N	13.816	°W	35.42	27.97
fish30	05/11/05	09:06	0.768	°N	12.403	°W	36.08	26.63
fish31	05/11/05	15:00	0.122	°N	11.900	°W	35.99	26.64
fish32	06/11/05	09:00	1.688	°S	10.493	°W	36.14	25.94
fish33	06/11/05	21:03	3.192	°S	9.322	°W	36.31	25.87
fish34	07/11/05	08:20	4.813	°S	8.059	°W	36.03	24.51
fish35	08/11/05	09:03	8.356	°S	5.285	°W	36.01	23.44

Name	Date	Time (UTC)	Latitude		Longitude		Salinity	Temperature [°C]
fish36	08/11/05	15:05	8.982	°S	4.799	°W	36.09	23.26
fish37	08/11/05	20:38	9.768	°S	4.173	°W	36.14	22.93
fish38	09/11/05	08:50	11.550	°S	2.764	°W	36.42	22.16
fish39	09/11/05	20:58	11.996	°S	2.409	°W	36.41	21.94
fish40	10/11/05	09:05	13.801	°S	0.969	°W	36.54	20.89
fish42	10/11/05	15:01	14.534	°S	0.382	°W	36.52	20.79
fish43	10/11/05	21:03	15.426	°S	0.337	°E	36.48	20.27
fish44	11/11/05	09:02	17.248	°S	1.813	°E	35.95	19.19
fish45	11/11/05	15:03	17.960	°S	2.384	°E	35.97	19.09
fish46	11/11/05	21:03	18.814	°S	3.094	°E	35.82	18.97
fish47	12/11/05	09:00	20.570	°S	4.544	°E	35.79	18.97
fish48	12/11/05	15:09	21.292	°S	5.145	°E	35.77	19.24
fish49	12/11/05	21:00	22.168	°S	5.879	°E	35.62	18.68
fish50	13/11/05	08:53	23.971	°S	7.402	°E	35.43	18.10

Tab. 1.2: CTD/rosette stations. Major tracer stations in bold

Station	Date	Time [UTC]	Latitude		Longitude		Water depth	CTD winch length [m]
PS69/001-3	15.10.05	12:56	49.728	°N	3.761	°W	76	66
PS69/002-3	16.10.05	13:06	46.818	°N	5.303	°W	1013	198
PS69/003-1	16.10.05	18:36	46.406	°N	5.914	°W	4360	4333
PS69/004-3	18.10.05	13:05	45.863	°N	6.624	°W	4766	196
PS69/005-3	19.10.05	13:12	46.217	°N	4.095	°W	161	151
PS69/006-2	20.10.05	07:26	45.750	°N	5.525	°W	4620	4623
PS69/006-4	20.10.05	10:25	45.748	°N	5.519	°W	4616	4614
PS69/006-7	20.10.05	12:42	45.735	°N	5.521	°W	4616	196
PS69/006-8	20.10.05	13:32	45.741	°N	5.526	°W	4619	195
PS69/007-3	21.10.05	13:21	45.917	°N	4.592	°W	4039	196
PS69/008-3	27.10.05	13:39	33.562	°N	14.506	°W	3915	201
PS69/009-3	28.10.05	13:36	29.600	°N	16.319	°W	3673	200
PS69/010-3	29.10.05	13:33	25.531	°N	17.861	°W	3204	200
PS69/011-2	30.10.05	10:55	22.500	°N	20.500	°W	4136	4128
PS69/011-5	30.10.05	13:01	22.500	°N	20.503	°W	4138	197
PS69/011-7	30.10.05	14:00	22.500	°N	20.500	°W	4135	958
PS69/011-8	30.10.05	14:53	22.500	°N	20.500	°W	4136	196
PS69/011-9	30.10.05	15:23	22.501	°N	20.498	°W	4136	154
PS69/012-3	31.10.05	13:38	18.374	°N	20.928	°W	3112	198
PS69/013-3	01.11.05	13:36	13.905	°N	20.816	°W	4382	197
PS69/014-2	02.11.05	09:06	10.623	°N	20.131	°W	4828	4817
PS69/014-4	02.11.05	11:05	10.625	°N	20.130	°W	4828	195
PS69/014-5	02.11.05	11:41	10.624	°N	20.128	°W	4824	492
PS69/014-7	02.11.05	12:39	10.621	°N	20.133	°W	4825	200

Station	Date	Time [UTC]	Latitude		Longitude		Water depth	CTD winch length [m]
PS69/014-9	02.11.05	13:19	10.616	°N	20.136	°W	4833	137
PS69/015-3	03.11.05	13:30	7.023	°N	17.488	°W	4859	201
PS69/016-3	04.11.05	13:33	3.697	°N	14.717	°W	4768	197
PS69/017-3	05.11.05	13:30	0.269	°N	12.013	°W	4613	205
PS69/018-2	05.11.05	22:53	0.694	°S	11.267	°W	3877	3848
PS69/018-4	06.11.05	00:34	0.695	°S	11.265	°W	3879	494
PS69/018-6	06.11.05	01:40	0.696	°S	11.265	°W	3880	256
PS69/019-3	06.11.05	13:24	2.156	°S	10.135	°W	3866	199
PS69/020-3	08.11.05	13:11	8.796	°S	4.978	°W	4274	197
PS69/021-2	09.11.05	12:11	11.870	°S	2.516	°W	5595	1978
PS69/021-5	09.11.05	13:21	11.867	°S	2.513	°W	5716	195
PS69/021-8	09.11.05	14:17	11.863	°S	2.512	°W	5747	198
PS69/021-9	09.11.05	16:16	11.863	°S	2.513	°W	5749	5744
PS69/021-10	09.11.05	18:17	11.863	°S	2.514	°W	5744	788
PS69/021-11	09.11.05	19:20	11.863	°S	2.514	°W	5746	1966
PS69/022-3	10.11.05	13:05	14.267	°S	0.596	°W	5429	198
PS69/023-3	11.11.05	13:57	17.867	°S	2.321	°E	5471	198
PS69/024-3	12.11.05	13:31	21.106	°S	4.995	°E	2405	196
PS69/025-2	13.11.05	13:07	24.527	°S	7.877	°E	4716	198
PS69/026-2	13.11.05	19:08	25.001	°S	8.281	°E	4697	4666
PS69/026-4	13.11.05	21:52	25.002	°S	8.286	°E	4698	4404
PS69/026-5	14.11.05	00:12	25.004	°S	8.285	°E	4699	3430
PS69/026-7	14.11.05	02:29	25.005	°S	8.284	°E	4698	759
PS69/026-8	14.11.05	03:36	25.005	°S	8.285	°E	4698	1991
PS69/027-3	14.11.05	13:33	25.963	°S	9.364	°E	4719	197

2. METEOROLOGICAL CONDITIONS

Klaus Buldt
Deutscher Wetterdienst

RV *Polarstern* started its journey on 13 October, 2005 at 09:30 local. A large high over Russia which had dominated the weather situation at home for quite a while caused beautiful weather as we left Bremerhaven with light easterly winds, blue sky and temperatures around 15°C. But already in the evening RV *Polarstern* reached a weak trough extending from southern Norway to the English Channel. Crossing this the wind changed from east to southeast and increased to about 5 – 6 Bft. During the first half of the night some showers occurred.

While passing the English Channel weather remained calm with still easterly winds of 4 Bft. In the morning of 14 October some drizzle caused poor visibility but later in the day scattered skies were observed and it stayed dry.

At this time a low over Spain was filling while moving towards the northwest of France. In the evening of 15 October until the morning of the 16 overcast skies were observed but it stayed dry. The easterly wind still did not come up to more than 4 Bft.

On Sunday 16 October we reached the working area in the Bay of Biscay. The frontal system of an intensive depression at 57°N 30°W approached from the west but did not reach the outmost parts of the Bay of Biscay before the next evening. Then some showers where observed together with again easterly to southeasterly winds of 4 Bft. This did not generate much of a wind sea but a swell of up to 3 m rolled in from the west towards our position.

The depression described remained stationary during the following days. So the weather in the working area was dominated by instable air masses causing showers and even some thunderstorms in the night from 18 to 19. Then the wind shifted southwest to west and increased to an average of 5 - 6 Bft. For a few hours Bft 7 was registered during the night.

With the approach of a new low at 50°N 15°W the wind was backing south to southeast again on 20 October. During the next night the depression deepened and moved towards the Irish Sea. As the front moved through the wind shifted again to southwest and increased rapidly to 7 Bft with gusts up to 8 Bft. The sea state reached a height of about 3 m.

A secondary low developed on 21 October in about the area mentioned and took almost the same route. So the weather situation recurred in an interval of about 24 hrs.

Leaving the operation area in the evening of 21 October we crossed the cold front of this system. In the following hours the southwesterly wind increased to 8 Bft. During the night showers and thunderstorms were observed.

Approaching Cape Finnisterre it took until the evening of 22 October before the northwesterly wind decreased to about 4 Bft. During this period the swell was still running in from the west with about 2,5 to 3 m wave height.

RV *Polarstern* entered port at Vigo in the morning of 23 October. For a short period a ridge of the subtropical high over the Azores influenced the weather over the northwest of Spain. It brought us nice and calm autumn days during our stay in this Spanish harbour with a gentle breeze, almost blue skies and temperatures around 17°C.

Setting sail again on 25 October we were back to the weather situation described above. The cold front of a depression over the North Sea running down to Northwest Spain caused some rain in the morning. Just out of the harbour the southerly wind increased rapidly to 7 Bft. As we gained distance to the coastline the wind force decreased slowly again to about 6 Bft.

At the same time a strong cyclone developed near 48°N 29°W. While moving northeast its frontal system approached the course of RV *Polarstern* on the 27. Before the frontal clouds had reached us the southerly wind increased to 7 Bft. Embedded in the cold front some huge clusters brought heavy showers during the night while the wind force increased for a short period up to 9 Bft with gusts of 11 Bft. All this caused a sea state of about 3.5 m and gave us a restless night.

The southern parts of this front diminished rapidly during the early morning of the 27. This led to a quick decrease of wind force to only 3 - 4 Bft. However, in the beginning some rain as well as showers in the afternoon where observed while the front was moving northeast.

Due to the fact that the northern frontal zone reached as far south as 20°N in the eastern Atlantic the subtropical high normally found in the area of the Azores stayed far in the west during the following days. This constellation brought us a few days with light winds from north, scattered clouds and temperatures around 22° C.

As on 31 October the high had finally moved to a position around 30°N 25°W it started to weaken. So the northeasterly trade wind just reached 4 Bft but later in the day short periods with 5 - 6 Bft were registered.

On 2 November we got to the northern verge of the Intertropical Convergence Zone (ITCZ) which at this time appeared to be only little active. The first showers and short thunderstorms were observed in the night from 3 to 4. The easterly wind just reached 2 - 3 Bft. On 5 November while crossing the equator we had finally left the ITCZ.

Compared to other voyages the trade wind area was found to be extremely calm this year. During the first days wind force went up to just 4 – 5 Bft. Clear to scattered skies dominated this period but in the morning of the 7 November one single shower

was observed. From the 8 November onwards cloudiness increased due to a well defined trade wind inversion. RV *Polarstern* encountered large areas of stratiform low clouds. For several days overcast to broken conditions dominated interrupted only by short intervals of fair weather around noon and early afternoon.

On 10 November a shallow depression developed off the coast of southwest Africa. It caused little disturbance to the trade winds on our course. Wind force went down to only 3 - 4 Bft. As on the 13 November this low had filled and moved to the southern tip of the African continent weather condition improved to scattered skies in the morning and fair conditions during the rest of the day.

When we entered the area of the southeasterly trade winds a light to moderate swell of up to 2 m was running in from the south.

Due to an increasing pressure gradient between the subtropical high in the South Atlantic and a hardly moving low over Namibia wind force went up to 6 Bft late in the evening of the 14 November. But already a few hours later wind decreased again to 4 – 5 Bft. These conditions together with scattered skies as well as sunny spells lasted until we reached Cape Town in the morning of 17 November.

3. ACOUSTICS

3.1 Studies to minimize the acoustic impact of the Atlas hydrosweep and parasound echosounders on the marine environment in the Bay of Biscay

Monika Breitzke[1)], Saad El Naggar[1)], Dorothea Graffe[1)], Gerhard Kuhn[1)], Fred Niederjasper[1)], Ulrich Lütticke[2]

[1)]Alfred-Wegener-Institut
[2)]Atlas Hydrographic GmbH

Objectives and system description
To minimize the acoustic impact of RV *Polarstern*'s hull-mounted scientific sonars on the marine environment the ATLAS Hydrographic GmbH developed various options to reduce the source levels of its hydrosweep and parasound echosounder systems.

Hydrosweep
Hydrosweep is a multibeam sonar, which transmits and receives acoustic waves of 15.5 kHz frequency within a fan of 90° to 120° opening angle athwart ship and 2° opening angle along the ship. The travel times of the reflections from the sea floor, combined with the sound velocity (profile) of the water column are used to derive high-resolution bathymetric maps which reveal the topography of the ocean floor in great detail. The amplitudes of the reflections from the sea floor, sampled by 2000 points along the swath, simultaneously provide sidescan sonar images which indicate high and low scattering areas on the sea floor by light and dark gray-shaded colours. The currently installed Hydrosweep DS-2 system includes an upgrade which allows (1) to use 240 "soft" beams (HDBE Mode = High Definiton Bearing Estimation Mode) instead of the conventional 59 "hard" beams of the former system versions for high-resolution bathymetric surveys and (2) to reduce the source level manually and automatically (ASLC mode = Automatic Source Level Control Mode). A correctly working HDBE mode is mandatory for an application of the ASLC mode. Three different settings can be used to control the source level: (1) Standard, (2) Maximum Source Level, (3) Automatic Source Level Control (ASLC).

In case of a "Standard" source level control the system is running in the high-resolution HDBE mode with a maximum constant source level of 239 dB in the deep sea, an operator-defined coverage of the transmission and receiver swaths of 90° to 120°, a "Start Time Variable Gain" (Start TVG) set by the operator, and an automatically determined "Actual Time Variable Gain" (Actual TVG) optimized according to the level of the received data.

In case of a "Maximum Source Level" control the transmitted source level and the transmission and receiver swath widths are defined manually by the operator. The time variable gain can either be determined automatically or manually. In case of an automatic gain control the "Start TVG" is set by the operator and the "Actual TVG" is optimized within a range of ±12 dB according to the computed S/N ratio of the

received data. Ideally, a value of 18 dB is chosen for the "Start TVG" so that a maximum gain of 30 dB can be reached. In case of a manual gain control both "Start TVG" and "Actual TVG" are set manually to the same constant value, maximum to 18 dB. If the maximum source level and the (manually defined) gain are chosen too low, the outer beams of the swath might become unusable.

In case of an "Automatic Source Level Control (ASLC)" the system tries to optimize and reduce the source level automatically so that operator-defined values for the maximum source level, the receiver swath width and the S/N ratio of the received data are fulfilled. This is reached by decreasing the transmission source level and increasing the "Actual TVG" simultaneously such that the computed S/N-ratio and the desired coverage of the received data is higher than or equal to the operator-defined value. Again, a "Start TVG" of maximum 18 dB can be chosen by the operator, whereas the "Actual TVG" is varied automatically by ±12 dB. Shortly before RV *Polarstern* left the shipyard and Bremerhaven for the ANT-XXIII/1 cruise a new, improved software version had been installed for the Hydrosweep DS-2 system in which some bugs of the preceding version particularly regulating the automatic source level control had been fixed and newly programmed.

Parasound

Parasound works as both low-frequency sediment echosounder to image the upper 5 -100 m of the sediment coverage of the ocean floor and as high-frequency echosounder to determine the water depth. It makes use of the parametric effect, which produces waves of low secondary frequency through non-linear acoustic interaction of two finite, high-amplitude waves of high primary frequencies. If these two frequencies are very similar and the corresponding sound waves are emitted simultaneously with sufficient high amplitudes, a signal of the difference frequency is generated. This new low-frequency signal is travelling within the emission cone of the original high-frequency waves, which is limited to an opening angle of 4° for the parasound system. Frequencies of 18 kHz and 20.5 - 23.5 kHz are used for the high-amplitude primary signals to produce user-selectable frequencies of 2.5 - 5.5 kHz for the secondary parametric signal. Signal durations can be varied between 1 - 8 periods of the emitted sine wave signals. Typically, parametric signals of 4 kHz and 2 periods length are used for sediment echosounding, whereas the 18 kHz primary signal serves for the water depth determination. Since the two-way travel time in the deep sea is long compared to the length of the reception window (max. 266 ms), parasound first determines the water depth using the 18 kHz signal, and then sends out a burst of pulses at 400 ms intervals (pulse trains) until the first echo returns (Pilot-tone mode). This emission sequence produces non-equidistant shot intervals and a non-equidistant, water depth dependent coverage on the sea floor. The current Parasound DS-2 system uses a software version which was completely renewed and installed in spring 2003. In addition to the new windows-driven Parastore-3 control and recording software it includes options to record reflections from the complete water column and to swivel the roll and pitch angles of the transmission and receiving cone by ±5°, so that the signal penetration can always be perpendicular to the sea floor within these limits. An automatic source level control comparable to the ASLC mode of the current Hydrosweep DS-2 version is not available yet but will be included in the future Parasound DS-3 system probably scheduled for installation in RV *Polarstern* in 2007.

Objectives
During the first leg of ANT-XXIII/1 both echosounder systems were applied to pursue the following objectives:

1. Detailed test of the newly installed software version of the Hydrosweep DS-2 system, particularly of the high-resolution HDBE mode and without and with manually and automatically controlled source levels (ASLC mode).

2. Comparison of the data quality of the new high-resolution hydrosweep bathymetric data (HDBE mode) without and with manually and automatically (ASLC mode) reduced source levels recorded during this cruise with formerly recorded conventional hydrosweep data (59 "hard" beams, no source level reduction) at already established test sites.

3. Verification of a correct operation of the current Parasound DS-2 system version and test of some new options like swivelling the emission and receiving cone.

4. Recording of a digital parasound reference data set which allows comparing the data quality of future parasound system versions and upgrades (e.g. DS-3 in 2007) with that of the preceding system. Such a reference data set does not exist up to now.

Work at sea
To meet these objectives we mainly followed the tracks of the former RV *Polarstern* cruises ANT-VIII/1 and ANT-XV/1 and revisited three well-known sites and two new sites in the Bay of Biscay where bathymetric data has already been collected with the Hydrosweep DS-1 and the first version of the Hydrosweep DS-2 system (59 "hard" beams only). These well-known sites are Location 1, 2b and the Canyon de Noirmoutier. The two new sites are named Location 1a and 2d (Fig. 3.1). Usually, hydrosweep and parasound data were collected simultaneously with few exceptions, where parasound was switched off to test its influence on the quality of the hydrosweep data (Table 1.1, Table 1.2). Data recording started shortly after RV *Polarstern* had passed the Strait of Dover and had left the 12 nm zones of Great Britain and France. On approaching the Bay of Biscay both systems were either run with their standard parameter settings, or different software options were tested to collect experience for the detailed surveys at Locations 1a, 1, 2b, 2d and the Canyon de Noirmoutier. As standard parameter settings a frequency of 4 kHz and a signal duration of 2 periods was used for the parasound system, and the HDBE mode with 120°/100° transmission/receiver swath widths and no source level limitation ("Standard" source level control) was used for the hydrosweep system. Additionally, the hydrosweep data received by the 59 hard beams was continuously recorded via a serial interface installed on RV *Polarstern*. In what follows the local setting of the test sites and the experiments conducted there are described. Table 1.1 and table 1.2 give an overview on the different parameter settings of the hydrosweep and parasound systems.

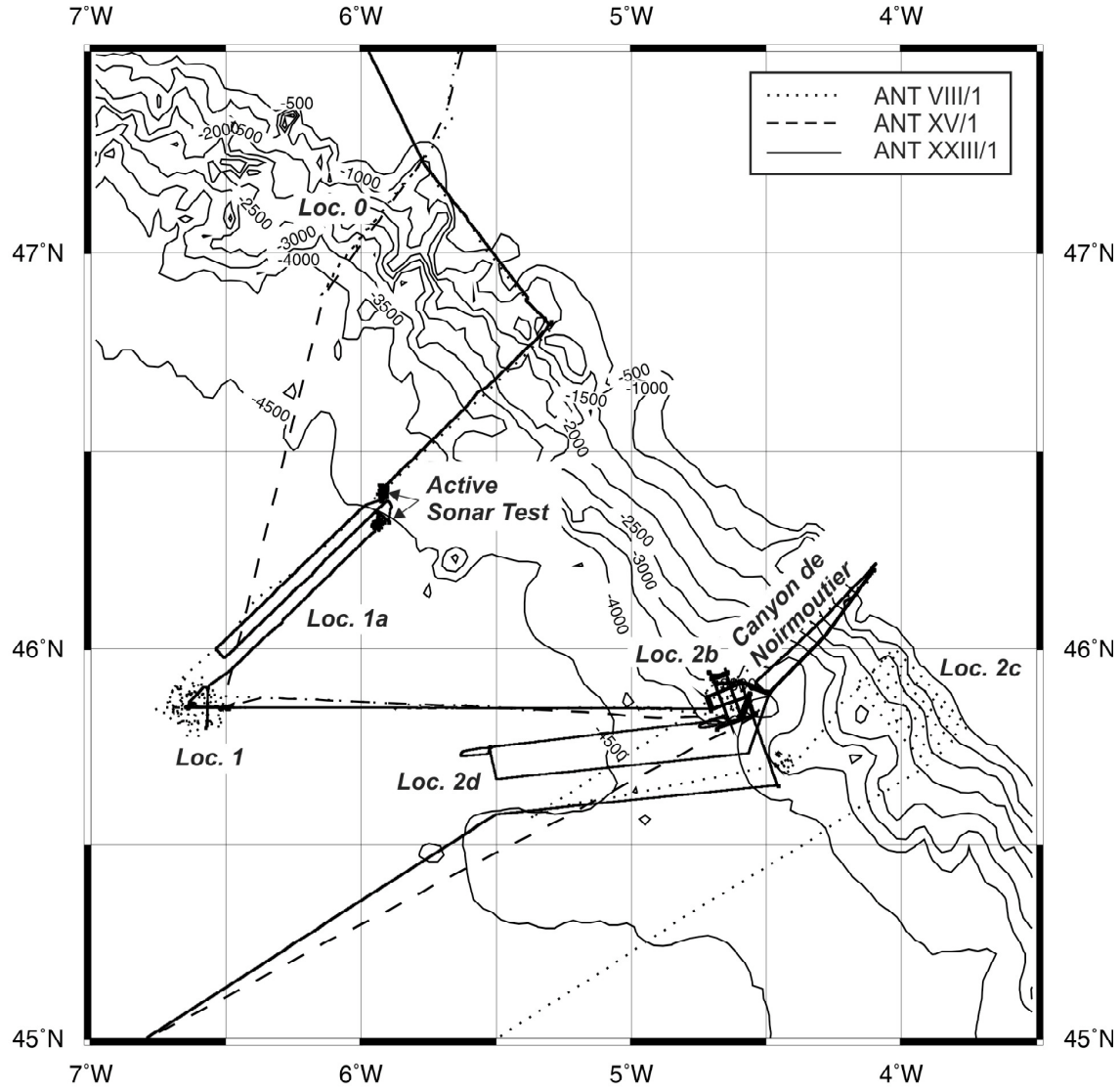

Fig. 3.1: ANT-XXIII/1 cruise track and test sites for the acoustic parasound and hydrosweep echosounder systems in the Bay of Biscay in comparison to the tracks of the former RV Polarstern *cruises ANT-VIII/1 and ANT-XXIII/1*

Location 1a

Location 1a lies on the continental slope northeast of location 1, between about 46°22.5'N 5°54.4'W and 45°58.5'N 6°30.4'W (Fig. 3.2). The water depth varies between about 4600 and 4800 m. It was chosen because during the test of an active sonar system at the northeastern end of the profile lines the barely visible target buoy was lost during daytime, and some time had to be spent with other experiments until nighttime when the buoy could more easily be found again and recovered by its blinking flash light.

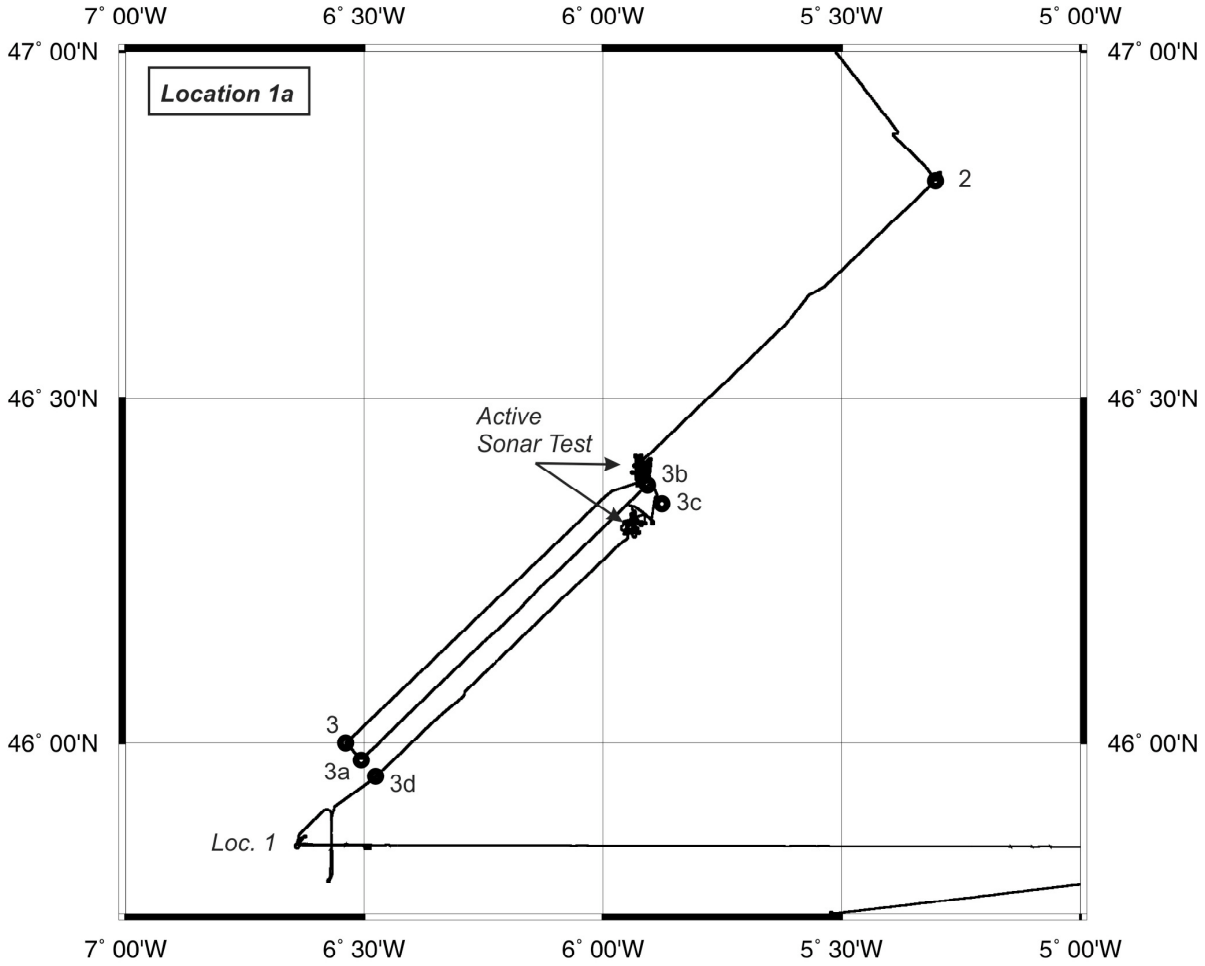

Fig. 3.2: ANT-XXIII/1 cruise track and waypoint numbers at the acoustic test site "Location 1a" in the Bay of Biscay

Three parallel, NE-SW oriented lines were surveyed up- and downslope. For parasound a range of 5,000 m was used along the first two lines, whereas a range of 10,000 m was used along the third line so that the influence of the different non-equidistant shot intervals and the different number of pulses per pulse train on the image of the sediment coverage can be compared.

Hydrosweep was run in the HDBE mode ("Standard" source level control) with 120° transmission swath width and variations in the receiver swath widths of 120°, 100° and 90° along the first line to study the bathymetric data quality for different receiver coverages. Additionally, it was tested and observed, if the mean sound velocity c_{mean} was computed correctly by the new hydrosweep software. Along the second line tests with an automatic source level control using the HDBE and ASLC modes and a maximum source level of 239 dB, transmission/receiver swath widths of 120°/90° and variations of the S/N-ratio were carried out to study if the new software adjusts the

source level in a sensible way. The third line was routinely run in the HDBE mode ("Standard" source level control) with 120°/100° transmission/receiver coverages.

Location 1

Location 1 is a deep sea site with an average water depth of 4800 m, located at 45°51.0'N 6°34.15'W (Fig. 3.3). According to the hydrosweep data collected during ANT-VIII/1 the bathymetry is almost flat with maximum depth variations of 75 m.

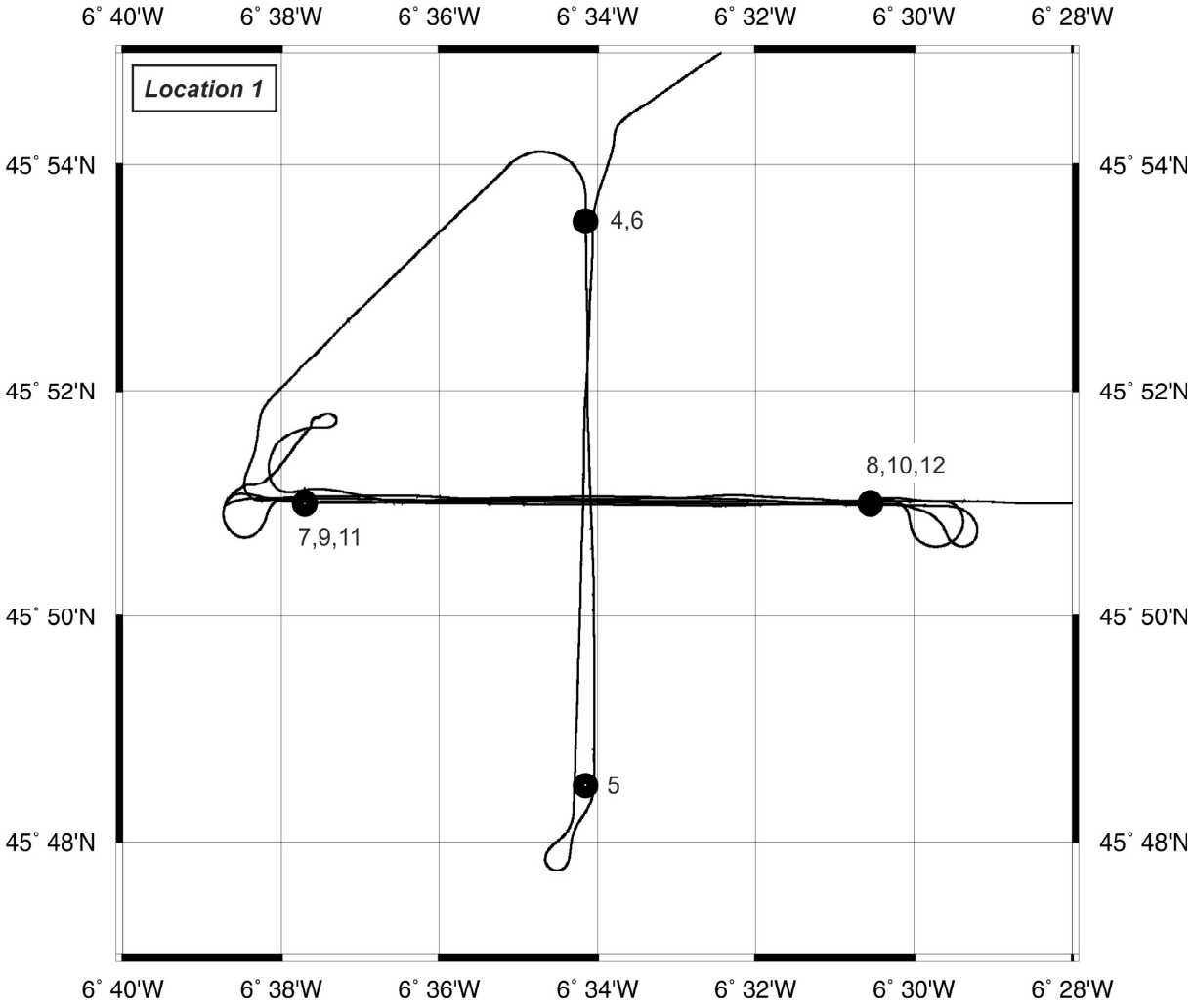

Fig. 3.3: ANT-XXIII/1 cruise track and waypoint numbers at the acoustic test site "Location 1" in the Bay of Biscay

Two crossing lines of 5 nm length oriented N-S and W-E were studied. Each line was surveyed at least twice with courses in opposite directions to calibrate the two motion sensors (MINS 1, MINS 2) of RV *Polarstern*, each along one line. For this purpose, hydrosweep was run in the HDBE calibration mode with alternate soundings forward

and athwart ship, 90°/90° transmission/receiver swath widths and "Standard" source level control. An analysis of this data will provide the roll and pitch offsets of both motion sensors.

The parasound range was set constantly to 10,000 m along both lines, so that the reproducibility of the image of the sediment coverage by opposite course directions can be verified and a potential inaccuracy in the vertical beam-steering can be identified. Furthermore, during the way back on the W-E profile, the values for the positions of the parasound transducer and the motion and heave sensors were varied because a residual, uncompensated heave was noticed in the parasound data collected in the shallow water of the English Channel.

Additionally, the W-E profile was surveyed three more times. During these runs hydrosweep was switched back to the HDBE survey mode with 120°/120° transmission/receiver swath widths, "Maximum Source Level" control, a manually fixed "Start" and "Actual TVG" of 18 dB during the first two, and an automatically adjusted "Actual TVG" during the third of these three runs. As maximum source level we began with 239 dB on the first line and reduced it to 233 dB after about 2.5 nm distance. The second line began with a source level limited to 230 dB and continued with 227 dB after 2.5 nm distance. Along the third line, where an automatically adjusted "Actual TVG" was used, maximum source levels were limited to 239 and 227 dB along the first and last 2.5 nm distance.

Parasound was switched back to a range of 5,000 m during the first two of these three runs, with values for the positions of the parasound transducer and the motion and heave sensors kept constant compared to the last line surveyed with range 10,000 m. Thus, the reproducibility of the image of the sediment coverage by opposite course directions, and a potential inaccuracy in the vertical beam-steering can be verified again for a range setting of 5,000 m. Additionally, the different images of the sediment coverage achieved by the different number of pulses per train and the different, non equidistant shot-intervals in the 5,000 and 10,000 m ranges can be compared. During the third of these three lines parasound was switched off to study its influence on the quality of the hydrosweep data.

Canyon de Noirmoutier, Location 2b, Location 2d

The Canyon de Noirmoutier incises the French continental slope between 46°11.6'N 04°06.7'W and 45°53.3'N 04°29.3'W (Fig. 3.4). Water depths range from about 200 to 4,300 m. At the canyon's southern end, on the lower continental slope, Location 2b covers a small NW-SE oriented ridge rising from about 4,300 to 3,300 m water depth (Fig. 3.5). Both the Canyon de Noirmoutier and Location 2b were already studied twice with RV *Polarstern* by a small grid of profile lines, first during ANT-VIII/1 with Hydrosweep DS-1 and second during ANT-XV/1 with the first version of Hydrosweep DS-2. The site named Location 2d is new and connects the lower continental slope with about 4,300 m water depth to the deep sea with about 4,800 m water depth by three parallel profile lines (Fig. 3.6).

During this cruise, first Location 2b and the Canyon de Noirmoutier were surveyed by a small grid and several up- and downslope profiles. A break for a geochemical water sampling station in the deep sea at the eastern end of the profiles of Location 2d

followed. After having finished this station Location 2b and the Canyon de Noirmoutier were revisited again for hydrosweep and parasound surveys with other parameter settings. By leaving, approaching and leaving Location 2b for the geochemical sampling station in the deep sea and for Vigo the three profiles of Location 2d were collected automatically.

On the way from Location 1 to Location 2b several parameter settings for the source level control of hydrosweep were tested. First, hydrosweep was run in the HDBE mode with 120° transmission swath width and "Maximum Source Level" control. The receiver swath was confined to 120°, 110° and 100°, and the maximum source level was fixed to 239, 233 and 230 dB. Subsequently, a test with the HDBE and ASLC modes and fixed maximum source level was conducted, including transmission/receiver coverages of 120°/100°, a maximum source level of 233 dB and an S/N-ratio of 15 dB.

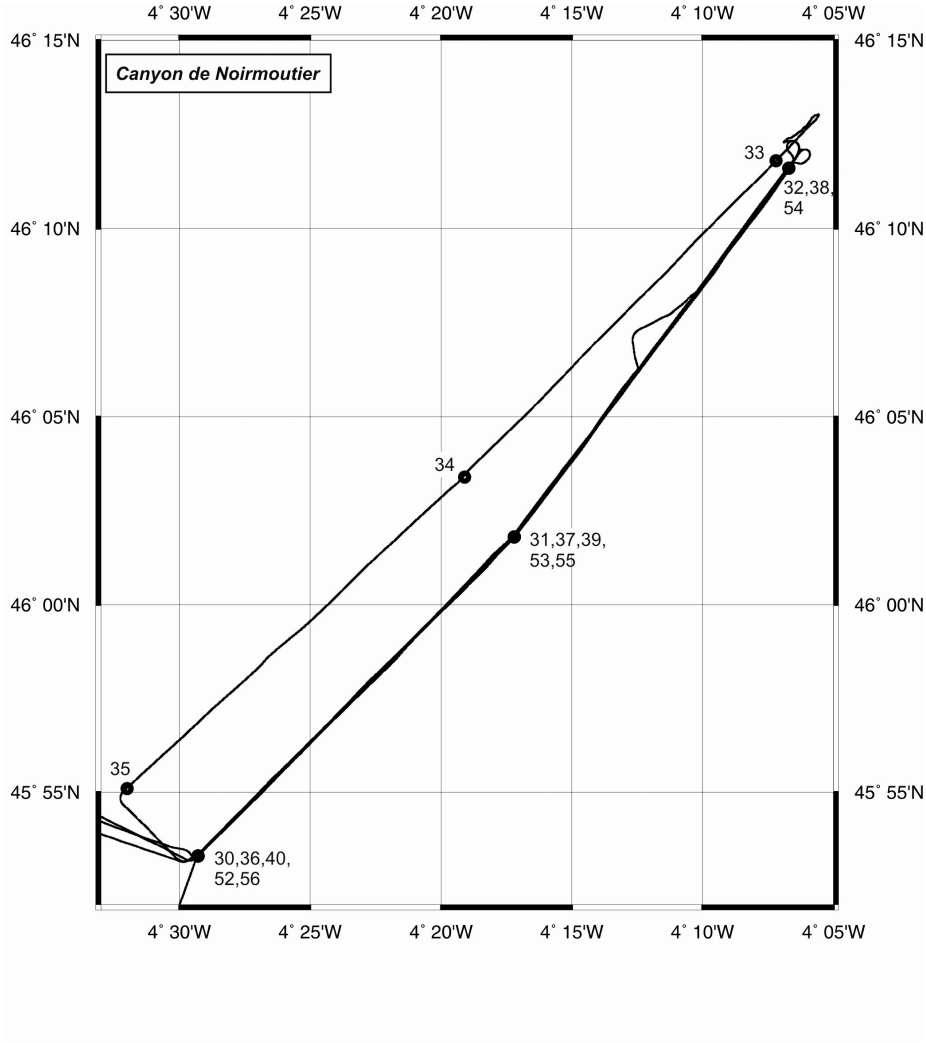

Fig. 3.4: ANT-XXIII/1 cruise track and waypoint numbers at the acoustic test site "Canyon de Noirmoutier 1" on the French continental slope northeast of the test site "Location 2b" in the Bay of Biscay

The two southernmost profiles of Location 2b were surveyed 3 and 4 times in opposite directions with different ship velocities and each line with another motion sensor to calibrate and determine potential offsets of the MINS 1 and MINS 2, to verify possible time and position errors produced by the data filtering of the motion sensors, and to identify possible roll, pitch and heading errors. During these studies hydrosweep was run in the HDBE survey mode ("Standard" source level control) with 90°/90° transmission/receiver swath widths and a "Start TVG" of 10 dB. Subsequently, the complete grid of profile lines was surveyed once in the HDBE mode ("Standard" source level control) with 120°/100° transmission/receiver swath widths and a "Start TVG" of 10 dB. The grid was studied a second time after the Canyon de Noirmoutier had been surveyed twice with hydrosweep in the HDBE mode and a "Maximum Source Level" control" set to 233 dB, 120°/100° transmission/receiver swath widths and an automatic gain control with 18 dB "Start TVG". After a break for the geochemical water sampling station in the deep sea, this grid was surveyed twice again, first in the HDBE mode with a "Maximum Source Level" control" set to 230 dB, a transmission/receiver coverage of 120°/100° and an automatic gain control with 18 dB "Start TVG", and second in the HDBE mode with "Standard" source level control, 120°/120° transmission/receiver coverages and an automatic gain control with 18 dB a "Start TVG".

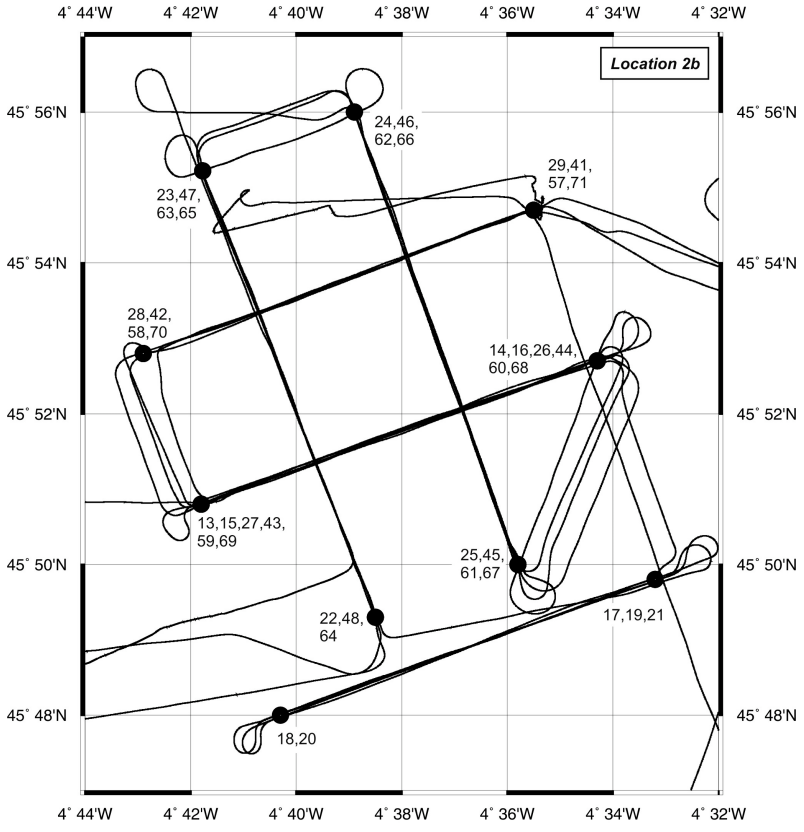

Fig. 3.5: ANT-XXIII/1 cruise track and waypoint numbers at the acoustic test site "Location 2b" at the southwestern end of the Canyon de Noirmoutier in the Bay of Biscay

The Canyon de Noirmoutier was first surveyed by two different profile lines, one in the canyon axis, the other slightly shifted to the northwestern canyon flank. The line in the canyon axis was run three times, first upslope in the HDBE mode ("Standard" source level control) with 120°/100° transmission/receiver coverages and 10 dB "Start TVG", a second time upslope in the HDBE and ASLC modes with no source level limitation, 120°/100° transmission/receiver coverages, a S/N ratio of 15 dB and a "Start TVG" of 18 dB, and third downslope with the same parameter settings for about 60 - 70% of the profile line and a limitation of the maximum source level to 233 dB in the lower part of the canyon. The line shifted to the northwestern flank was run in the HDBE mode ("Standard" source level control) with 120°/100° transmission/receiver swath widths and 10 dB "Start TVG". After the break for the geochemical water sampling station two additional lines were recorded along the canyon axis, one upslope, and one downslope. This survey started with the HDBE mode and a "Maximum Source Level" control confined to 230 dB, 18 dB "Start TVG" and an automatically adjusted "Actual TVG". During the survey the operator tried to optimize the source level manually such that sufficient receiver coverage and a sufficient S/N-ratio could be reached with a minimum source level.

The three lines of Location 2d were mainly dedicated to collect parasound data in an area with rather flat topography and significant signal penetration. Hydrosweep was run in the HDBE mode ("Standard" source level control) with 120°/120° transmission/receiver coverages along the northernmost line and 120°/100° coverages along the two southern lines.

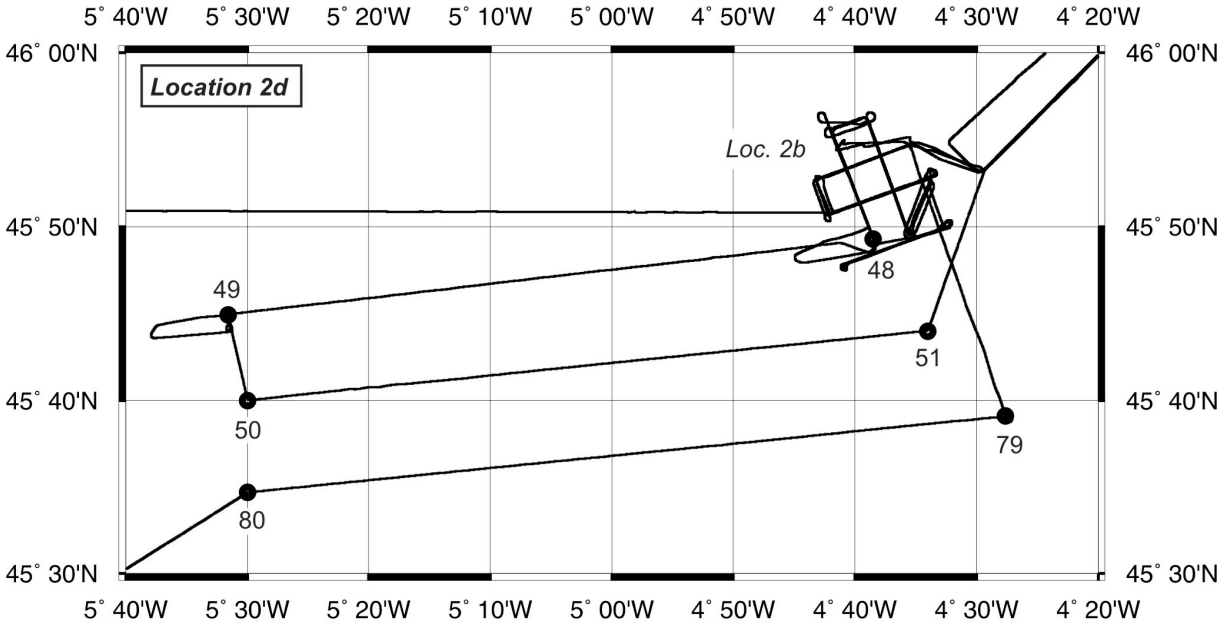

Fig. 3.6: ANT-XXIII/1 cruise track and waypoint numbers at the acoustic test site "Location 2d" between the test site "Location 2b" and a geochemical water sampling station in the deep sea

For all parasound data collected along the Canyon de Noirmoutier and at Locations 2b and 2d the standard parameter settings of 4 kHz frequency, 2 periods length and a range of 5000 m were used. Only in the shallow parts of the canyon with water depths shallower than 1000 m the range was adjusted appropriately to 1000, 500 and 200 m. Additionally, parasound was switched off when Location 2b and the Canyon de Noirmoutier were revisited after the geochemical water sampling station in the deep sea, because the rather rough topography in this area did not allow to collect high-quality data suitable to act as reference data for future parasound recordings, and because there was no need to collect data along the same lines several times. Thus, it was a good occasion to study if the hydrosweep data quality is affected if both systems run simultaneously.

Preliminary results

The hydrosweep and parasound tests were finished and the data recording was switched off about 12 - 24 hours before RV *Polarstern* arrived in Vigo, having recorded multibeam and echosounder data of about 650 nm track length. A detailed data analysis particularly for the hydrosweep data has still to be carried out at home. This includes a detailed, careful comparison of single shots, of single track lines and of the bathymetric maps which can be created from the small grid of profile lines collected at Location 2b for the different parameter settings during this cruise and with the data of the former cruises ANT-VIII/1 and ANT-XV/1. Nevertheless, some general conclusions can be drawn from the "online" observation of the hydrosweep system during the surveys:

1. The HDBE mode seemed to work correctly without any problems or artefacts.

2. The ASLC mode (with no source level limitation) only reduced the source level appropriately without significant loss of data quality and according to the given S/N-ratio and receiver coverage in the rather smooth, flat area of Location 1b. Along the steep slope of the Canyon de Noirmoutier it completely failed upslope, and lost a complete package of the outer beams downslope. Hence, generally the source level regulation algorithm does not work correctly but has still to be improved so that it could be used with less manual control than was necessary during this test cruise.

3. If a "Maximum Source Level Control" (239, 233, 230, 227 dB) is used in combination with fixed values for the "Start" and "Actual TVG" (18 dB) the quality of the outer beams increasingly worsens, so that the coverage usable to create bathymetric maps decreases. In case of a maximum source level of 227 dB the usable coverage only amounts to about the single water depth, even in flat areas.

4. If a "Maximum Source Level Control" is used in combination with an automatic gain control (18 dB "Start TVG") the "Actual TVG" obviously enhances the received data such that the reduction in the source level is compensated, at least in flat areas. Nevertheless, though a detailed data analysis is remaining, a source level reduction to less than 230 dB did not seem to be appropriate in the deep sea.

5. Generally, the operation of the hydrosweep system with reduced source levels obviously need more experienced operators than were necessary for the

"standard" system because the operator continuously has to watch the data quality online and may have to change parameters appropriately.

The parasound system still incorporates some major and minor bugs:

1. In shallow water the heave compensation is not completely removing the ship's up and down movements, but obviously there is still some residual heave in the data. It is not clear if this is due to a remaining error in the Parastore-3 software or due to some time delay introduced by the transfer of the heave sensor data via the motion sensors MINS 1 or MINS 2 to the recording programme.

2. The range 2,000 m does not work correctly (PAR pilot mode). Parasound always transmits only one pulse instead of a pulse train and in intervals of about 8 s instead of 3.34 s. A transmission interval of about 8 s is typical for a range of 5,000 m, whereas an interval 3.34 s is required for a range of 2,000 m and is displayed correctly in the corresponding menu of the Parastore-3 programme.

3. The range 7,000 m does not work correctly. The number of pulses per train and the transmission intervals are equivalent to those used with a range setting of 10,000 m, though a shorter transmission interval is displayed in the menu of the Parastore-3 programme.

4. The tick increment and the position of the labels along the time/depth axis of both online screen and online plot are confusing if a recording window length of 100 m is used. It would be more appropriate and easier to read if the total window length would be divided into 10 parts instead of the 8 parts used now. This would lead to a depth increment of 10 m in case of a 100 m window and to a depth increment of 20 m in case of a 200 m window instead of the 12 and 25 m used now.

Apart from these bugs the parasound system worked well and allowed to collect a useful reference data set. Figures 3.7 to 3.10 present some examples from the English Channel, Locations 1a, 1, and 2d.

The English Channel southwest of Dover is characterized by pronounced, asymmetric sand ripples of about 5 to 10 m height and about 50 - 500 m length (Fig. 3.7).They lie on the erosional surface of the "normal" sea floor which cuts older dipping, outcropping layers. The type and shape of these ripples strongly vary along the ship's track. For example, the three profiles shown in figure 3.7 were recorded continuously along about 41 km length and over 2 hours duration.

The lower French continental slope at location 1a between waypoints 3a and 3b shows typical hemipelagic sedimentation with parallel subbottom layers and a signal penetration of about 30 m at the southwestern end of the profile (Fig. 3.8). These layers are cut by a large slump of unknown thickness because the parasound signals did not penetrate the slump body but only show its surface at the sea floor.

The sediments at Location 1 at the southwestern end of the profiles of Location 1a as well reveal this hemipelagic parallel subbottom layering with a signal penetration between 30 and 50 m on both the N-S and the W-E profile line (Fig. 3.9). Accordingly, Location 2d between waypoints 50 and 51 is characterized by the same type of hemipelagic sedimentation (Fig. 3.10).

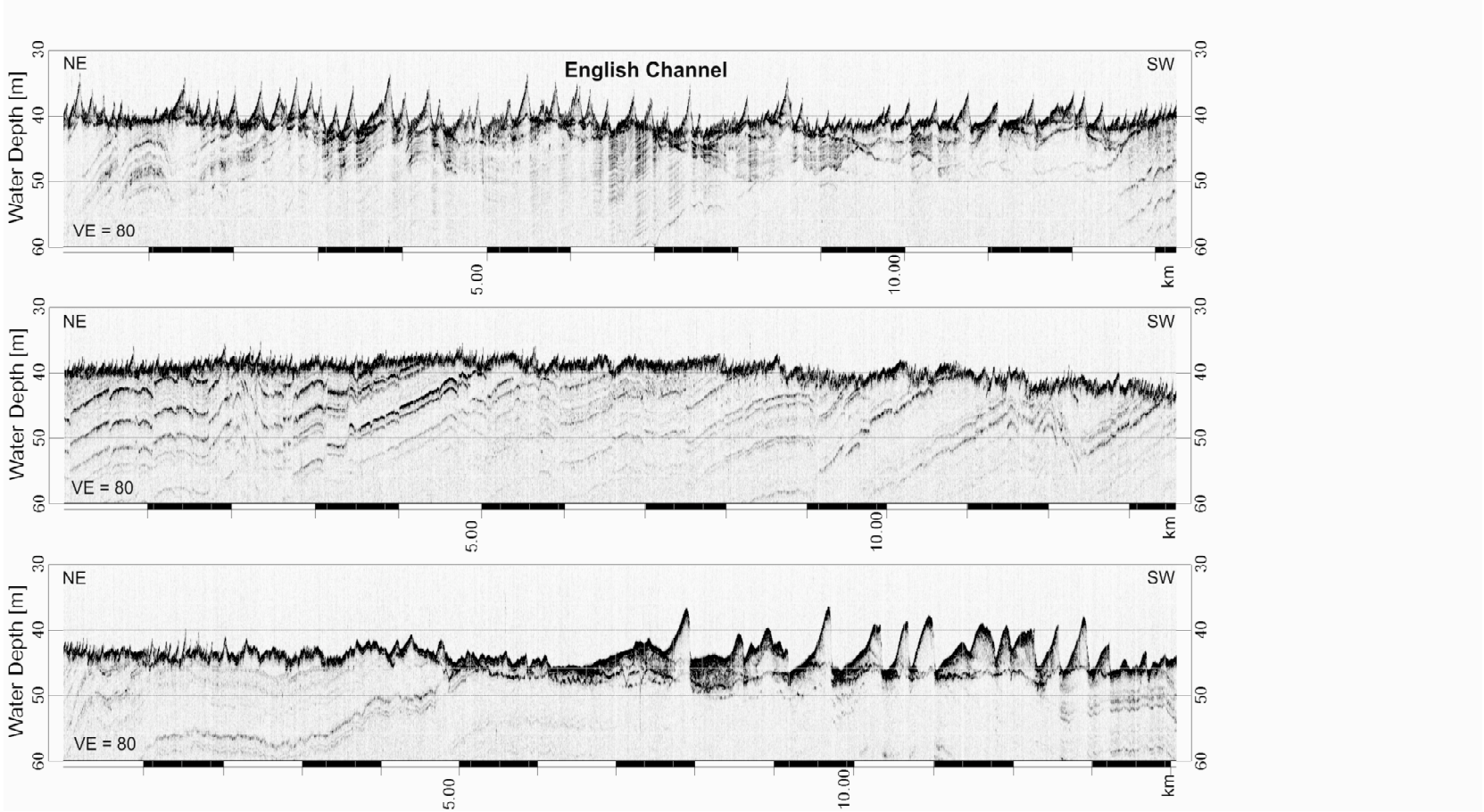

Fig. 3.7: Continuous parasound profile recorded in the English Channel southwest of the Strait of Dover over about 2 hours duration and along about 41 km track length. Sediments are characterized by pronounced sand ripples and a heavily eroded sea surface.

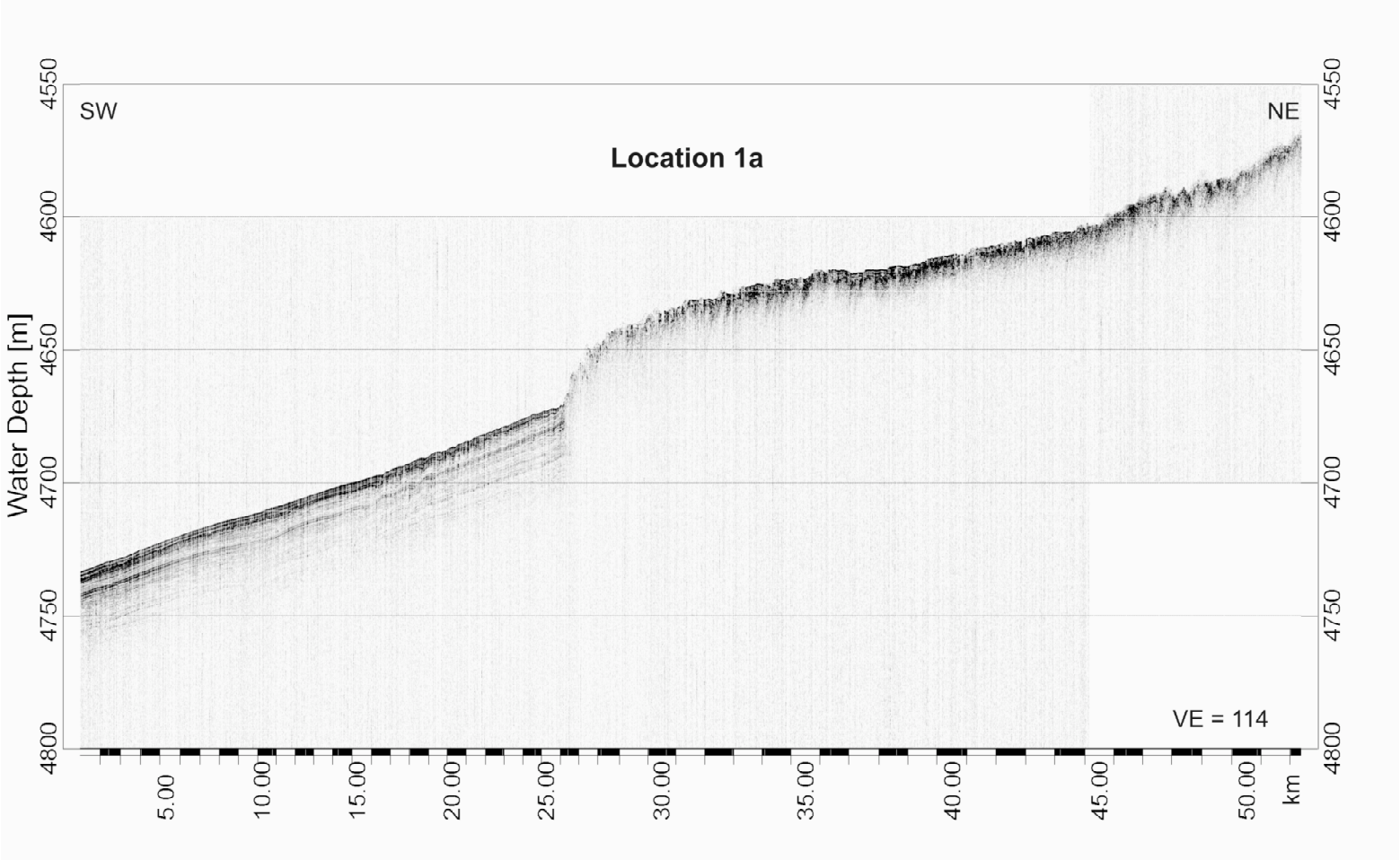

Fig. 3.8: Parasound profile recorded at Location 1a (between waypoints 3a and 3b) on the lower French continental slope. The profile is characterized by subparallel hemipelagic layers and a transparent slump of unknown thickness.

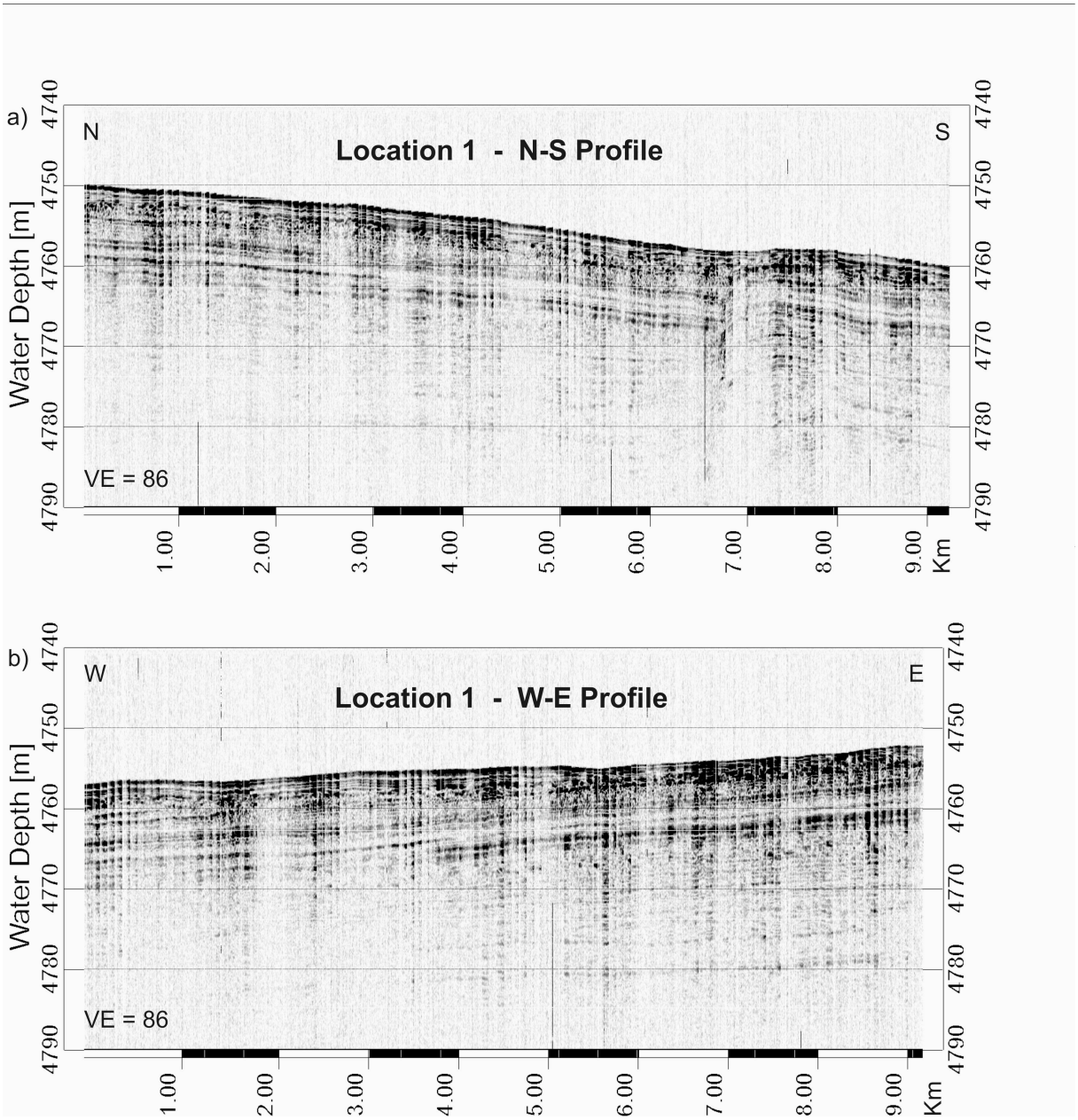

Fig. 3.9: N-S and W-E running parasound profiles recorded at Location 1 in the deep sea. Both profiles show the typical subparallel hemipelagic sedimentation.

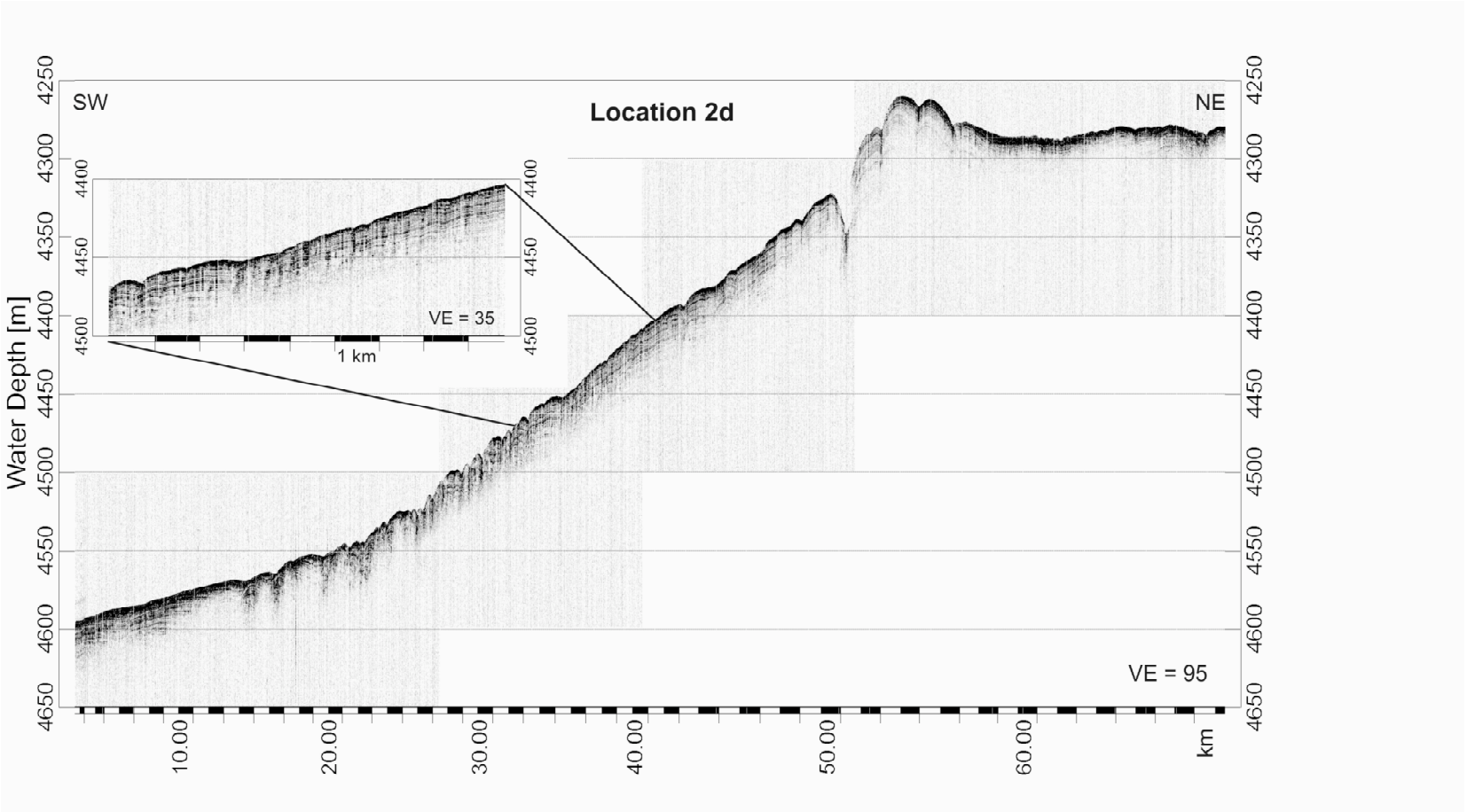

Fig. 3.10: Parasound profile recorded at Location 2d on the lower French continental slope between waypoints 50 and 51. Similar to the profiles displayed in figures 3.7, 3.8 and 3.9 it is characterized by subparallel hemipelagic layers, too.

Tab. 3.1: List of waypoints, geographical coordinates, date and time of the hydrosweep profiles and variation of the hydrosweep parameter settings

Waypoint (begin of profile	Date	Time UTC	Latitude	Longitude	Waypoint (end of profile)	Time (end)	Distance [nm] between WP	Survey Speed (schedule)	Gyro/Motion Sensor #	Transmit Angle	Receive Angle	HDBE Mode	Parameters	TVG	Calibration Mode	PARASOUND On/Off	Comment
																	Approaching Location 1
1	16.10.05	08:10	47 13.320	-5 46.080	2		30.9	-	2	120	100	Standard			never	on	start of data recording; WP1 to WP2: test of various parameter settings
2	?	?	46 48.900	-5 18.190	3	12:58	70.7		2	120	100	Standard			never	on	
3	17.10.05	12:58	46 00.000	-6 32.330	3a	13:11	2.0	-	2	120	100	Standard			never	on	connection between waypoints
3a	17.10.05	13:11	45 58.500	-6 30.400			34.6	-	2	120	100	Standard			never	on	WP 3a to WP 3b: test of various parameter settings
	17.10.05	13:59	46 05.000	-6 20.800			-	-	2	120	90	ASLC	Max. Source Lev. 239 dB Desired S/N 10 dB Desired Coverage 90° **EqFp** (= Equal Footprint)		never	on	
	17.10.05	14:35	46 09.000	-6 14.200			-	-	2	120	90	ASLC	Max. Source Lev. 239 dB Desired S/N 20 dB Desired Coverage 90° EqFp		never	on	
~3b	17.10.05	16:28	46 22.400	-5 54.400			-	-	2	120	90	ASLC	Max. Source Lev. 239 dB Desired S/N 15 dB Desired Coverage 90° EqFp		never	on	WP 3b: Stop for active sonar test station
	18.10.05	04:51	46 18.100	-5 56.900			34.5	-	2	120	100	Standard	**EqSp** (= Equal Spacing)		never	on	leaving active sonar test station towards WP 3d
3d	18.10.05	08:03	45 57.000	-6 28.600			5.2	-	2	120	100	Standard	EqSp		never	on	
	18.10.05	08:32	45 54.000	-6 33.900	4	08:37	-	-	2	90	90	Standard	EqSp		alternate	on	alternate calibration mode for roll/pitch calibration

Waypoint (begin of profile	Date	Time UTC	Latitude	Longitude	Waypoint (end of profile)	Time (end)	Distance [nm] between WP	Survey Speed (schedule)	Gyro/Motion Sensor #	Transmit Angle	Receive Angle	HDBE Mode	Parameters	TVG	Calibration Mode	PARASOUND On/Off	Comment
																	Location 1 (N-S Profile)
4	18.10.05	08:37	45 53.500	-6 34.150	5	09:07	5.0	10	2	90	90	Standard	EqSp		alternate	on	N-S profile
5	18.10.05	09:20	45 48.500	-6 34.150	6	09:49	5.0	10	2	90	90	Standard	"		alternate	on	S-N profile
6	18.10.05	09:49	45 53.500	-6 34.150	7	10:22	3.5	10	**1**	90	90	Standard	"		alternate	on	connection to W-E profiles; change from MINS 2 to MINS 1
																	Location 1 (W-E Profile)
7	18.10.05	10:22	45 51.000	-6 37.700	8	10:51	5.0	10	1	90	90	Standard	"		alternate	on	W-E profile
8	18.10.05	11:07	45 51.000	-6 30.550	9	11:37	5.0	10	1	90	90	Standard	"		alternate	on	E-W Profile; stop for station
9	18.10.05	13:30	45 51.000	-6 37.700			5.0	10	**2**	**120**	**120**	Max Level	Max. SL 239 dB	manual 18 dB	never	on	begin of profile (W-E)
	18.10.05	13:47	45 51.000	-6 34.500				10	2	120	120	Max Level	Max. SL 233 dB	"	never	on	middle of profile
	18.10.05				10	14:00								"	never	on	end of profile
10	18.10.05	14:14	45 51.000	-6 30.550			5.0	10	2	120	120	Max Level	Max. SL 230 dB	"	never	on	begin of profile (E-W)
	18.10.05	14:33	45 51.000	-6 34.500						120	120	Max Level	Max. SL 227 dB	"	never	on	middle of profile
	18.10.05				11	14:49									never	on	end of profile
11	18.10.05	15:03	45 51.000	-6 37.700	12	15:29	5.0	10	2	120	120	Max Level	Max. SL 227 dB	Start 18 Act. 18	never	**off**	profile WP 11 to WP 12 (W-E); TVG Act. at end of profile: 30 dB
																	Location 1 to 2b
12	18.10.05	15:30	45 51.000	-6 30.800			75.9	10	2	120	120	Max Level	Max. SL 230 dB	Start 18 Act. 30	never	**on**	
	18.10.05	16:04	45 51.000	-6 21.500			-	10	2	120	120	Max Level	Max. SL 233 dB	Start 18 Act. 29	never	on	
	18.10.05	16:38	45 51.000	-6 12.900			-	10	2	120	120	Max Level	Max. SL 239 dB	Start 18 Act. 24	never	on	
	18.10.05	17:18	45 51.000	-6 05.800			-	10	2	120	120	Max Level	Max. SL 239 dB opt (s. Comment)	Start 18	never	on	opt = manually optimized depth window

Waypoint (begin of profile	Date	Time UTC	Latitude	Longitude	Waypoint (end of profile)	Time (end)	Distance [nm] between WP	Survey Speed (schedule)	Gyro/Motion Sensor #	Transmit Angle	Receive Angle	HDBE Mode	Parameters	TVG	Calibration Mode	PARASOUND On/Off	Comment
														Act. 25			
	18.10.05	17:53	45 51.000	-5 55.000			-	10	2	**120**	**100**	ASLC	Max. SL 233 dB, S/N 15 dB, Coverage 100°	Start 18 Act. 30	never	on	
	18.10.05	21:52	45 50.800	-4 54.800				10	2	90	90						sound velocity profile changed
	18.10.05	21:57	45 50.000	-4 53.000				10	**1**	90	90						change from MINS 2 to MINS 1
	18.10.05				13	22:46											end of profile
																	Location 2b (parallel profiles and grid)
13	18.10.05	22:46	45 50.800	-4 41.800	14	00:05	5.6	**4**	**1**	**90**	**90**	Standard			never	on	northern SW-NE profiles
14	19.10.05	00:21	45 52.700	-4 34.300	15	00:59	5.6	**10**	1	90	90	Standard			never	on	“
15	19.10.05	01:12	45 50.800	-4 41.800	16	01:44	5.6	10	1	90	90	Standard			never	on	“
16	19.10.05	01:44	45 52.700	-4 34.300	17	02:07	3.0	10	1	90	90	Standard			never	on	connection
17	19.10.05	02:07	45 49.800	-4 33.200	18	02:47	5.3	10	1	90	90	Standard			never	on	southern SW-NE profile
18	19.10.05	03:01	45 48.000	-4 40.300	19	03:29	5.3	10	1	90	90	Standard			never	on	“
19	19.10.05	03:45	45 49.800	-4 33.200	20	04:23	5.3	10	**2**	90	90	Standard			never	on	“
20	19.10.05	04:35	45 48.000	-4 40.300	21	05:04	5.3	10	2	90	90	Standard			never	on	“
21	19.10.05	05:17	45 49.800	-4 33.200	22	05:44	3.7	10	2	**120**	**100**	Standard			never	on	connection
22	19.10.05	05:44	45 49.300	-4 38.500	23	06:25	6.3	10	2	120	100	Standard	EqFp		never	on	survey of the total grid
23	19.10.05	06:25	45 55.220	-4 41.770	24	06:41	2.1	10	2	120	100	Standard	“		never	on	
24	19.10.05	06:41	45 56.000	-4 38.900	25	07:18	6.4	10	2	120	100	Standard	“		never	on	
25	19.10.05	07:18	45 50.000	-4 35.800	26	07:55	2.9	10	2	120	100	Standard	“		never	on	
26	19.10.05	07:55	45 52.700	-4 34.300	27	08:20	5.6	10	2	120	100	Standard	“		never	on	
27	19.10.05	08:20	45 50.800	-4 41.800	28	08:36	2.1	10	2	120	100	Standard	“		never	on	
28	19.10.05	08:36	45 52.800	-4 42.900	29	09:10	5.5	10	2	120	100	Standard	“		never	on	

Waypoint (begin of profile	Date	Time UTC	Latitude	Longitude	Waypoint (end of profile)	Time (end)	Distance [nm] between WP	Survey Speed (schedule)	Gyro/Motion Sensor #	Transmit Angle	Receive Angle	HDBE Mode	Parameters	TVG	Calibration Mode	PARASOUND On/Off	Comment
29	19.10.05	09:10	45 54.700	-4 35.500	30	09:38	4.5	10	2	120	100	Standard	"		never	on	connection
																	Canyon de Noirmoutier
30	19.10.05	09:38	45 53.300	-4 29.300	31	10:48	12.0	10	2	120	100	Standard			never	on	
31	19.10.05	10:48	46 01.800	-4 17.200	32	11:56	12.2	10	2	120	100	Standard			never	on	
32	19.10.05	11:56	46 11.600	-4 06.700	33		0.4	10	2	120	100	Standard			never	on	station on the shelf; connection
33	19.10.05	13:35	46 11.800	-4 07.200	34	14:58	11.8	10	2	120	100	Standard			never	on	
34	19.10.05	14:58	46 03.400	-4 19.100	35	16:19	12.2	10	2	120	100	Standard			never	on	
35	19.10.05	16:19	45 55.100	-4 32.000	36	16:38	2.6	10	2	120	100	Standard			never	on	connection
36	19.10.05	16:38	45 53.300	-4 29.300	37	17:44	12.0	10	2	120	100	ASLC	Max. SL 239 dB Desired S/N 15 dB Desired Coverage 100°		never	on	
37	19.10.05	17:44	46 01.800	-4 17.200	38	18:52	12.2	10	2	120	100	ASLC	"		never	on	17:50 HDBE failed (ASLC automatically changed parameter settings such that HDBE could not work correctly any more)
38	19.10.05	19:04	46 11.600	-4 06.700	39	20:22	12.2	10	2	120	100	ASLC	"		never	on	
39	19.10.05	20:22	46 01.800	-4 17.200			12.0	10	2	120	100	ASLC	"		never	on	
	19.10.05	20:56:50			40	21:40	-	"	"	"	"	ASLC	Max. SL. 233 dB		never	on	Max. Source Level reduced to 233 dB
																	Location 2b (grid)
40	19.10.05	21:40	45 53.300	-4 29.300			4.5	10	2	120	100	ASLC	Max. SL 233 dB		never	on	connection
	19.10.05	22:05			41	22:11						Max Level	Max. SL 233 dB				change from ASLC to Max. Level
41	19.10.05	22:11	45 54.700	-4 35.500	42	22:45	5.5	10	2	120	100	Max Level	"		never	on	
42	19.10.05	22:45	45 52.800	-4 42.900	43	23:03	2.1	10	2	120	100	Max Level	Max. SL 233 dB		never	on	connection
43	19.10.05	23:03	45 50.800	-4 41.800	44	23:36	5.6	10	2	120	100	Max Level	"		never	on	
44	19.10.05	23:37	45 52.700	-4 34.300	45	00:05	2.9	10	2	120	100	Max Level	"		never	on	connection

Waypoint (begin of profile	Date	Time UTC	Latitude	Longitude	Waypoint (end of profile)	Time (end)	Distance [nm] between WP	Survey Speed (schedule)	Gyro/Motion Sensor #	Transmit Angle	Receive Angle	HDBE Mode	Parameters	TVG	Calibration Mode	PARASOUND On/Off	Comment
45	20.10.05	00:05	45 50.000	-4 35.800	46	00:44	6.4	10	2	120	100	Max Level	"		never	on	
46	20.10.05	00:44	45 56.000	-4 38.900	47	01:01	2.1	10	2	120	100	Max Level	"		never	on	connection
47	20.10.05	01:01	45 55.220	-4 41.770	48	01:38	6.3	10	2	120	100	Max Level	"		never	on	WP 48: end of grid survey
																	From Loc. 2b to station at WP 49 and back to Canyon de Noirmoutier
48	20.10.05	01:38	45 49.300	-4 38.500				10	2	120	100	Standard			never	on	leaving towards station at WP 49
~49 (an)	20.10.05	06:50	45 44.933	-5 31.596				10	2	120	100	Standard			never	on	arriving at station; standby
~49	20.10.05	14:51	45 44.933	-5 31.596	50	15:25	5.1	10	2	120	100	Standard	EqFp		never	on	leaving station
50	20.10.05	15:25	45 40.000	-5 30.000	51	19:16	39.3	10	2	120	100	Standard	"		never	on	
51	20.10.05	19:16	45 44.000	-4 34.000	52	20:09	9.9	10	2	120	100	Standard	"		never	on	connection
																	Canyon de Noirmoutier
52	20.10.05	20:09	45 53.300	-4 29.300			12.0	10	2	120	100	Max Level	Max. SL 230 dB, EqFp		never	**off**	Maximum Level mode with varying Max. SL; Parasound off
	20.10.05	20:22						10	2	120	100	Max Level	Max. SL 227 dB		never	off	EqFp until end of 21.10.05
	20.10.05	20:37						10	2	120	100	Max Level	Max. SL 224 dB		never	off	
	20.10.05	20:47						10	2	120	100	Max Level	Max. SL 222 dB		never	off	
	20.10.05	20:58						10	2	120	100	Max Level	Max. SL 221 dB		never	off	
	20.10.05	21:07						10	2	120	100	Max Level	Max. SL 218 dB		never	off	
					53	21:21											end of profile
53	20.10.05	21:21	46 01.800	-4 17.200			12.2	10	2	120	100	Max Level	Max. SL 213 dB		never	off	
	20.10.05	21:32						10	2	120	100	Max Level	Max. SL 218 dB		never	off	
	20.10.05	21:59						10	2	120	100	Max Level	Max. SL 213 dB		never	off	

Waypoint (begin of profile	Date	Time UTC	Latitude	Longitude	Waypoint (end of profile)	Time (end)	Distance [nm] between WP	Survey Speed (schedule)	Gyro/Motion Sensor #	Transmit Angle	Receive Angle	HDBE Mode	Parameters	TVG	Calibration Mode	PARASOUND On/Off	Comment
	20.10.05	22:03						10	2	120	100	Max Level	Max. SL 212 dB		never	off	
	20.10.05	22:07						10	2	120	100	Max Level	Max. SL 207 dB		never	off	
	20.10.05	22:28	46 12.000	-4 06.500	~54	22:28		10	2	120	100	Max Level	Max. SL 207 dB		never	off	end of profile 22:28; note written somewhat later
54	20.10.05	22:39	46 11.600	-4 06.700			12.2	10	2	120	100	Max Level	Max. SL 207 dB		never	off	
	20.10.05	23:13						10	2	120	100	Max Level	Max. SL 207 dB		never	**on**	Parasound on
	20.10.05	23:19						10	2	120	100	Max Level	Max. SL 207 dB		never	**off**	Parasound off
	20.10.05	23:20						10	2	120	100	Max Level	Max. SL 212 dB		never	off	
	20.10.05	23:22								120	100	Max Level	Max. SL 218 dB		never	off	
	20.10.05	23:37								120	100	Max Level	Max. SL 222 dB		never	off	
	20.10.05	23:45								120	100	Max Level	Max. SL 227 dB		never	off	
	21.10.05	00:04			55	00:05				120	100	Max Level	Max. SL 224 dB		never	off	
55	21.10.05	00:05	46 01.800	-4 17.200			12.0	10	2	120	100	Max Level	Max. SL 224 dB		never	off	
	21.10.05	00:41								120	100	Max Level	Max. SL 222 dB		never	off	
	21.10.05	00:44			56	01:24				120	100	Max Level	Max. SL 218 dB		never	off	
56	21.10.05	01:24	45 53.300	-4 29.300	57	01:50	4.5	10	2	120	100	Max Level	Max. SL 218 dB		never	off	connection
																	Location 2b (grid 2x)
57	21.10.05	01:50	45 54.700	-4 35.500	58	02:30	5.5	10	2	120	100	Max Level	Max. SL 230 dB EqFp		never	off	Maximum Level mode Max. SL 230 dB
58	21.10.05	02:32	45 52.800	-4 42.900	59	02:45	2.1	10	2	120	100	Max Level	"		never	off	connection
59	21.10.05	02:47	45 50.800	-4 41.800	60	03:15	5.6	10	2	120	100	Max Level	"		never	off	
60	21.10.05	03:29	45 52.700	-4 34.300	61	03:52	2.9	10	2	120	100	Max Level	"		never	off	connection

Waypoint (begin of profile	Date	Time UTC	Latitude	Longitude	Waypoint (end of profile)	Time (end)	Distance [nm] between WP	Survey Speed (schedule)	Gyro/Motion Sensor #	Transmit Angle	Receive Angle	HDBE Mode	Parameters	TVG	Calibration Mode	PARASOUND On/Off	Comment
												Level					
61	21.10.05	04:06	45 50.000	-4 35.800	62	04:48	6.4	10	2	120	100	Max Level	"		never	off	
62	21.10.05	05:01	45 56.000	-4 38.900	63	05:23	2.1	10	2	120	100	Max Level	"		never	off	connection
63	21.10.05	05:37	45 55.220	-4 41.770	~64	06:16	6.3	10	2	120	100	Max Level	"		never	off	
~64 (an)	21.10.05	06:16	45 40.800	-4 39.100													course changed for station shortly before WP 64
64	21.10.05	08:18	45 49.300	-4 38.500	65	09:02	6.3	10	2	120	120	Standard	EqFp		never	off	
65	21.10.05	09:02	45 55.220	-4 41.770	66	09:34	2.1	10	2	120	120	Standard	"		never	off	connection
66	21.10.05	09:34	45 56.000	-4 38.900	67	10:13	6.4	10	2	120	120	Standard	"		never	off	
67	21.10.05	10:13	45 50.000	-4 35.800	68	10:39	2.9	10	2	120	120	Standard	"		never	off	connection
68	21.10.05	10:40	45 52.700	-4 34.300	69	11:20	5.6	10	2	120	120	Standard	"		never	off	
69	21.10.05	11:20	45 50.800	-4 41.800	70	10:40	2.1	10	2	120	120	Standard	"		never	off	connection
70	21.10.05	11:41	45 52.800	-4 42.900	71	12:14	5.5	10	2	120	120	Standard	"		never	off	WP 71: station started at 12:14
																	Leaving for Vigo
71	21.10.05	15:58	45 54.700	-4 35.500				10	2	120	100	Standard	"		never	**on**	Parasound on
79	21.10.05	?	45 39.100	-4 27.600				10	2	120	100	Standard	"		never	on	
80	21.10.05	21:30	45 34.700	-5 30.000				10	2	120	100	Standard	"		never	on	end of profile 21.30
-	22.10.05	07:00	44 33.000	-7 47.600									"				data recording off

Tab. 3.2: List of waypoints, geographical coordinates, date and time of the parasound profiles and variation of the parasound parameter settings

Waypoint (begin of profile)	Date	Time UTC	Latitude	Longitude	Waypoint (end of profile)	Time (end)	Distance [nm] between WP	Survey Speed (schedule)	Gyro/Motion Sensor#	Frequency [kHz]	Number of Periods	Range [m]	Position of PARASOUND Transducer (x/y/z)	Position of Motion Sensor (x/y/z)	Comment
															Location 1a
	14.10.05	22:20			2	ca. 11:00		-	2	4	2	100, 200, 500, 1000, 5000			start of data recording
2	?	?	46 48.900	-5 18.190	3	12:58	70.7		2	4	2	5000			profile interrupted for sonar test
3	17.10.05	12:58	46 00.000	-6 32.330	3a	13:11	2.0	-	2	4	2	5000			connection between waypointsl
3a	17.10.05	13:11	45 58.500	-6 30.400	~3 b	16:28	34.6	-	2	4	2	5000			at the end of the profile stop for search of the triple mirror and active sonar test
~3b	17.10.05	16:28	46 22.400	-5 54.400	3d	08:03	34.5	-	2	4	2	5000			
3d	18.10.05	08:03	45 57.000	-6 28.600	4	08:37	5.2	-	2	4	2	5000			leaving towards location 1
															Location 1 (N-S Profile)
4	18.10.05	08:37	45 53.500	-6 34.150	5	09:07	5.0	10	2	4	2	10000	0/0/0	0/0/0	N-S profile
5	18.10.05	09:20	45 48.500	-6 34.150	6	09:49	5.0	10	2	4	2	10000	0/0/0	0/0/0	S-N profile; verification of the N-S profile and a potential residual error in vertical beam steering
6	18.10.05	09:49	45 53.500	-6 34.150	7	10:22	3.5	10	1	4	2	10000	0/0/0	0/0/0	connection to W-E profiles; change from MINS 2 to MINS 1
															Location 1 (W-E Profile)
7	18.10.05	10:22	45 51.000	-6 37.700	8	10:51	5.0	10	1	4	2	10000	0/0/0	0/0/0	W-E profile
8	18.10.05	11:07	45 51.000	-6 30.550	9	11:37	5.0	10	1	4	2	10000	0.97/0.00/0.00	-4.10/0.35/8.50	E-W Profile; position of transducer and motion sensor according to values noted by the bathymetry group; check, if and how the positions of the transducer and motion sensor affect the recorded data; after WP 9: stop for station; on station test of different transducer and motion sensor positions; tests with beam steering

Waypoint (begin of profile)	Date	Time UTC	Latitude	Longitude	Waypoint (end of profile)	Time (end)	Distance [nm] between WP	Survey Speed (schedule)	Gyro/Motion Sensor#	Frequency [kHz]	Number of Periods	Range [m]	Position of PARASOUND Transducer (x/y/z)	Position of Motion Sensor (x/y/z)	Comment
9	18.10.05	13:30	45 51.000	-6 37.700	10	14:00	5.0	10	2	4	2	5000	0.97/0.00/0.00	-4.10/0.35/8.50	W-E profile; comparison of data quality recorded with ranges 10000 and 5000 m
10	18.10.05	14:14	45 51.000	-6 30.550	11	14:49	5.0	10	2	4	2	5000	0.97/0.00/0.00	-4.10/0.35/8.50	E-W profile; check, if and how the positions of the transducer and motion sensor affect the recorded data
11	18.10.05	15:03	45 51.000	-6 37.700	12	15:29	5.0	10	2	off	off	off			W-E profile; Parasound off
															Location 1 to 2b
12	18.10.05	15:30	45 51.000	-6 30.800	13	22:46	75.9	10	2	4	2	5000	0.97/0.00/0.00	-4.10/0.35/8.50	connection between Loc. 1 and 2b/Canyon de Noirmoutier
															Location 2b (parallel profiles and grid)
13	18.10.05	22:46	45 50.800	-4 41.800	14	00:05	5.6	4	1	4	2	5000	0.97/0.00/0.00	-4.10/0.35/8.50	northern SW-NE profiles
14	19.10.05	00:21	45 52.700	-4 34.300	15	00:59	5.6	10	1	4	2	5000	0.97/0.00/0.00	-4.10/0.35/8.50	"
15	19.10.05	01:12	45 50.800	-4 41.800	16	01:44	5.6	10	1	4	2	5000	0.97/0.00/0.00	-4.10/0.35/8.50	"
16	19.10.05	01:44	45 52.700	-4 34.300	17	02:07	3.0	10	1	4	2	5000	0.97/0.00/0.00	-4.10/0.35/8.50	connection
17	19.10.05	02:07	45 49.800	-4 33.200	18	02:47	5.3	10	1	4	2	5000	0.97/0.00/0.00	-4.10/0.35/8.50	southern SW-NE profile
18	19.10.05	03:01	45 48.000	-4 40.300	19	03:29	5.3	10	1	4	2	5000	0.97/0.00/0.00	-4.10/0.35/8.50	"
19	19.10.05	03:45	45 49.800	-4 33.200	20	04:23	5.3	10	2	4	2	5000	0.97/0.00/0.00	-4.10/0.35/8.50	"
20	19.10.05	04:35	45 48.000	-4 40.300	21	05:04	5.3	10	2	4	2	5000	0.97/0.00/0.00	-4.10/0.35/8.50	southern SW-NE profile; Parastore-3 break down at 04:28; restart
21	19.10.05	05:17	45 49.800	-4 33.200	22	05:44	3.7	10	2	4	2	5000	0.97/0.00/0.00	-4.10/0.35/8.50	connection
22	19.10.05	05:44	45 49.300	-4 38.500	23	06:25	6.3	10	2	4	2	5000	0.97/0.00/0.00	-4.10/0.35/8.50	survey of the grid
23	19.10.05	06:25	45 55.220	-4 41.770	24	06:41	2.1	10	2	4	2	5000	0.97/0.00/0.00	-4.10/0.35/8.50	"
24	19.10.05	06:41	45 56.000	-4 38.900	25	07:18	6.4	10	2	4	2	5000	0.97/0.00/0.00	-4.10/0.35/8.50	"
25	19.10.05	07:18	45 50.000	-4 35.800	26	07:55	2.9	10	2	4	2	5000	0.97/0.00/0.00	-4.10/0.35/8.50	"
26	19.10.05	07:55	45 52.700	-4 34.300	27	08:20	5.6	10	2	4	2	5000	0.97/0.00/0.00	-4.10/0.35/8.50	"
27	19.10.05	08:20	45 50.800	-4 41.800	28	08:36	2.1	10	2	4	2	5000	0.97/0.00/0.00	-4.10/0.35/8.50	"

Waypoint (begin of profile)	Date	Time UTC	Latitude	Longitude	Waypoint (end of profile)	Time (end)	Distance [nm] between WP	Survey Speed (schedule)	Gyro/Motion Sensor#	Frequency [kHz]	Number of Periods	Range [m]	Position of PARASOUND Transducer (x/y/z)	Position of Motion Sensor (x/y/z)	Comment
28	19.10.05	08:36	45 52.800	-4 42.900	29	09:10	5.5	10	2	4	2	5000	0.97/0.00/0.00	-4.10/0.35/8.50	"
29	19.10.05	09:10	45 54.700	-4 35.500	30	09:38	4.5	10	2	4	2	5000	0.97/0.00/0.00	-4.10/0.35/8.50	connection
															Canyon de Noirmoutier
30	19.10.05	09:38	45 53.300	-4 29.300	31	10:48	12.0	10	2	4	2	5000	0.97/0.00/0.00	-4.10/0.35/8.50	upslope
31	19.10.05	10:48	46 01.800	-4 17.200	32	11:56	12.2	10	2	4	2	5000, 1000, 500, 200	0.97/0.00/0.00	-4.10/0.35/8.50	upslope
32	19.10.05	11:56	46 11.600	-4 06.700	33		0.4	10	2	4	2	200	0.97/0.00/0.00	-4.10/0.35/8.50	station on the shelf; connection
33	19.10.05	13:35	46 11.800	-4 07.200	34	14:58	11.8	10	2	4	2	200, 500, 1000, 5000	0.97/0.00/0.00	-4.10/0.35/8.50	downslope
34	19.10.05	14:58	46 03.400	-4 19.100	35	16:19	12.2	10	2	4	2	5000	0.97/0.00/0.00	-4.10/0.35/8.50	downslope
35	19.10.05	16:19	45 55.100	-4 32.000	36	16:38	2.6	10	2	4	2	5000	0.97/0.00/0.00	-4.10/0.35/8.50	connection
36	19.10.05	16:38	45 53.300	-4 29.300	37	17:44	12.0	10	2	4	2	5000	0.97/0.00/0.00	-4.10/0.35/8.50	upslope
37	19.10.05	17:44	46 01.800	-4 17.200	38	18:52	12.2	10	2	4	2	5000	0.97/0.00/0.00	-4.10/0.35/8.50	upslope
38	19.10.05	19:04	46 11.600	-4 06.700	39	20:22	12.2	10	2	4	2	5000	0.97/0.00/0.00	-4.10/0.35/8.50	downslope
39	19.10.05	20:22	46 01.800	-4 17.200	40	21:40	12.0	10	2	4	2	5000	0.97/0.00/0.00	-4.10/0.35/8.50	downslope
															Location 2b (grid)
40	19.10.05	21:40	45 53.300	-4 29.300	41	22:11	4.5	10	2	4	2	5000	0.97/0.00/0.00	-4.10/0.35/8.50	connection
41	19.10.05	22:11	45 54.700	-4 35.500	42	22:45	5.5	10	2	4	2	5000	0.97/0.00/0.00	-4.10/0.35/8.50	survey of the grid
42	19.10.05	22:45	45 52.800	-4 42.900	43	23:03	2.1	10	2	4	2	5000	0.97/0.00/0.00	-4.10/0.35/8.50	"
43	19.10.05	23:03	45 50.800	-4 41.800	44	23:36	5.6	10	2	4	2	5000	0.97/0.00/0.00	-4.10/0.35/8.50	"
44	19.10.05	23:37	45 52.700	-4 34.300	45	00:05	2.9	10	2	4	2	5000	0.97/0.00/0.00	-4.10/0.35/8.50	"
45	20.10.05	00:05	45 50.000	-4 35.800	46	00:44	6.4	10	2	4	2	5000	0.97/0.00/0.00	-4.10/0.35/8.50	"

Waypoint (begin of profile)	Date	Time UTC	Latitude	Longitude	Waypoint (end of profile)	Time (end)	Distance [nm] between WP	Survey Speed (schedule)	Gyro/Motion Sensor#	Frequency [kHz]	Number of Periods	Range [m]	Position of PARASOUND Transducer (x/y/z)	Position of Motion Sensor (x/y/z)	Comment
46	20.10.05	00:44	45 56.000	-4 38.900	47	01:01	2.1	10	2	4	2	5000	0.97/0.00/0.00	-4.10/0.35/8.50	"
47	20.10.05	01:01	45 55.220	-4 41.770	48	01:38	6.3	10	2	4	2	5000	0.97/0.00/0.00	-4.10/0.35/8.50	WP 48: end of grid survey
															From Loc. 2b to station at WP 49 and back to Canyon de Noirmoutier
48	20.10.05	01:38	45 49.300	-4 38.500	~49	06:50		10	2	4	2	5000	0.97/0.00/0.00	-4.10/0.35/8.50	leaving towards station at WP 49; standby on station
~49	20.10.05	14:51	45 44.933	-5 31.596	50	15:25	5.1	10	2	4	2	5000	0.97/0.00/0.00	-4.10/0.35/8.50	leaving station
50	20.10.05	15:25	45 40.000	-5 30.000	51	19:16	39.3	10	2	4	2	5000	0.97/0.00/0.00	-4.10/0.35/8.50	
51	20.10.05	19:16	45 44.000	-4 34.000	52	20:09	9.9	10	2	4	2	5000	0.97/0.00/0.00	-4.10/0.35/8.50	connection
															Canyon de Noirmoutier
52	20.10.05	20:09	45 53.300	-4 29.300	53	21:21	12.0	10	2	off	off	off			Parasound off
53	20.10.05	21:21	46 01.800	-4 17.200	~54	22:28	12.2	10	2	off	off	off			"
54	20.10.05	22:39	46 11.600	-4 06.700	55	00:05	12.2	10	2	off	off	off			"
55	21.10.05	00:05	46 01.800	-4 17.200	56	01:24	12.0	10	2	off	off	off			"
56	21.10.05	01:24	45 53.300	-4 29.300	57	01:50	4.5	10	2	off	off	off			"
															Location 2b (grid 2x)
57	21.10.05	01:50	45 54.700	-4 35.500	58	02:30	5.5	10	2	off	off	off			Parasound off
58	21.10.05	02:32	45 52.800	-4 42.900	59	02:45	2.1	10	2	off	off	off			"
59	21.10.05	02:47	45 50.800	-4 41.800	60	03:15	5.6	10	2	off	off	off			"
60	21.10.05	03:29	45 52.700	-4 34.300	61	03:52	2.9	10	2	off	off	off			"
61	21.10.05	04:06	45 50.000	-4 35.800	62	04:48	6.4	10	2	off	off	off			"
62	21.10.05	05:01	45 56.000	-4 38.900	63	05:23	2.1	10	2	off	off	off			"
63	21.10.05	05:37	45 55.220	-4 41.770	~64	06:16	6.3	10	2	off	off	off			"
64	21.10.05	08:18	45 49.300	-4 38.500	65	09:02	6.3	10	2	off	off	off			"

Waypoint (begin of profile)	Date	Time UTC	Latitude	Longitude	Waypoint (end of profile)	Time (end)	Distance [nm] between WP	Survey Speed (schedule)	Gyro/Motion Sensor#	Frequency [kHz]	Number of Periods	Range [m]	Position of PARASOUND Transducer (x/y/z)	Position of Motion Sensor (x/y/z)	Comment
65	21.10.05	09:02	45 55.220	-4 41.770	66	09:34	2.1	10	2	off	off	off			"
66	21.10.05	09:34	45 56.000	-4 38.900	67	10:13	6.4	10	2	off	off	off			"
67	21.10.05	10:13	45 50.000	-4 35.800	68	10:39	2.9	10	2	off	off	off			"
68	21.10.05	10:40	45 52.700	-4 34.300	69	11:20	5.6	10	2	off	off	off			"
69	21.10.05	11:20	45 50.800	-4 41.800	70	10:40	2.1	10	2	off	off	off			"
70	21.10.05	11:41	45 52.800	-4 42.900	71	12:14	5.5	10	2	off	off	off			"
															Leaving for Vigo
71	21.10.05	15:58	45 54.700	-4 35.500				10	2	4	2	5000	0.97/0.00/0.00	-4.10/0.35/8.50	Parasound on
79	21.10.05	?	45 39.100	-4 27.600	80	21:30		10	2	4	2	5000, 10000	0.97/0.00/0.00	-4.10/0.35/8.50	end of profile 21.30
-	22.10.05	07:00	44 33.000	-7 47.600					2	4	2	5000		"	data recording off

3.2 Test of the ELAC NDS3070 collision avoidance sonar in the Bay of Biscay

Saad El Naggar[1)], Ekkehard Schütt[1),)] Monika Breitzke[1)], and Rüdiger Schönwetter[2)]
not on board: Olaf Boebel[1)]

[1)]Alfred-Wegener-Institut
[2)]L3 Communications ELAC Nautik GmbH

Objectives
To mitigate the acoustic impact of seismic surveys on the marine environment tools are needed. They are still being developed and will allow to monitor safety radii around and beneath RV Polarstern within which at least some species of marine mammals are likely to be subject to behavioural disturbance and/or physical damage due to the received sound pressure levels (e.g. temporary or permanent threshold shifts).

According to the regulations defined by the National Marine Fisheries Service, USA the 180 dB_{RMS} sound pressure level is presently considered to be the threshold above which marine mammals might possibly experience temporary threshold shifts.

Internationally, three methods for monitoring the safety radii are applied: (1) Visual monitoring, (2) passive acoustic monitoring, (3) active acoustic monitoring. For RV *Polarstern* visual monitoring is realized by binoculars and for limited sectors by infrared cameras. For passive acoustic monitoring a 600 m long streamer consisting of three 10 m long sections of 5 hydrophones has been developed. This test study is intended to be a first step towards the development of an active acoustic monitoring system, which has the advantage that marine mammals neither have to be visible at the sea surface nor have to vocalize to be detected, as is necessary for visual or passive monitoring systems.

The ELAC NDS3070 collision avoidance sonar has been selected as a potential first prototype for an active whale detection sonar for RV *Polarstern*. In its active panorama mode the ELAC NDS3070 collision avoidance sonar operates with 30 kHz and allows to monitor a spherical sector of 360° horizontal and 26° vertical angle (from sea surface) around the ship. Assuming a detection probability of 90% and a false alarm rate of 0.5 % theoretical computations show that an object with a target strength of -6 dB can be detected to a distance of up to 1,500 m (under ideal sea and velocity conditions). A value of -6 dB was chosen because it is approximately the minimum target strength of a small whale hit at its head or tail by sound waves. To test this active sonar under "real" conditions the sonar head was installed in the moon pool and sonar signals were generated and received by mobile transmission and receiving cabinets brought onboard RV *Polarstern* for this study.

Objectives were:
- to test if such sonar systems can generally be used for marine mammal detection in the presence of the rather loud background noise of RV *Polarstern*,

- to determine the detection ranges for an object of known target strength under the "real" environmental conditions prevailing during the test study in the Bay of Biscay.

Sea trials
On 16 October 2005, 21.00 h, the sonar tests were started in the Bay of Biscay at location 46° 24' N; 05° 55'W, and were completed on 18 October 2005; 06:00 h at location 46° 17' N; 05° 58' W. A sound velocity profile in the test location was measured by using a CTD-system down to 500 m water depth. This sound velocity profile was used for the theoretical computation of detection ranges under the actual environmental conditions. Subsequently, an object (triple mirror) with a calibrated target strength of -6 dB was deployed and positioned in a certain water depth of 70 m and 170 m respectively by appropriate buoys and weights. The target was acoustically measured by various angles and distances using a spiral-shaped course so that its detect ability can be verified as function of angle and range (Fig. 3.11 and Fig. 3.12). This experiment was repeated for different ship's speeds and different acoustic noise produced by other active sonars like hydrosweep, parasound, fishery sonar and Dolog. The sea trial was also repeated for different water depths (70 m, 170 m) of the triple mirror.

The position of the triple mirror was recorded by using a recording GPS-receiver fixed on the buoy. The distance between ship and target was acoustically measured and will be later calculated by using the position data from the target and the ship.

First results
The tests have shown that the used sonar system is able to acoustically detect a target of –6 dB in the horizontal range between 200 and 1,000 m and in the vertical range between 50 and 200 m with both frequencies 30 and 70 kHz. The detect ability was strongly affected by the noise produced by other active sonars. The system tested here is able to detect objects, like whales, in the mentioned range and if a narrow band filter (± 0,5 kHz) is used by the receiver units.

Figure 3.13 shows a screen shoots of target and ship noise produced by propeller and other machineries.

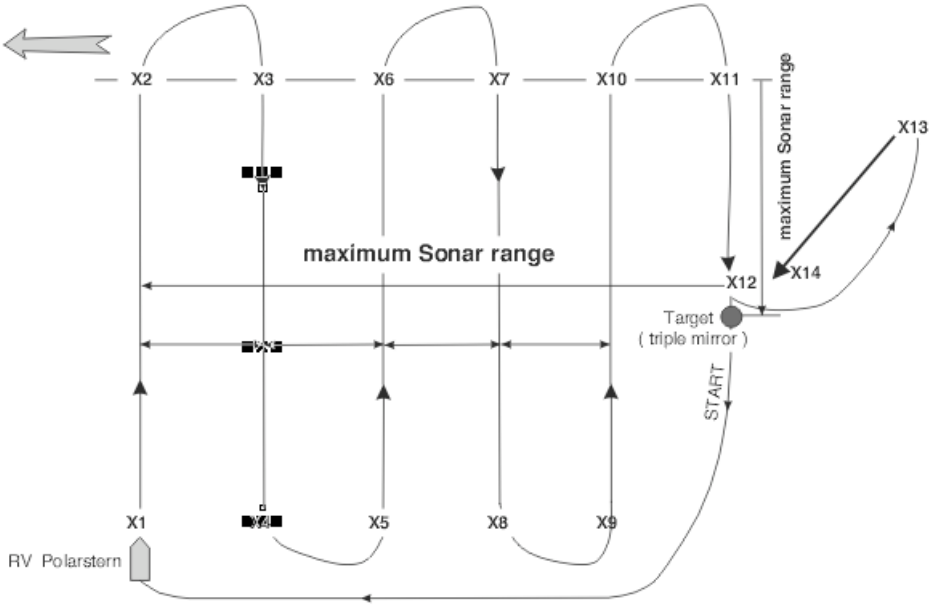

Fig. 3.11: The first test scenario. Course track for RV Polarstern approaching the calibration target (triple mirror) by various angles

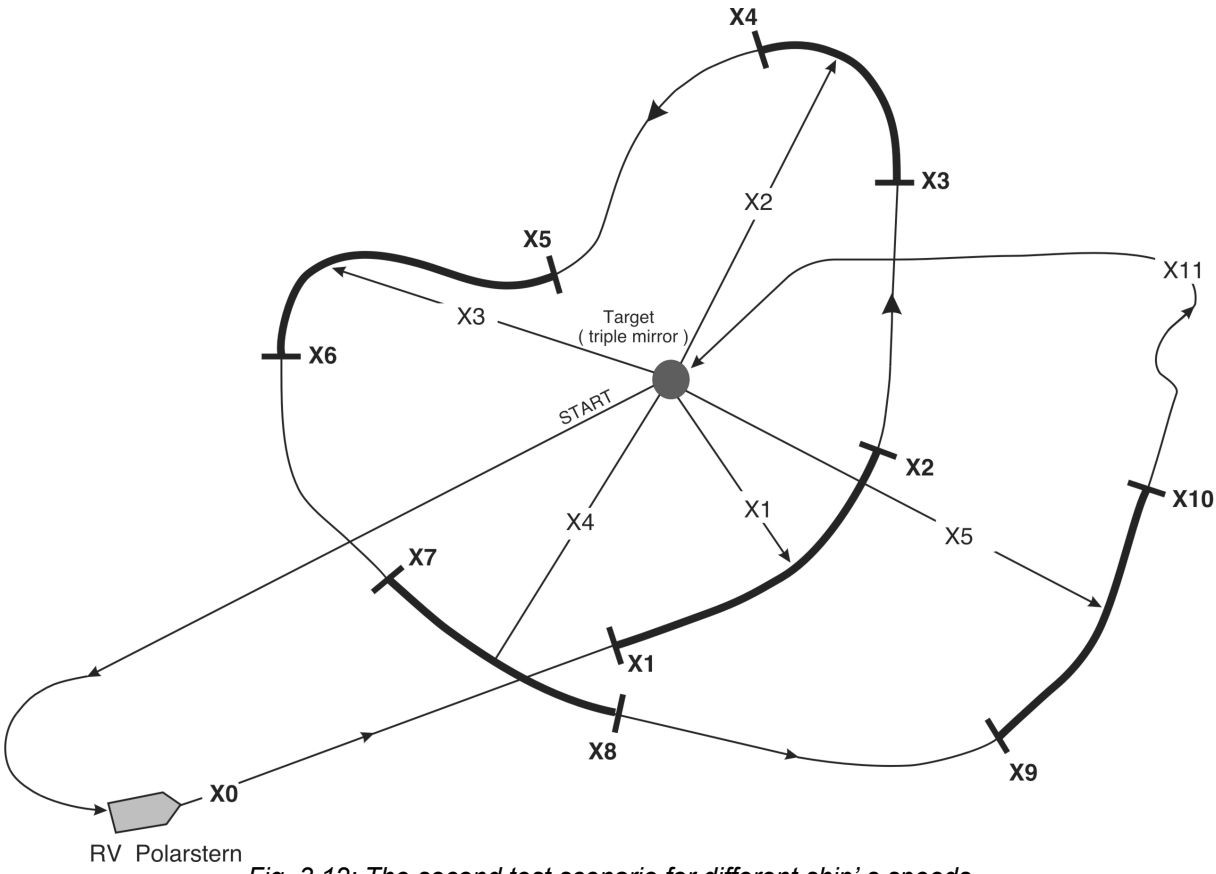

Fig. 3.12: The second test scenario for different ship' s speeds

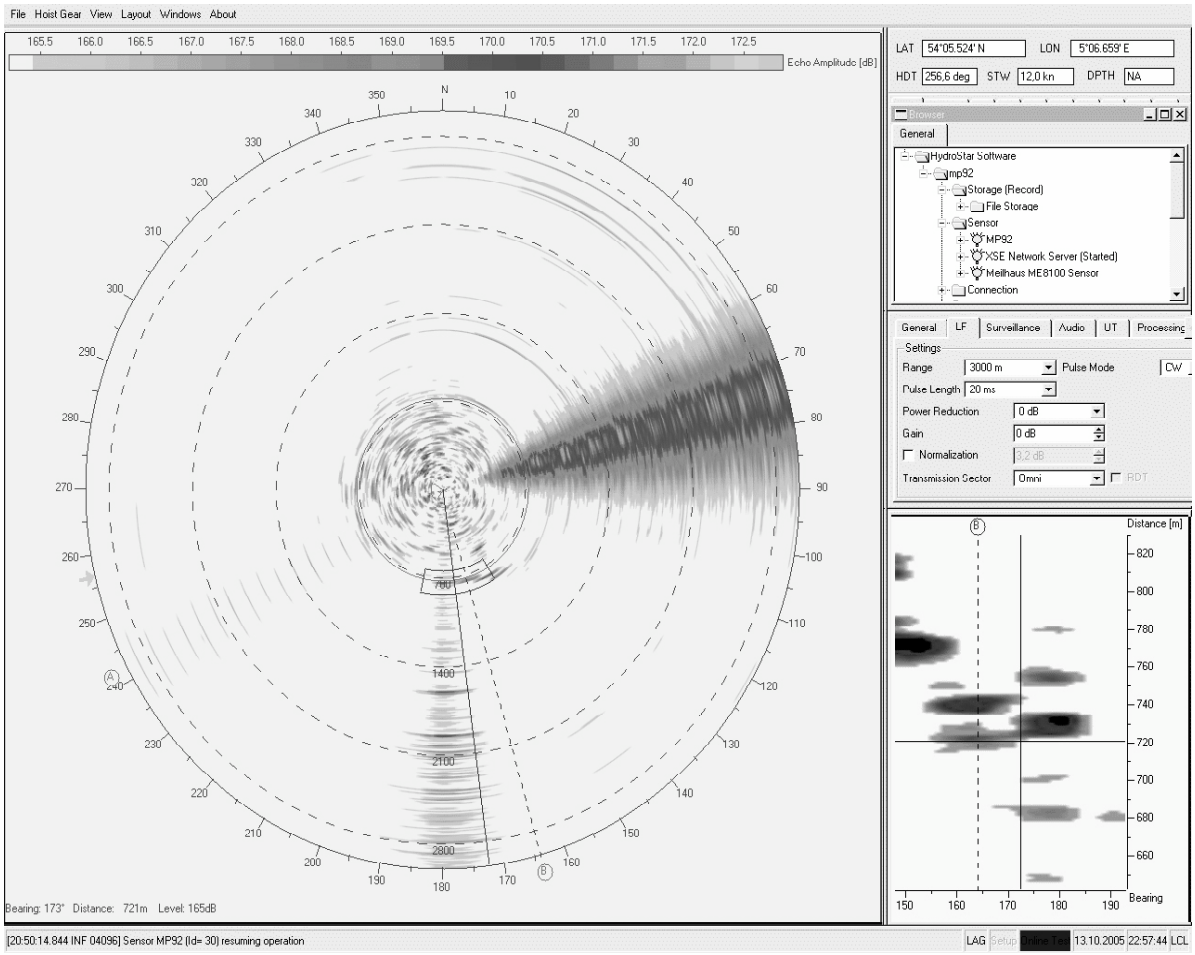

Fig. 3.13: Shows a screen shot of target and ship noise produced by propeller and other machineries

4. TRACER STUDIES

4.1 GEOTRACES pilot study

Michiel Rutgers van der Loeff[1)], Ingrid Vöge[1)], Walter Geibert[1)], Delphine Dissard[1)], Martin Frank[2)], Peter Croot[2)], Christian Schlosser[2)], Sebastian Steigenberger[2)], Jörg Rickli[3)], Jan Scholten[4)], Janine Gastaud[4)], Ursula Hennings[5)], Timo Daberkow[6)], Corinna Harms[6)]
not on board: Gereon Budéus[1)], Jelle Bijma[1)], Streu[2)], Pohl[5)], Balzer[6)]

[1)]Alfred-Wegener-Institut
[2)]IFM-GEOMAR
[3)] ETH Zürich
[4)]MEL Monaco
[5)]IOW
[6)]Universität Bremen

Objectives of the GEOTRACES programme

Our knowledge of ocean circulation and global biogeochemical cycles has a strong basis in the GEOSECS programme, conducted in the 1970s. The ensuing development of analytical techniques now allows studies of trace elements and their isotopes (TEIs) at concentration levels and at space and time resolution that were inconceivable during the GEOSECS era. These developments include clean sampling, sensitivity, miniaturisation, automation, *in-situ* techniques or entirely new detection principles. This means that detailed mapping can be obtained of far more tracers including their isotopic composition with the potential to provide unique insights into a wide range of oceanic processes. This opportunity was the stimulus of the recently inaugurated GEOTRACES programme. This programme is endorsed by SCOR, which has recently also approved the GEOTRACES science plan (http://www.geotraces.org/).

The two primary objectives for the GEOTRACES programme are:

- to determine global distributions of selected TEIs in the ocean; and
- to evaluate the oceanic sources, sinks, and internal cycling of these TEIs and thereby characterize more completely their global biogeochemical cycles.

The central point in the concept of GEOTRACES is to measure a wide set of tracers in parallel. Only if the tracers are measured in the same water masses we can be confident to use them as mutual support in the interpretation. The radionuclides can help to explain the history of particle flux of the water mass, the trace metals can track the history of dust inputs and the REE and soluble radionuclides trace the origin of the water masses. This integrating concept, as it can now be applied due to methodological advances, has not been fully used in previous studies.

The Atlantic transit of ANT-XXIII/1 served as a pilot study for such an integrated approach. While this expedition could not yet fulfil the GEOTRACES objective to obtain full-depth multi-tracer transects across ocean basins, we could already learn a great deal from surface transects with a limited number of deep casts. Surface waters are, by nature, the part of the water column that is expected to experience the

greatest temporal variability. We passed water masses characterized by very different inputs: the upwelling area off West Africa, dust inputs off Sahara and the very low inputs in the South Atlantic gyre, and we could measure the effect of these variable inputs on a wider range of tracers than it has been possible before.

4.1.1 Hydrography

Kerstin Hans,
Alfred-Wegener-Institut
not on board: Gereon Budéus, Alfred-Wegener-Institut

Work at sea
CTD and water sampler
Routinely, a CTD/water-sampler system with 24 bottles was used on stations. When more than 24 samples were requested, additional casts had to be performed. To reflect this in the data file name, the last digit refers to the cast number (starting with 0 for the first cast on a station). The Niskin bottles contained a volume of 12 l. The instruments used were a SBE 911+ with duplicate temperature and conductivity sensors, and additional sensors connected to the A/D input. These additional sensors were for oxygen concentrations, transmission, Chlorophyll fluorescence, and Gelbstoff fluorescence.

The sensor listing reads:

pressure, S/N 68997
temperature, primary, SBE3+, S/N 2460
temperature, secondary, SBE3+, S/N 2417
conductivity, primary, SBE4, S/N 2054
conductivity, secondary, SBE4, S/N 2055
oxygen, SBE43, S/N 48
transmissometer, CST_267DR
chlorophyll fluorescence, Dr. Haardt backscat 1996
ys fluorescence, Dr. Haardt backscat S/N 8070

The entire system worked faultlessly, with the restriction known from the previous cruise that the oxygen sensor was drifting so that absolute values are not correct. No attempt for *in-situ* calibrations has been made on board.

The CTD data have been processed and plotted immediately after each station in order to obtain a fast quality control. No problems have been encountered. Sea-Bird's following routines were used: datcnv, split, celltm, filter (low pass on p, 150 ms), loopedit, binavg (1 dbar bins). Sensor alignment was performed by the Deck Unit with standard advance on C. The subsequent processing and plotting was done on a SUN workstation under Solaris using proprietary routines. The plotted differences between the temperature and conductivity sensor pairs revealed negligible calibration differences and time drifts. The operator on board was K. Hans, data responsibility at AWI is with G. Budéus.

On all major stations samples of the water column were collected for nutrient analysis. These samples were poisoned with $HgCl_2$ and will be analysed at AWI (G. Kattner).

4.2 Controlling factors of the behaviour of natural Thorium, lead and Polonium isotopes in seawater

Rutgers van der Loeff, Ingrid Vöge, Walter Geibert,
Alfred-Wegener-Institut

Work at sea
Particle-reactive trace elements are removed from the water column by adsorption on sinking particles. The efficiency of this scavenging process depends on the particle rain rate and particle composition. The cruise track offered the opportunity to study the scavenging over a wide range of scavenging conditions.

Scavenging of ^{234}Th
^{234}Th is produced by decay of ^{238}U in seawater and decays with a half life of 24.1 days. Scavenging causes a depletion of ^{234}Th with respect to ^{238}U in surface waters. We expected to find a pattern of depletion that mirrors the combined effect of varying particle flux and composition along the cruise track. We have measured ^{234}Th with two techniques: The classical technique requires the filtration of 20-l samples taken from the ship's seawater supply to determine the particulate ^{234}Th content and the subsequent co-precipitation of ^{234}Th on MnO_2 in the filtrate. This technique was used in coordination with the trace metal sampling (Table 1.1).

In addition we have tested a new automated technique. Five-liter samples of the ship's seawater supply are automatically filtered and filled into a container where reagents are added to form a MnO_2 precipitate. After a period of at least one hour, the precipitate is filtered over a second filter. The filter is washed with distilled water, dried and beta counted on board ship. Quartz fiber filters are used throughout because they have the lowest beta background. The new automated procedure uses 5 cm diameter filter units that are counted in a 10-position beta counter. As the background count rate of this counter on board ship was high (around 1 cpm) and rather variable, we decided to abandon the first filtration and measure total ^{234}Th exclusively.

Preliminary results
The results (Fig. 4.1) show the general validity of the automated procedure. Negligible scavenging is found around 30°N and around 5°N. Some removal is found in the intermediate zone, 10 - 20 °N and in the Biscay area. The strongest removal is found south of the equator in the South Atlantic Gyre which was apparently more productive than we had expected.

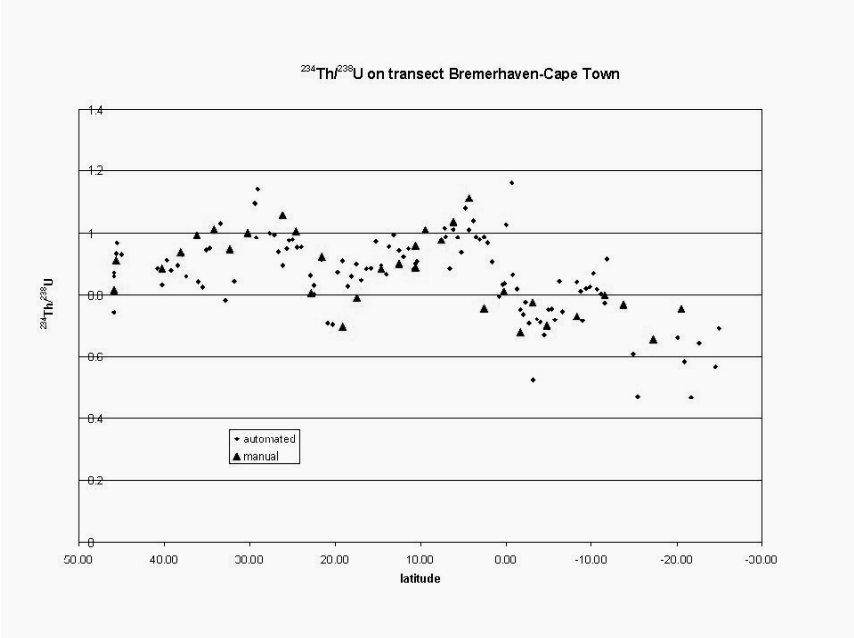

Fig. 4.1: Distribution of total $^{234}Th/^{238}U$ in surface waters as measured with the 20-l technique (triangles) and with the automated 5-l procedure (dots)

In parallel to the ^{234}Th measurements we also took samples to determine the distribution of ^{210}Pb and ^{210}Po in surface waters.

Enrichment of inorganic colloids by means of a large volume centrifuge

The colloidal size fraction of seawater, filling the gap between particulate (e.g. algae) and truly dissolved substances (e.g. salt), has been a target of marine geochemistry for many years. A focus of previous investigations had been placed on organic components of the colloidal fraction. Inorganic colloidal substances were not considered to represent an important component of sea water. In order to screen seawater for potential inorganic colloids, we have enriched the smallest possible size fractions from large volumes of sea water in order to obtain a sufficient amount of material for analysis. This was accomplished by a continuous flow centrifuge that had been connected to the seawater supply. Particles and colloids from about 1 m^3 of seawater at 18 locations were collected at a flow rate of ~350 l/hour at about 16000 x g. The sample collection is suitable for trace element analysis, as the inlet system and the collecting surface is made from titanium or teflon® only.

The given acceleration should be sufficient to efficiently collect particles much smaller than 2 µm in diameter, dependent on their density. This size fraction is expected to contain clay minerals, which would be overlooked in conventional analytic techniques. In order to identify these clay minerals (if present), analysis will include electron microscopy and the measurement of specific elements (Ti, ^{232}Th, Si). Sampling problems were arising from the surface of the teflon® sheets, that led in some cases to a potential loss of water drops from the upper part of the centrifuge rotor, where the smalles particles must be expected.

Experimental study of Th adsorption onto particles

In an experimental study, the adsorption of Thorium onto clay particles was compared in filtered (0.2 µm) and ultrafiltered (<10000 Da, Vivaflow 200 PES membrane) surface water and deep sea water from the Bay of Biscay and from station PS69/14 (southern dust station). Small amounts of Thorium together with a clay mineral standard (SW-y2 Montmorillonite from clay minerals repository, @ 1 mg/l) were added to these water types to test the hypothesis whether the natural colloidal composition of seawater is affecting the sorption kinetics of Th. For comparison, the same water types were also monitored without particles added. Both experiments were lasting five days, and almost all 300 subsamples (particulate and dissolved separately) could be measured on-board with the seagoing Risoe beta counter GM25-5. Preliminary results for the Bay of Biscay water indicate that the absence of colloids is favouring adsorption of Th to the walls of the vessel in both deep and surface water, as seen in poor recoveries for ultrafiltered water (Fig. 4.2 a, b).

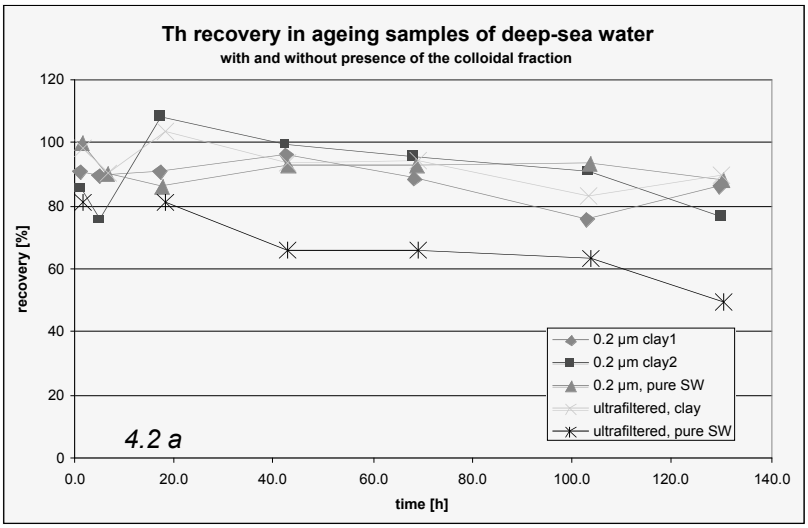

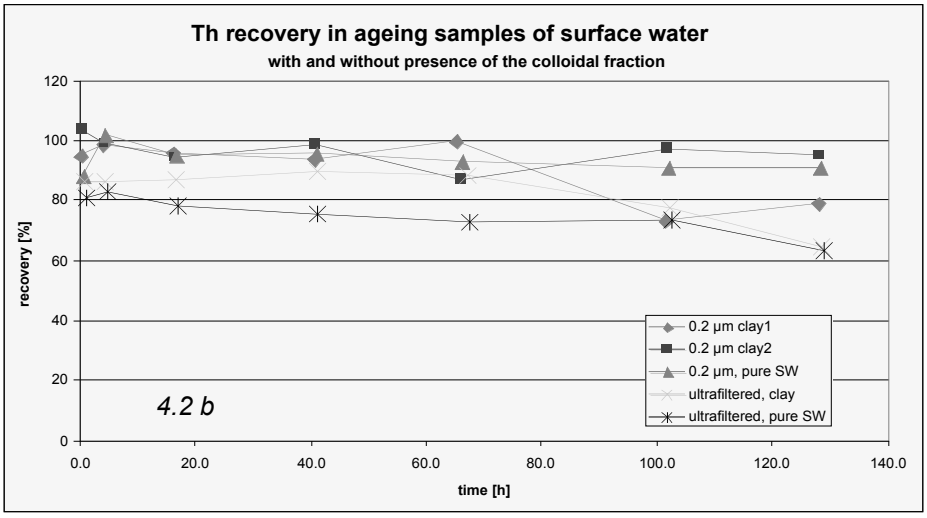

Fig. 4.2: Temporal evolution of Th recovery during in-vitro experiments with water from the Bay of Biscay in deep sea (upper panel, Fig. 4.2 a) and surface water (lower panel, Fig.4.2 b). Errors are estimated to be 3 % (1 σ).

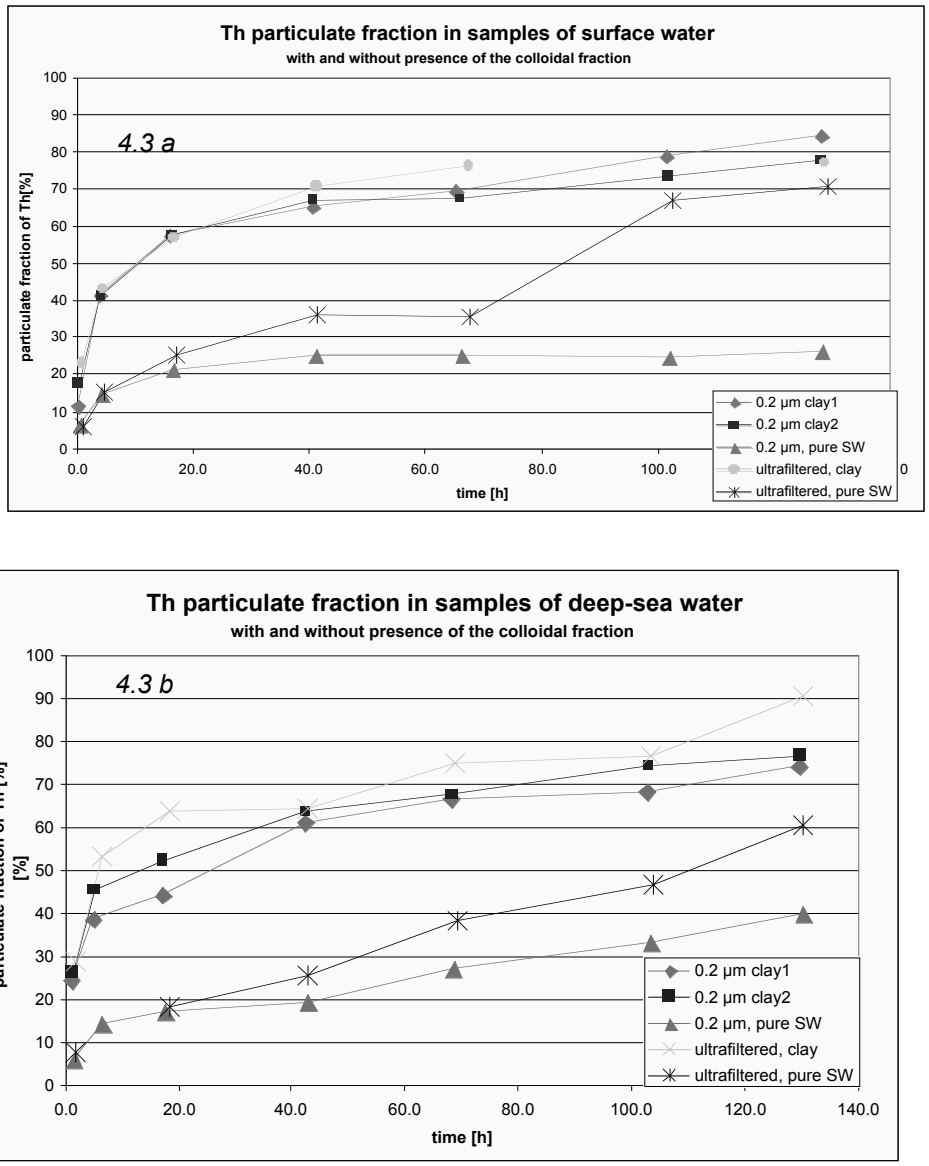

Fig. 4.3: Temporal evolution of the particulate fraction of ^{234}Th during in-vitro experiments with water from the Bay of Biscay in deep sea (upper panel, Fig.4.3 a) and surface water (lower panel, Fig. 4.3.b). Errors are estimated to be 3 % (1 σ).

Particulate fractions of Th are not zero, not in filtered and not even in ultrafiltered seawater (Fig. 4.3). This must be due to the new formation of particles from the colloidal or dissolved pool of substances. Particle formation is not even decreased in ultrafiltered water. However, a trend can be seen that later adsorption of Th onto particles is favoured by previous ultrafiltration. Together with the observations from the recoveries, it can be preliminarily concluded that colloids play a role in keeping Th apparently dissolved.

Sampling of dissolved organics
At five stations, the dissolved organic fraction was enriched from 36-48 l of filtered seawater on PPL solid phase extraction cartridges. The samples were prepared for later analysis of DOC composition via FT-ICR-MS (B. Koch, AWI). Additionally, subsamples (and replicates) were taken for the determination of DOC concentrations.

Cooperation with particle optics
During the expedition, cooperations with groups investigating optical properties of seawater were arising. Studies of angular scattering in seawater due to colloids and small particles accompanying the Th sorption experiments were conducted by D. Stramski on a daily basis during the sorption experiment with water from the dust station. The combination of chemical and optical monitoring of seawater may turn out to be a powerful tool for colloid and small particle characterization.

Studies on light absorption in seawater due to humic substances were performed by R. Röttgers. Comparisons between filtered, ultrafiltered and organics-depleted seawater (by PPL extraction) were providing some insights into possible effects of the different fractions on light absorption in the sample.

4.3 Intercomparison of techniques for the analysis of TH-230, rare earth elements and the isotopic composition of ND

Michiel Rutgers van der Loeff[1)], Ingrid Vöge, Walter Geibert[1)], Martin Frank[2)], Jörg Rickli[3)], Jan Scholten[4)],

[1)]Alfred-Wegener-Institut
[2)]IFM-GEOMAR
[3)] ETH Zürich
[4)] Marine Environment Laboratory (MEL), Monaco

not on board: Andersson, Stockholm; Jeandel, LEGOS-Toulouse; Henderson, Oxford; Zhong, Quingdao, China

Objectives
One of the objectives of this expedition was to provide opportunities for the development of appropriate sampling and analytical techniques for the GEOTRACES programme. We selected station 69/21 in the Angola Basin (11°52'S, 2°31'W) to collect two rosette casts at mid-water depth (2,000 m) purely for intercomparison purposes. One cast was devoted to intercomparison of ^{230}Th and ^{231}Pa techniques, a second cast for the intercomparison of techniques for the analysis of rare earth elements and the isotopic composition of Nd.

Work at sea
Sampling of ^{230}Th in the water column
The measurement of ^{230}Th and particularly ^{231}Pa in the water column is still challenging because the concentrations of these isotopes in sea water are very low (down to fg/L).

Within the last few years, a dramatic change in measurement techniques has taken place, from radiometrical determination towards mass spectrometry. As a

consequence, the main problems in measurement have shifted. Whereas radiometric determinations were requiring large volume samples (several hundreds of litres), typically obtained by *in-situ* pumps, the mass spectrometric approach only requires about 5 l (^{230}Th) to 20 l (^{231}Pa), obtained from Niskin bottles. Radiometric data were in most cases not affected much by blank contributions. This has changed with the low volumes that are used for mass spectrometry - clean sample processing is now crucial for reliable mass-spectrometric ^{230}Th and ^{231}Pa data.

The quick development in measurement techniques within the last years has led to a number of individual approaches in the analysis, typically determined by the requirements of the different groups (e.g., which other isotopes are to be analyzed), and by individual experience.

In order to compare the effects of different sample preparation methods, we took 24 samples of 2 l volume from deep-sea water (Station 69/21, 2,000 m). From these samples, ^{230}Th will be measured according to different sample preparation protocols. The results will provide information about the most suitable ways for Thorium analysis. Additionally, a series of 10 l containers were filled with the same sample for an intercomparison of ^{230}Th and ^{231}Pa analysis between different laboratories. Using this approach, the effects of different treatments during sampling, storage, and purification of Thorium when analysing a single deep water sample for ^{230}Th by means of mass spectrometry can be quantified.

Furthermore, a test batch of Eichrom MnO_2-resin was applied to enrich trace elements from 20 l of seawater. If this method proves to be successful, this would open a possibility to analyze a wider spectrum of trace elements on a single sample in the near future.

Isotopic composition of Neodymium

Fifteen rosette bottles were collected in one cast at 2,000 m depth in the Angola Basin (station 69/21) and filled into cubitainers. The combined sample was filtered with a peristaltic pump over 0.45 µ nuclepore filters and the filtrate was filled into cleaned 10 - l bottles and acidified with suprapur HCl for analysis of Nd isotopic composition. A similar sampling of surface water was done by collecting water from the towed fish. A special fish sample (number 41) was collected for this purpose on 10 November 2005 at 14° 21'S, 0°32'W, salinity 36.49, temperature 20.89°C. These samples were filtered and acidified as the deep-water sample. Each of the following participating labs will obtain six 10 - l samples, three from 2,000 m depth and three from surface water: LEGOS Toulouse (Catherine Jeandel), IFM-GEOMAR Kiel (Martin Frank), Laboratory of Isotope Geology Stockholm (Per Andersson), and AWI Bremerhaven (Michiel Rutgers van der Loeff).

4.4 Distribution of anthropogenic and natural radionuclides in surface waters of the East Atlantic

Jan Scholten, Jan Gastaud,
Marine Environment Laboratory (MEL), Monaco

Objectives

Full oceanographic transects of natural and anthropogenic radionuclides through the Atlantic Ocean are sparse. The investigations of MEL during the *Polarstern* cruise aim at a better understanding of the distribution of natural isotopes (^{230}Th, ^{232}Th, ^{231}Pa, ^{210}Po, ^{210}Pb) and anthropogenic radionuclides (such as ^{90}Sr, ^{137}Cs, plutonium isotopes, americium, ^{99}Tc, ^{129}I) in surface waters in relation to aeolian deposition, hydrography, bioproductivity and particle scavenging. More specifically the investigations focused on the following objectives:

- gradients in the anthropogenic radionuclide concentrations between the North and South Atlantic;
- the effect of bioproductivity and dust supply on anthropogenic radionuclide distribution;
- relation between the distribution of anthropogenic radionuclides and the spreading of deep water masses in the Cape Basin;
- ^{232}Th and ^{210}Pb in surface waters and their potential as tracers for aeolian dust deposition;
- distribution of ^{230}Th and ^{232}Th in particulate (>0.45 µm, >0.2 µm), colloidal (>10 kDa) and "truly" dissolved (< 10 kD) phases;
- the role of surface water mass mixing on the ^{230}Th and ^{231}Pa distribution in shallow water;
- aeolian deposition of natural and anthropogenic radionuclides;
- intercalibration of analytical procedures for the determination of radionuclides.

Work at sea

Sampling during ANT-XXIII/1 focused on surface as well as on deep waters. For the determination of anthropogenic radionuclides 300 l of surface water was sampled daily using the "Klaus Pump" between Vigo and the Cape Basin. The water was filtered (size 0.45 µm) and filled in two separate precipitation tanks followed by several chemical separation procedures which pre-concentrate plutonium isotopes, ^{90}Sr and ^{137}Cs from the seawater. The resulting precipitates were collected in 20 to 30 l plastic containers for the transport to the home lab. For measurements of ^{129}I, ^{3}H and ^{14}C, 1 l of water was filled in three separate bottles.

A parallel sampling for anthropogenic radionuclides was conducted using a cartridge filtration system. This system consisted of one Cuno pre-filter (1 µm pore size) followed by three cartridges impregnated with MnO_2. About 1000-1600 l of water was allowed to pass over these cartridges. These large volumes are necessary to allow for the measurements of ^{242}Am and ^{238}Pu which occur in very low concentrations. For the determination of anthropogenic radionuclides in deep-water samples were collected in the Cape Basin. In five depth levels up to 80 l were obtained and filled in cub containers for further analyses in the home lab.

For determination of natural radionuclides (^{210}Po/^{210}Pb (selected), ^{230}Th, ^{232}Th, ^{231}Pa (selected)) further sampling of surface waters between 45°N and 8°S was conducted using the fish and/or snorkel. A volume of 50 l was filtrated through 0.45 µm and 0.2 µm sized filters. The colloidal phase was separated using Vivaflow ultrafiltration. The fraction < 10 KDa was pre-concentrated for further analyses of ^{230}Th and ^{232}Th isotopes in the home lab.

At hydrocast stations "Dust North" (PS69/011), "Dust South" (PS69/014) and at equatorial upwelling (PS69/018) the upper (≤ 1,000 m) water column was sampled in 10 depth levels. A volume of about 40-50 l was obtained for measurements of natural radionuclides (^{232}Th, ^{230}Th, ^{231}Pa, ^{210}Po/^{210}Pb). Particulate matter (>0.45 µm) was collected by filtration of about 30 l; and the filtrate was processed for further ^{210}Po/^{210}Pb analyses in the home lab. In the Angola Basin and in the Cape Basin additional sampling of deep waters for determination of Thorium isotopes and ^{231}Pa was conducted.

Expected results
The results obtained during RV *Polarstern* ANT-XXIII/1 are expected to provide a baseline for radionuclide distributions in the East Atlantic and new insights about the behaviour of radionuclides along gradients of bioproductivity and atmospheric deposition.

4.5 Radiogenic (Hafnium-Neodymium), cosmogenic (^{10}Beryllium) and stable (Silicon) isotopes in Atlantic seawater

Martin Frank[1)] [1)]IFM-GEOMAR
Jörg Rickli[2)] [2)]ETH Zürich

Objectives
As a contribution to the evolving international GEOTRACES programme, which is aimed at a better understanding of the biogeochemical cycling of trace metals in the ocean, sampling for measurements of four different dissolved metal isotope systems was performed.

Radiogenic (Hafnium-Neodymium) isotopes
The Sm/Nd and Lu/Hf isotope systems vary largely between continental lithologies due to fractionation processes in the earth's mantle during the formation of the continental crust. Thereby the elements Nd and Hf preferentially partition into the crust whereas Sm and Lu tend to remain in the mantle. Radioactive ^{147}Sm and ^{176}Lu slowly decay into ^{143}Nd and ^{176}Hf, respectively, with long half-lives on the orders of billions of years. These isotopes are expressed as ratios with primordial isotopes of the same element, which have never experienced any radiogenic ingrowth (^{144}Nd and ^{176} Hf). The crustal fractionation processes have led to differences in ^{143}Nd/^{144}Nd and ^{176}Hf/^{177}Hf in continental rocks, despite the very long half-lives of the parent isotopes. Old cratonic continental rocks, such as in Canada or Greenland have the

lowest (least radiogenic) isotope ratios (ε_{Nd} = -25 to -60 and ε_{Hf} = -50 to -80), whereas young mantle-derived rocks, such as around the Pacific, have the highest (most radiogenic) ratios (ε_{Nd} = +5 to +10 and ε_{Hf} = +10 to +20).

In order to have more handy numbers for these very small isotopic differences, the Nd isotope ratios are expressed as ε_{Nd} values:

$$\varepsilon_{Nd} = \frac{\frac{^{143}Nd}{^{144}Nd}sample - \frac{^{143}Nd}{^{144}Nd}CHUR}{\frac{^{143}Nd}{^{144}Nd}CHUR} x10000$$

where CHUR is the $^{143}Nd/^{144}Nd$ of the chondritic uniform reservoir (presently 0.512638). Analogous to Nd, Hf isotope ratios are given as ε_{Hf} values, with a $^{176}Hf/^{177}Hf$ for CHUR of 0.282169). These ratios can be measured precisely (0.2 to 0.5 ε_{Nd} and ε_{Hf} units) with modern mass spectrometry (Thermal Ionisation Mass Spectrometers (TIMS) or in the case of Hf isotopes exclusively with Multiple Collector Inductively Coupled Plasma Mass Spectrometers (MC-ICPMS)).

Both metals are transferred into the ocean via weathering processes such as riverine inputs, dust inputs, or leaching of shelf sediments, but these inputs are still quite poorly characterized and quantified. The residence times of Hf and Nd in seawater are on the order of 500 - 2000 years, which prevents complete homogenisation of the isotopic signatures, but at the same time allows for a long distance transport within particular water masses. Dissolved Nd isotopes in seawater have thus been used as quasi-conservative chemical tracers for ocean circulation and weathering inputs in the present and past ocean. Hf isotopes cannot yet be used reliably, mainly due to the extremely low concentrations in seawater between 0.1 and 1 pmol/l, which have until recently prevented isotopic measurements. The only available information for the Hf isotopic composition exists for deep waters and has been obtained from the isotopic composition hydrogenetic ferromanganese crusts, which incorporate trace metals from seawater druing growth. These results indicate that the Hf isotope compositions in seawater does not reflect the bulk isotopic composition of the rocks that they are weathered from but that for a given Nd isotope ratio the Hf isotope ratio is offset towards higher values (Fig. 4.4). This has been interpreted in terms of weathering effects (different minerals in rocks have different Hf isotope compositions and weather at different rates), which makes the combination of these two isotope systems a potentially powerful geochemical proxy for continental weathering in the present and past oceans. Clearly, however, a proof from combined Hf and Nd isotope measurements of seawater is required.

In addition, there are still large uncertainties as to the quantitative importance of dust inputs versus riverine supplies for the dissolved oceanic budgets of both Nd and Hf, which have prevented full exploitation of the potential of these isotope systems. Continental weathering inputs need to be better constrained and quantified in order to apply these systems reliably for example as quantitative proxies for past ocean circulation.

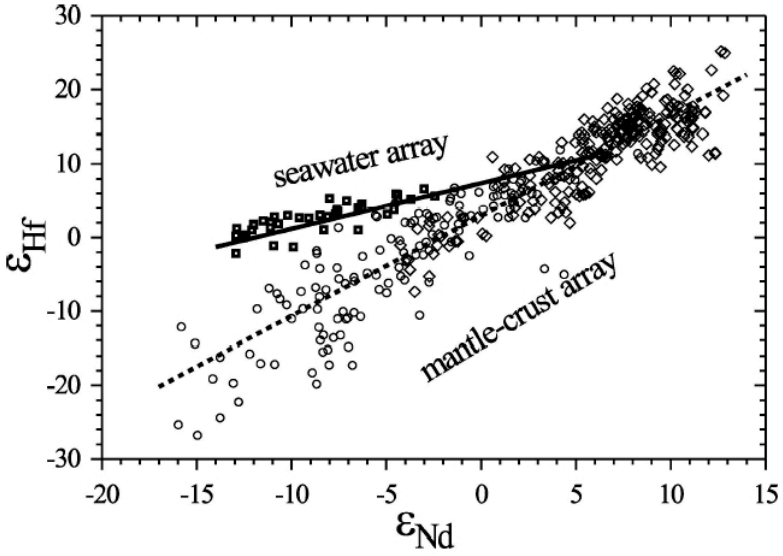

Fig. 4.4: ε_{Nd} versus ε_{Hf} for continental rocks (open circles), oceanic basalts (open diamonds), and surfaces of ferromanganese crusts and nodules (open squares) which represent today´s deep water isotope composition.

There have been two main scientific goals for this cruise:

a) The first Hf isotope analyses for Atlantic seawater

At ETH Zurich we have developed a method to extract and measure the Hf isotope composition from the same filtered 60 l seawater samples for deep waters and 120 - 140 l samples for surface waters, which have with lower concentrations. These large volumes of water are required because we need at least 5-10 nanograms of Hf in total for a reliable measurement of the Hf isotope composition. Neodymium and Be can be separated from the same samples and will then be available in comfortable quantities for high precision measurements. On this cruise we aimed to sample the main water masses characterizing the Atlantic meridional overturning circulation. We have collected samples from Mediterranean Outflow Water (MOW) at a water depth of 900 m in the Bay of Biscaye, from Eastern North Atlantic Deep Water (ENADW) at 2,500 m depth in the eastern North Atlantic, from Antarctic Intermediate Water (AAIW) at several locations in the equatorial Atlantic, the Angola Basin and the Cape Basin at depths around 800 m, NADW at depths between 2,300 and 4,500 m in the Angola Basin and the Cape Basin, and finally Antarctic Bottom Water (AABW) at a depth 4,700 m in the Cape Basin. This coverage will for the first time provide the opportunity to groundtruth the indirect observations from the ferromanganese crust deposits and will serve as a basis for further applications of Hf isotopes in marine research.

b) Quantification of the influence of dust dissolution on the dissolved Hf and Nd isotope composition of seawater

The second scientific goal of the cruise is the investigation of the influence of dust input on the dissolved isotopic composition of Nd and Hf. After introduction of dust into seawater a certain amount dissolves and is released to seawater. This release

depends on the composition of the source rocks of the dust and the respective elements. Estimates for the amount of dust dissolving in seawater range between near nothing and 25 % percent and are subject to ongoing debate. The surface water transect sampled on this cruise enables a direct investigation of the influence of dust dissolution on the Nd isotope composition of seawater because the Saharan source rocks of the dust have a significantly different isotopic signature to the dissolved isotopic composition of eastern North Atlantic waters. In addition, the Nd isotope signature of the Northern Sahara (very low, ε_{Nd} on the order of -11 to -20) is different to that in the southern Sahara (higher ε_{Nd} = -8 to -11). From the direct measurements of the Nd concentrations and isotope composition of the waters we expect new and systematic insights into the importance of dust dissolution for these metals, which will also have implications for the prcesses controlling other trace metals, in particular micronutrients such as Fe. Analogous to Nd we will gain a first direct insight into the importance of dust dissolution for Hf, which has so far been predicted to be of minor importance for the Hf budget of seawater. It will further enable to compare the released isotope signature of Hf with that of the source rocks in order to investigate if the dissolution of dust is a process that releases the bulk Hf isotopic signature of the dust or, more likely, that of more labile mineral phases in the dust particles. For this purpurse we also plan to measure the isotopic composition of the detrital fraction of some of the particulate samples recovered with the large centrifuge (W. Geibert). We obtained 31 surface water samples covering the area of European dust sources, the major Saharan dust input regions, as well as potential southern African sources. In addition, we sampled the upper 200 m of the deep water profiles in the eastern north Atlantic and the Angola Basin at higher resolution in order to be able to find and analyse potential deeper maxima of Hf and Nd concentrations originating from older dust input events.

Beryllium isotopes

The element Be has one stable isotope, ^{9}Be, which is exclusively of terrigenous origin, whereas a second isotope, ^{10}Be, is cosmogenic forms in the upper atmosphere at a near constant rate and decays with a half-life of 1.5 million years. ^{10}Beryllium is transferred to the surface ocean via wet precipitaton. Be has a residence time in the ocean similar to Nd and Hf and the ^{10}Be/^{9}Be ratio has also been used as an isotopic water mass tracer. For Be isotopes already quite a number of measurements in the water column of the Atlantic exist, which is why the main focus will be the investigation of the dependence of changes of this ratio in the surface waters as a function of dust input and dissolution. This should release ^{9}Be and therefore lead to a decrease in the ratio, which should correlate to the changes observed in the radiogenic isotopes as well as to changes of the concentrations of other lithogenic elements such as Fe, Al and Ti.

Stable Silicon isotopes:

Si isotopes in seawater have been shown to fractionate as a function of Si utilization by opaline phytoplankton (diatoms). Diatoms prefer the lighter Si isotopes for the production of their opal frustules which leaves the surface waters enriched in the heavier Si isotopes. This enrichment is a function of the availability of Si and if supply is diminished, for example by stratification of the water column or phytoplankton blooms, fractionation becomes stronger and the Si isotope composition becomes

heavier. It has recently become possible to measure the stable Si isotope composition (δ^{30}Si) of seawater by MC-ICPMS, which enables precise measurements and at the same time a much higher sample throughput than with other methods. This will lead to a wide-spread application of this relatively new isotopic tool. The main goal of this cruise is to see if the changes in surface water productivity along the cruise track, observed for example from chlorophyll and ^{234}Th measurements, are reflected in the Si isotope composition of Atlantic seawater. In addition, the influence of dust will be investigated because it has a δ^{30}Si value of 0 ‰ and if there is significant inputs of Si from dissolution of dust this should also be visible in changes of the concentrations as well as the isotopic composition of dissolved Si.

Work at sea

Since there was no possibility to produce any data on board of the ship for the planned isotope measurements we had to take large quantities of water samples under clean conditions. Sampling took place using different devices. For the surface samples we mainly used the towed fish of Peter Croot's group but also several samples were taken with a snorkel under the hull of RV *Polarstern* and we also used the seawater intake system to investigate if this system is clean enough for future measurements of the isotopes of interest. We took 31 samples of 140 l which were transported to the ship laboratory in 50 l PE bottles. In addition we took 29 samples of 60 - 96 litres from the water profiles that were recovered with the niskin bottles of the rosette. The water was filtered trough a 0.45 µm filter into precleaned 20 l cubitainers. 2 l of the filtered waters for all samples were collected separately, one for concentration measurements of Nd and Hf, as well as Si isotope and Si concentration measurements, and one for the measurement of Be concentrations. In addition, we sampled 0.5 l separately for the determination of Rare Earth Elements (REEs) to be performed at Oxford University. All filtered water samples were then acidified to a pH of about 2 by addition of suprapure (elbow-desitilled) concentrated HCl and 0.3 ml of a 0.3 g/g FeCl solution werde added. Finally, between 0.5 and 1 ml of a 1000 ppm Be carrier solution were added for the isotope dilution measurements of ^{10}Be concentrations. The samples were then left overnight to equilibrate with the Be carrier and were then precipitated with suprapure ammonia at a pH of 7.5-8.5. The samples were then shaken occasionally during two days and finally the Fe hydroxide precipitate settled at the bottom of the cubitainers. The supernate was syphoned off and the precipitate transferred into another 20 l bottle and left to settle again for another day. The supernate was syphoned off again, so that about 1 litre was left, which was transferred into 2 l bottles and closed for transport and further chemical purification steps and measurement of the Hf and Nd isotope compositions and concentrations in the clean lab facilities at the Institute for Isotope Geology and Mineral Resources at ETH Zurich. During this purification procedure the Be fractions will be collected and further treated at IFM-GEOMAR in Kiel for final measurement at the Accelerator Mass Spectrometry (AMS) facility at ETH Zurich.

Link to other GEOTRACES-related projects on this cruise

The goals of our isotope studies are strongly linked to those of other GEOTRACES-related groups on board of this cruise. This linkage is the core concept of the forthcoming GEOTRACES programme, which is based on a holistic coverage and

investigation of many trace metal and isotope systems together with a range of ancillary parameters in order to improve our understanding of their biogeochemical cycling. We will closely collaborate with the groups of Peter Croot and Timo Daberkov on the abundances of Fe, Al and Ti, which are clearly influenced by dust input and its inorganic dissolution. This will be essential for the correct interpretation of our radiogenic and cosmogenic isotope data. We will also collaborate closely with the groups of Michiel Rutgers van der Loeff and Rüdiger Röttgers for comparison with the chlorophyll and productivity measurements, as well as the ^{234}Th measurements, without which the Si isotope data cannot be interpreted correctly.

4.6 Cation incorporation into foraminiferal shells

Delphine Dissard
Alfred-Wegener-Institut

Objectives

The cation composition of foraminifera shells isolated from marine sediments is used as proxy for temperature, salinity and carbonate chemistry of surface seawater during the time the shells were formed. A proper use of this proxy requires the establishment of a relationship between cation incorporation into foraminifera shells and surface seawater parameters over a range of environmental conditions.

Work at sea

In order to determine the cation incorporation into foraminiferal shells as a function of temperature, salinity, and sea water carbonate chemistry, planktonic foraminifera have been sampled continuously during the cruise ANT-XXIII/1 (Bremerhaven-Cape Town). More than seventy samples were collected during this transect, taken every eight hours, with a constant seawater flux of 3 m^3/h. The set-up was composed of a 1,000 l plastic container, in which the plankton net (250-125 µm) was fixed, and could be easily removed to collect the sample. The sea water was flushed from the membrane pump to avoid the disturbance of the material as much as possible. At the same time, water samples have been collected for later analyses of alkalinity and total CO_2 in order to determine the carbonate chemistry of the seawater. Seventy samples of seawater have therefore been collected and poisoned with $HgCl_2$, simultaneously of the plankton sampling, poisoned with formaldehyde 20 %. More than twenty water samples have also been collected from the CTD surface water with the same aim. No further analyses have been made on board, but it appears that planktonic foraminifera have been successfully sampled in a very well preserved state, and in a very important density during the second part of the cruise (Vigo - Cape Town) where the waters were rich. During the first part, and more precisely , in the Bay of Biscay, waters appeared to be very oligotrophic and planktonic foraminifera were present in a very low density. Together with culture experiments and numerical modelling we hope to be able to use this freshly collected material to improve existing proxy relationship and to develop new ones.

4.7 Continuous shipboard speciation measurements of dissolved Fe and Ti

Peter Croot[1)], Christian Schlosser[1)], Sebastian Steigenberger[2)]
[1)]IFM-GEOMAR
[2)]Alfred-Wegener-Institut

Objectives

While it is established now that Fe can be a (co)limiting nutrient for phytoplankton in High Nutrient Low Chlorophyll (HNLC) regions of the world (Boyd et al., 2000; Coale et al., 1998; Coale et al., 2004; Croot et al., 2001; Croot et al., 2005; Tsuda et al., 2003), we still know little about the processes by which Fe is supplied to the ocean and how processes in the ocean scavenge/uptake or remineralize dissolved Fe. By examining iron chemistry in a variety of different marine environments, such as encountered on ANT-XXIII/1, we can develop an overview of the key processes controlling the biogeochemistry of iron in seawater. From this basis we can start to quantify the fluxes involved in each individual process.

In many cases examination of other elements similar in chemistry to iron reveals more information on the key processes involved – such elements include Ti(IV), Al(III) and Mn(II). By comparison of the concentrations of these 3 strongly hydrolysed elements in the soluble, dissolved and particulate phases we hope to be able to better understand the processes affecting dust dissolution and particle scavenging in the surface ocean. The cruise track from Vigo to Cape Town allows comparison between high dust load regions affected by the Saharan and Namibian deserts, low dust regions in between and a zone of high biological productivity at the equator.

Titanium biogeochemistry in seawater has been studied very little in the open ocean, with only a single deep-water profile from the Pacific (Orians and Boyle, 1993; Orians et al., 1990) which showed picomolar concentrations in surface waters and increasing to ~300 pM in deep waters. There have been a few more studies in enclosed seas (van den Berg et al., 1994) and estuaries (Skrabal, 1995; Skrabal and Terry, 2002; Skrabal et al., 1992) but overall there is little information on the global Ti distribution in the ocean. Based on the work of Orians et al. (1990) Ti has a short residence time in the ocean and thus it would be predicted that if it is supplied predominantly by atmospheric sources that there would be a strong gradient in the vicinity of the Saharan dust plume. The present study through the use of a new voltametric technique, developed at IFM-GEOMAR that allows shipboard determination of pM levels of Ti, was set to test this hypothesis.

By comparison of the chemistries and distributions of Ti, Al and Fe this GEOTRACES study is aiming to improve our knowledge of the processes effecting trace metal distributions in the ocean with emphasis on dust impacted regions.

Work at sea

During ANT-XXIII/1 the trace metal group from IFM-GEOMAR in collaboration with co-workers from IOW, AWI and Universität Bremen undertook continuous near-surface sampling for the dust derived elements Fe, Al and Ti, using a towed fish and trace metal clean pumping system. This work was part of the German contribution for GEOTRACES and is also a continuation of similar earlier work performed on the RV *Polarstern* (ANT-XVIII/1) (Bowie et al., 2003; Sarthou et al., 2003) and the *Meteor*

(M55) (Croot et al., 2004) in the central Atlantic looking at the effect of Saharan dust deposition on surface seawater iron concentrations.

Water sampling

As Fe exists at extremely low levels in seawater, extreme caution is needed in taking samples at sea, because of the potential for contamination from the ubiquitous steel construction of modern research vessels. Thus for the purposes of the present work we employed a variety of techniques for obtaining clean water samples:

- Discrete water samples from depth were obtained via GO-FLO samplers deployed on a Kevlar line. Dissolved samples were collected after filtration through 0.2 μm cartridge filters with slight N_2 overpressure. All sample collection was carried out in the IFM-GEOMAR Clean Air Container situated on the working deck close to the Kevlar winch. Samples were taken from the following depths: 20, 40, 60, 80, 100, 120, 150 and 200 m.

- Surface water samples were collected from the IFM-GEOMAR towed fish deployed from a winch on the working deck some 3 - 4 m from the side of the ship and a depth of 2 -3 m. From the fish samples were pumped to the wet lab via a totally enclosed system with suction provided by Teflon diaphragm pumps. The water was then sent to several 20 or 50 l carboys for collection as part of the coordinated GEOTRACES sampling programme carried out during ANT-XXIII/1. Filtered samples were obtained by drawing a sample through a 0.2 μm cartridge filter using a second Teflon diaphragm pump. Sample Bottles were then filled under laminar flow clean air in a flow hood located on the same bench in the wet room. The entire system was self enclosed and the carboys for trace metal sampling were fitted with air vent filters to prevent contamination from the laboratory air.

- An alternative system for surface water samples was employed using the snorkel located in the moon pool of the ship. The sampling system was similar to that used in the wet-lab for the fish samples.

Initially it was assumed that it was not possible to take samples for Titanium from the CTD because of contamination from Ti components of the CTD itself. However, first comparisons between samples from the Niskins from the CTD rosette and the GOFLOs using the Kevlar wire showed no discernable differences. Therefore later sampling for Titanium involved the use of the CTD rosette system.

Trace metal sampling

Samples were analysed using a combination of online flow injection analysis (FIA) systems: Total Fe as Fe(II) via sulfite reduction and luminol chemiluminescence (Bowie et al., 1998; Powell et al., 1995), Fe(III) speciation measurements were performed using the voltametric reagent TAC (Croot and Johansson, 2000), Al(III) via a fluorescence technique (Hydes and Liss, 1976; Resing and Measure, 1994) and Ti(IV) via a new voltametric method developed at IFM-GEOMAR (Croot, in preparation).

Preliminary results

The distribution of samples is shown in figure 1.1. Approximately 50 samples from the underway fish/snorkel sampling system were analysed for dissolved Fe and Ti during this cruise. There was no apparent difference for dissolved Fe between the fish and snorkel systems, though the data set is limited (n=3). Samples were analysed for Fe and Ti from 6 deep stations, with samples for other dissolved elements (Cd, Zn, Pb, Cu, Co) collected and acidified for return to the laboratory in Kiel for later analysis. The samples for Fe were limited to the upper 200 m while Ti samples from the CTD were also utilized allowing a full depth profile to be obtained.
The initial results for dissolved Ti are shown in figure 4.5 and here it can be clearly seen that the Saharan dust plume has a strong influence on Ti concentrations in the eastern Atlantic. At the position of the ITCZ it is interesting to note, though, that there is a rapid decrease in Ti levels as the Southern Hemisphere air apparently contains much less dust or Ti-bearing aerosols.

Acknowledgements

The authors would like to show their deep thanks and appreciation to the officers and crew of the RV *Polarstern*, for all their efforts in helping us throughout the duration of ANT-XXIII/1. Thanks also to the Chief Scientist, Dr. Michiel Rutgers van der Loeff and to the AWI for making this cruise possible. Special thanks to all our GEOTRACES colleagues who helped performing the sampling programme during this cruise: Ingrid Vöge, Jan Scholten, Martin Frank, Jörg Rickli, Timo Daberkow, Corinna Harms and Ursula Hennings. This work was made possibly specifically through funding from the DFG (CR145/7), AWI and IFM-GEOMAR.

References

Bowie, A.R., Achterberg, E.P., Mantoura, R.F.C. and Worsfold, P.J., 1998. Determination of sub-nanomolar levels of iron in seawater using flow injection with chemiluminescence detection. Analytica Chimica Acta, 361: 189-200.

Bowie, A.R. et al., 2003. Shipboard intercomparison of dissolved iron in surface waters along a north-south transect of the tropical Atlantic Ocean. Marine Chemistry, 84: 19-34.

Boyd, P.W. et al., 2000. Mesoscale iron fertilisation elevates phytoplankton stocks in the polar Southern Ocean. Nature, 407: 695-702.

Coale, K.H. et al., 1998. IronEx-I, an insitu iron-enrichment experiment: Experimental design, implementation and results. Deep-Sea Research II, 45: 919-945.

Coale, K.H. et al., 2004. Southern Ocean Iron Enrichment Experiment: Carbon Cycling in High- and Low-Si Waters. Science, 304(5669): 408-414.

Croot, P.L. and Johansson, M., 2000. Determination of iron speciation by cathodic stripping voltammetry in seawater using the competing ligand 2-(2-Thiazolylazo)-p-cresol (TAC). Electroanalysis, 12(8): 565-576.

Croot, P.L., Streu, P. and Baker, A.R., 2004. Short residence time for iron in surface seawater impacted by atmospheric dry deposition from Saharan dust events. Geophysical Research Letters, 31: L23S08, doi:10.1029/2004GL020153.

Croot, P.L. et al., 2001. Retention of dissolved iron and FeII in an iron induced Southern Ocean phytoplankton bloom. Geophysical Research Letters, 28: 3425-3428.

Croot, P.L. et al., 2005. Spatial and Temporal distribution of Fe(II) and H2O2 during EISENEX, an open ocean mesoscale iron enrichment. Marine Chemistry, 95: 65-88.

Hydes, D.J. and Liss, P.S., 1976. Fluorimetric method for determination of low concentrations of dissolved aluminum in natural waters. Analyst, 101: 922-931.

Mahowald, N. et al., 1999. Dust sources and deposition during the last glacial maximum and current climate: A comparison of model results with paleodata from ice cores and marine sediments. Journal of Geophysical Research, 104(D13): 15895-15916.

Orians, K.J. and Boyle, E.A., 1993. Determination of Picomolar Concentrations of Titanium, Gallium and Indium in Sea-Water by Inductively-Coupled Plasma-Mass Spectrometry Following an 8-Hydroxyquinoline Chelating Resin Preconcentration. Analytica Chimica Acta, 282(1): 63-74.

Orians, K.J., Boyle, E.A. and Bruland, K.W., 1990. Dissolved titanium in the open ocean. Nature, 348: 322-325.

Powell, R.T., King, D.W. and Landing, W.M., 1995. Iron distributions in surface waters of the south Atlantic. Marine Chemistry, 50: 13-20.

Resing, J.A. and Measure, C.I., 1994. Fluorometric Determination of Al in Seawater by Flow Injection Analysis with In-Line Preconcentration. Analytical Chemistry, 66: 4104-4111.

Sarthou, G. et al., 2003. Atmospheric iron deposition and sea-surface dissolved iron concentrations in the East Atlantic. Deep-Sea Research, 50: 1339-1352.

Skrabal, S.A., 1995. Distributions of Dissolved Titanium in Chesapeake Bay and the Amazon River Estuary. Geochimica Et Cosmochimica Acta, 59(12): 2449-2458.

Skrabal, S.A. and Terry, C.M., 2002. Distributions of dissolved titanium in porewaters of estuarine and coastal sediments. Marine Chemistry, 77: 109-122.

Skrabal, S.A., Ullman, W.J. and Luther, G.W., 1992. Estuarine distributions of dissolved titanium. Marine Chemistry, 37: 83-103.

Tsuda, A. et al., 2003. A Mesoscale Iron Enrichment in the Western Subarctic Pacific Induces a Large Centric Diatom Bloom. Science, 300(5621): 958-961.

van den Berg, C.M.G., Boussemart, M., Yokoi, K., Prartono, T. and Campos, M.L.A.M., 1994. Speciation of aluminium, chromium and titanium in the NW Mediterranean. Marine Chemistry, 45: 267-282.

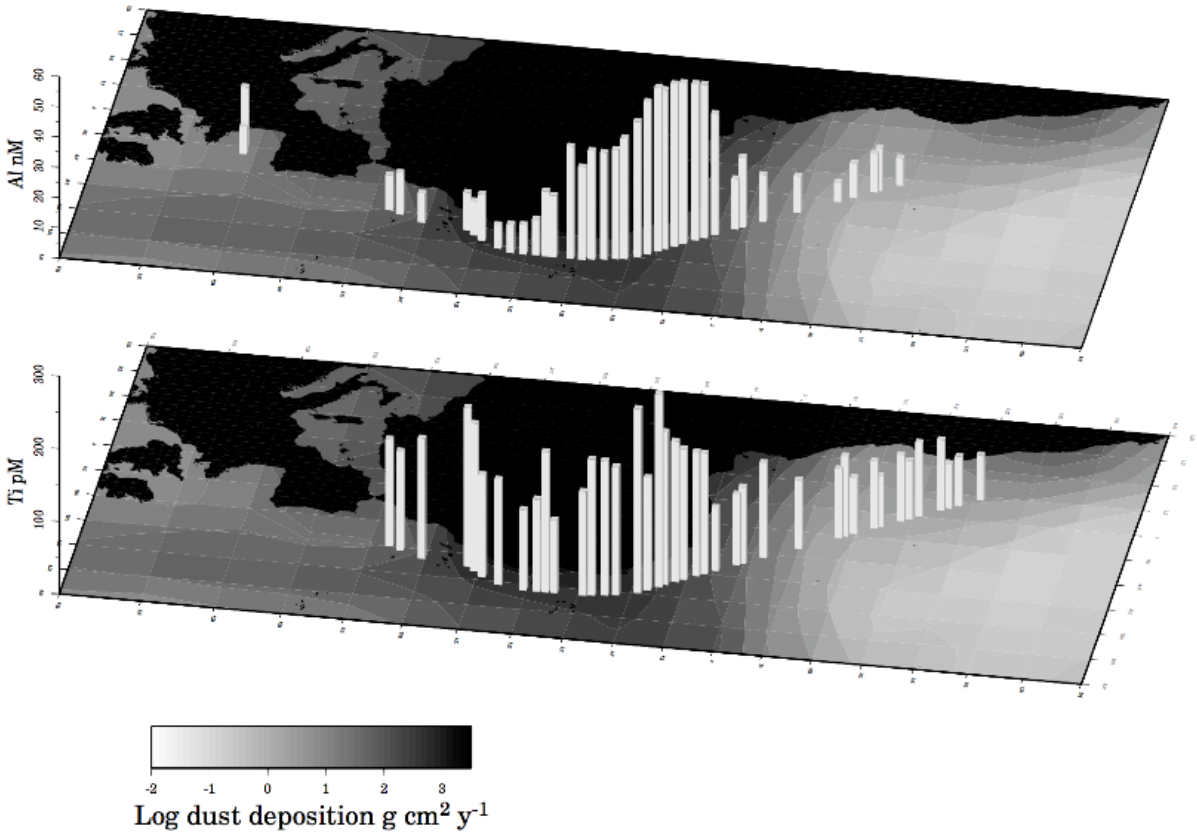

Fig. 4.5: Preliminary map of surface Ti (below; Croot, Schlosser and Steigenberger, section 4.7) and Al (above; Daberkow and Harms, section 4.7-A) distribution during ANT-XXIII/1 superimposed on modelled dust deposition from (Mahowald et al., 1999)

4.7.1 Scavenged-type trace metals in solution, colloids and particles of an Atlantic Ocean surface section; dissolved aluminium

Time Daberkow, Corinna Harms,
IUP University of Bremen, Institut für Umweltphysik, Universität Bremen

Objectives / expected results

Particle-water interaction is a key process in the biogeochemical cycling of chemical elements in the ocean. Uptake into/onto particulate matter and subsequent sinking (scavenging) exerts major control on the chemical composition of seawater. This process maintains the rather low concentrations of many elements in seawater. Marine Particles can be classified into different size fractions: (i) there are relatively large/heavy, fast sinking particles, which are responsible for the vertical transport towards the sediment; most of the mass resides (ii) in small, almost unsinkable

suspended particulate matter (SPM) of biogenic and terrestrial origin; and (iii) the colloidal fraction which passes the filter membranes (< 0.4 µm) which are typically used to separate the SPM from the dissolved fraction. Thus, the fraction classically regarded as dissolved, needs to be divided into the colloidal fraction(s) and the "truly" dissolved fraction. The role of this colloidal fraction in the interactions between dissolved and particulate matter in the ocean and its trace element composition is still widely unknown. Although being part of the operationally defined dissolved fraction, the colloidal size fraction including the elements adsorbed on the colloids may have biogeochemical properties different from those of “truly” dissolved elements.

The comparison of trace element composition of the different fractions in seawater (SPM, dissolved, colloidal and “truly” dissolved) and the additional comparison to the composition of aerosol particles and rainwater samples are expected to provide important clues on the transport and sorption mechanisms (sorption of trace elements onto colloids and sorption on suspended particles) as well as on the general biogeochemical behaviour of the analyzed trace elements (e.g. Fe, Co, Ni, Cu, Zn, Cd, Pb) in the ocean.

With Fe being a prominent example, many of the trace element studied here are essential for marine life, and thus also for the biogenically induced particle flux within the water column. These trace elements cover a broad range of chemical properties, enabling the study of relevant biogeochemical processes in greater detail.

Work at sea / preliminary results

During the cruise ANT-XXIII/1 surface water samples were collected for the analysis of different trace elements in the mentioned fractions. Dissolved samples have been separated into “truly” dissolved and colloidal sample material using cross-flow ultra filtration (CFUF, with nominal mass cut-offs at 30,000, 10,000, and 5,000 Da).

To have an indicator for the input of particles/dust from the atmosphere, the concentration of total dissolvable aluminium (TD-Al) was analyzed using the Lumogallion fluorescence method.

Sampling was conducted over the whole transact (see Fig. 4.5 and Table 1.1) covering different regions of input and production and also includes a few water column profiles (not listed in Table 1.1). Surface water sampling was done via the side towed fish (sampling depth ca. 3 m). Where this was not possible due to heavier sea state a snorkel system below the ship (sampling depth ca. 12 m) was used for seawater supply.

Fractionation by ultra filtration and SPM-filtration each had been done once a day, sampling of unfiltered and prefiltered water twice a day; frequency of aluminium sampling/analyzing varied from once a day at the beginning and end of the transect up to four times a day at the dust input regions.

4.7.2 Elemental Ratios in Particulate Samples along a meridional transect in the Atlantic

Peter Croot[1)], Christian Schlosser[1)], [1)]IFM-GEOMAR
Sebastian Steigenberger[2)]) [2)]Alfred-Wegener-Institut
not on board: R. Sherrell, Rutgers University, New Brunswick, New Jersey, USA

Objectives

Trace element ratios in particulate matter from surface waters reflect the nature of the particles themselves and can provide information on the processes that formed them. In particular in regions of high productivity the content of the mostly organic particles reflect the concentrations of the bio available fraction of the metals in seawater; this may include changes in the Cd:P or Zn:P ratio or in the Fe:P ratio. In contrast in regions with a high dust load, the particles may reflect more the inorganic/crustal signature of the aerosol source regions. The Rutgers group of Prof. Rob Sherrell have a strong history of developing and applying ICPMS techniques to the problem of element ratios in particulate matter (Berman-Frank et al., 2001; Cullen and Sherrell, 1999; Cullen et al., 1999; Cullen et al., 2003; Field et al., 1999; Sterner et al., 2004). By measuring elemental ratios in particles collected during ANT-XXIII/1 we hope to gather further information on the way in which particle supply and production, scavenging and dissolution controls dissolved metal concentrations in the open ocean and in turn how this may effect primary productivity.

Work at sea

In the present work we obtained surface and near surface samples along the meridional transect during ANT-XXIII/1. Sampling was conducted in two modes:

- Surface sampling from the FISH at the same time as the main GEOTRACES sample collection took place in the wet lab. This involved collecting 20 l of seawater into a trace metal clean carboy and filtering through either 47 mm quartz or polycarbonate filters. All sample manipulations and filtration took place in a class 100 laminar flow bench. The filters were then later dried on the laminar flow bench and stored until shipping for later analysis at Rutgers.

- Depth resolved sampling was performed at several of the GEOTRACES stations during ANT-XXIII/1. This involved filtering 2 l of seawater collected from the GO-FLO samplers through 13 mm quartz fibre filters while under low N_2 overpressure in the IFM-GEOMAR clean container. Typically samples were obtained from 20, 60, 100 and 200 m. The filters were then dried in the clean room using a small incubator and stored until shipping for later analysis at Rutgers.

The collected samples will be analysed by ICP-MS in the laboratory at Rutgers. The present study was a pilot study to examine the feasibility of combining this type of sampling with work on the dissolved metals in the water column carried out by the trace metal group at the IFM-GEOMAR. This is an international collaboration between Germany and the USA as an initial contribution to German GEOTRACES.

References

Berman-Frank, I., Cullen, J.T., Shaked, Y., Sherrell, R.M. and Falkowski, P.G., 2001. Iron availability, cellular iron quotas, and nitrogen fixation in Trichodesmium. Limnology and Oceanography, 46: 1249-1260.

Cullen, J.T. and Sherrell, R.M., 1999. Techniques for determination of trace metals in small samples of size-fractionated particulate matter: phytoplankton metals off central California. Marine Chemistry, 67: 233-247.

Cullen, J.T., Lane, T.W., Morel, F.M.M. and Sherrell, R.M., 1999. Modulation of cadmium uptake in phytoplankton by seawater CO2 concentration. Nature, 402: 165-167.

Cullen, J.T., Chase, Z., Coale, K.H., Fitzwater, S.E. and Sherrell, R.M., 2003. Effect of iron limitation on the cadmium to phosphorous ratio of natural phytoplankton assemblages from the Southern Ocean. Limnology and Oceanography, 48: 1079-1087.

Field, M.P., Cullen, J.T. and Sherrell, R.M., 1999. Direct determination of 10 trace metals in 50 uL samples of coastal seawater using desolvating micronebulization sector field ICP-MS. Journal of Analytical Atomic Spectrometry, 14: 1425-1431.

Sterner, R.W. et al., 2004. Phosphorus and trace metal limitation of algae and bacteria in Lake Superior. Limnology and Oceanography, 49: 495-507.

4.8 Deposition of trace metals to Atlantic surface waters

Peter Croot[1)], Christian Schlosser[1)], [1)]IFM-GEOMAR
Sebastian Steigenberger[2)]) [2)]Alfred-Wegener-Institut
not on board: A. Baker, School of Environmental Sciences, University of East Anglia, UK

Objectives

Transport of airborne dust from the continents provides a route by which Fe can enter remote surface ocean waters. This transport can be of particular importance for supplying iron to HNLC regions where Fe is the limiting nutrient. The episodic nature of dust transport makes many aspects of this deposition uncertain – how much is soluble, what is the redox speciation and how much is deposited in rainfall? Previous work by the group of Dr. Alex Baker (UEA) has shown the importance of aerosol solubility and mass loading to the deposition of Fe to the Atlantic (Baker et al., 2003). Simultaneous measurements of aerosol loadings and water column concentrations through an international collaboration between IFM-GEOMAR and UEA have shown short residence times for particle reactive metals such as iron directly under the Saharan dust plume (Croot et al., 2004). By undertaking simultaneously atmospheric and water sampling it allows a more comprehensive examination of the processes involved in atmospheric deposition of trace metals to the surface ocean.

Work at sea

During ANT-XXIII/1 aerosol samples were collected using a Graseby-Anderson high-volume sampler provided by UEA. Samples collected during the transect past West Africa showed visual evidence of Saharan dust with a reddish-brown colour. Daily

samples for aerosol dust were collected during the cruise north of the ITCZ with 2 day sampling to the south, because of the expected lower dust loadings. Samples were collected during steaming time and were turned off during the daily bio-optics station, when the ship would be orientated so the working deck was towards the sun and there was a large risk of contamination of the filters from the smokestack. The filters were processes under trace metal clean conditions under a class 100 laminar flow hood. The collected filters will be analysed in the laboratory in Norwich upon return for dust derived elements (Ca, Fe, Al, Mn, Ti) and macronutrients. The resulting data will be used in conjunction with the simultaneous measurements of metal concentrations in the upper water column to construct estimates of dust supply and residence time of trace metals to the Eastern Atlantic.

References

Baker, A.R., Kelly, S.D., Biswas, K.F., Witt, M. and Jickells, T.D., 2003. Atmospheric deposition of nutrients to the Atlantic Ocean. Geophysical Research Letters, 30(24).

Croot, P.L., Streu, P. and Baker, A.R., 2004. Short residence time for iron in surface seawater impacted by atmospheric dry deposition from Saharan dust events. Geophysical Research Letters, 31: L23S08, doi:10.1029/2004GL020153.

4.9 Hydrogen Peroxide (H_2O_2) in the upper water column along an Atlantic meridional transect

Peter Croot[1)], [1)]IFM-GEOMAR
Sebastian Steigenberger[2)]) [2)]Alfred-Wegener-Institut

Objectives

H_2O_2 is a short lived photochemically produced trace oxidant found in the sunlit water column. Information on H_2O_2 concentrations allows us to constrain the oxidation time of reduced metal species (e.g. Cu(I), Fe(II)) in the ocean where H_2O_2 is the principal oxidant, this information is important for understanding the biogeochemical cycling of these metals. Furthermore H_2O_2 can be used as a tracer for vertical mixing in surface waters and/or a tracer of recent (last few days) rain events. For ANT-XXIII/1 our objective was to make a synoptic survey of H_2O_2 throughout the Eastern Atlantic and examine the influence of different biogeochemical provinces on its formation and decay.

Hydrogen peroxide (H_2O_2) is the most stable intermediate in the four-electron reduction of O_2 to H_2O and may function as an oxidant or a reductant. H_2O_2 is principally produced in the water column by photochemical reactions involving dissolved organic matter (DOM) and O_2 (Cooper et al., 1988; Scully et al., 1996; Yocis et al., 2000; Yuan and Shiller, 2001). Open ocean H_2O_2 concentrations show a distinct exponential profile with a maximum at the surface consistent with the photochemical flux. Concentrations can reach up to 300 nmol L-1 in equatorial and tropical regions with high DOM concentrations such as in the Amazon plume in the Atlantic (Yuan and Shiller, 2001). In regions with low DOM and low sunlight, surface H_2O_2 levels are much lower with values in the Southern Ocean of 10-20 nmol L-1

(Sarthou et al., 1997). Rainwater is a major potential source for H_2O_2 to surface seawater as it is preferentially removed from the atmosphere, relative to other peroxides, during convective events (Croot et al., 2004b). Due to its high solubility in water, scavenging of H_2O_2 in deep convection is around 55-70 % (Cohan et al., 1999). Mixing ratios of H_2O_2 in the marine troposphere show a strong latitude dependence with a maximum over the equator, suggesting that the air to surface flux at the equator should be high (Weller and Schrems, 1993).

H_2O_2 is also produced by biological processes in the ocean with observations from the Sargasso Sea (Palenik and Morel, 1988) and in phytoplankton cultures (Palenik et al., 1987) of production in the dark. Most studies to date have suggested that the major production pathway in the water column for H_2O_2 is from photochemical production, however in a few cases in the Southern Ocean, distinct H_2O_2 maximums at depth, corresponding to the chlorophyll maximum, suggest a significant biological source of H_2O_2 (Croot et al., 2004a). The 'dark decay life-time' of H_2O_2 can vary from hours to weeks in the ocean (Petasne and Zika, 1997), but typically may be around 4 days in the open ocean (Plane et al., 1987). Overall the decay rate of H_2O_2 is apparently controlled by several factors: H_2O_2 concentration, colloid concentration, bacteria/cyanobacteria numbers and temperature (Wong et al., 2003; Yuan and Shiller, 2001).

Work at sea

During ANT-XXIII/1 samples were taken for H_2O_2 from the upper 200 m during the daily bio-optics CTD cast and sampling was limited to at most 7 depths due to the water requirements (multiple bottles) from the other groups sampling this cast. For the bio-optics cast the chlorophyll maximum, near surface water and 200 m depth was always sampled and other sample depths were chosen according to examination of the CTD profile, targeting apparent mixing environments, with at least one sample from deeper in the observed mixed layer.

Methods

H_2O_2 measurements in surface waters

Seawater samples were obtained using Niskin bottles on a standard CTD rosette. Samples were drawn into 100 ml low density brown polyethylene bottles which were impervious to light. Samples were analyzed within 1 - 2 hours of collection where possible and were not filtered. In the present work H_2O_2 was measured using a flow injection chemiluminescence (FIA-CL) reagent injection method (Yuan and Shiller, 1999). In brief, the chemiluminescence of luminol is catalysed by the reaction of H_2O_2 present in the sample with Co^{2+} at alkaline pH. H_2O_2 standards were made by serial dilution from a primary stock solution (30% Fluka - Trace Select). The concentration of the primary standard was determined by direct spectrophotometry of the solution (ε= 40.9 mol L^{-1} cm^{-1}, (Hwang and Dasgupta, 1985)). Secondary standards were analysed with a spectrophotometric method using Cu(II) and 2,9-dimethyl-1,10-phenanthroline (Kosaka et al., 1998). Seawater samples were measured directly by FIA-CL, while rainwaters were diluted, up to 1:100, with ultrapure water (18 MΩ). Sample concentrations were corrected daily for the reagent blank (Yuan and Shiller, 1999) and for H_2O_2 in the ultrapure water (20 - 60 nmol L^{-1}). Samples were analyzed

using 5 replicates: typical precision was 2 - 3 % through the concentration range 1 - 100 nM, the detection limit (3σ) was typically 0.6 nmol L^{-1}.

Preliminary results and discussion

H_2O_2 profiles were measured at 18 stations during the course of ANT-XXIII/1 from a wide range of upper ocean environments (Fig. 4.6). Initial analyses suggest that mixing processes strongly controlled the vertical distribution of H_2O_2 more so than the light attenuation, though presently the influence of the CDOM concentrations on the production has not be factored in. Highest surface concentrations were found in the ITCZ due to the supply by rain but high concentrations were found also throughout dry regions of the tropics suggesting significant photochemical production in some areas.

Later work will include comparing the H_2O_2 profiles with the simultaneous bio-optical measurements made at each station and the mixing information provided by the CTD. Using this approach it should be possible to determine the major processes (e.g. active mixing, rain inputs of H_2O_2, production via photolysis or phytoplankton production of H_2O_2) controlling the distribution of H_2O_2 in the upper water column along the ANT-XXIII/1 transect.

Acknowledgements

The authors would like to show their deep thanks and appreciation to the crew of the RV *Polarstern*, for all their efforts in helping us throughout ANT-XXIII/1. Thanks also to the Chief Scientist, Dr. Michiel Rutgers van der Loeff and to the AWI for making this cruise possible.

References

Cohan, D.S., M.G. Schultz, D.J. Jacob, B.G. Heikes, and D.R. Blake, Convective injection and photochemical decay of peroxides in the tropical upper troposphere: Methyl iodide as a tracer of marine convection, Journal of Geophysical Research-Atmospheres, 104 (D5), 5717-5724, 1999.

Cooper, W.J., R.G. Zika, R.G. Petasne, and J.M.C. Plane, Photochemical Formation of H2O2 in Natural Waters Exposed to Sunlight, Environmental Science and Technology, 22, 1156-1160, 1988.

Croot, P.L., P. Laan, J. Nishioka, V. Strass, B. Cisewski, M. Boye, K. Timmermans, R. Bellerby, L. Goldson, and H.J.W. de Baar, Spatial and Temporal distribution of Fe(II) and H2O2 during EISENEX, an open ocean mesoscale iron enrichment, submitted to Marine Chemistry, 2004a.

Croot, P.L., P. Streu, I. Peeken, K. Lochte, and A.R. Baker, Influence of ITCZ on H2O2 in near surface waters in the equatorial Atlantic Ocean, Geophysical Research Letters (accepted), 2004b.

Hwang, H., and P.K. Dasgupta, Thermodynamics of the Hydrogen Peroxide-Water System, Environmental Science and Technology, 19, 255-258, 1985.

Kosaka, K., H. Yamada, S. Matsui, S. Echigo, and K. Shishida, Comparison among the methods for hydrogen peroxide measurements to evaluate advanced oxidation processes: Application of a spectrophotometric method using copper(II) ion and

2.9 dimethyl-1,10-phenanthroline, Environmental Science & Technology, 32 (23), 3821-3824, 1998.

Palenik, B., and F.M.M. Morel, Dark production of H2O2 in the Sargasso Sea, Limnology and Oceanography, 33, 1606-1611, 1988.

Palenik, B., O.C. Zafiriou, and F.M.M. Morel, Hydrogen peroxide production by a marine phytoplankter, Limnology and Oceanography, 32, 1365-1369, 1987.

Petasne, R.G., and R.G. Zika, Hydrogen peroxide lifetimes in south Florida coastal and offshore waters, Marine Chemistry, 56 (3-4), 215-225, 1997.

Plane, J.M.C., R.G. Zika, R.C. Zepp, and L.A. Burns, Photochemical modeling applied to natural waters, in Photochemistry of environmental aquatic systems, edited by R.G. Zika, and W.J. Cooper, pp. 215-224, American Chemical Society, Washington D.C., 1987.

Sarthou, G., C. Jeandel, L. Brisset, D. Amouroux, T. Besson, and O.F.X. Donard, Fe and H2O2 distributions in the upper water column in the Indian sector of the Southern Ocean, Earth and Planetary Science Letters, 147, 83-92, 1997.

Scully, N.M., D.J. McQueen, D.R.S. Lean, and W.J. Cooper, Hydrogen peroxide formation: The interaction of ultraviolet radiation and dissolved organic carbon in lake waters along a 43-75 degrees N gradient, Limnology and Oceanography, 41 (3), 540-548, 1996.

Weller, R., and O. Schrems, H2O2 in the Marine Troposphere and Seawater of the Atlantic Ocean, Geophysical Research Letters, 20, 125-128, 1993.

Wong, G.T.F., W.M. Dunstan, and D.B. Kim, The decomposition of hydrogen peroxide by marine phytoplankton, Oceanologica Acta, 26 (2), 191-198, 2003.

Yocis, B.H., D.J. Kieber, and K. Mopper, Photochemical production of hydrogen peroxide in Antarctic Waters,, Deep Sea Research Part I : Oceanographic Research, 47(6), 1077-1099, 2000.

Yuan, J., and A.M. Shiller, Determination of Subnanomolar Levels of Hydrogen Peroxide in Seawater by Reagent-Injection Chemiluminescence Detection, Analytical Chemistry, 71, 1975-1980, 1999.

Yuan, J., and A.M. Shiller, The distribution of hydrogen peroxide in the southern and central Atlantic ocean, Deep-Sea Research II, 48, 2947-2970, 2001.

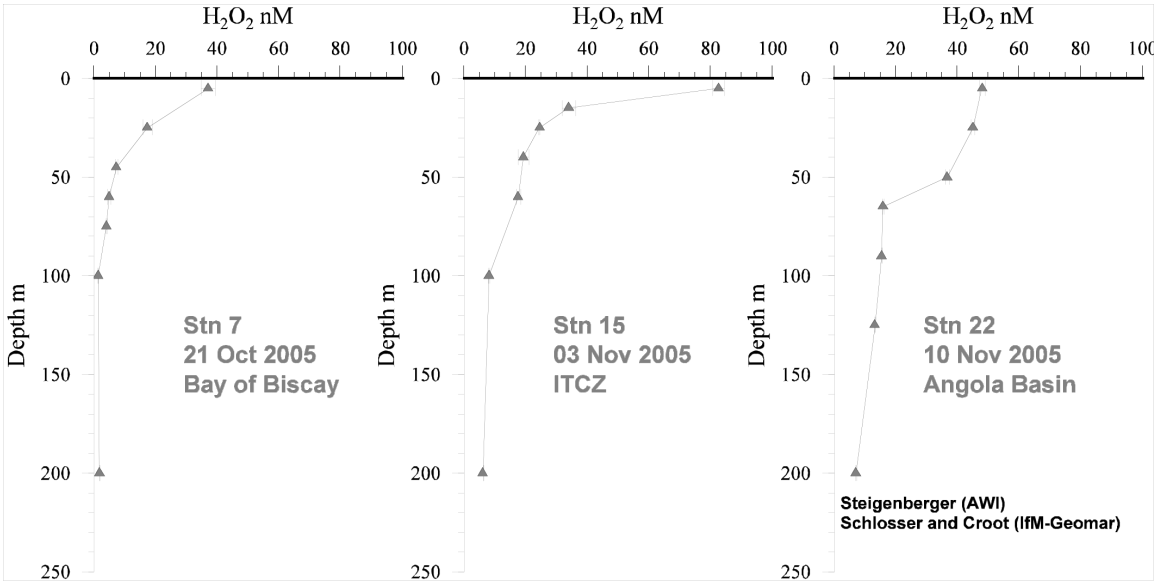

Fig. 4.6: The vertical distribution of H_2O_2 from some representative stations during ANT-XXIII/1. Of particular note is the strong mixing in the upper water column in the Angola Basin and the rain impacted surface waters of the ITCZ.

4.10 Dissolved germanium in the Atlantic Ocean: a germane element for German geotraces

Peter Croot
IFM- GEOMAR
not on board: M. Ellwood, National Institute for Water and Atmosphere (NIWA), New Zealand

Objectives

Germanium (Ge) is a metalloid and exists in seawater primarily as Ge(OH)4, in a dissolved form analogous to nutrient silicon, Si(OH)4 (silicic acid). Ge has a similar nutrient-type profile to Si in the ocean as organisms which use silicon in their skeletons (Diatoms etc.) have only a small discrimination between Ge and Si. Similarly to Si, Ge shows similar inter-ocean differences in concentrations. Even though the bulk of oceanic Ge follows the silicon cycle, small differences exist that are useful to oceanographers. Thus the Ge:Si ratio in seawater can provide useful information on processes affecting the Ge and Si cycles. In the present work we obtained samples to examine the deep water distribution of Ge at a number of stations along the ANT-XXIII/1 transect in the Atlantic Ocean. This data will be used to examine what drives changes in the ratio between Ge and Si in the present day ocean and thus allow a test of the validity of the use of Ge/Si ratios in sediments as paleo proxies for productivity and Silicate utilization.

Work at sea

Samples were collected from the CTD rosette and filtered through 0.45 μm syringe filters before being shipped to New Zealand for analysis in the laboratory of Dr. Michael Ellwood (NIWA). During ANT-XXIII/1, samples from 4 deep water stations were sampled for Germanium:

Bay of Biscay
Northern Dust Station
Southern Dust Station
Cape Basin

4.11 Mercury distribution in Eastern Atlantic surface waters and the calibration of methods in the framework of geotraces

Ursula Hennings
Institut für Ostseeforschung (IOW)
not on board: Pohl, IOW

Objectives
On the *Polarstern* cruise ANT-XXIII/1 samples were taken to study two main objectives:

- sampling and determination of mercury (Hg) in the surface water of the eastern Atlantic Ocean by high frequency under consideration of the main oceanic regimes and meteorological systems, including an oceanic region which is affected by high Saharan dust deposition;

- to calibrate our sample handling and analytical methods for trace elements like Cd, Pb, Cu, Zn, Ni, Co, Mn, Fe with the sample handling and analytical methods of colleagues from the national and international GEOTRACES community.

Work at sea
Surface water samples for the determination of Hg and Cd, Pb, Cu, Zn, Ni, Co, Mn, Fe were collected in a high frequency with a “Clean water sampling Fish” provided by IFM-GEOMAR between the cruise transect Vigo – Cape Town. Samples were taken three times and in the dust input region of North West Africa four times a day.

Besides the sampling of surface water, two depth profiles for the direct determination of Hg with 20 and one depth profile with samples from 17 depth horizons were taken by CTD/rosette.

Mercury concentrations were directly analysed on board of RV *Polarstern* by using cold vapour technique with mercury amalgamation and enrichment on a gold net and the determination by fluorescence detection.

For the determination of the other metals (Cd, Pb, Cu, Zn, Ni, Co, Mn, Fe), 120 samples were divided in unfiltered and filtered samples, acidified and stored. Analyses will be carry out in the home laboratory.

Preliminary results
First results show that the concentrations of mercury in the surface water are ranging on a very low level between 1,0 and 4,0 pmol/l. The slightly enhanced concentrations were observed in the region of North West Africa and are possibly due to the atmospheric dust input by trade winds from the North African desserts.

A detailed analysis of the data will be carried out in the laboratory of the Baltic Sea Research Institute, by a partly repetition of sample measurements.

4.12 Selected persistent organic pollutants (POPs) in air and water

Armando Caba[1)], Annika Jahnke[1)], Rosalinda Gioia[2)], Luca Nizzetto[3)],

[1)]GKSS Forschungszentrum Geesthacht
[2)]University Lancaster
[3)]University Insubria/University Rhode Island

Objectives

Several leading groups of Environmental Chemistry joined the RV *Polarstern* during the first cruise leg of expedition ANT-XXIII from 13 October to 17 November 2005. Their common interest was the determination of trace organic contaminants in moderate latitudes of the Northern and Southern Hemisphere in order to further investigate the circulation, fate and behaviour of these global key contaminants.

RV *Polarstern* had been shown to be well suited for the sampling of these trace compounds. The chemical measurement programme during ANT-XXIII/1 concentrated on the determination of selected POPs in air and water. The contaminants which are investigated can be subdivided into two major groups:

1. The „classical“ POPs like polychlorinated dibenzodioxins and -furans (PCDD/Fs) as well as polycyclic aromatic hydrocarbons (PAHs) which are formed during combustion processes, polychlorinated biphenyls (PCBs) used in transformers, and selected organochlorine pesticides,

2. „new“ and emerging POPs like the polybrominated diphenylether (PBDEs) flame retardants and polyfluorinated compounds (PFCs).

By combining short-term atmospheric samples with the collection of representative water samples across different regions of the Atlantic, answers are sought as to whether atmospheric transport or the marine phytoplankton productivity are controlling the transport and settling flux of POPs.

POPs such as polychlorinated biphenyls (PCBs), polybrominated diphenyl ethers (PBDEs), organochlorine pesticides (HCHs, HCBs, DDTs etc.), polyflourinated compounds (PFCs), and combustion-derived polychlorinated dibenzo-p-dioxins/furans (PCDD/Fs) are investigated. The overall ship’s track from the North Sea into the Cape Basin implies a great opportunity to monitor the air concentrations of POPs from source regions to remote areas as well as the exchange of pollutants between the Northern and Southern hemisphere. We expect to see spatial trends in air concentrations that provide some evidence for the global fractionation theory. It is generally assumed that the atmosphere can serve as pathway for the delivery of these pollutants to water and terrestrial surfaces. Therefore, POPs can undergo long-range atmospheric transport (LRAT) with high volatile compounds condensing in colder (polar) regions and less volatile compounds condensing in warmer regions close to sources. This will probably not occur in one step, but in a number of steps of volatilization followed by deposition, according to seasonal fluctuations in temperature. The effect of this will be a relative enrichment of the more volatile compounds in cold areas, while less volatile compounds are enriched in moderate

latitudes. Criteria for global fractionation behaviour of chemicals are various physical-chemical properties such as vapour pressure, the octanol-air partition coefficient (K_{OA}), the octanol-water partition coefficient (K_{OW}) and the Henry's Law Constant.

PCBs are a class of compounds with a variety of different physical-chemical properties. There are 209 congeners relative to the number of chlorine atoms on the molecule and the position that these atoms occupy. Therefore, with all these differences in physical-chemical properties, PCBs are ideal to investigate and find evidence of the global fractionation theory. These properties are very dependent on temperature and will therefore greatly influence the global transport of POPs.

Growth in interest on PBDE flame retardants has been as exponential as their apparent increase in the environment over the past 20-25 years in North America and Europe. Toxicological studies of limited PBDE congeners indicate that they are potential thyroid disruptors and developmental neurotoxicants. However, there is still very little information on PBDE contamination and its spatial trend over the regions of the world. The investigation which follows air sample collection on RV *Polarstern* will attempt to comprehensively understand the spatial and temporal trend of contamination by PBDEs in the atmosphere.

Polyfluorinated organic acids and their derivatives are produced by industry in very large quantities and are used for many purposes. Perfluoroalkyl sulfonates are used as surfactants and for surface treatment in carpets, leather, paper, packaging and upholstery. In addition, some sulfonated and carboxylated PFCs have been used in or as fire-fighting foams, paints, alkaline cleaners, shampoos, and insecticide formulations. Due to the large production quantities and the persistence in the environment, polyfluorinated compounds are meanwhile globally distributed. Perfluorooctanesulfonic acid (PFOS) and perfluorinated carboxylic acids such as perfluorooctanoic acid (PFOA) have been detected in organisms from remote locations such as in blood of ringed seals, polar bears, mink, birds and fishes as well as in human blood.

Due to the findings of PFCs in numerous biota samples, it is of special interest to investigate their long-range transport. Two transportation processes from sources to remote locations have been proposed: On the one hand, PFCs could be transported by means of oceanic currents in the water phase due to their high polarity, especially since some of the PFCs have been found in North Sea and Arctic sea water. On the other hand, some precursors of perfluorinated sulfonic and carboxylic acids are highly volatile and can lead to an increased input of PFCs from the atmosphere. The investigation of the wide scale distribution of perfluorinated acids in the sea water of the North Sea and Atlantic Ocean is an ideal complementation to the simultaneous measurements in the atmosphere. ANT-XXIII/1 was especially suitable for these investigations as this cruise leg ranged from the likely sources (European continent) to remote areas where direct inputs are lacking.

Work at sea

Air sampling

Two different high-volume air samplers (Hi-Vols) were used to collect air on board of RV *Polarstern* during ANT-XXIII/1. Totally, more than 160 air samples were collected on the cruise track from Bremerhaven to Cape Town (see Table 4.1 to Table 4.3). Table 4.1 shows samples collected using the Lancaster University Hi-Vols, which will

be used to determine PCB and PBDE concentrations. Table 4.2 represents samples collected using the Hi-Vols from University of Rhode Island (URI) and Arizona State University, respectively, and the samples collected for the determination of TSP (Total Suspended Particulate) using a TSP sampler belonging to Lancaster University. Samples from the URI Hi-Vol will be used to investigate the concentration of PCDD/Fs in the atmosphere. Table 4.3 shows sampling volumes and locations for the samples taken with the GKSS Hi-Vols in order to determine PFCs in air.

Tabl. 4.1: Sample collection with the Lancaster Hi-Vols during ANT-XXIII/1

Sample I.D.	Sample Duration (mins)	Air Vol. (m^3)	LAT	LONG
ANT K1	720	124	50°50.035-50°4.3 N	1°0.5E-2°2.9 W
ANT R1	720	156	50°50.035-50°4.3 N	1°0.5E-2°2.9 W
ANT K2	729	154	50 °2.0 -49° 12.0 N	2°40.24-5° 3.9 W
ANT R2	729	164	51 °2.0 -49° 12.0 N	2°40.24-5° 3.9 W
ANT K3	692	154	49° 9.1 - 47° 18.47N	5° 11.29- 5 °49.84 W
ANT R3	693	155	49° 9.1 - 47° 18.47N	5° 11.29- 5 °49.84 W
ANT K4	585	129	47° 9.1-46° 24.16N	5° 41.33-5°54.39 W
ANT R4	585	129	47° 9.1-46° 24.16N	5° 41.33-5°54.39 W
Biscay 1	2065	467	46° 24.11-46° 1.84 N	5° 54.89- 6 21.24 W
ANTR5	180	41	45° 38.86-45° 34.98 N	4° 30.43-5° 25.52 W
ANTK5	180	40	45° 38.86-45° 34.98 N	4° 30.43-5° 25.52 W
ANT R6	700	153	44° 8.4-42°51.00 N	8° 41.76- 10° 5.6 W
ANT K6	707	153	44° 8.4-42°51.00 N	8° 41.76- 10° 5.6 W
ANT R7	800	179	40° 26.7- 38° 3.34 N	10° 14.5 - 11° 40.36 W
ANT K7	800	177	40° 26.7- 38° 3.34 N	10° 14.5 - 11° 40.36 W
ANT R8	0	NA		
ANT K8	625	131	38° 2.52 - 36° 21.76 N	11° 40.88 - 12° 44.98 W
ANT R9	844.2	191	32° 45.05 - 30° 19.80 N	14° 59.87- 16° 27.12 W
ANT K9	843	186	32° 45.05 - 30° 19.80 N	14° 59.87- 16° 27.12 W
ANT R10	380.4	86	30° 15.73 - 29° 0.1 N	16° 26.54 - 15° 54.12 W
ANT K10	587.4	128	30° 15.73 - 28°17.75 N	16° 26.54 - 15 °24.77W
NO DATA				
ANT K11	707.4	154	28° 17.15 - 26° 10.95N	15° 24.04 - 17° 8.0 W
ANT R12	583.2	136	25° 59.87- 24° 36.53N	17° 20.44- 18° 53.08 W
ANT K12	606	127	25° 59.87- 24° 36.53 N	17° 20.44- 18° 53.08 W
ANT R13	580.8	131	24° 34.66 - 22° 30.69 N	18° 55.21 - 20° 29.54 W
ANT K13	579	122	24° 34.66 - 22° 30.70 N	18° 55.21 - 20° 29.55 W
ANT R14	677.4	152	22° 30.02 - 21° 36.22 N	20° 29.85 - 20°.51.37 W
ANT K14	677.4	147	22° 30.02 - 21° 36.22 N	20° 29.85 - 20°.51.37 W
ANT R 15	763.2	167	21° 36.01 - 19° 6.7 N	20° 51.47 -20° 54.60 W
ANT K 15	744	155	21° 36.01 - 19° 6.7 N	20° 51.47 -20° 54.60 W
ANT R 16	674.4	147	19° 5.9 - 17° 6.4 N	20° 54.63 -20° 57.09 W
ANT K 16	674.4	144	19° 5.9 - 17° 6.4 N	20° 54.63 -20° 57.09 W
ANT R 17	769.2	174	17° 5.9 - 14° 36.47 N	20° 57.10 -20° 58.17 W
ANT K 17	769.2	160	17° 5.9 - 14° 36.47 N	20° 57.10 -20° 58.17 W
ANT R 18	720	161	14° 35.34 - 12° 31.39 N	20° 57.93 - 20° 31.72 W
ANT K 18	720	153	14° 35.34 - 12° 31.39 N	20° 57.93 - 20° 31.72 W
ANT R 19	703.2	154	12° 30.26 - 10° 37.39 N	20° 31.48 - 20° 7.9 W

Sample I.D.	Sample Duration (mins)	Air Vol. (m^3)	LAT	LONG
ANT K 19	703.2	145	12° 30.26 - 10° 37.39 N	20° 31.48 - 20° 7.9 W
NO DATA 02/11/05 SHIP STOPPED AT STATION/WIND SPEED VERY LOW AROUND 1 m/s / NO DAY SAMPLE				
NO DATA 02/11/05 SHIP STOPPED AT STATION/WIND SPEED VERY LOW AROUND 1 m/s / NO DAY SAMPLE				
ANT R 20	680.4	156	9° 17.10 - 7° 30.18 N	19° 23.80 - 17° 53.65 W
ANT K 20	710.4	154	9° 17.10 - 7° 30.18 N	19° 23.80 - 17° 53.65 W
ANT R 21	431.4	99	7° 29.15 -6° 9.3 N	17° 53.09 - 16° 46.30 W
ANT K 21	431.4	94	7° 29.15 -6° 9.3 N	17° 53.09 - 16° 46.30 W
ANT R 22	655.2	141	6° 8.92 - 4°13.66 N	16° 45.52 - 15° 9.71 W
ANT K 22	654	141	6° 8.92 - 4°13.66 N	16° 45.52 - 15° 9.71 W
ANT R 23	555	128	4° 11.33 - 2° 54.55 N	15° 7.77 - 14° 4.1 W
ANT K 23	549	119	4° 11.33 - 2° 54.55 N	15° 7.77 - 14° 4.1 W
ANT R 24	718.2	161	2° 54.24 - 1° 4.44 N	14° 3.86 - 12° 38.44 W
ANT K 24	718.2	155	2° 54.24 - 1° 4.44 N	14° 3.86 - 12° 38.44 W
ANT R 25	723	167	1° 3.7N - 0° 28.43 S	12° 37.87 - 11° 26.21 W
ANT K 25	723	159	1° 3.7N - 0° 28.43 S	12° 37.87 - 11° 26.21 W
ANT R 26	703.8	160	0° 28.57 - 1° 25.73 S	11° 26.09 - 10° 41.655 W
ANT K 26	699	149	0° 28.57 - 1° 25.73 S	11° 26.09 - 10° 41.655 W
ANT R 27	711	162	1° 26.03 - 2° 54.60 S	10° 41.42 - 9° 32.49 W
ANT K 27	711	156	1° 26.03 - 2° 54.60 S	10° 41.42 - 9° 32.49 W
ANT R 28	711	160	2° 55.76 - 4° 37.72 S	9° 31.59 - 8° 12.23 W
ANT K 28	711	157	2° 55.76 - 4° 37.72 S	9° 31.59 - 8° 12.23 W
ANT R 29	726	152	4° 38.19 - 6° 21.45 S	8° 11.79 - 6° 51.11 W
ANT K 29	726	161	4° 38.19 - 6° 21.45 S	8° 11.79 - 6° 51.11 W
ANT R 30	717	164	6° 21.89 - 8° 6.60 S	6° 50.77 - 5° 28.69 W
ANT K 30	716.4	158	6° 21.89 - 8° 6.60 S	6° 50.77 - 5° 28.69 W
ANT R 31	699	161	8° 7.03 - 9° 32.39 S	5° 28.35 - 4° 21.18 W
ANT K 31	699	155	8° 7.03 - 9° 32.39 S	5° 28.35 - 4° 21.18 W
ANT R 32	726	163	9° 33.10 - 11° 18.98 S	4° 21.18 - 2° 56.91 W
ANT K 32	726	161	9° 33.10 - 11° 18.98 S	4° 21.18 - 2° 56.91 W
ANT R 33	730.86	169	11° 19.43 - 11° 51.79 S	2° 56.56 - 2° 30.34 W
ANT K 33	729	156	11° 19.43 - 11° 51.79 S	2° 56.56 - 2° 30.34 W
ANT R 34	700.2	157	11° 51.79 - 13° 32.36 S	2° 30.84 - 1° 10.70 W
ANT K 34	699	147	11° 51.79 - 13° 32.36 S	2° 30.84 - 1° 10.70 W
ANT R 35	709.2	166	13° 34.24 - 15° 9.98 S	1° 9.19 W - 0° 7.6 E
ANT K 35	706.2	156	13° 34.24 - 15° 9.98 S	1° 9.19 W - 0° 7.6 E
ANT R 36	726	164	15° 10.42 - 17° 1.16 S	0° 8.0 - 1° 37.64 E
ANT K 36	724.8	162	15° 10.42 - 17° 1.16 S	0° 8.0 - 1° 37.64 E
ANT R 37	735	173	17° 1.4 - 18° 38.78 S	1° 37.88 - 2° 57.36 E
ANT K 37	735	161	17° 1.4 - 18° 38.78 S	1° 37.88 - 2° 57.36 E
ANT R 38	687	156	18° 39.23 - 20° 20.30 S	2° 57.72 - 4° 21.10 E
ANT K 38	687	154	18° 39.23 - 20° 20.30 S	2° 57.72 - 4° 21.10 E
ANT R 39	ND	ND	20° 21.94 - 21° 53.24S	ND
ANT K 39	688.2	158	20° 21.94 - 21° 53.24S	4° 22.47 -5° 38.55 E
ANT R 40	660	146	21° 54.42 - 23° 46.50 S	5° 39.53 - 7° 14.11 E
ANT K 40	740.4	159	21° 54.42 - 23° 46.50 S	5° 39.53 - 7° 14.11 E
ANT R 41	698.4	152	23° 46.95 - 25° 0.05 S	7° 14.50 - 8° 16.93 E
ANT K 41	699	153	23° 46.95 - 25° 0.05 S	7° 14.50 - 8° 16.93 E
ANT R 42	723	152	25°.0.05 - 25° 22.27 S	8° 16.93 - 8° 41.85 E
ANT K 42	725.4	152	25°.0.05 - 25° 22.27 S	8° 16.93 - 8° 41.85 E

Sample I.D.	Sample Duration (mins)	Air Vol. (m^3)	LAT	LONG
ANT R 43	664.2	147	25° 23.91 - 26° 29.44 S	8° 43.68 - 9° 57.99 E
ANT K 43	664.2	143	25° 23.91 - 26° 29.44 S	8° 43.68 - 9° 57.99 E
ANT R 44	687	157	26° 29.57 - 27° 57.06 S	9° 58.12 - 11° 38.30 E
ANT K 44	687	142	26° 29.57 - 27° 57.06 S	9° 58.12 - 11° 38.30 E
9 FIELD BLANKS				

Tab. 4.2: Sample collection using the URI and Arizona State University Hi-Vols and the TSP sampler during ANT-XXIII/1

Date	Dioxine/Furans sampling		TSP sampling		Mean Latitude	Mean Longitude	Mean Air temp. (°C)	Type *
	Sample ID	Total Vol. (m^3)	Sample	Total Vol. (m^3)				
14-Oct-05	Diox/Furans 1	490	TSP 1	702	50 28.09 N	0 15.81 W	16.52	D
15-Oct-05	Diox/Furans 2	545	TSP 2	781	49 43.69 N	3 45.64 W	15.75	D
15-Oct-05	Diox/Furans 3	477	TSP 3	683	48 23.95 N	6 12.71 W	14.83	C
16-Oct-05	Diox/Furans 4	235	TSP 4	337	46 43.45 N	5 26.43 W	14.36	C
16-Oct-05	Diox/Furans 5	512	TSP 5	733	46 24.53 N	5 54.12 W	14.21	D
17-Oct-05	Diox/Furans 6	497	TSP 6	712	46 2.15 N	6 29.03 W	16.3	C
17-Oct-05	Diox/Furans 7	491	TSP 7	703	46 18.36 N	5 55.73 W	16.49	C
18-Oct-05	Diox/Furans 8	487	TSP 8	697	45 51.02 N	6 35.90 W	15.74	D
18-Oct-05	Diox/Furans 9	551	TSP 9	789	45 49.98 N	4 33.01 W	15.64	D
19-Oct-05	Diox/Furans 10	498	TSP 10	713	46 13.00 N	4 5.69 W	16.33	D
19-Oct-05	Diox/Furans 11	260	TSP 11	373	45 52.91 N	4 40.46 W	16.18	D
21-Oct-05	Diox/Furans 12	468	TSP 12	670	45 54.98 N	4 35.49 W	16.74	C
25-Oct-05	Diox/Furans 13	573	TSP 13	820	39 12.77 N	10 55.37 W	18.94	C
26-Oct-05	Diox/Furans 14	349	TSP 14	499	37 30.16 N	12 1.60 W	20.34	C
27-Oct-05	Diox/Furans 15	483	TSP 15	691	33 25.96 N	14 34.87 W	20.28	C
27-Oct-05	Diox/Furans 16	441	TSP 16	631	31 41.29 N	15 38.45 W	21.4	C
28-Oct-05	Diox/Furans 17	471	TSP 17	675	29 49.64 N	16 29.07 W	22.4	C
28-Oct-05	Diox/Furans 18	481	TSP 18	688	27 31.11 N	15 37.79 W	22.29	C
29-Oct-05	Diox/Furans 19	431	TSP 19	617	23 24.80 N	19 49.21 W	24.54	C
29-Oct-05	Diox/Furans 20	706	TSP 20	1011	20 42.66 N	20 52.59 W	24.66	D
30-Oct-05	Diox/Furans 21	493	TSP 21	705	18 24.65 N	20 55.48 W	25.26	D
31-Oct-05	Diox/Furans 22	446	TSP 22	639	18 24.65 N	20 55.48 W	26.03	D
31-Oct-05	Diox/Furans 23	542	TSP 23	776	16 14.97 N	20 58.15 W	28.12	D
01-Nov-05	Diox/Furans 24	470	TSP 24	674	13 48.07 N	20 47.91 W	28.77	D
01-Nov-05	Diox/Furans 25	388	TSP 25	556	11 23.86 N	20 17.52 W	29.11	D
02-Nov-05	Diox/Furans 26	355	TSP 26	508	8 26.63 N	18 41.35 W	29.22	C
03-Nov-05	Diox/Furans 27	240	TSP 27	344	7 1.47 N	17 28.70 W	29.2	C
03-Nov-05	Diox/Furans 28	432	TSP 28	618	4 25.01 N	15 19.16 W	28.67	C
04-Nov-05	Diox/Furans 29	384	TSP 29	550	2 1.98 N	13 23.18 W	27.43	C
05-Nov-05	Diox/Furans 30	340	TSP 30	487	0 20.14 N	12 4.00 W	26.55	C
05-Nov-05	Diox/Furans 31	394	TSP 31	564	0 41.74 S	11 15.83 W	25.92	C
06-Nov-05	Diox/Furans 32	413	TSP 32	592	2 9.24 S	10 8.20 W	26.05	C
06-Nov-05	Diox/Furans 33	438	TSP 33	627	3 44.82 S	8 53.38 W	25.03	C
07-Nov-05	Diox/Furans 34	389	TSP 34	557	5 25.54 S	7 33.04 W	24.46	C

Date	Dioxine/Furans sampling		TSP sampling		Mean Latitude	Mean Longitude	Mean Air temp. (°C)	Type *
	Sample ID	Total Vol. (m^3)	Sample	Total Vol. (m^3)				
07-Nov-05	Diox/Furans 35	377	TSP 35	539	7 9.52 S	6 13.47 W	24.16	C
08-Nov-05	Diox/Furans 36	387	TSP 36	554	8 47.67 S	4 58.69 W	23.32	C
08-Nov-05	Diox/Furans 37	467	TSP 37	668	10 14.39 S	3 48.05 W	22.58	C
09-Nov-05	Diox/Furans 38	342	TSP 38	490	11 51.81 S	2 30.73 W	22.17	C
09-Nov-05	Diox/Furans 39	414	TSP 39	593	12 41.34 S	1 51.44 W	21.66	C
10-Nov-05	Diox/Furans 40	402	TSP 40	576	14 22.55 S	0 30.50 W	20.61	C
10-Nov-05	Diox/Furans 41	538	TSP 41	770	16 10.63 S	0 56.61 E	19.54	C
11-Nov-05	Diox/Furans 42	436	TSP 42	624	17 51.64 S	2 18.81 E	19.14	C
11-Nov-05	Diox/Furans 43	504	TSP 43	722	19 31.13 S	3 40.38 E	18.86	C
12-Nov-05	Diox/Furans 44	478	TSP 44	684	21 10.88 S	5 3.16 E	18.96	C
13-Nov-05	Diox/Furans 45	343	TSP 45	491	25 0.25 S	8 17.06 E	18.17	C
14-Nov-05	Diox/Furans 46	435	TSP 46	623	25 54.30 S	9 18.04 E	18.3	C

Tab. 4.3: Sample collection with the GKSS Hi-Vols during ANT-XXIII/1

	START				STOP				
Sample	Date	UTC	Lat	Long	Date	UTC	Lat	Long	Volume
ANTXXIII-1_01	20051013	19.40h	54°7,95 N	5°33,46 E	20051016	17.38h	46°24,45 N	5°55,00 W	954,4
ANTXXIII-1_02	20051013	19.30h	54°8,09 N	5°36,78 E	20051016	17.20h	46°24,47 N	5°55,05 W	993,1
ANTXXIII-1_03	20051016	18.14h	46°24,43 N	5°54,89 W	20051019	16.25h	45°54,39 N	4°31,74 W	944,0
ANTXXIII-1_04	20051016	18.08h	46°24,47 N	5°54,89 W	20051019	16.25h	45°54,39 N	4°31,74 W	1218,1
ANTXXIII-1_05	20051019	17.03h	45°56,51 N	4°24,76 W	20051021	11.00h	45°51,78 N	4°37,91 W	834,8
ANTXXIII-1_06	20051019	17.07h	45°57,03 N	4°24,00 W	20051021	11.00h	45°51,78 N	4°37,91 W	671,9
ANTXXIII-1_07	20051025	13.15h	41°13,94 N	9°50,40 W	20051025	13.25h	41°13,00 N	9°52,26 W	Field blank
ANTXXIII-1_08	20051025	13.15h	41°13,94 N	9°50,40 W	20051025	13.25h	41°13,00 N	9°52,26 W	Field blank
ANTXXIII-1_09	20051025	19.52h	40°7,32 N	10°25,10 W	20051028	09.24h	30°14,71 N	16°30,16 W	967,0
ANTXXIII-1_10	20051028	10.11h	30°6,65 N	16°34,93 W	20051031	12.04h	18°31,74 N	20°55,34 W	1011,8
ANTXXIII-1_11	20051028	10.15h	30°5,95 N	16°35,33 W	20051031	12.10h	18°30,56 N	20°55,35 W	1618,0
ANTXXIII-1_12	20051031	12.33h	18°26,02 N	20°55,44 W	20051103	22.07h	5°58,14 N	16°36,89 W	1399,2
ANTXXIII-1_13	20051031	12.36h	18°25,44 N	20°55,46 W	20051103	22.12h	5°57,35 N	16°36,25 W	1787,6
ANTXXIII-1_14	20051103	22.41h	5°52,88 N	16°32,50 W	20051107	08.04h	4°46,39 S	8° 5,37 W	1370,3
ANTXXIII-1_15	20051103	22.45h	5°52,26 N	16°31,99 W	20051107	08.09h	4°47,11 S	8°4,81 W	1610,4
ANTXXIII-1_16	20051108	10.20h	8°32,53 S	5°8,32 W	20051111	12.16h	17°43,04 S	2°11,73 E	1121,9
ANTXXIII-1_17	20051108	10.28h	8°33,66 S	5°7,43 W	20051111	12.20h	17°43,65 S	2°12,22 E	1322,4
ANTXXIII-1_18	20051111	12.46h	17°47,47 S	2°15,33 E	20051114	12.32h	25°55,68 S	9°19,59 E	1173,4
ANTXXIII-1_19	20051111	12.48h	17°47,76 S	2°15,57 E	20051114	12.39h	25°56,49 S	9°20,47 E	1208,3
ANTXXIII-1_BL1	20051013	19.50h	54°7,76 N	5°30,13 E	20051103	22.21h	5°55,96 N	16°35,07 W	Blank
ANTXXIII-1_BL2	20051016	18.20h	46°24,38 N	5°54,87 W	20051021	11.00h	45°51,78 N	4°37,91 W	Blank
ANTXXIII-1_BL3	20051103	22.53h	5°51,03 N	16°30,96 W	20051114	12.37h	25°56,25 S	9°20,23 E	Blank

Glass Fiber Filters (GFFs) precombusted at 450°C overnight were used to capture the particles and particle-bound species, and two cylindrical 3-inch-diameter polyurethane foam (PUF) adsorbants were used downstream to capture the gas-phase contaminants. Prior to use, the PUFs for the Lancaster and URI Hi-Vols were cleaned with an Accelerated Solvent Extraction (ASE) system using dichloromethane (DCM) as solvent. After cleaning, the PUFs were desiccated under vacuum to remove excess solvent and stored frozen in pre-cleaned aluminum tins. The PUF adsorbant and XAD-2 resin for PFCs sampled with the GKSS Hi-Vols were

precleaned by Soxhlet extraction with methanol and ethyl acetate. After sample collection, GFFs and PUFs / XAD-2 resin were sealed and stored frozen until analysis. As low concentration levels are expected to be found in remote regions, all the pre-cleaning procedures were performed in clean room facilities at Lancaster University and GKSS.

Short-term air samples (12 hours) were collected on the cruise track from Bremerhaven to Cape Town. These samples are useful to investigate the day-night cycle of PCBs over the ocean and whether the marine phytoplankton is controlling the atmospheric concentrations of POPs in the marine atmosphere. Concerning volatile PFCs, sampling took 3 days because of the expected extremely low concentrations. All the laboratory extractions, clean-up and analyses will be performed in clean room facilities at Lancaster University, UK, and GKSS-Research Centre in Geesthacht, Germany. Field blanks were collected in order to define blank-based limits of detection (LODs) and limits of quantification (LOQs) for each sampling matrix (PUF, XAD-2 and GFF) as the average contaminant mass of field blanks plus 3 standard deviations.

Passive air sampling

Ten passive air samplers were deployed on board of the ship to look at the ship background concentrations of POPs. Duplicate passive samplers for classical as well as new and emerging POPs were deployed on the observation deck near the Hi-Vols, in the GKSS container where matrices are treated before and after sampling, on the back of the ship, in the -25º C freezer where air samples are stored and in the wet lab, where water sampling is performed. Polyurethane Foam (PUF) samplers are used to passively sample air. The advantage of passive samplers compared with active samplers is that they are cheap because they are not power consuming and they are easy to deploy. The surface of the PUF comes into contact with vapour phase species in the atmosphere and it will respond through three different steps:

- **Initial linear** uptake of the compound to the surface
- **Curvilinear portion** of the uptake as equilibrium is approaching
- **Equilibrium** between the air concentration and the surface.

The mass of the compound held by the surface when it is at equilibrium with the air will depend on temperature, the type of the surface and the physico-chemical properties of the respective POPs. The uptake is also influenced by the size or capacity of the subsurface compartment, the suface area and the thickness of the sampler. These factors above can be varied depending on the compound of interest, the deployment/sampling time and the sensitivity of the analytical instrumentation. Time to reach equilibrium with the sampler device vary between compounds and increases with K_{OA}.

Previous studies on RV *Polarstern* where passive samplers were also deployed showed that the ship does not contribute to PCB contamination and this allowed us to conduct research on POPs on this research vessel even at very low concentrations. We expect to see the same results about the ship background contamination during this cruise leg.

Water sampling

Daily water sampling was performed simultaneously to the air sampling in order to investigate the mechanisms controlling the air-water exchange flux. The water samples were taken from the clean seawater system (stainless steel pipe / Klauss pump) of RV *Polarstern* (11 m depth).

The majority of samples have been extracted with solid-phase adsorber columns based on styrene/divinylbenzole copolymer, while a number of 0.5 l (deep) water samples are taken to the clean laboratories for extraction and analysis. A mixture of deuterated internal standards are added prior to extraction to control the extraction efficiency and to calculate the concentrations of the observed contaminants. Sample volumes of 10 or 20 liters, respectively, were used for extraction to compare different factors of preconcentration. After pumping the seawater through the columns they were rinsed with precleaned Milli-Q water and dried. Elution will be done after the cruise in the land-based clean laboratory. One part of the replicate samples will be processed and determined by the Federal Maritime Agency (BSH, Hamburg, Germany), while the other samples will be analysed at the Norwegian Institute for Air Research (NILU, Tromsoe, Norway).

Tabl. 4.4: Water sample collection (Lancaster University / URI) during ANT-XXIII/1

Sampling ID	Total volume (L)	Latitude	Longitude
WAT 1 15.10	517	49°37.05- 48° 48.69N	3° 59.13 5° 53.43 W
WAT 2 22.10	659	44°7.6-42°52.70 N	8° 43.60-10°6.73 W
WAT 3 26.10	792	37° 52.189- 36° 5.2 N	11° 47.579 -12° 55.51 W
WAT 4 28.10	588	30° 9.981 - 28° 27.65 N	16° 32.958 - 15° 31.35 W
WAT 5 29.10	721	26° 0.9 - 24° 46.72 N	17° 20.13 - 18° 41.79 W
WAT 6 31.10	731	18° 47.84612 - 17° 5.51 N	20° 55.00351 - 20° 57.10 W
WAT 7 03.11	970	7° 15.47 - 5° 34.54 N	17° 41.63 - 16° 17.18 W
WAT 8 05.11	789	0° 57.03 N - 0° 37.35 S	12° 32.71 - 11° 19.26 W
WAT 9 05-06.11	856	0° 39.47 - 1° 28.93 S	11° 17.62 - 10° 39.15 W
WAT 10 06.11	639	1° 32.53 - 2° 59.39 S	10° 36.35- 9° 31.59 W
WAT 11 06-07	784	3° 0.56 - 4° 42.10 S	9° 27.85 - 8° 8.87 W
WAT 12 08.11	897	8° 13.49 - 9° 49.55 S	5° 23.29 - 4° 7.65 W
WAT 13 10.11	819	13° 42.16 - 15° 20.63 S	1° 2.88W - 0° 16.22 E
WAT 14 12.11	628	20° 26.75 - 22° 14.41 S	4° 26.43 - 5° 56.4 E
WAT 15 13.11	830	23° 52.72 - 25° 0.07 S	7° 19.40 - 8° 16.90 E
4 Field blanks			

Tab. 4.5: Water sample collection (GKSS) during ANT-XXIII/1

Sample name	Date	UTC	Lat.	Long.	Temp. K	Sal. K	#	Blanks	Std. add.	NILU	CTD
ANTXXIII-1_NEP001ff	20051015	11.24h	49°44,533´N	3°41,167´W	15.7	35.27	3			2	
ANTXXIII-1_NEP004ff	20051016	06.55h	47°26,852´N	5°55,999´W	15.8	35.48	4			1	2
ANTXXIII-1_NEP008ff	20051017	06.33h	46°23,946´N	5°55,449´W	17.1	35.60	4			1	
ANTXXIII-1_NEP012ff	20051018	06.35h	46°6,446´N	6°14,381´W	17.6	35.64	4	1		1	
ANTXXIII-1_NEP017ff	20051019	06.11h	45°53,297´N	4°40717´W	18.5	35.55	4	1		1	
ANTXXIII-1_NEP022ff	20051020	06.42h	45°44,918´N	5°31,621´W	18.4	35.71	4	2		1	5
ANTXXIII-1_NEP028ff	20051021	06.30h	45°49,533´N	4°40,447´W	18.2	35.58	4			1	
ANTXXIII-1_NEP032*ff	20051022	06.28h	44°36,782´N	7°39,234´W	17.6	35.70	4			1	
ANTXXIII-1_NEP036*ff	20051025	08.56h	41°47,354´N	9°30,349´W	17.3	35.71	4			1	
ANTXXIII-1_NEP040ff	20051026	07.45h	38°5,274´N	11°39,147´W	20.4	36.33	4			1	
ANTXXIII-1_NEP044*ff	20051027	08.57h	34°11,671´N	14°6,682´W	21.7	36.49	4			1	
ANTXXIII-1_NEP048ff	20051028	08.20h	30°25,604´N	16°23,686´W	23.0	36.88	4			1	
ANTXXIII-1_NEP052*ff	20051029	08.25h	26°15,163´N	17°3,376´W	24.3	36.93	4			1	
ANTXXIII-1_NEP056ff	20051030	08.11h	22°38,455´N	20°23,699´W	25.0	36.57	4			1	6
ANTXXIII-1_NEP060ff	20051031	08.13h	19°16,878´N	20°54,392´W	24.8	36.29	4			1	
ANTXXIII-1_NEP064ff	20051101	08.32h	14°42,730´N	20°59,493´W	28.2	35.75	4	1		1	
ANTXXIII-1_NEP069ff	20051102	08.18h	10°37,430´N	20°7,968´W	29.1	35.54	4	1		1	8
ANTXXIII-1_NEP074ff	20051103	08.25h	7°40,910´N	18°2,941´W	29.3	34.99	4	2		1	
ANTXXIII-1_NEP080ff	20051104	08.29h	4°22,795´N	15°17,309´W	28.5	34.27	3			1	
ANTXXIII-1_NEP083ff	20051105	21.17h	0°41.606´S	11°15,990´W	25.9	36.00	3			1	5
ANTXXIII-1_NEP089ff	20051106	BL	-	-	-	-		4		1	
ANTXXIII-1_NEP093ff	20051108	08.22h	8°15,815´S	5°21,448´W	23.7	35.98	3	1		1	
ANTXXIII-1_NEP097ff	20051109	08.10h	11°27,144´S	2°50,433´W	22.0	36.30	3			1	7
ANTXXIII-1_NEP100ff	20051110	10.15h	13°58,200´S	0°50,015´W	20.9	36.50	3			1	
ANTXXIII-1_NEP103ff	20051111	08.30h	17°10,448´S	1°45,196´E	19.3	35.96	3			1	
ANTXXIII-1_NEP106ff	20051112	08.07h	20°26,414´S	4°26,158´E	18.8	35.71	3			1	
ANTXXIII-1_NEP109ff	20051112	Std.add.	-	-	-	-			4	1	
ANTXXIII-1_NEP113ff	20051113	08.57h	23°58,865´S	7°24,649´E	18.4	35.53	3			1	7
ANTXXIII-1_NEP116ff	20051114	08.22h	25°28,634´S	8°49,063´E	18.1	35.60	3			1	
TOTAL							**98**	**13**	**4**	**30**	**40**

4.13 Long-term trends and seasonal variability of the ^{13}C signature of dissolved inorganic carbon (DIC) in surface waters of the Atlantic Ocean

Delphine Dissard
Alfred-Wegener-Institut
not on board: Körtzinger, IfM-GEOMAR

Objectives

The project is a continuation of a long-term observation study of the ^{13}C signature of dissolved inorganic carbon (DIC) in surface waters of the Atlantic Ocean, which commenced in 2003. The biannual sampling based on transits of RV *Polarstern* to/from the Southern Ocean will provide insight into the seasonality and interannual variability of the $\delta^{13}C$-DIC in contrasting climatic and biogeochemical regimes (subtropical vs. subpolar, oligotrophic vs. mesotrophic, thermally vs. biologically controlled CO_2 system). It may also permit quantification of the Suess effect on $\delta^{13}C$-DIC if maintained as a long-term project.

A similar scientific question has been addressed successfully at the oceanic time-series stations such as the Bermuda Atlantic Time Series Study (BATS) and the Hawaii Ocean Time Series. In addition, sampling programmes have been mounted on „Volunteer Observing Ships“ in the North Pacific and North Atlantic. Within the EU-funded project CARBOOCEAN, IFM-GEOMAR has measured δ^{13}C-DIC along a trans-Atlantic VOS line since 2005. The present long-term sampling programme based on RV *Polarstern* transits will represent a significant extension of the CARBOOCEAN study.

Work at Sea

Subsamples of the seventy surface water samples collected for the study of cation incorporation in foraminifera shells in relation to the carbonate chemistry of seawater (see section 4.6) have been prepared for analyses of δ^{13}C and δ^{18}C in the laboratory in Kiel (A. Körtzinger, IFM-GEOMAR).

5. SATELLITE GROUND TRUTH AND ATMOSPHERIC STUDIES

5.1 Bio-optical measurements

Dariusz Stramski[1)], Rick A. Reynolds[1)], Malgorzata Stramska[2)], Slawomir Kaczmarek[3)], Rüdiger Röttgers[1)], Kerstin Heymann[4)], Andreas Ruser[5)],

[1)]UCSD-Scripps, University of California
[2)]UCSD Hancock Institute for Marine Studies, University of Southern California
[3)]Institute of Oceanology, Polish Academy of Sciences
[4)]GKSS Forschungszentrum Geesthacht, Institute für Küstenforschung
[5)]FTZ Westküste

Objectives

The execution of the bio-optics research programme on the ANT-XXIII/1 cruise was a collaboration of two groups, one group from the US institutions (Scripps Institution of Oceanography and University of Southern California) including a representative from a Polish institution (Institute of Oceanology) and the other group from Germany (GKSS and FTZ Westküste). The primary objectives associated with our participation in the cruise were:

1. to collect a comprehensive suite of bio-optical data in various provinces of the Atlantic Ocean covering the northern and southern tropical regions west off Africa;
2. to develop algorithms for estimating particulate organic carbon (POC) concentration in the surface ocean from satellite observations of ocean colour;
3. to advance an understanding of the interactions of light with various seawater constituents, especially suspended particulate matter and coloured dissolved organic matter;
4. to validate the satellite-derived ocean colour data products with our *in-situ* data collected under sunny skies.

Among the several tasks that we pursued on the cruise, the development of an algorithm for remote sensing of POC is perhaps most explicitly related to current trends in ocean biogeochemistry and climate research, in which an understanding of processes that regulate atmospheric CO_2 plays a pivotal role. Uncertainties about various carbon reservoirs and fluxes lead to difficulties in balancing the contemporary carbon budget at global scale. Therefore, improving measurement capabilities and accuracy of carbon estimates for various compartments of the Earth system is essential. POC in the surface ocean is one such compartment of substantial interest. Changes in surface POC result from biological/chemical processes and transformation of POC in the water column, as well as export of POC to the interior of the ocean. The sinking of POC is part of the biological pump, which provides a mechanism for storing carbon in the deep ocean, a long-term sink for atmospheric CO_2. The distributions and dynamics of POC in the upper ocean are driven by temporally and spatially varying processes that cannot be efficiently examined solely

from ship measurements or other *in-situ* observing platforms. Satellite sensors provide a unique tool for long-term synoptic observations of surface ocean with the global extent of coverage. The capability to estimate chlorophyll *a* concentration from remotely-sensed ocean colour has long been established and utilized. However, development of a similar capability for estimating POC is still in its infancy and at present, POC is not among the standard data products of NASA's and other satellite missions.

During the ANT-XXIII/1 cruise on *RV Polarstern* we made an advancement towards developing a capability for global monitoring of POC from satellites. For achieving this goal, it is necessary to conduct a specially designed set of bio-optical measurements over a range of biogeochemical provinces of the world's ocean. The existing historical data are by far insufficient for the development of basin-scale POC algorithms for the Atlantic and other ocean regions. This is because simultaneous measurements of POC and other properties of suspended particulate matter, along with optical measurements of spectral ocean reflectance, spectral light backscattering, angular distribution of light scattering, and spectral absorption properties, have not been made in the past. The ANT-XXIII/1 expedition provided an excellent opportunity to carry out such research across the Atlantic Ocean including tropical waters of both the northern and southern hemispheres.

Work at sea

Our activities at sea included: (i) *in-situ* optical measurements; (ii) on-board optical and particle analyses of discrete water samples obtained from CTD/rosette casts and underway surface water sampling (Fish and Snorkel), and (iii) collection of particulate matter by filtration of the discrete water samples for various post-cruise analyses.

Overall we made *in-situ* (in-water) optical measurements at 26 stations, and additionally we worked on water samples obtained from 33 surface water sampling events. The *in-situ* optical measurements were normally made at stations near local noon (24 stations). Making measurements at this time of the day provided us with an extra opportunity to collect sea-truth data for validation of satellite observations of ocean colour. If skies were clear, we made atmospheric measurements of the aerosol optical thickness at five wavelengths within the spectral region from near ultraviolet to near infrared. These additional atmospheric measurements can be particularly useful for satellite data validation. On two occasions (i.e., at two major GEOTRACES stations), we made *in-situ* measurements of the optical properties of seawater during nighttime hours.

Our underway work on surface water samples was usually conducted twice a day, that is for the morning (09:00) and the evening (21:00) sampling events. These underway measurements were complemented by continuous measurements of particle properties and chlorophyll fluorescence made with a flow-cytometer and a Fasttracka fluorometer using surface water which was pumped from below the ship in the moon pool.

In addition, we made some pilot measurements of light scattering of filtered and ultrafiltered seawater samples to address the question of potential role of colloidal

particles to optical scattering in the ocean. This was done in collaboration with scientists involved in ultrafiltration of seawater (Walter Geibert, Timo Daberkow). Finally, as a collaboration with Walter Geibert, we participated in his experiment on spontaneous formation of particles in filtered seawater, in which we made measurements of angular pattern of light scattering.

Below we describe in greater detail our measurements and analyses that were carried out at near-noon stations and underway surface water sampling events.

Near-noon optical stations

In-water optical profiles were made throughout the upper ocean layer (typically down to 210 m and occasionally to 250-280 m) with two instrument packages. First, we used the Multisensor Datalogger System (MDS) for measuring the inherent optical properties of ocean water. This system was deployed at 26 stations. MDS is equipped with SeaBird Sealogger 25 with temperature, conductivity, and pressure sensors, two beam transmissometers (c-Star, WetLabs) allowing the determination of the beam attenuation coefficient at two wavelengths of light of 488 and 660 nm, chlorophyll fluorometer (WetStar, WetLabs), Hydroscat-6 and two a-βeta instruments (HobiLabs) allowing the determination of optical backscattering coefficient at eight wavelengths (420, 442, 470, 510, 555, 589, 620, and 671 nm), LISST-100 (Sequoia) instrument for measuring the volume scattering function (VSF) in forward directions at 532 nm and for determining the particle size distribution, and spectrofluorometer Fluoroprobe (bbe Moldaenke) for identifying various phytoplankton groups through fluorescence excitation at 450, 525, 570, 590, and 610 nm with emission at 680 nm. Because of the instrument failure, LISTT-100 was used only during the first part of the cruise in the Bay of Biscay and at the first station after leaving Vigo.

For measuring the natural light field within the upper water column (down to 150 - 200 m), we deployed a freefall spectroradiometer (SPMR, Satlantic). It is essential that this mode of SPMR deployment made it possible to measure the light field away from ship perturbations. SPMR measured the spectral downwelling irradiance (E_d) and upwelling radiance (L_u) at 13 wavelengths covering the visible spectral range from UV through the red portion of the spectrum, i.e., 339, 380, 412, 442, 470, 490, 510, 532, 555, 590, 620, 666, and 682 nm. Among the various properties, the spectral reflectance (i.e., ocean colour) can be determined from the SPMR measurements, which is of direct importance to the development of ocean colour algorithms and validation of satellite-derived data products. During each deployment of SPMR, we made 3 or 4 repetitive vertical casts. At the last 8 stations south of the equator we used two SPMR instruments for intercalibration purposes and for ensuring better quality of final radiometric data. Overall, we made 105 vertical casts with SPMR instruments at 24 daytime stations.

The *in-situ* optical measurements with MDS and SPMR were accompanied by a CTD/rosette cast down to 200 m to collect discrete water samples. As a standard approach, we collected water from 4 depths, that is surface, chlorophyll fluorescence maximum, 200 m, and one depth either above or below chlorophyll maximum. These discrete water samples were filtered to collect particulate matter for post-cruise analyses of POC, phytoplankton pigments, mass concentration of total suspended

matter (TSM), and absorption spectra. The POC samples were taken in duplicate. A significant portion of phytoplankton pigment and TSM samples were also taken in duplicate, for example as a general rule we took duplicate samples of the surface water. The phytoplankton pigment samples were stored in liquid nitrogen and will be analyzed after the cruise with HPLC (High Performance Liquid Chromatography) method. The TSM and POC samples were dried on board and will be analyzed after the cruise with standard gravimetric and high temperature combustion methods, respectively. The particulate absorption samples will be measured after the cruise with a spectrophotometric transmittance-reflectance method. All these methods are consistent with JGOFS or NASA recommendations and protocols.

From two depths (surface and chlorophyll maximum), we took additional samples for phytoplankton pigments, TSM, and absorption spectra for inter-comparison of results between the two participating groups. For these samples, the pigments and the spectral absorption of particulate matter and coloured dissolved organic matter (CDOM) were analyzed on board the ship using an HPLC system and a spectrophotometer. In addition to our routine water sampling within the top 200 m layer at optical stations, we took samples for POC and TSM from greater depths at 4 major GEOTRACES stations.

Overall, during ANT-XXIII/1 we collected 286 sample filters for post-cruise POC analysis, 270 samples for HPLC pigment analysis, 233 samples for TSM analysis, and 240 samples for particulate absorption analysis. These numbers include both "in-water" stations as well as underway surface sampling events.

The spectral absorption measurements of particles and CDOM were also made on board on discrete water samples using a newly designed absorption meter, the so-called Point-Source Integrating-Cavity Absorption Meter (PSICAM). This instrument consists of a spherical cavity made of a highly reflective material (that can be filled with water sample) and a light source in the centre of the cavity. The optical signal is measured with a commercial spectroradiometer (Ramses, Trios). The PSICAM provides a sensitive tool for measuring particulate absorption without adverse effects associated with particle scattering, which represents a significant advantage compared to other traditional methods. The instrument was used here for the first time to test its performance and accuracy in relatively clear open-ocean waters. The PSICAM results will be compared to the results from the spectrophotometric determinations of CDOM and particle absorption.

Our routine work on discrete water samples also included on-board measurements of volume scattering function VSF (i.e., scattered intensity as a function of scattering angle) with a Dawn EOS (Enhanced Optical System) scattering meter equipped with a laser operating at 532 nm (Wyatt Tech.). Eighteen photodetectors are spaced around its sample cell in a multi-angle geometry, ensuring that measurements of VSF are made simultaneously over a range of scattering angles from about 20 to 150^{o}. In addition, the instrument is equipped with a polarization device that provides measurement of scattering for vertically and horizontally polarized incident beam. Such measurements have seldom been made in oceanography. These measurements are important not only to the characterization of optical backscattering and remote sensing applications but also to many fundamental questions in ocean

optics itself. For surface water samples, the scattering measurements with Dawn-EOS on untreated samples were followed by measurements on acidified samples (acetic acid at a 0.05 % final concentration). The acidification treatment results in dissolution of particulate $CaCO_3$, if present in water (for example, coccolithophorid phytoplankton). The difference between the two measurements provides a measure of scattering due to particulate $CaCO_3$. The knowledge of scattering associated with particulate inorganic carbon (PIC) will be essential to the development of POC algorithm, in which the contribution of PIC can be viewed as an unwanted source of bias or noise.

Each final VSF that will be determined from Dawn-EOS measurements will actually represent an average function obtained with very many "snapshot" measurements of the angular distribution of scattered light for both the vertically polarized and the horizontally polarized incident laser beam. Specifically, each determination of final VSF consisted of 3 replicate measurements, and each of the replicate measurements consisted of 1440 "snapshot" measurements for vertically polarized light over a 3-min period and 1440 "snapshot" measurements for horizontally polarized light over a 3-min period. The final VSF for any given sample is an average of 4320 measurements for vertical polarization and 4320 measurements for horizontal polarization. Overall, during the cruise we acquired about 1120 time series runs of angular pattern of scattering, each of 3-min duration. This data set essentially represents about 930,000 snapshot measurements of "unpolarized" volume scattering function of seawater (note that the same number applies to snapshot measurements with horizontally and vertically polarized incident beam). This is a very large and unique data set on angular light scattering. Our initial analysis of this enormous amount of data will focus on calculating one average VSF for a given sample. However, we expect that there might be an important and useful information contained in the statistical variability of VSF within a given sample, and we plan to explore this variability as well.

Two other types of measurement that were performed on board *RV Polarstern* on discrete water samples were focused on particle analysis with a FlowCam system (Fluid Imaging) and a Cytobuoy flow-cytometer (Cytosense). FlowCam images, counts, and measures particles in fluids, providing a capability for identification and sizing of particles as small as a few micrometers. The instrument allows the user to trigger particle analysis by light scatter and fluorescence, which provides information about plankton community structure. Approximately 40 water samples were analyzed with FlowCam; these samples consisted of surface water at all near-noon optics stations, and generally the fluorescence maximum as well. For each sample, 500 to 3000 individual particles within the size range ~1 - 100 μm were imaged with a CCD camera and saved to a file. Characteristics of each particle (size, shape, forward light scatter, fluorescence of chlorophyll or phycoerythrin) were also measured and associated with each particle image. The Cytobuoy system allows the counting and sizing of particles from about 1 to 600 μm, and measures back- and side-scattering, as well as fluorescence emission in the orange and red portions of the spectrum. These flow cytometry data can be used for fingerprinting different algal groups.

During the first part of the cruise in the Bay of Biscay we also used LISST-100 in a bench-top mode of operation to measure VSF (at 532 nm) in the forward scattering

directions for discrete water samples. These measurements, along with data from Dawn-EOS, will provide a nearly full angular information on VSF in the range of scattering angles from about 0.1 to 150^{o}. In addition, the scattering data from LISST-100 will be inverted to yield the particle size distribution in the range from about 1 to 250 μm.

Underway surface water sampling

Samples of surface water taken from Fish or Snorkel were filtered for post-cruise analysis of POC, HPLC pigments, TSM, and particulate absorption spectra. These samples were also measured with Dawn-EOS light scattering instrument and the PSICAM absorption instrument as described above. This work was done on samples from 33 Fish/Snorkel sampling events that typically occurred twice a day, in the morning (09:00) and in the evening (21:00).

The Cytobuoy system was acquiring data hourly during the whole cruise (with minor interruptions) for water samples taken from a depth of about 11 m below the ship. A Fasttracka fluorometer was also used to make continuous measurements on water taken from that 11 m depth. This provided a continuous monitoring of photophysiological characteristics and general biomass of phytoplankton (in terms of chlorophyll fluorescence) during the cruise.

Status of data at the end of the cruise and expected results

A broad suite of instruments and sensors used in our measurements produce large amounts of diverse data that require significant effort of processing and quality control to produce final results. During the cruise our focus was on the acquisition of data and verification of quality of raw data being acquired. While we inspected some example raw data for specific patterns and features, the present status of data does not allows us to comment on preliminary results. Immediately upon the cruise our optical instrumentation will be calibrated in specialized facilities, which will allow us to start data processing with both pre-cruise and post-cruise calibration. This is essential to ensure the best possible quality of final results. After data quality control and data processing to physical units is completed, we will embark on various types of analysis.

We expect to establish relationships between the optical properties of the ocean (spectral reflectance, scattering, and absorption) and seawater constituents (POC, TSM, and phytoplankton pigments, especially chlorophyll *a*) over a range of water types encountered during the cruise. Some of these relationships will be used in the development of novel remote sensing algorithms for estimating POC. Our data will be explored to advance an understanding of the optical variability caused by changes in the composition of optically significant water constituents. Example issues include the optical effects due to changes in the ratio of POC to TSM, changes in phytoplankton pigment composition, changes in the contribution of PIC, changes in particle size distribution, and the presence of colloidal matter in water. This understanding is critical to various fundamental and applied-oriented questions in bio-optical oceanography and ocean colour remote sensing, including the performance of novel POC algorithms that we wish to develop. In addition, using the data collected at "clear-sky" stations we will carry out a match-up analysis with simultaneous satellite-

derived data, specifically from the SeaWiFS instrument on Orb Image satellite. This will allow us to contribute to the current effort of validating standard satellite-derived ocean colour data products such as spectral water-leaving radiance and chlorophyll *a* concentration.

Collaboration/links to other projects

The execution of the overall bio-optics research programme on ANT-XXIII/1 was a collaboration of two groups, one group from the US institutions (Scripps Institution of Oceanography and University of Southern California) including a representative from a Polish institution (Institute of Oceanology) and the other group from Germany (GKSS and FTZ Westküste). Owing to this collaboration, we acquired a comprehensive and unique set of bio-optical data. The collaboration between the two groups will continue in the phase of data analysis and preparation of manuscripts for publication.

A collaboration was also initiated between our optics group and chemical oceanographers involved in the GEOTRACES programme. This collaboration has potential to lead to interesting new insights in the fields of both ocean optics and ocean biogeochemistry. During the cruise we made light scattering measurements with Dawn-EOS instrument on filtered (0.2 µm and 1 µm) and ultrafiltered (10 and 30 kDa) seawater to test the hypothesis about the contribution of colloidal particles to light scattering in the ocean. The samples of seawater filtrate for these measurements were provided by Walter Geibert (AWI) and Timo Daberkow (University of Bremen). We also made scattering measurements with Dawn-EOS as part of the experiment conducted by Walter Geibert on spontaneous formation of particles in filtered (0.2 µm) seawater and ultrafiltered (10 kDa) seawater. These measurements were carried out daily over a period of 10 days. We expect that the light scattering measurements will provide a clear evidence of particle formation and temporal evolution in the newly formed particulate assemblage. We plan to continue our collaboration in the phase of data analysis and interpretation.

5.2 Spectral UVB and UVA measurements and ozone distributions

Sigrid Wuttke, Saad El Naggar, Otto Schrems, Thaddäus Bluszcz,
Alfred-Wegener-Institut
not on board: Otto Schrems, Alfred-Wegener-Institut

Introduction

Due to the ozone depletion in Antarctica during the last 25 years, increased levels of solar UVB radiation have been observed. Since 1994, a personal dosimetry programme has been carried out at the permanent German Antarctic *Neumayer* Station (70° 39’ S, 08° 15’ W) to quantify the impacts of incident UVB radiation on human beings in Antarctica. This programme includes the use of different radiation detectors, including personal dosimeters and a UV spectrometer. The electronic dosimeter (ELUV-14) was especially developed at AWI (El Naggar et al., 1995).

To support this programme and link the Antarctic radiation conditions to radiation conditions in other climate zones, ozone and UV measurements are carried out during the cruises of RV *Polarstern* between Bremerhaven and Cape Town.

Objectives
The objectives during ANT-XXIII/1 include the investigation of incident UV radiation in dependence of latitude focussing on the influence of variable ozone content in the atmosphere. In detail the following objectives will be addressed:

- determination of global UVB doses as a function of latitude, sun elevation and total ozone column with different radiation detectors,
- assessing the different UV radiation conditions in a variety of climate zones and a large range of solar zenith angles,
- measuring spectral UVB distributions during the cruise using the AWI-Spectrometer,
- determination of the meridional ozone variations using the ECC radio sondes.

Work at sea
The work programme on board RV *Polarstern* consists of carrying out daily UV-measurements using the AWI-spectrometer, Eluv-14 dosimeter and the Solar-Light Model 501 Biometer. During the cruise, the radiometric stability and the wavelength alignment of the spectroradiometer is tested on a regular basis. The stability tests are performed with a 150 W tungsten halogen lamp which is incorporated in a mobile calibration unit. The wavelength alignment is tested with a low pressure mercury lamp.

To support the radiation measurements, daily launches of ECC ozone sondes in combination with VAISALA radio sondes are performed. These balloon borne measurements provide information on the vertical distribution of ozone, temperature and humidity in the atmosphere.

The data collected during the cruise are checked with different quality control procedures. These include initial comparisons of the different radiation sensors, comparisons to a radiative transfer model, investigation of diurnal cycles of erythemal irradiance.

Instruments
Solar spectral UV irradiance is recorded with the AWI-UV-Spectrometer. This instrument consists of a Bentham 150 DTM double monochromator with 32 Multi Channel Photomultiplier Plate to measure UVB irradiance (290 to 320 nm). The single channels of the UVB instrument are 1.35 nm apart and the resolution is about 2 nm. To detect UVA irradiance (320 to 400 nm) an Oriel single monochromator with 256 diode array detector is used. This instrument has a resolution of 2 nm, but the channels have a step width of only 0.65 nm. Both parts of the AWI-UV-spectrometer are operated in a temperature stabilised box and are driven by the same software. The spectra of UV irradiance are stored every minute.

Erythemal irradiance is recorded by two different types of instruments: the personal UVB-Dosimeter ELUV-14, and the Solar Light Model 501 Biometer. Both instruments are broadband detectors with a response similar to the erythemal action spectrum. Data are stored in daily files in 1 minute and 5 minute records for the ELUV dosimeters and the Biometer, respectively.

Ozone profiles are determined with balloon borne ECC Ozone Sondes. In addition to the ECC sonde, a VAISALA radio sonde (RS 92) is attached to the balloon as well. This way, the vertical distribution of ozone, temperature and humidity in the atmosphere can be measured. Such a balloon is launched every day. Data is transmitted by the radio sonde at a predetermined frequency every 5 seconds.

During conditions with direct sun total ozone column is measured by a portable Solar Light Microtops Ozonometer. This hand held instrument is a portable sun photometer with three channels (305, 312, 320 nm) for the detection of total ozone column.

Preliminary Results

Measurements of spectral UVB and UVA irradiance

The AWI-UV-spectrometer was set up on the Peildeck on the starboard side of RV *Polarstern*. It was operated in a continuous modus, thus spectra have been recorded day and night. Frequent mobile calibrations have been performed in order to test the radiometric stability of the instrument. The time series of the radiometric stability of the UVB and UVA instrument are presented in figure 5.1 and figure 5.2, respectively. The radiometric stability is expressed by ratios of measurements of the calibration lamp. The measurement of the calibration lamp on 11 October 2005 is in the denominator to have a common reference. This day was chosen because it was the day after setting up the instrument on the ship. Ideally, the ratio remains one over the sampling period.

The UVB instrument shows significant changes in its response during the cruise. These changes of sensitivity in the order of 20 % compared to 11 October 2005 for some channels may be due to changes in humidity in the instruments housing. Another reason might be slight shifts of mechanical parts in the monochromator due to the ship's movements. Despite these large changes in sensitivity the absolute values of incident UV irradiance can still be calculated applying the measurements of the mobile calibration lamp. The low sensitivity on 17 October 05 is due to a failure of the temperature stabilisation in the spectrometer's housing. The response of the UVA instrument shows changes of only up to ±5%.

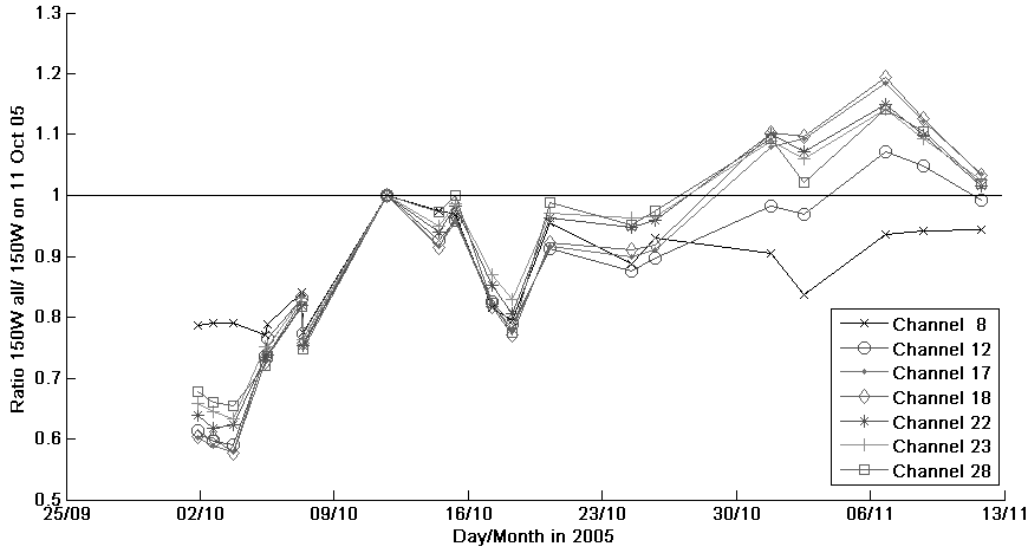

Fig. 5.1: Time series of radiometric stability of the AWI-UVB-spectrometer during the voyage ANT-XXIII/1. The response of the spectrometer increased significantly. This change in radiometric response has to be accounted for when calculating the absolute values of UVB irradiance.

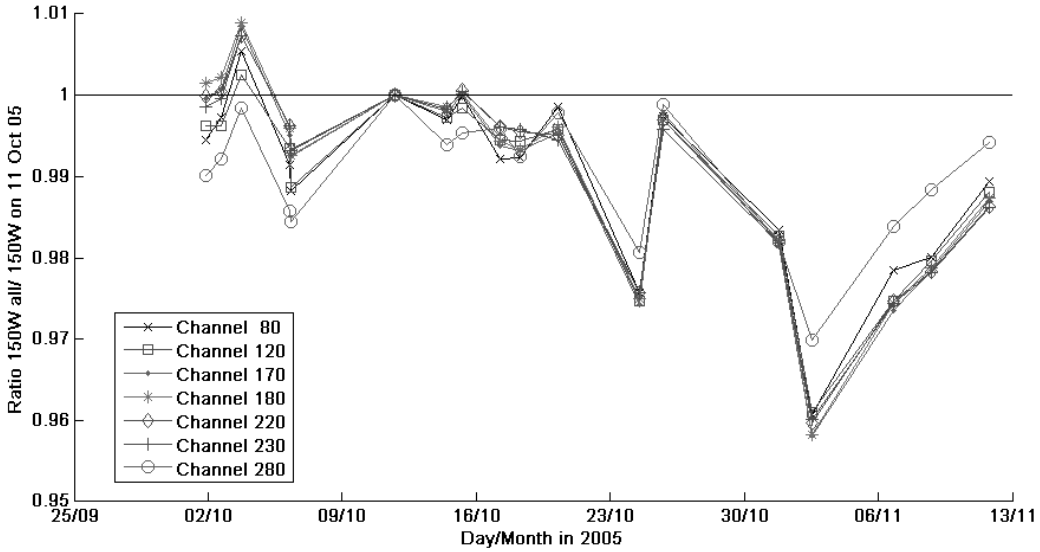

Fig. 5.2: Time series of radiometric stability of the AWI-UVA-spectrometer during the voyage ANT-XXIII/1. The response of the UVA spectrometer remained within ±5% during the entire cruise.

To finally calculate absolute values of spectral irradiance, the following uncertainties have to be taken into account:

- Change in radiometric stability (Bernhard and Seckmeyer, 1999);
- possible wavelength shifts (Slaper et al., 1997);
- correction for the deviation of the input optics from the ideal cosine response (Bernhard and Seckmeyer, 1997);
- stray light corrections, especially at the short wavelength in the UVB;
- shadowing effects of the ship;
- ship's movements.

So far, the data shown in this section are corrected for the change in radiometric stability and the correction for the deviation from the ideal cosine response.

The time series of UVB irradiance as measured during ANT-XXIII/1 is presented in figure 5.3. The UVB irradiance is integrated between from 290 to 320 nm. The two data gaps on 18 and 24 October are due to a failure in the instrument's temperature stabilisation.

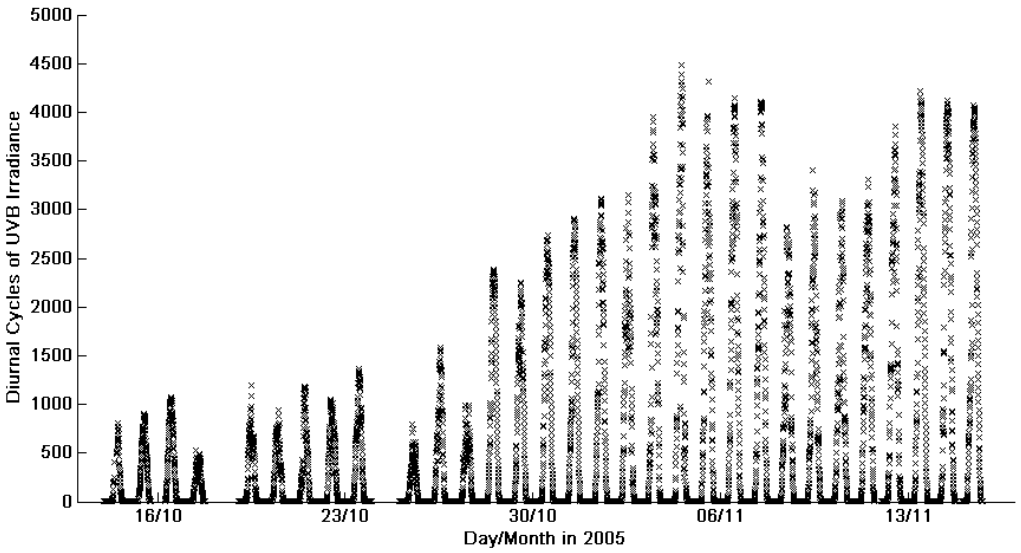

Fig. 5.3: Diurnal cycles of integrated UVB irradiance during ANT-XXIII/1

Various integrals of UV irradiance at noon are shown in figure 5.4 and figure 5.5. The UVB integral comprises the wavelength range from 290 to 320 nm (Fig. 5.4). The UVA integral has boundaries from 320 to 400 nm, and the complete UV integral from 290 and 400 nm (Fig. 5.4). The noon time integrals are derived from the measurements of spectral UV irradiance as well as from model calculations. The freely available library for radiative transfer calculations LibRadtran (Mayer and Kylling, 2005) was used to calculate spectral irradiance at the surface. The most important input parameters comprise the solar zenith angle (SZA), the total ozone column, surface albedo and a default aerosol parameterisation. The SZA was calculated according to the position of the ship and the time referring to the measured spectra. The total ozone column is derived from the ozone profiles obtained from the launches of the ozone sondes. The albedo was considered to be constant with 0.2 and a default aerosol parameterisation for a marine environment has been used. For future analyses it is intended to use aerosol optical depths that are obtained from LIDAR group. Also, an albedo depending on solar zenith angle and wavelength will be applied. The model calculations do not include clouds. Therefore, the modelled UV irradiance is expected to be larger than the measurement.

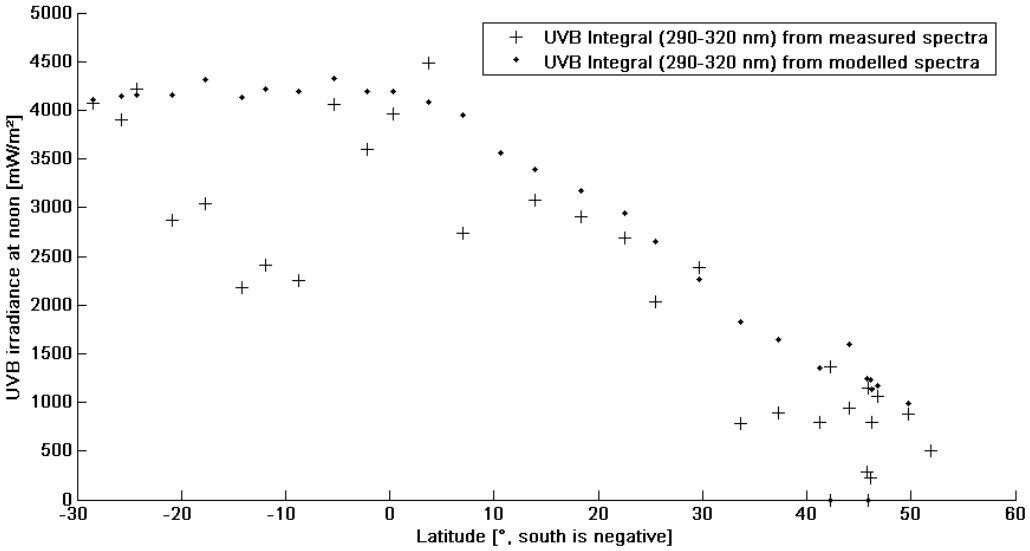

Fig. 5.4: Noontime values of measured and modelled UVB irradiance during ANT-XXIII/1 in dependence of latitude

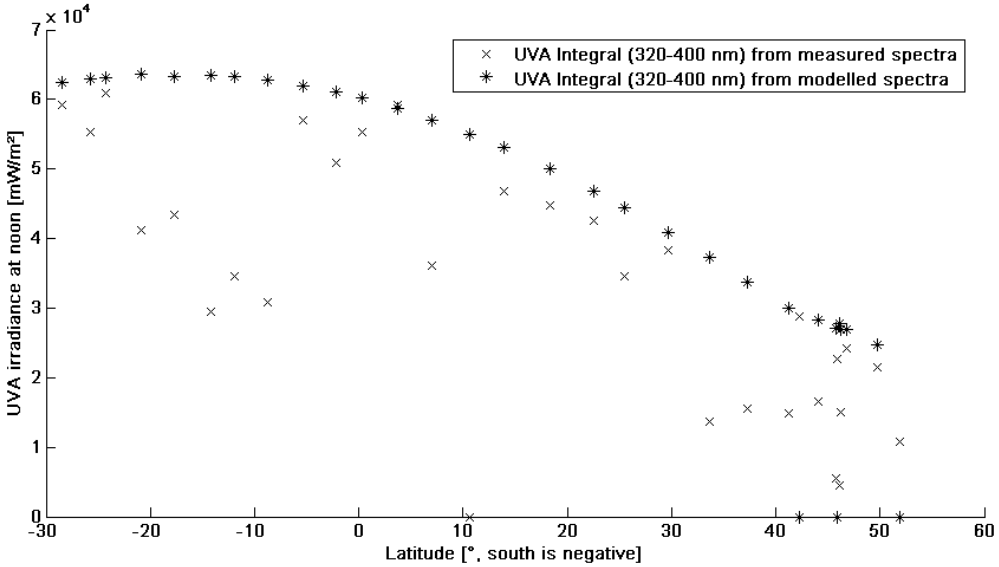

Fig. 5.5: Noontime values of measured and modelled UV and UVA irradiance during ANT-XXIII/1 in dependence of latitude

It can be seen from figure 5.4 that the fraction of UVB irradiance is significantly lower than the fraction of UVA irradiance (see Fig. 5.5). However, the biological effectiveness is much higher in the UVB. Therefore, it is the wavelength region of interest for a number of UV effects studies.

UVB dosimetry measurements

For measurements of the erythemally weighted UVB irradiance, a Biometer, type 501 from Solar Light, and an Eluv-14 dosimeter are installed next to the spectrometer.

Tab. 5.1: Summary of parameters relevant for the analysis of UVB irradiance during ANT-XXIII/1 (13.10.05 – 17.11.05)

Date	Zenith Time [UTC]	Latitude [deg]	Longitude [deg]	UV-B Dose [J/m^2]	Erythem Dose [J/m^2]	Erythem Dose [MED]	Ozone [DU]	Max.Sun Elevation [°]
13.10.2005				7560.393	337.470	1.607		
14.10.2005	11:50	51.90	2.50	5414.924	451.710	2.151		30
15.10.2005	12:15	49.70	-3.73		795.270	3.787	311	31.8
16.10.2005	12:21	46.82	-5.30	16562.703	980.701	4.670	290	34.3
17.10.2005	12:26	46.07	-6.45	7156.845	410.340	1.954	293	34.7
18.10.2005	12:27	45.85	-6.63		754.320	3.592	337	34.6
19.10.2005	12:25	46.20	-6.30	12721.256	714.840	3.404	304	33.9
20.10.2005	12:22	45.73	-5.50	11190.360	633.570	3.017	273	34
21.10.2005	12:18	45.92	-4.60	13467.242	796.530	3.793		33.4
22.10.2005	12:36	44.00	-8.92	15535.212	889.770	4.237	207	34.9
23.10.2005	12:35	42.24	-8.73	18766.472	1095.150	5.215		36.4
24.10.2005	12:35	42.24	-8.73		1098.930	5.233		36
25.10.2005	12:40	41.27	-9.80	8322.892	478.800	2.280	298	36.7
26.10.2005	12:47	37.27	-12.17	19698.595	1193.220	5.682	292	40.3
27.10.2005	12:58	33.55	-14.50	12610.849	733.950	3.495	311	43.7
28.10.2005	13:05	29.60	-16.32	37692.704	2375.311	11.311	280	47.3
29.10.2005	13:11	25.53	-17.87	34260.962	2523.780	12.018	261	51
30.10.2005	13:22	22.50	-20.5	43289.569	3150.421	15.002	248	53.8
31.10.2005	13:24	18.37	-20.92	44319.931	3339.840	15.904	265	57.6
01.11.2005	13:23	13.90	-20.82	48211.250	3411.030	16.243	270	61.7
02.11.2005	13:21	10.62	-20.00	39227.834	2975.700	14.170	272	64.7
03.11.2005	13:10	7.00	-17.50	57060.104	3990.628	19.003	249	68
04.11.2005	12:59	3.70	-14.70	58954.769	4005.960	19.076	252	71
05.11.2005	12:48	0.27	-12.00	62879.989	4683.209	22.301	257	74.1
06.11.2005	12:41	-2.17	-10.13	67547.151	5095.859	24.266	268	76
07.11.2005	12:30	-7.37	-7.62	63897.726	4609.079	21.948	265	78.9
08.11.2005	12:20	-8.78	-4.97	43178.078	3124.380	14.878	288	82,1
09.11.2005	12:10	-11.87	-2.50	45140.534	3441.689	16.389	291	84.9
10.11.2005	12:03	-14.25	-0.62	43492.717	3129.630	14.903	304	87
11.11.2005	11:51	-17.68	2.18	53284.042	3866.100	18.410	280	89.9
12.11.2005	11:40	-20.95	4.85	58952.823	4346.369	20.697	302	86.9
13.11.2005	11:29	-24.4	7.77	71120.688	5320.769	25.337	297	83.7
14.11.2005	11:23	-25.81	9.19	73776.530	5421.568	25.817	296	82.5
15.11.2005	11:10	-28.5	12.28	73021.665	5311.110	25.291	314	80.1

In table 5.1, relevant data of the UVB measurements are presented. These data include the time and location of the maximal elevation of the Sun for each day, as well as the total ozone column. Further the daily erythemal doses as measured with the Biometer are given in J/m^2 as well as in MED. MED (Minimum Erythemal Dose) is

an artificial unit describing the sun-burning effectiveness. The biological effective dose of 1 MED = 210 J/m^2, would cause minimal redness of the average skin (Solar Light, 1993).

Figure 5.6 shows the UVB unweighted and erythemally weighted daily doses during the cruise. On 8 November 2005, a heavy cloud cover prevailed causing the very low dose for this day. The maximal dose of 73776.530 J/m^2 (UVB unweighted) and 5421.568 J/m^2 (erythemally weighted = 25.82 MED) were recorded on 14 November 2005 at sun's elevation of 82.5°. The expected UV maximum should be on 11 November 2005 at sun elevation of 89.9°. However, a stratiform cloud cover prevented the dose from being maximal. The cloud cover on this day reduced the dose to 18.4 MED.

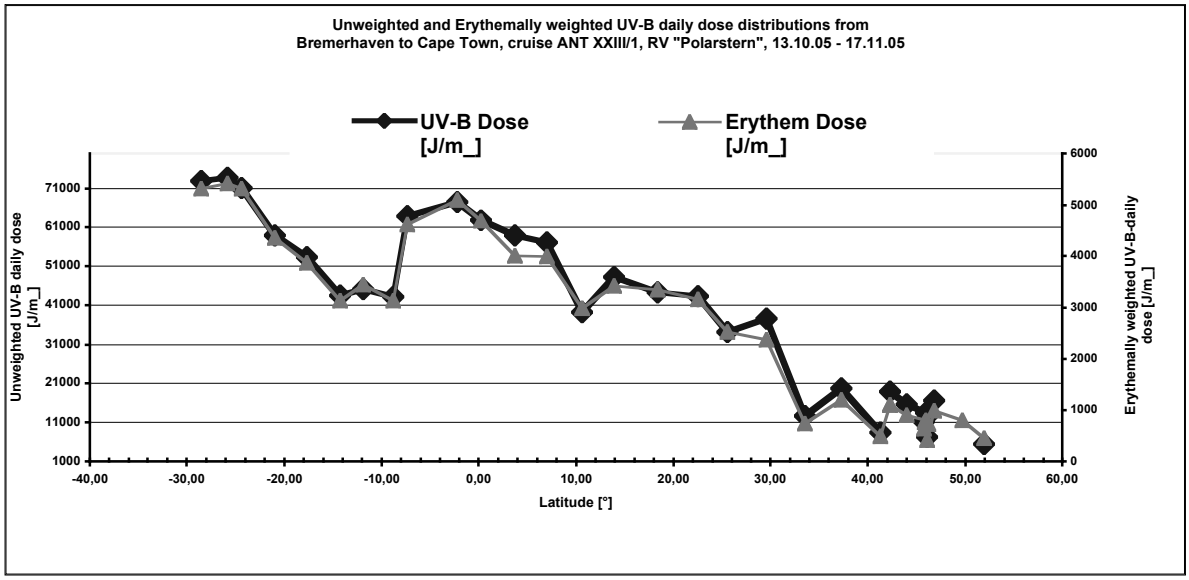

Fig. 5.6: UVB Dose (erythemally weighted and unweighted) in dependence of latitude between Bremerhaven and Cape Town during ANT-XXIII/1

Ozone sounding

Ozone sounding using ECC-sondes and VAISALA RS-92-SGP radio sondes were successfully carried out on a daily basis between 15 October 2005 and 15 November 2005. A total of 29 ozone profiles were recorded. All relevant data are presented in Table 5.2.

Tab. 5.2: Summary of all ozone sounding data collected during ANT-XXIII/1 13.10.05 – 17.11.05

Date	Start Time [UTC]	Latitude [deg]	Longitude [deg]	Max.Height [m]	Ozone Measured [DU]	Ozone Residual [DU]	Ozone Total [DU]	Max. Sun Elevation [°]
13.10.2005								
14.10.2005								30
15.10.2005	11:20	49.70	-3.57	32107	263.9	46.6	311	31.8
16.10.2005	11:10	46.95	-5.50	33355	253.4	36.4	290	34.3
17.10.2005	11:04	46.27	-6.12	35367	262	31	293	34.7
18.10.2005	11:12	45.85	-6.60	32897	289.7	46.9	337	34.6
19.10.2005	12:06	46.12	-4.17	34705	267.5	36	304	33.9
20.10.2005	11:07	45.75	-5.52	35368	250	23.4	273	34
21.10.2005								33.4
22.10.2005	11:20	44.20	-8.53	33365	181.7	25.6	207	34.9
23.10.2005								36.4
24.10.2005								36
25.10.2005	11:05	41.5	-9.66	32692	250.4	47.5	298	36.7
26.10.2005	11:00	37.65	-11.93	33959	255.50	36.87	292	40.3
27.10.2005	11:00	33.93	-14.28	31682	247.6	63.7	311	43.7
28.10.2005	11:04	30.04	-16.62	32626	229.7	50.2	280	47.3
29.10.2005	16:50	25.18	-18.25	34053	219.86	40.77	261	51
30.10.2005	11:01	22.5	-20.5	33226	203.36	44.55	248	53.8
31.10.2005	11:01	18.83	-20.92	33175	214.86	50.23	265	57.6
01.11.2005	11:02	14.34	-20.91	32091	211.19	58.98	270	61.7
02.11.2005	11:00	10.62	-20.13	29659	188	84.2	272	64.7
03.11.2005	10:55	7.38	-17.8	33586	210.87	37.89	249	68
04.11.2005	11:00	4.066	-15.02	33503	214.4	37.59	252	71
05.11.2005	11:03	0.55	-12.23	32944	214.03	43.13	257	74.1
06.11.2005	10:55	-1.9	-10.33	33180	222.75	44.8	268	76
07.11.2005	10:55	-5.12	-7.82	33000	220.3	44.63	265	78.9
08.11.2005	14:58	-8.9	-4.86	34705	249	38.81	288	82.1
09.11.2005	11:04	-11.81	-2.56	33978	247.31	43.91	291	84.9
10.11.2005	10:57	-14	-0.8	33172	252.27	52.05	304	87
11.11.2005	20:05	-18.62	2.94	34846	251.8	28.1	280	89.9
12.11.2005	10:55	-20.79	4.73	32864	249.49	52.33	302	86.9
13.11.2005	10:52	-24.2	7.60	32097	238.58	58.83	297	83.7
14.11.2005	10:54	-25.71	9.08	34104	254.4	41.98	296	82.5
15.11.2005	11:03	-28.47	12.24	31832	247.97	66.02	314	80.1

Figure 5.7 shows the preliminary results of the latitudinal distribution of the total ozone column. The total ozone column was changing between 337 DU in the North decreasing to 249 DU in the equator area and increasing again in the South to 314 DU.

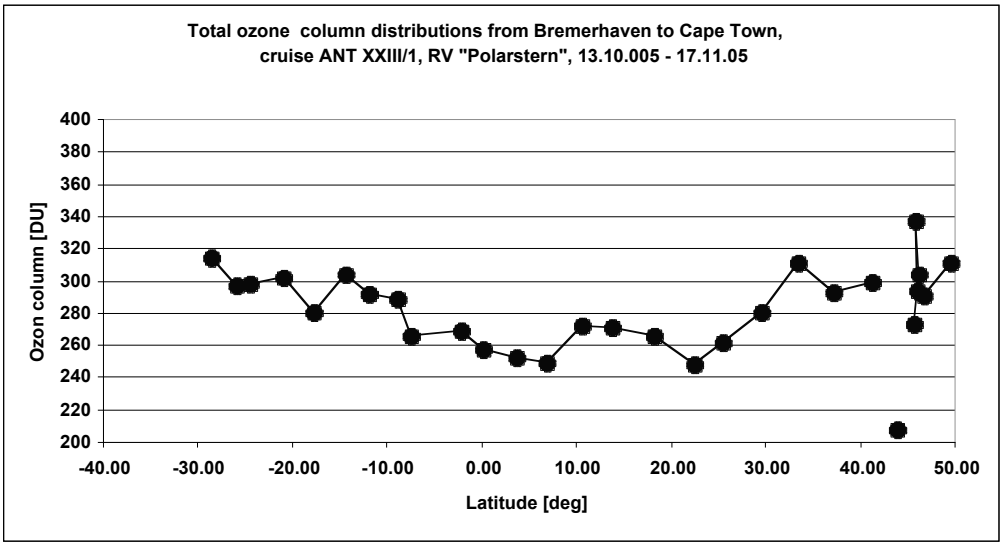

Fig. 5.7: Latitudinal distribution of total ozone column between Bremerhaven and Cape Town during ANT-XXIII/1

Two ozone profiles are shown in figure 5.8. One profile was measured on 18 October 2005 in the Northern hemisphere. The profile on 6 November 2005 was measured just south of the equator. The typical increase of ozone concentration in the lower troposphere is a typical feature of Northern hemisphere ozone profiles. This increase is due to the presence of trace gases due to anthropogenic emission. With the help of these pollutants tropospheric ozone can be generated. The atmosphere in the Southern hemisphere is comparably clean, therefore ozone is not generated in the lower troposphere (WMO, 2003). The stratospheric ozone maximum can be observed in both profiles. As expected, this ozone layer is at a higher altitude in the tropics compared to the mid-latitudes.

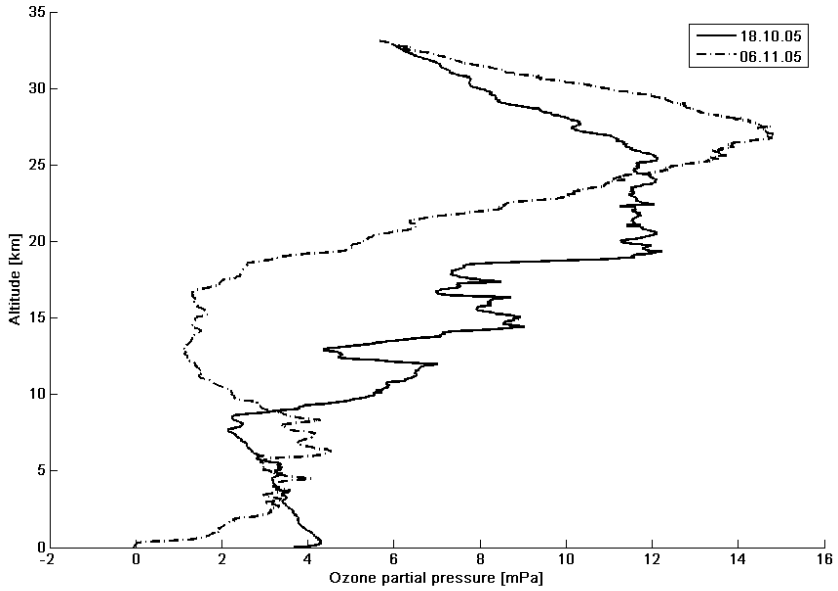

Fig. 5.8: Two ozone profiles measured during ANT-XXIII/1. One ozone profile was measured in the Northern hemisphere (18 October 05) and on just south of the equator (6 November 05). The stratospheric ozone maximum around 25 km can be observed in both profiles

Further analyses

To further assess latitudinal variations in UV irradiance in dependence of SZA, ozone column and clouds, systematic comparisons between the radiative transfer model and the measured UV spectra will be performed. The use of model calculations will yield a quantification of the attenuation of incident UV radiation by clouds. Another aspect that will be addressed in more detail is the amplification of incident UV levels, especially of erythemal irradiance, with decreasing ozone columns.

References

Bernhard, G. and G. Seckmeyer, Uncertainty of measurements of spectral solar UV irradiance, *J. Geophys. Res.,* **104(D12),** 14321-14345, 1999.

Bernhard G., and G. Seckmeyer, New Entrance Optics for Solar Spectral UV Measurements (Technical Note), *Photochem. Photobio.,* **65(6),** 923-930, 1997.

El Naggar, S., H. Gustat, H. Magister, and R. Rochlitzer, An electronic personal UV-B-dosimeter, *Photochem. Photobiol.,* **31,** 83-86, 1995.

Mayer, B., and A. Kylling, Technical note: The libRadtran software package for radiative transfer calculations: Description and examples of use, *Atmos. Chem. Phys.,* **5,** 1855-1877, 2005.

Slaper, H., H.A.J.M. Reinen, M. Blumthaler, M. Huber, F. Kuik, Comparing ground-level spectrally resolved solar UV measurements using various instruments: A technique resolving effects of wavelength shift and slit width, *Geophys. Res. Lett.,* **22,** 2721-2724, 1995.

Solar Light Co. Inc., UV-Biometer User's Manual, Solar Light Co. Inc, Philadelphia, PA, USA, 45 pp, 1993.

WMO (World Meteorological Organization), *Scientific Assessment of Ozone Depletion: 2002,* Global Ozone and Research Monitoring Project – Report No. 47, 498 pp., Geneva, 2003.

5.3 LIDAR measurements of aerosols and cirrus clouds

Franz Immler, ÖzdenTerli, Wilfried Ruhe,
Alfred-Wegener-Institut
not on board: Otto Schrems, Alfred-Wegener-Institut

Objectives

Objectives of our investigations were the observations of aerosols and cirrus clouds in extended regions of the northern and southern hemisphere (50°N bis 30°S) to complete the data sets obtained during previous cruises of RV *Polarstern* (Immler and Schrems, 2002 and 2003). The lidar method offers the opportunity to detect atmospheric aerosols and cirrus clouds over a wide range of optical depths and with high vertical and high time resolution. The backscatter data of our lidar provide a detailed picture of the vertical structure of the clouds. With the help of radiosondes launched every day from RV *Polarstern* the temperature of the cirrus clouds as well as the structure of the tropopause could be characterized.

For the measurements aboard RV *Polarstern* our new lidar system (ComCAL) which uses a Nd:YAG laser with 20 Hz repetition rate and 200 mJ pulse energy at 1064 nm, 532 nm and 355 nm were deployed. The backscatterd light is collected by means of a 40 cm telescope. The whole system is mounted in a 20 feet laboratory container and was placed on the helicopter deck. Measurements were planned to be performed continuously throughout the cruise as far as the meteorological conditions allow to do so.

We expected to observe tropospheric aerosols and in particular Saharan dust layers in the region of 35°N to 7°N and in altitude ranges up to about 6 km. Concerning the observation of cirrus clouds special attention was paid to high-altitude tropical cirrus. Additionally we expected that the backscatter signals provide a detailed picture of the vertical structure of the cirrus clouds, which frequently extend to more than 1000 km horizontally and which can persist for several days. On the basis of the obtained data certain cloud properties will be derived.

Work at sea

The ComCAL (Compact Cloud Aerosol LIDAR) is a recently built lidar system that went on its first field campaign. It was located at the helicopter deck. To obtain the data, we needed clear sky conditions. In addition to measure as often as possible, the daily work was to monitor and optimise the system. This means enhancing and assimilating the control-and acquisition software under real world conditions. Also testing and improving the different hardware devices was one of the tasks for this cruise. In further expeditions ComCAL is supposed to be as a shipborne lidar for full automatic operation. Therefore automatic start up and shut down procedures were developed that are based on POLDAT data for ceiling, precipitation and time. During the cruise, the amount of overal measuring time was more than 130 hours which is a satisfying yield, compared to about 100 hours measured during the ANT-XXI/1 cruise with the MARL system. Most of the data was measured between 30°N and the equator showing interesting results on aerosols as well as clouds.

Expected results / preliminary results

From 29 October until 3 November we detected Saharan dust near the Inter-tropical convergence zone (ITCZ) at about 26° to 9° North. The dust is visible in the backscatter (532 nm parallel polarized, Fig. 5.9) and in the volume depolarisation (Fig. 5.10).

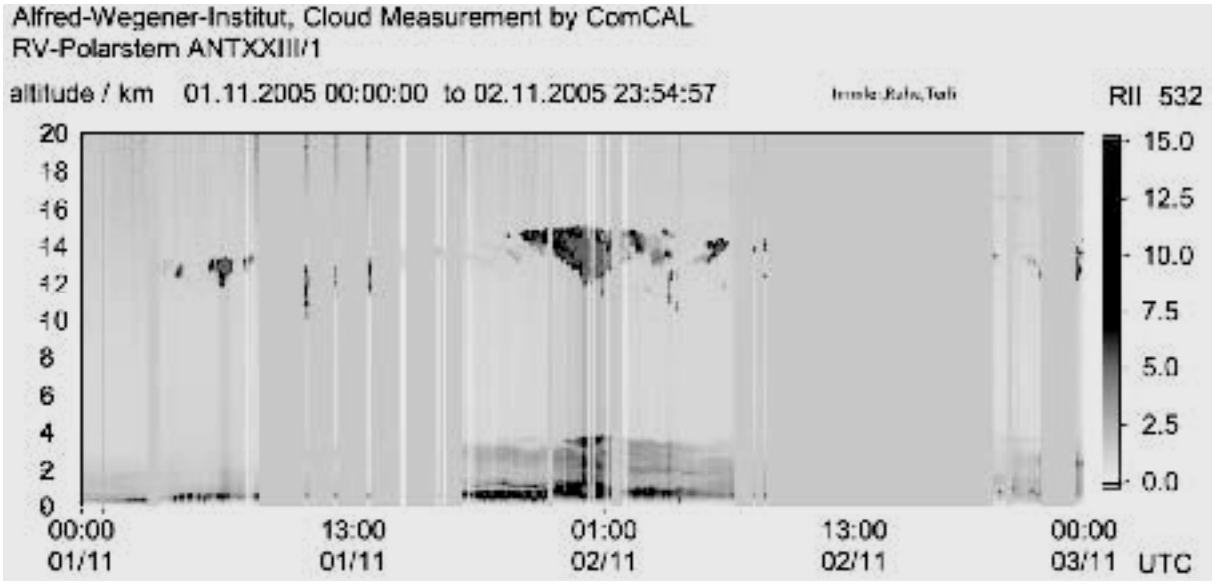

Fig. 5.9: Backscatter at 532 nm (parallel polarized) wavelength. At 1:00 o`clock the top height of Saharan dust layer was about 4 kilometers.

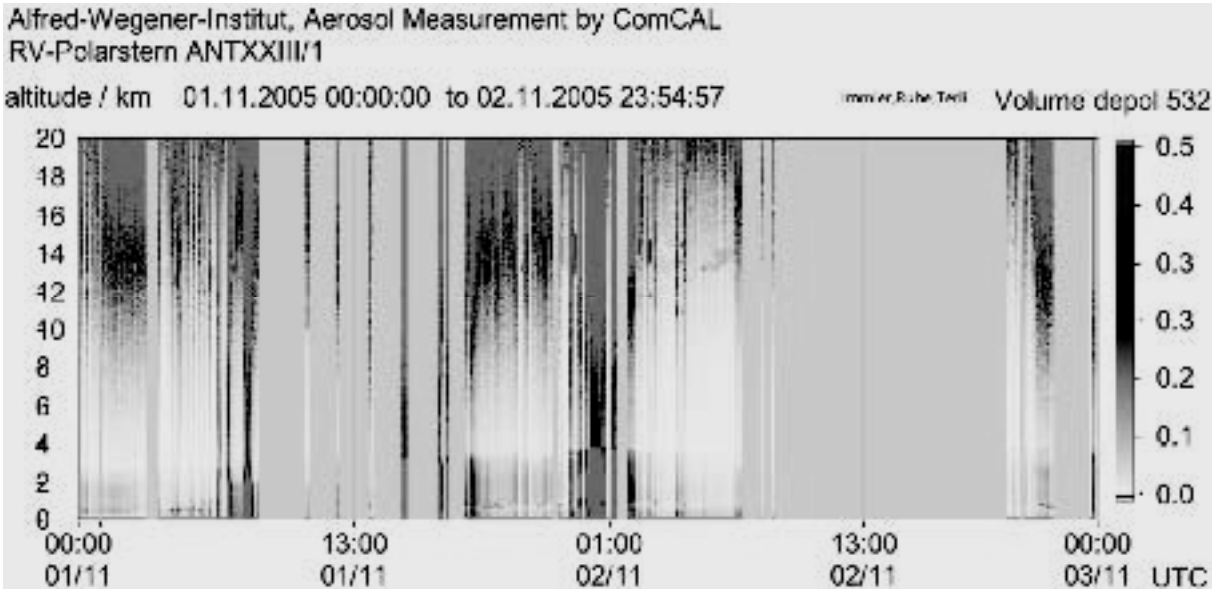

Fig. 5.10: As expected the volume depolarisation at the wavelength 532 nm shows also Saharan dust up to about 4 kilometers.

Ultra thin tropical cirrus

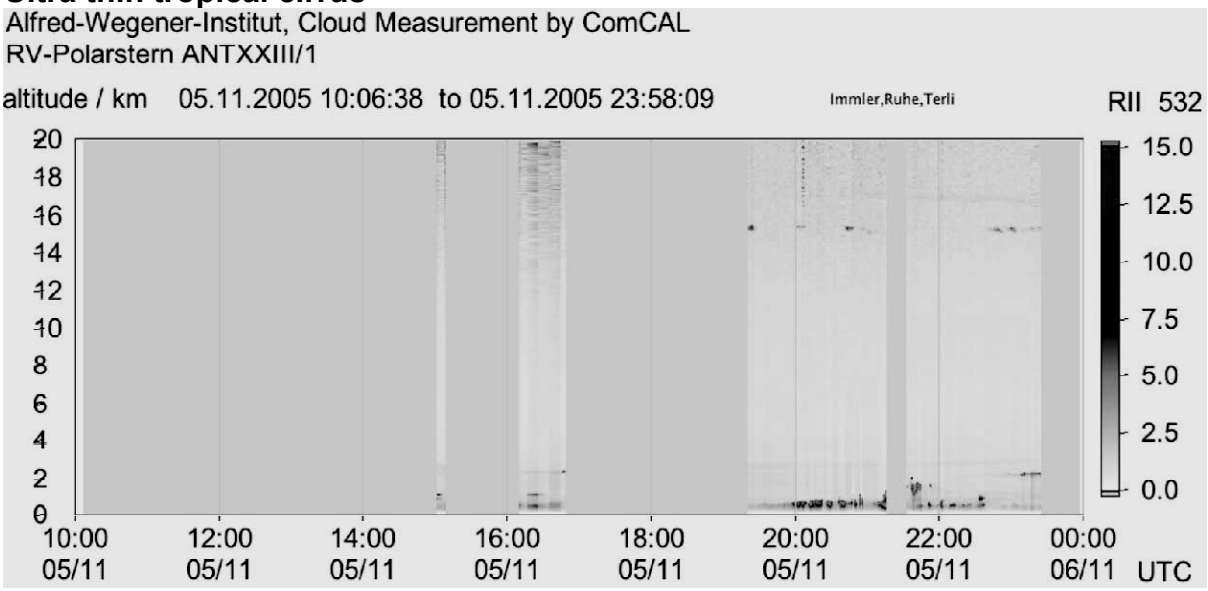

Fig. 5.11: A layer of subvisible cirrus is detected at about 15.5 and 17 km. According to data from the radiosonde the Tropopause was at about 18 km.

Comments

This results are preliminary and particularly the Saharan dust will be verified with backward trajectories to determine the sources.

Links with other projects

The Lidar measurements will contribute to the EU project SCOUT-O3 and to the virtual institute PEP (Pole – equator – Pole).

References

F. Immler and O. Schrems, Determination of tropical cirrus properties by simultaneous Lidar and radiosonde measurements, Geophys. Res. Lett. Vol. 29, NO.23, 2090, doi:10.1029/200GL015076, 2002

F. Immler and O. Schrems, Vertical profiles, optical and mircrophysical properties of Saharan dust layers determined by a ship-borne lidar, Atmos. Chem. Phys. 3, 1353-1364, 2003

5.4 Atmospheric trace gas measurements using the solar absorption spectrometry in the infrared spectral region, FTIR-measurements

Tsidu Gizaw Mengistu, Thomas Weinzierl
Institut für Umweltphysik, Bremen University
not on board: T. Warneke, V. Velazco, J. Notholt, Institut für Umweltphysik, Bremen University; O. Schrems, Alfred-Wegener-Institut

Objectives

The FTIR spectroscopy using the sun or moon as a light sources has been established throughout the last decades as a suitable tool to study the composition of the atmosphere. Feeding the solar light on the entrance aperture of a spectrometer allows to record absorption spectra over a wide spectral range from the infrared to the UV. The solar light is received using the solar tracker with two movable plane mirrors following the course of the sun and correcting for the ship movements. If the spectra are recorded in high resolution the spectral features are well separated. After the interferograms are recorded they are Fourier transformed yielding the required spectra.

Since the solar spectrum is well known the absorption lines can be assigned either to the solar system or to the Earth's atmosphere. The position of the spectral line can in most cases unambiguously be assigned to a specific atmospheric gas and the absorption depth is related to the total amount of atmospheric gas. Column amount of, in total about 20, tropospheric and stratospheric gases can be determined. Furthermore, concentration profiles of a few gases can be retrieved based on collisional broadening of spectral lines, which diminishes with altitude in response to exponential decrease in pressure.

Work at sea

In order to assign a spectral feature either to solar system or the Earth's atmosphere, the measurement should be done under cloud free conditions. In view of this, the ANT-XXIII/1 expedition can be characterized by cruise track of overcast to scattered clouds from Bremenhaven to Vigo, scattered clouds in the morning to nearly clear sky in the afternoon in the cruise leg from Vigo to 5^{o} S during the period from 25 October to 5 November 2005, and overcast sky in the period 8 - 12 November 2005 and sunny weather in the remaining two days of the planned measurement period of this leg of the cruise before Cape Town. The measurements during this expedition, therefore, cover only small part of the tropics in the southern hemisphere, which is between equator and 5^{o} S while there were very good measurement coverages in the northern hemisphere tropics. Despite the data gap during 8 - 12 November 2005, the scientific topics that are planned to be investigated on the basis of these measurements can be carried out.

Data quality

The quality of geophysical quantities derived from FTIR solar radiance measurements depends on the quality and self-consistency of spectral radiances. There are lot of processes by which the signal is affected on its way from the instrument entrance optics through the interferometer, the detectors, and the signal processing.

Investigations described in this section focus on the characterization of the instrument line shape (ILS). The ILS of an ideal interferometer of finite optical path difference but infinitesimal field of view is the sinc function. Contrary to that, in the case of a real interferometer, misalignment, self-apodization through off-axis beams within the finite field of view, and diffraction effects cause deviations from the ideal line shape. ILS distortions can also be caused due to path difference dependent fringe amplitude and sampling errors. It has been known that a typically aligned FTIR spectrometer may have an additional loss of modulation efficiency in the order of 25 % at a maximal path difference.

For making infinite-resolution spectral radiative transfer calculations comparable to finite-resolution FTIR measurements, the synthetic infinite-resolution spectra have to be convolved with the theoretical sinc function. In this preliminary analysis, it is assessed whether the ideal ILS, as described by sinc function, is appropriate and accurate. For this purpose we use an additional ILS model (Hase et al.,1999) henceforth called ILS correction model, and check if the ILS can further be improved. Moreover, the extent of required correction is also used to monitor the quality (Hase et al.,1999, Mengistu et al., 2003) of the FTIR measurements during the course of this cruise.

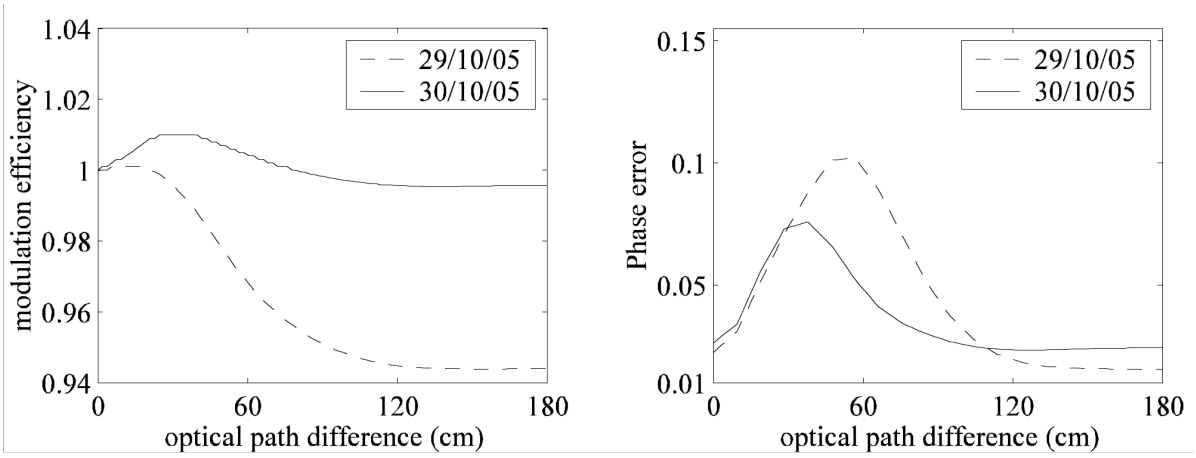

Fig. 5.12: ILS correction. Left panel: Modulation efficiency as a function of optical path difference. Right panel: Phase correction as a function of optical path difference.

The driving parameters of the ILS correction model are linear modulation efficiency at maximum optical path difference and phase correction. If the theoretical sinc function was sufficient enough to describe the observations, modulation efficiency at maximum optical path difference would have been one and the phase correction would have been zero. The phase error describes the asymmetry of imperfect ILS. Figure 5.12 shows an optical path dependent modulation efficiency correction for 29 - 30 October 2005 and corresponding phase corrections. On 29 October pronounced modulation efficiency fluctuations and more phase corrections were required. Based on these quality indicators, the set-up was further checked and the alignment of the aperture was improved. Following this change, gas cell measurement was made on 30 October. The outcome of the ILS analysis for this measurement revealed that the corrections required are smaller than those required on 29 October. In this manner,

the FTIR measurements were monitored for its quality during the course of the expedition.

Expected results

The ILS analysis has shown that the FTIR measurements during ANT-XXIII/1 expedition are of high quality. Further analysis which requires computer codes for line by line radiative transfer and non-linear iterative inversion algorithms will be made after the cruise at our office. The atmospheric trace species determined from the analysis will be used to study different atmospheric processes. Processes like biomass burning, increasing trend of stratospheric water vapour in the last few decades and condensation history of water vapour are a few examples among many interesting topics that can be studied on the basis of the trace gases derived from FTIR solar measurements.

The composition of the tropical stratosphere is determined by two sources: airmass with tropospheric composition that enters the stratosphere and local stratospheric chemistry. The measurements will help us understand the extent to which these processes determine stratospheric composition. Moreover, like other similar expeditions in the past which took place during the same period of the year, the measurements may capture tropical biomass burning emissions and emissions from the northern hemisphere (Notholt et al., 2003).

Compounds like CO, C_2H_6, OCS, HCN and CH_2O are short lived species of interest. The long lived species such as CO_2 and CH_4 can now be retrieved with improved precision of less than 0.5 % to detect small atmospheric variability. Trace gases like O_3, CH_4, CH_2O or CO can be used for satellite validation. The main water vapour isotope, $H_2{}^{16}O$, and its heavier isotopes, like HDO and $H_2{}^{18}O$ will be retrieved to study the condensation history of airmass and isotopic entry ratio from troposphere to the stratosphere. This will be complemented by coincident observations from MIPAS onboard ENVISAT satellite.

References

F. Hase, T. Blumenstock and C. Paton-Walsh, Analysis of instrumental line shape of high-resolution FTIR-spectrometers using gas cell measurements and a new retrieval software, Applied Optics, pp. 3417 - 3422, 1999.

G. Mengistu Tsidu, M. Kiefer, T. von Clarmann, H. Fischer, B. Funke, U. Grabowski, F. Hase, M. Höpfner, M. López-Puertas, and G. P. Stiller, Validation of MIPAS/ENVISAT Level-1B data products, H.-L. Huang, D. Lu, Y. Sasano (Eds.), Optical Remote Sensing of the Atmosphere and Clouds III, Proc. of SPIE, Vol. 4891, pp. 483-496, 2003.

J. Notholt, Z. Kuang, C.P. Rinsland, G.C. Toon, M. Rex, N. Jones, T. Albrecht, H.Deckelman, J. Krieg, C.Weinzierl, H. Bingemer, R. weller, O. Schrems, Enhanced upper tropical tropospheric COS: Impact on the stratospheric aerosol layer, Science, 300,307-310, 2003.

5.5 MAXDOAS observations of tropospheric and stratospheric trace gases

Thomas Wagner
Institut für Umweltphysik, Universität Heidelberg
not on board: Roman Sinreich, Ossama Ibrahim, Barbara Dix, Udo Friess, Ulrich Platt, Institut für Umweltphysik, Universität Heidelberg

Objectives

As in several previous years, a MAXDOAS instrument is installed on board of the RV *Polarstern*. This time, it was designed to perform measurements during the whole cruise ANT-XXIII from October 2005 to May 2007. MAXDOAS observations during extended ship cruises are important for several reasons. First, measurements carried out with one instrument over large ranges of latitude and longitude yielding very homogenous data sets. Thus they allow to study the variations of atmospheric trace gases on a global scale. Second, it is possible to reach remote regions, especially polar regions, where peculiar phenomena (e.g. the bromine explosion) occur. Finally, the global data sets are well suited for the validation of satellite data. The MAXDOAS measurements are carried out in the UV spectral range, where the specific absorption features of many atmospheric trace gases (like O_3, NO_2, BrO, OClO, SO_2, and HCHO) can be analysed. Our instrument observes scattered solar photons in various directions; thus they yield (limited) information on the atmospheric height profiles of these trace gases. We describe the measurement principle, the instrumental set-up and the data analysis and present first results.

Measurement principle

The Multi AXis Differential Optical Absorption Spectroscopy (MAX-DOAS) technique allows to separate the absorptions taken place at different altitudes in the atmosphere by observing scattered sun light from a variety of viewing directions (see Fig. 5.13) (Hönninger and Platt, 2002; Leser et al., 2003; Von Friedeburg et al., 2003; Bobrowski et al., 2003; van Roozendael et al., 2003; Wittrock et al., 2003; Hönninger et al., 2004; Heckel et al., 2004). This is possible because for most measurement conditions, the observed light is scattered in the free troposphere. Thus, air masses located close to the ground are traversed on a slant absorption path determined by the viewing direction; in contrast, stratospheric air masses are traversed on a slant absorption path determined by solar zenith angle (see Fig. 5.14, Fig. 5.15).

In addition to the partial columns of various trace gases (like NO_2, BrO, HCHO, etc.see Table 5.3) also information on the aerosol profile can be retrieved (Wagner et al., 2004).

Tab. 5.3: Data products of the DOAS ship measurements

Trace gas	Spectral range	Tropopsheric and/or stratospheric columns
O_3	UV / vis	Strat/trop
NO_2	UV / vis	Strat/trop
BrO	UV	Strat/trop
OClO	UV / vis	Strat
HCHO	UV	Trop
O_4	UV / vis	Trop
SO_2	UV	Trop
IO	UV / vis	Strat?/trop

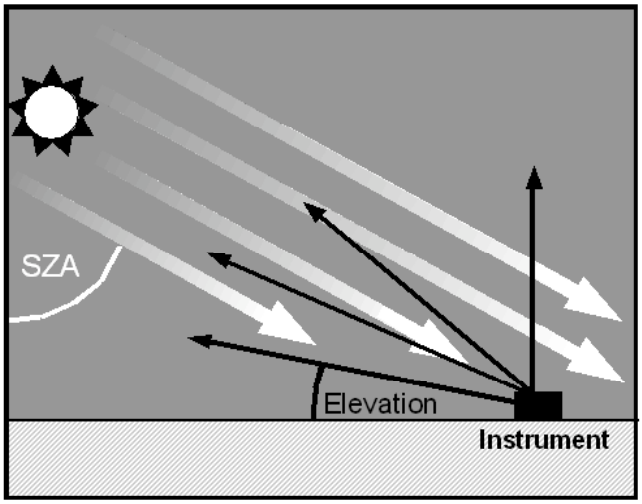

Fig. 5.13: Scheme of the MAX-DOAS observation geometry. Scattered sunlight is observed under various elevation (and often also azimuth) angles. Often the elevation angle of the telescopes is defined with respect to the ground. The solar zenith angle (SZA) is defined as the angle between the incident sunlight and the zenith.

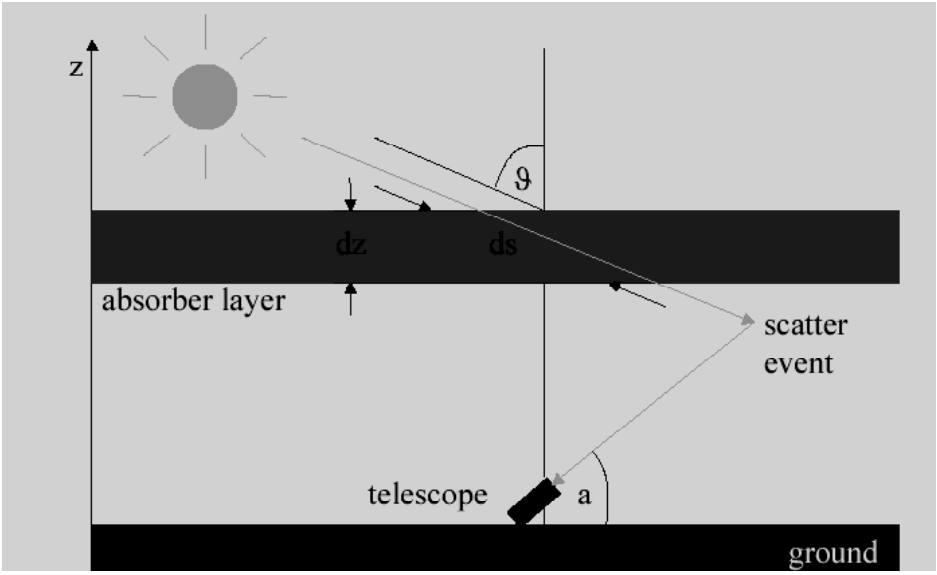

Fig. 5.14: The path length through the stratosphere is mainly determined by the solar zenith angle (SZA); from observations made at different SZA, the stratospheric trace gas absorption can be retrieved.

The sensitivity of DOAS observations of scattered light is usually quantified by the so called air mass factor, which is the ratio of the trace gas concentration integrated along the light path (SCD) and the vertically integrated trace gas concentration (VCD).

AMF = SCD/VCD

It is usually determined from numerical radiative transfer calculations (Solomon et al., 1987; Marquard et al., 2000). According to the altitude of a trace gas in the atmosphere, the respective AMF depends strongly on the SZA or the elevation angle (see Fig. 5.16, Fig. 5.17).

For the analysis of the MAXDOAS observations a new radiative transport model (TRACY) will be used, which is based on the backward Monte Carlo method (von Friedeburg, 2003; von Friedeburg et al., 2004; Wagner et al., 2004). It was explicitly designed for the correct treatment of spatial gradients, which is important for the correct interpretation of MAXDOAS observations.

In addition to the retrieval of concentration profiles of the atmospheric trace gases, also profiles of aerosol properties (like extinction, single scattering albedo, and phase function) can be analysed from MAXDOAS of the oxygen dimer O_4 (Wagner et al., 2004; Sinreich et al., 2005).

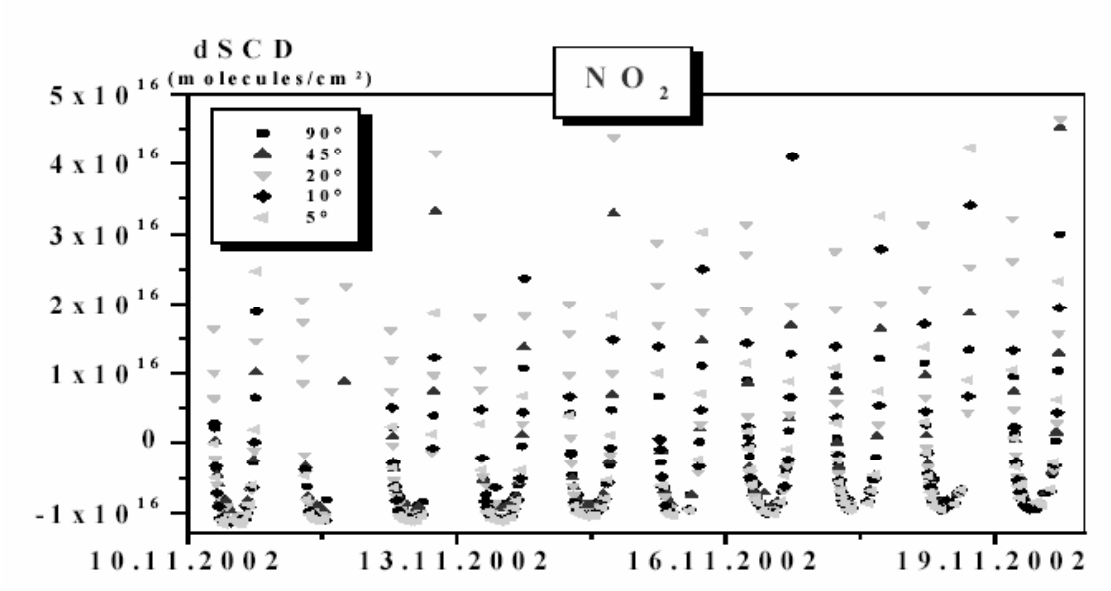

Fig. 5.15: Diurnal distribution of the NO_2 dSCD for a region of unpolluted tropospheric air masses. The bathtub like daily variation is typical for a purely stratospheric absorber [Halasia, 2004]. It is caused by the light path variations due to the position of the sun.

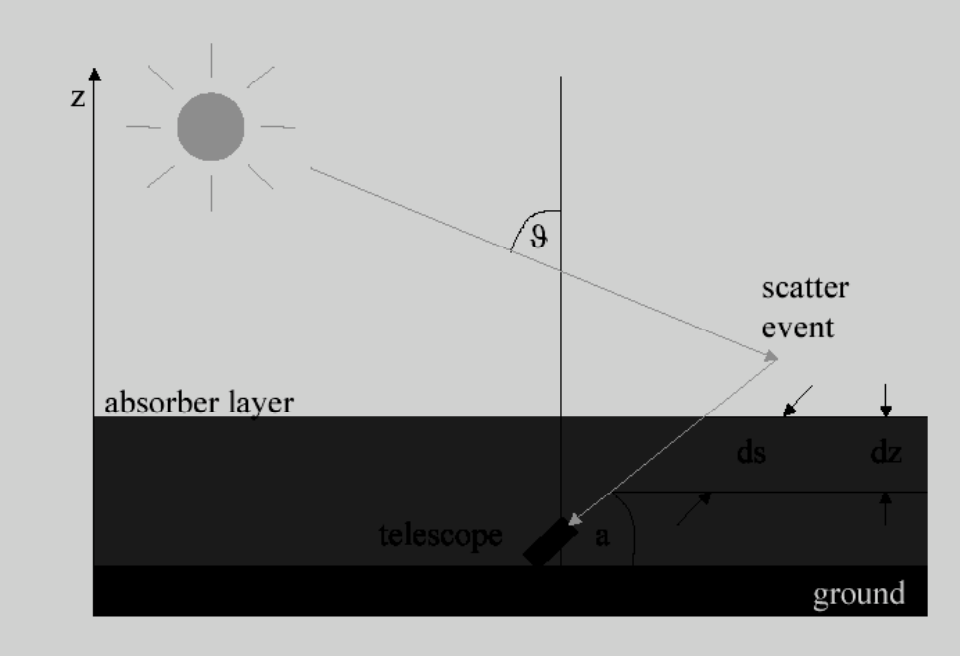

Fig. 5.16: The path length through the boundary layer is mainly determined by the viewing angle of the telescopes.; from observations made at different viewing angles, the boundary layer trace gas absorption can be retrieved.

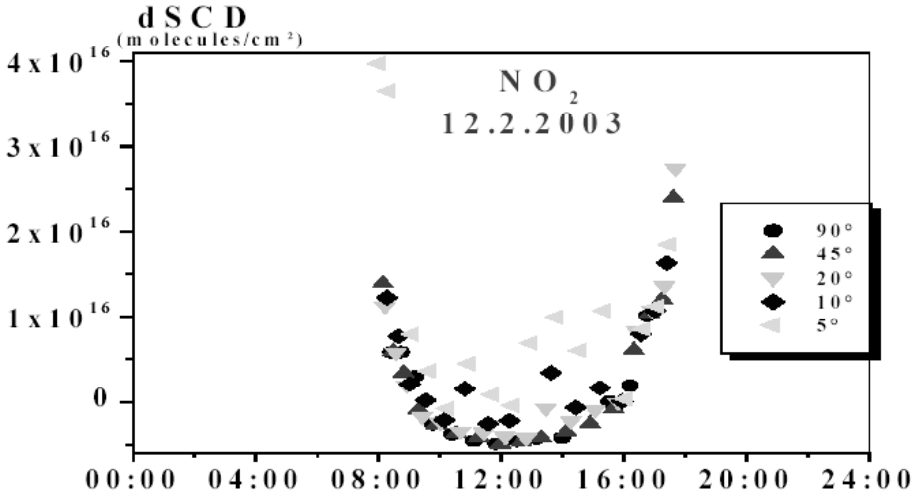

Fig. 5.17: Diurnal distribution of the NO_2 dSCD for a region of polluted tropospheric air masses. The different DSCDs for the different elevation angles are typical for an atmospheric absorber close to the ground [Halasia, 2004].

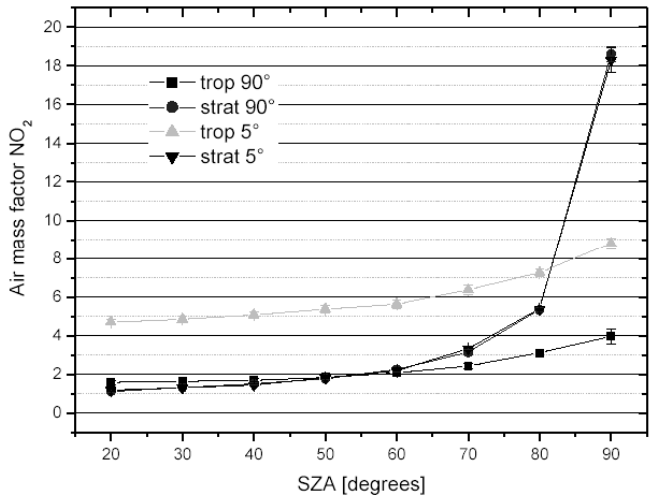

Fig. 5.18: Tropospheric and stratospheric air mass factors of NO_2 for elevation angles 5° and 90° calculated with the Heidelberg radiative transfer model TRACY. The AMFs for stratospheric concentrations mainly depend on the SZA; the AMFs for stratospheric concentrations mainly depend on the elevation angle.

Work at sea

The instrument consists of an indoor and an outdoor set-up. Both are connected via electric cables and glass fibres. The telescope is mounted in a small heated box, which is moved by a stepper motor to allow elevation angles between 0° (to the horizon) and 90° (to the zenith).

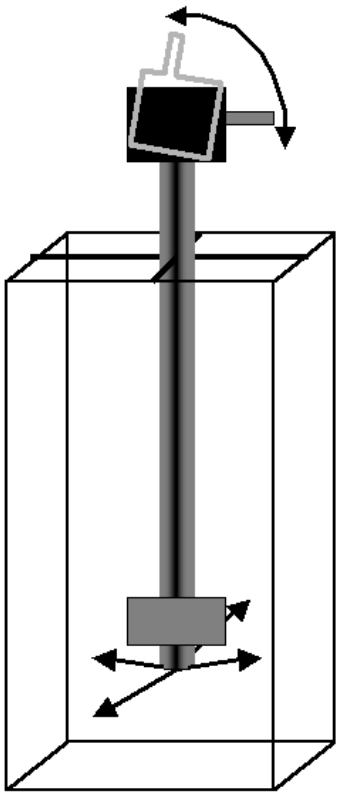

Fig. 5.19: Outdoor set-up of the MAX-DOAS instrument. To become independent of the ship movements, the telescope box is mounted atop a large pendulum with a heavy lead-weight at the bottom. The telescope box is moved by a stepper motor to allow elevation angles between 0° (to the horizon) and 90° (to the zenith).

To become independent of the ship movements, the telescope box is mounted atop a large pendulum with a heavy lead-weight at the bottom (see Fig. 5.19). In order to prevent the swinging axis from reaching a resonance frequency a gentle damping was added. The collected light is conducted via a quartz fibre (diameter: 800 µm) to the spectrograph mounted under deck in the observation room of the ship.

The light is fed into an Ocean Optics USB 2000 spectrograph that dispersed the light with a grating and mapped it onto a one dimensional CCD array with 2048 elements. The covered wavelength range reaches from 290nm to 430 nm, thus enabling the analysis of O_3, NO_2, BrO, OClO, HCHO, and SO_2. The spectral resolution is about 0.9nm FWHM.

The spectrometer is mounted into a modified hermetic Dewar vessel. In order to avoid ambient air from penetrating into the protective vessel it had been evacuated and filled up with gaseous Argon up to 1.2bar prior to the expedition. Stable measurement conditions and low detector noise could be achieved by cooling the spectrograph down to ca. 0°C by a two-stage Peltier cooling unit. A radiator with fan served as a lid for the Dewar, the fan blowing away the heat created in the cooling process. The electronic signal that is produced in the detector array by the incoming light was sent via an integrated analogue to digital converter (ADC) to a read-out unit of a computer, which stored and imaged the spectra.

Spectra are taken about every 2 minutes between sunrise and sunset. Measurements at 6 elevation angles (1°, 3°, 6°, 10°, 30°, 90°) are performed sub-sequentially. During the night automatic measurements of offset and dark current are taken. The correct time (UTC) and position of the ship is provided automatically from the bord computer system.

Data analysis
The measured spectra are analysed using the DOAS method [Platt, 1994]. To the (logarithm of the) measured spectrum several trace gas cross sections as well as a Ring spectrum [Grainger and Ring, 1962; Bussemer, 1993], a Fraunhofer reference spectrum and a polynomial of low degree are fitted by means of a least squares fitting routine [Gomer et al., 1993; Stutz and Platt, 1996]. The wavelength calibration is performed by fitting the measured spectra to a high resolution solar spectrum [Kurucz et al., 1984]. Examples of the DOAS analysis of the various trace gases are shown in figure 5.20.

Because the Fraunhofer spectrum also contains atmospheric absorption structures of the atmospheric trace gases the result of the DOAS analysis represents the difference of the SCDs of the measured spectrum and of the Fraunhofer spectrum. From the observations of the SCD under changing SZA and/or elevation angles the partial trace gas columns in the boundary layer and the stratosphere can be analysed.

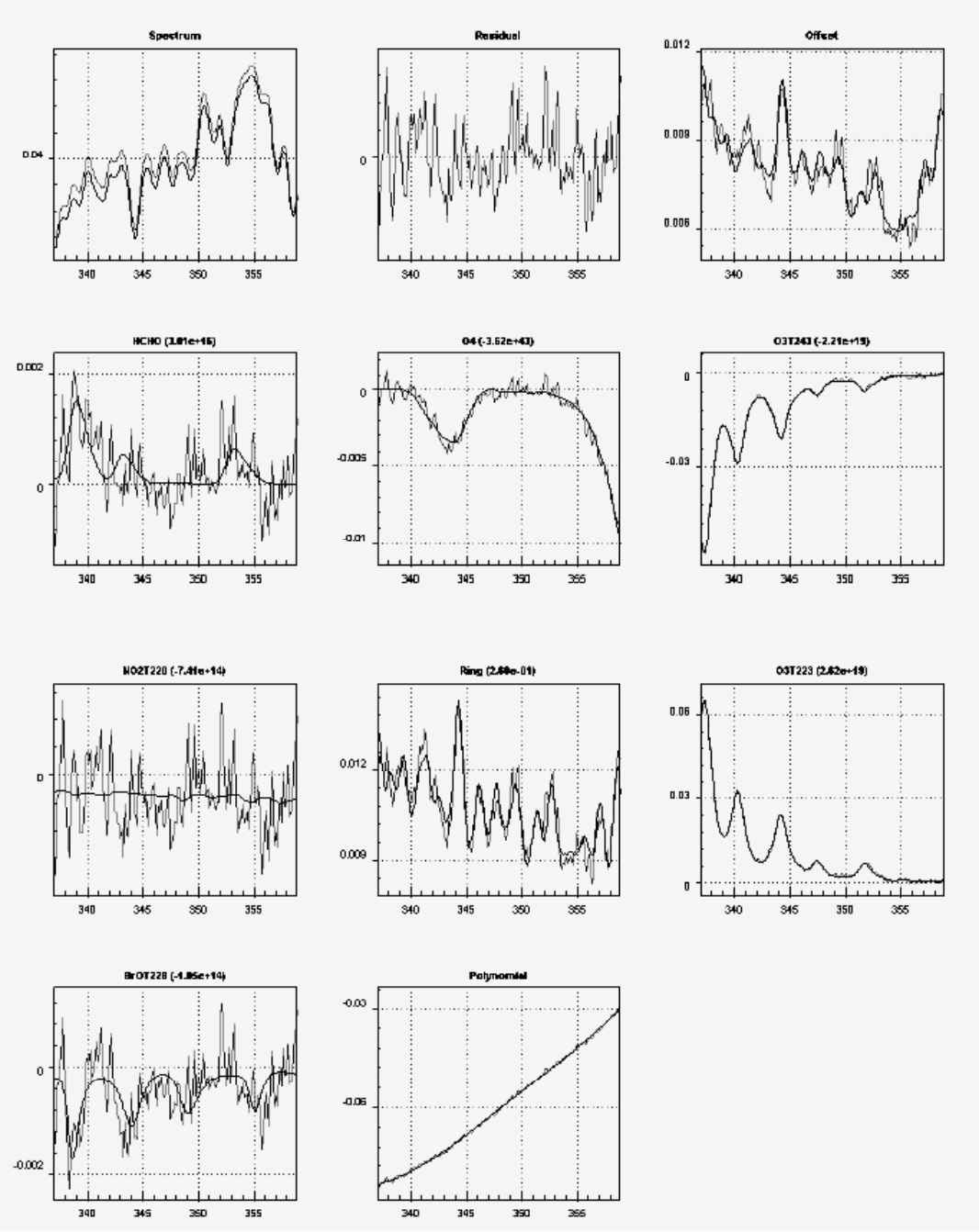

Fig. 5.20: Exemplary analysis result of a HCHO fitting procedure in the UV spectral range [Halasia, 2004]. Besides the HCHO absorption also the absorptions of other atmospheric trace gases are analysed simultaneously. The black lines indicate the laboratory spectra of the trace gas cross sections scaled to absorptions found in the measured spectrum (red line).

Preliminary results

One of the main foci of the MAXDOAS observations during this cruise is the observation of tropospheric BrO amounts. BrO can be present at a ppt-level in the troposphere; possible precursors could be released from biological activity in the ocean.

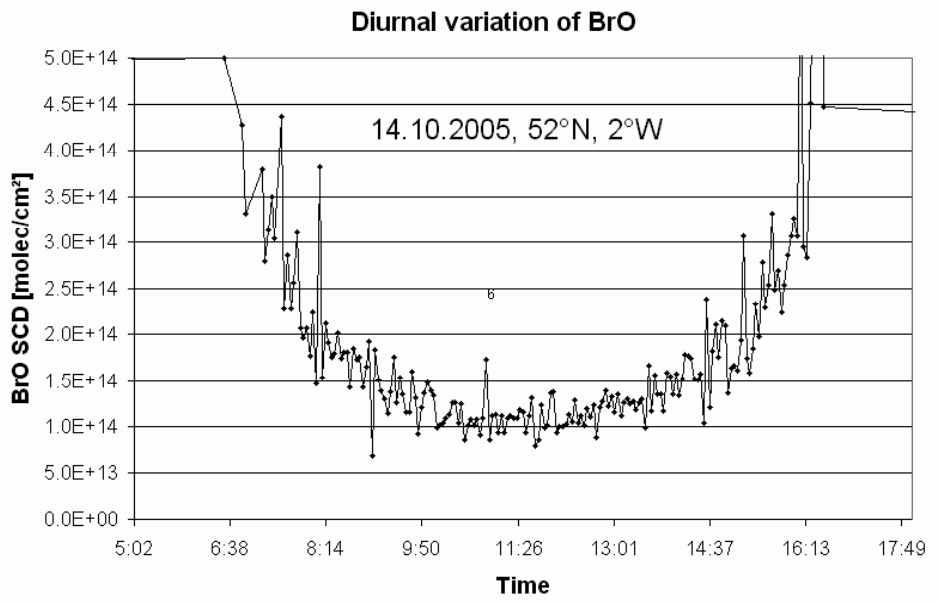

Fig. 5.21: Diurnal variation of the total BrO SCD for a day with almost no BrO in the troposphere. The measurements at the different elevation angles show similar values.

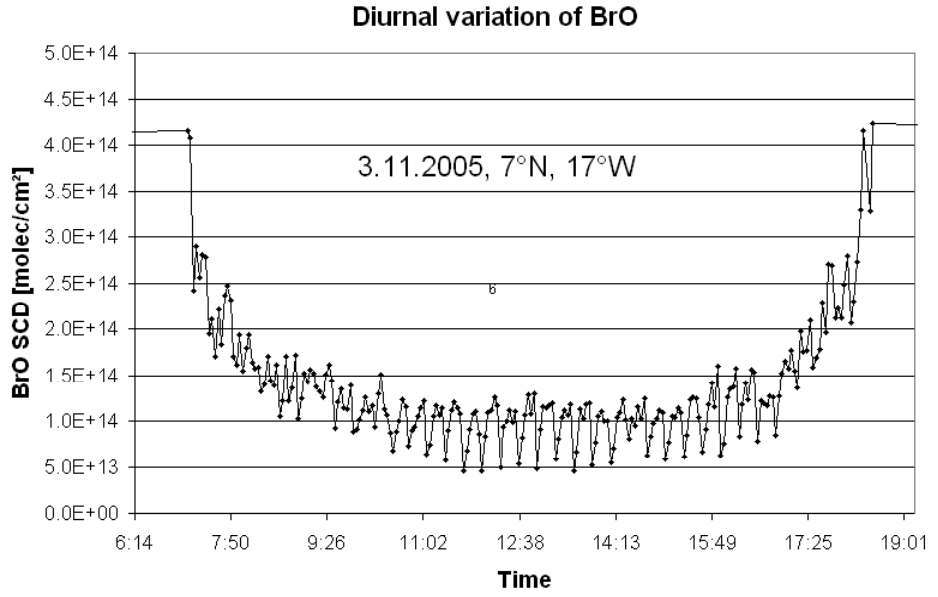

Fig. 5.22: Diurnal variation of the total BrO SCD for a day with BrO present in the troposphere. The measurements at the different elevation angles show systematically different values.

Figure 5.21 and figure 5.22 show the diurnal cycle of the total BrO SCD for two selected days. For both days, the overall U-shaped variation is caused by the influence of the solar position on the stratospheric BrO profile: during sunset and sunrise the stratospheric absorption is very long causing high BrO SCDs. On the first day, measurements at the different elevation angles of the telescope show almost similar values. On the second day, however, the BrO SCDs for the different elevation angles show clearly distinct values. These are caused by BrO located in the troposphere. From these systematic differences the tropospheric BrO column density can be derived. Figure 5.23 shows preliminary results of daily averaged tropospheric BrO column densities measured on the Atlantic transect during ANT-XXIII/1.

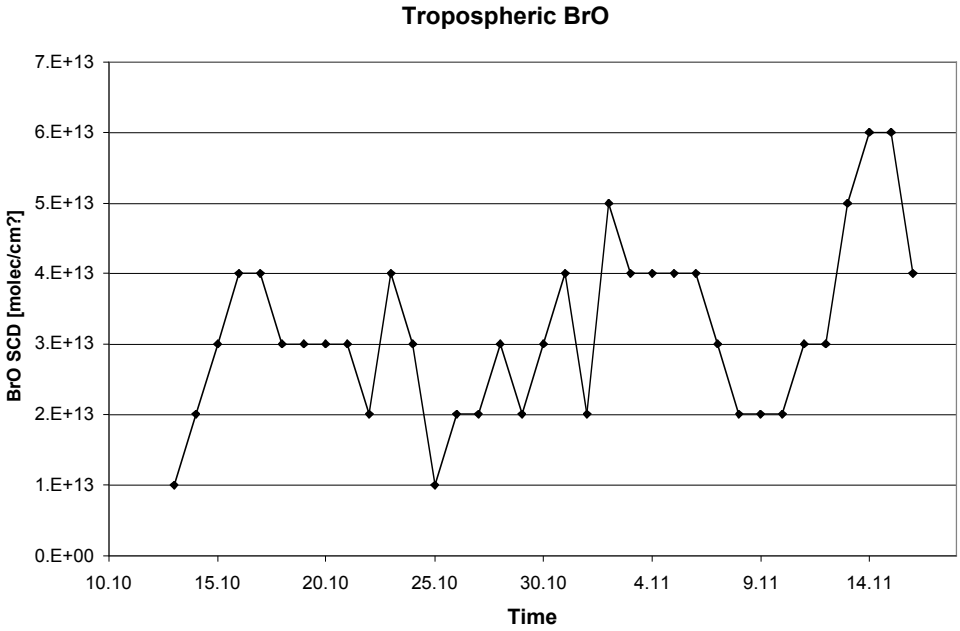

Fig. 5.23: Tropospheric BrO SCDs measured at 3° degree telescope elevation. The lowest values were found close to the coast (at Bremerhaven and Vigo); the heighest values are found in the south-east Atlantic.

Acknowledgements

Many thanks to the RV *Polarstern*-Crew for their great help and hospitality and to the AWI for providing this unique opportunity to perform measurements on the RV *Polarstern*. Special thanks go to Peter Gerchow for his great help to optimise the computer performance.

We also want to thank the workshop at the Institut für Umweltphysik for their competent support in building the MAX-DOAS instrument.

References

Bobrowski, N., Hönninger, G., Galle, B., and Platt, U.: Detection of bromine monoxide in a volcanic plume, Nature, 423, 273–276, 2003.

Bussemer, M., Der Ring-Effekt: Ursachen und Einfluß auf die spektroskopische Messung stratosphärischer Spurenstoffe, Diploma thesis, University of Heidelberg, 1993.

Gomer, T., T. Brauers, F. Heintz, J. Stutz, and U. Platt, MFC user manual, version 1.98, Institut für Umweltphysik, University of Heidelberg, Germany, (http://ich313.ich.kfa-juelich.de/Mfc/mfc.htm), 1993.

Grainger, J.F., and J. Ring, Anomalous Fraunhofer line profiles, Nature, 193, 762, 1962.

Halasia, Magdalini-Anastasia, SMAX-DOAS observation of atmospheric trace gases on the Polarstern ANT/XX-expedition from October 2002 until February 2003, Diploma thesis, University of Heidelberg, 2004.

Heckel, A., A. Richter, T. Tarsu, F. Wittrock, C. Hak, W. Junkermann, and J. Burrows, DOAS off-axis measurements of Formaldehyde, paper in preparation for Atmos. Chem. Phys., 2004.

Hönninger G., and Platt U., The Role of BrO and its Vertical Distribution during Surface Ozone Depletion at Alert, Atmos. Environ., 36, 2481–2489, 2002.

Hönninger, G., C. von Friedeburg, and U. Platt, Multi Axis Differential Optical Absorption Spectroscopy (MAX-DOAS), Atmos. Chem. Phys., 4, 231-254, 2004.

Kurucz, R.L., I. Furenlid, J. Brault, and L. Testerman, Solar flux atlas from 296 nm to 1300 nm, National Solar Observatory Atlas No. 1, 1984.

Leser, H., Hönninger, G., and Platt, U., MAX-DOAS measurements of BrO and NO2 in the marine boundary layer, Geophys. Res. Lett., 30, 10, doi:10.1029/2002GL015811, 2003.

Marquard, L.C., T. Wagner, and U. Platt, Improved Air Mass Factor Concepts for Scattered Radiation Differential Optical Absorption Spectroscopy of Atmospheric Species, J. Geophys. Res.,105, 1315-1327, 2000.

Platt U., Differential optical absorption spectroscopy (DOAS), Air monitoring by spectroscopic techniques, M.W. Sigrist, Ed., Chemical Analysis Series, 127, John Wiley & Sons, Inc, 1994.

Sinreich, R., U. Friess, T. Wagner, U. Platt, Multi Axis Differential Optical Absorption Spectroscopy (MAX-DOAS) of Gas and Aerosol Distributions, Faraday Discuss., 153 – 164, 2005.

Solomon, S., A. L. Schmeltekopf, and R. W. Sanders, On the interpretation of zenith sky absorption measurements, J. Geophys. Res, 92, 8311-8319, 1987.

Stutz J., and U. Platt, Numerical analysis and error estimation of Differential Optical Absorption Spectroscopy measurements least-squares methods, Appl. Optics, 35, 6041-6053, 1996.

Van Roozendael, M., Fayt, C., Post, P., Hermans, C., Lambert, J.-C.: Retrieval of BrO and NO2 from UV-Visible Observations, in: Sounding the troposphere from space: a new era for atmospheric chemistry, Springer-Verlag, ISBN 3-540-40873-8, edited by Borell, P. et al., 2003.

Von Friedeburg, C., I. Pundt, K.-U. Mettendorf, T. Wagner, and U. Platt, Multi-AXis-(MAX) DOAS Measurements of NO2 during the BAB II Motorway Emission Campaign, accepted for Atmospheric Environment 2004.

Wagner, T., B. Dix, C.v. Friedeburg, U. Frieß, S. Sanghavi, R. Sinreich, and U. Platt, MAX-DOAS O4 measurements – a new technique to derive information on atmospheric aerosols. (I) Principles and information content, J. Geophys. Res., 109, D22205, doi:10.1029/2004JD004904.

Wittrock, F., H. Oetjen, A. Richter, S. Fietkau, T. Medeke, A. Rozanov, and J. P. Burrows, MAX-DOAS measurements of atmospheric trace gases in Ny-Ålesund, Atmos. Chem. Phys. Discuss., 3, 6109-6145, 2003.

5.6 Temperature Measurements in the Mesopause Region (~87 km)

Michael Bittner, Kathrin Höppner
Deutsches Zentrum für Luft-und Raumfahrt, Wessling, Germany

Objectives
The mesosphere can be seen as an Early Warning System for Climate Signals. This is because the air density of the mesopause region is about one millionth lower than the one at the ground. It is expected that the amplitude of climate signals should be much more pronounced and is therefore earlier detectable than in the lower layers of the atmosphere.

Measurements of temperature in the mesopause region are, however, difficult. Aircrafts and balloons cannot reach this altitude. Therefore, the use of satellite-based measurements for the continuous observation of the mesopause region with global coverage becomes more and more important. Processing of satellite-based data of these heights is, however, delicate; radiative transfer schemes need to take into account “Non-LTE-Effects”. Additionally, satellite-based sensors sensitivity may degrade over their lifetime due to the extreme conditions in space.

The German Remote Sensing Data Center (DFD) of the German Aerospace Center (DLR) has developed a mobile Infrared-Spectrometer GRIPS 4 (GRound-based Infrared P-branch Spectrometer). The measurement technique makes use of the so-called airglow: In the upper mesosphere atomic hydrogen reacts with ozone

$$O_3 + H \rightarrow O_2 + OH^* \text{ (exothermic 3.32 eV)}$$

forming excited hydroxyl molecules (OH*) in a layer of ~8 km thickness and a peak altitude of ~87 km. Chemically excited OH molecules emit near-infrared radiation from several rotational-vibrational transitions. These emissions are measured by ground-based instruments during nighttime (OH* concentrations during daytime are negligible). The measuring technique also allows measurements even if light clouds or haze are present. Details are given in Bittner et al. (2000, 2002).

A case study comparing SCIAMACHY data to GRIPS 1 (precursor of GRIPS 4) above Hohenpeissenberg (47.5°N / 11.1°E) has already been conducted and yielded a good agreement (von Savigny et al., 2004, Fig. 5.24). The primary objective of this campaign was to validate mesopause temperature measurements of ENVISAT-SCIAMACHY over different climate zones from Bremerhaven to Cape Town (ANT-XXIII/1) with one instrument.

Another objective was to generate a data series during the expedition which inherently is of scientific interest concerning the investigation of atmospheric

dynamics. One specific question was to quantify smaller scale temperature fluctuations (gravity waves) versus latitude. The campaign was part of the ESA (European Space Agency) project “SCIAMACHY Long Term Validation”.

Work at sea

The instrument GRIPS 4 was installed in the “Wissenschaftlicher Arbeitsraum” on deck A. Since the second night (14/15 October 2005) on board it measured continuously every night. The temporal resolution was about 3 minutes. Figure 5.25 shows a typical spectrum. The rotational temperature was derived from the OH*(3,1) vibrational P-branch using the relative intensities of the shown three rotational P1(2), P1(3), and P1(4) lines at 1524 - 1543 nm. Only one night was lost during the cruise due to bad weather conditions (heavy cloud coverage).

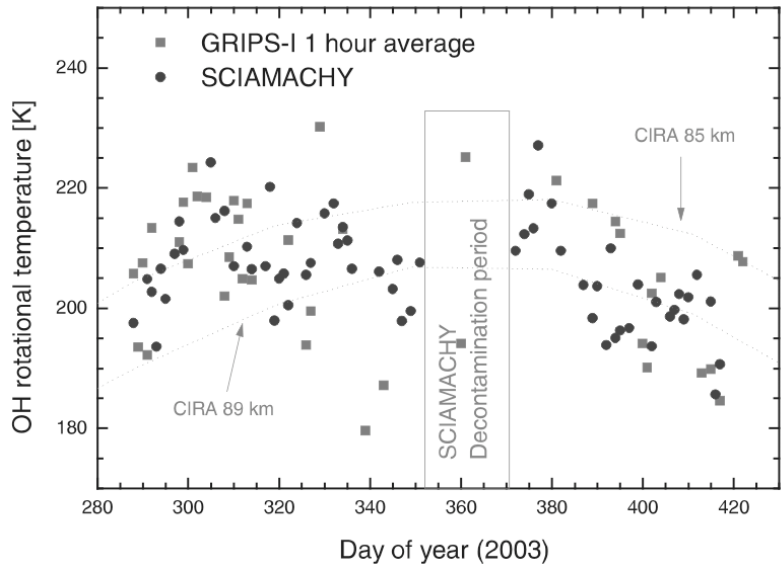

Fig. 5.24: Comparison of SCIAMACHY OH (3-1) rotational temperatures with collocated GRIPS-1 1-hour averages of ground-based OH (3-1) rotational temperature measurements at Hohenpeissenberg (47.5°N / 11.1°E) for period 15 October 2003 through 26 February 2004. The mean difference is about 2 Kelvin.

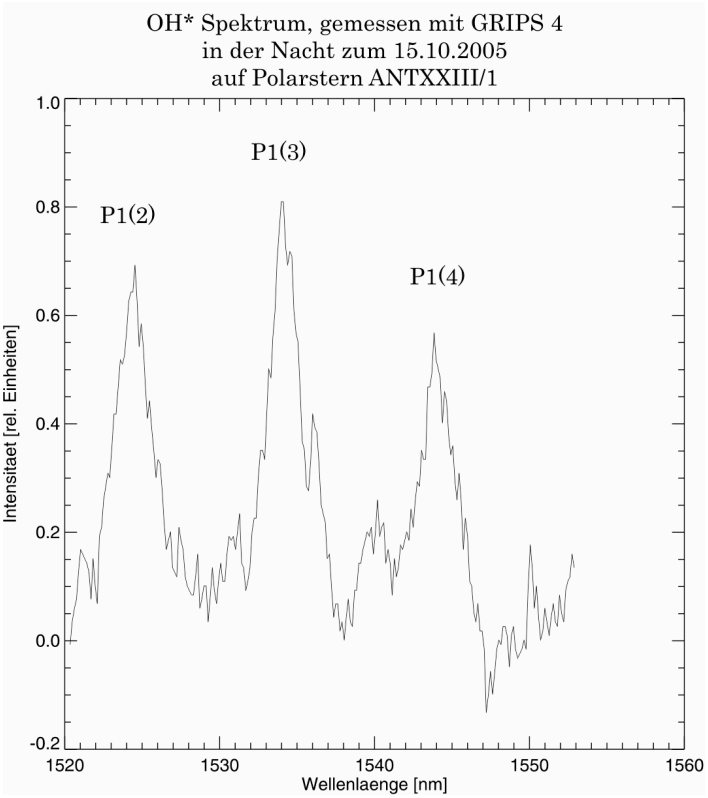

Fig. 5.25: OH spectrum, measured by GRIPS 4 on board RV* Polarstern *during the night 14/15 October, 2005.*

References

Bittner, M., D. Offermann, H.-H. Graef, M. Donner, and K. Hamilton, An 18 year time series of OH rotational temperatures and middle atmosphere decadal variations, J. Atmos. Sol. Terr. Phys., 64, 1147-1166, 2002

Bittner, M., D. Offermann, and H.-H. Graef, Mesopause temperature variability above a midlatitude station in Europe, J. Geophys. Res., 105, 2045-2058, 2000

von Savigny, C., K.-U. Eichmann, E.J. Llewellyn, H. Bovensmann, J.P. Burrows, M. Bittner, K. Höppner, D. Offermann, M.J. Taylor, Y. Zhao, W. Steinbrecht and P. Winkler, First retrieval of OH* rotational temperatures from satellite-based measurements of the (3-1) Meinel band emission, Geophys. Rel. Lett., 31, L15111 (10.1029/2004GL020410), 2004.

A.1 BETEILIGTE INSTITUTE / PARTICIPATING INSTITUTES ANT-XXIII/1

	Adresse /Address
Atlas Hydrographic GmbH	Kurfürstenallee 130 28211 Bremen / Germany
AWI	Stiftung Alfred-Wegener-Institut für Polar- und Meeresforschung in der Helmholtz-Gemeinschaft Postfach 12 01 61 27515 Bremerhaven / Germany
DLR	Deutsches Zentrum für Luft- und Raumfahrt (DLR) Münchner Strasse 20 D-82234 Wessling / Germany
DWD	Deutscher Wetterdienst Hamburg Abteilung Seeschifffahrt Bernhard-Nocht Str. 76 20359 Hamburg / Germany
ELAC-Nautik	L-3 Communications ELAC Nautik GmbH Neufeldtstrasse D-24118 Kiel / Germany
ETH Zürich	Institute for Isotope Geology and Mineral Resources Department of Earth Sciences ETH Zentrum, NO C61.1 Sonneggstrasse 5 CH-8092 Zurich / Switzerland
FIELAX	FIELAX GmbH Schifferstrasse 10-14 27568 Bremerhaven / Germany

	Adresse /Address
FTZ-Westküste	FTZ-Westküste Hafentrön 1 25761 Büsum / Germany
GKSS	GKSS Forschungszentrum Geesthacht, Institut für Küstenforschung, Max Planck- Str. 1, 21502 Geesthacht / Germany
IAP	Institut für Anorganische und Physikalische Chemie der Universität Bremen FB 02 – AG Meereschemie Postfach 330440 28334 Bremen / Germany
IFM-GEOMAR	Leibniz-Institut für Meereswissenschaften IFM-GEOMAR Düsternbrooker Weg 20 24105 Kiel/ Germany
impress	impress GmbH Varreler Landstrasse 28259 Bremen/ Germany
IOPAS	Institute of Oceanology Polish Academy of Sciences Powstancow Warszawy 55, 81–712 Sopot / Poland
IOW	Institut für Ostseeforschung Warnemünde, Seestrasse 15 D-18119 Warnemünde / Germany
IUP	Institut für Umweltphysik Universität Bremen – FB1 Postfach 330440 D-28334 Bremen / Germany
MEL-IAEA	Marine Environment Laboratory (IAEA- MEL) 4 Quai Antoine 1er MC-98000 Monaco / Monaco

	Adresse /Address
UCSD-Scripps	Marine Physical Laboratory Scripps Inst. Oceanography UCSD 9500 Gilman Drive m/c 0238 La Jolla, CA 92093-0238 / USA
University Heidelberg	Institut für Umweltphysik Universität Heidelberg Im Neuenheimer Feld 229 69120 Heidelberg / Germany
University Insubria	DBSF - Università dell'Insubria Via Dunant 3 21100 Varese / Italy
University Lancaster	Department of Environmental Science, I.E.N.S., Lancaster University Lancaster, LA1 4YQ / UK
UCSD-Hancock	Hancock Institute for Marine Studies University of Southern California Los Angeles, CA 90089-0371/ USA

A.2 FAHRTTEILNEHMER / PARTICIPANTS

Name	Vorname/ First Name	Institut Institute	Beruf / Profession
Bittner	Michael	DLR	Physicist
Bluszcz	Thaddäus	AWI	Technician
Breitzke	Monika	AWI	Geophysicist
Buldt	Klaus	DWD	Technician
Caba	Armando	GKSS	Engineer
Croot	Peter	IFM-GEOMAR	Scientist
Daberkow	Timo	University Bremen	Chemist
Dissard	Delphine	AWI	Student
El Naggar	Saad	AWI	Scientist
Frank	Martin	IFM-GEOMAR	Scientist
Gastaud	Janine	MEL Monaco	Student
Geibert	Walter	AWI	Scientist
Gioia	Rosalinda	University Lancaster	Student
Graffe	Dorothea	AWI	Engineer
Hans	Kerstin	AWI	Student
Harms	Corinna	University Bremen	Student
Hennings	Ursula	IOW	Engineer
Heymann	Kerstin	GKSS	Engineer
Hofmann	Jörg	FIELAX	Meteorologist
Höppner	Kathrin	DLR	Scientist
Immler	Franz	AWI	Physicist
Jahnke	Annika	GKSS	Scientist
Kaczmarek	Slawomir	IOPAS	Physicist
Kuhn	Gerhard	AWI	Geologist
Lütticke	Ulrich	Atlas Hydrographic	Engineer
Mengistu Tsidu	Gizaw	University Bremen	Physicist
Niederjasper	Fred	AWI	Geodesist
Nizzetto	Luca	University Insubria	Student

Name	Vorname/ First Name	Institut Institute	Beruf / Profession
Reynolds	Rick	UCLA	Scientist
Rickli	Jörg	ETH Zürich	Geologist
Röttgers	Rüdiger	GKSS	Scientist
Ruhe	Wilfried	impres	
Ruser	Andreas	FTZ Westküste	Scientist
Rutgers v.d.Loeff	Michael	AWI	Chemist
Schlosser	Christian	IFM-GEOMAR	Scientist
Scholten	Jan	MEL IAEA	Scientist
Schönwetter	Rüdiger	ELAC	Scientist
Schütt	Ekkehard	AWI	Engineer
Steigenberger	Sebastian	AWI	Student
Stramska	Malgorzata	UCLA	Scientist
Stramski	Dariusz	UCLA	Scientist
Terli	Özden	AWI	Student
Vöge	Ingrid	AWI	Lab assistant
Wagner	Thomas	Univ. Heidelberg	Physicist
Weinzierl	Thomas	University Bremen	Student
Wuttke	Sigrid	AWI	Scientist

A.3 SCHIFFSBESATZUNG / SHIP'S CREW

Reederei F.Laeisz G.m.b.H — Reise/journey ANT-XXIII/1
Nationality : GERMAN — Bremerhaven - Cape Town

No.	Name	Rank
01.	Pahl, Uwe / Schwarze, Stefan	Master
02.	Spielke, Steffen	1.Offc.
03.	Schulz, Volker	Ch.Eng.
04.	Bratz, Herbert	2.Offc.
05.	Wunderlich, Thomas	2.Offc.
06.	Niehusen, Frank	2.Offc.
07.	Uhlig, Heinz-Jürgen	Doctor
08.	Koch, Georg	R.Offc.
09.	Ziemann, Olaf	2.Eng.
10.	Simon, Wolfgang	2.Eng.
11.	Westphal, Henning	3.Eng.
12.	Holtz, Hartmut	Elec.Tech.
13.	Dimmler, Werner	Electron.
14.	Riess, Felix	Electron.
15.	Fröb, Martin	Electron.
16.	Feiertag, Thomas	Electron.
17.	Clasen, Burkhard	Boatsw.
18.	Neisner,Winfried	Carpenter
19.	Kreis, Reinhard	A.B.
20.	Schultz, Ottomar	A.B.
21.	Burzan, G.-Ekkehard	A.B.
22.	Schröder, Norbert	A.B.
23.	Moser, Siegfried	A.B.
24.	Pousada Martinez, S.	A.B.
25.	Hartwig-L., Andreas	A.B.
26.	Lamm, Gerd	A.B.
27.	Beth, Detlef	Storekeep.
28.	Hoppe, Kurt	Mot-man
29.	Fritz, Günter	Mot-man
30.	Krösche, Eckard	Mot-man
31.	Dinse, Horst	Mot-man
32.	Toeltl, Siegfried	Mot-man
33.	Fischer, Matthias	Cook
34.	Tupy,Mario	Cooksmate
35.	Martens, Michael	Cooksmate
36.	Dinse, Petra / Gaude, Hans Jürgen	1.Stwdess/Stwd
37.	Tillmann, Barbara	Stwdss/KS
38.	Streit, Christina	2.Stwdess
39.	Schmidt,Maria	2.Stwdess
40.	Deufl, Stefanie	2.Stwdess
41.	Tu, Jian Min	2.Steward
42.	Sun,Yong Sheng	2.Steward
43.	Yu, Chung Leung	Laundrym.

A.4 STATION LIST

Station	Date	Time	Position Lat	Position Lon	Depth [m]	Gear	Action
PS69/001-1	15.10.05	12:02	49° 43,27' N	3° 44,26' W	77	MSDL	start deployment
	15.10.05	12:07	49° 43,26' N	3° 44,36' W	79	MSDL	at depth: 42m
	15.10.05	12:10	49° 43,26' N	3° 44,40' W	75	MSDL	end deployment
PS69/001-2	15.10.05	12:18	49° 43,31' N	3° 44,62' W	75	SLS	start deployment
	15.10.05	12:43	49° 43,65' N	3° 45,36' W	75	SLS	end deployment
PS69/001-3	15.10.05	12:50	49° 43,66' N	3° 45,57' W	73	CTD/RO	start cast
	15.10.05	12:56	49° 43,70' N	3° 45,63' W	76	CTD/RO	at depth: 66m
	15.10.05	13:05	49° 43,76' N	3° 45,61' W	75	CTD/RO	end cast
PS69/002-1	16.10.05	11:58	46° 49,00' N	5° 18,15' W	1013	MSDL	start deployment
	16.10.05	12:09	46° 49,12' N	5° 18,07' W	1010	MSDL	at depth: 200m
	16.10.05	12:19	46° 49,20' N	5° 18,07' W	988	MSDL	end deployment
PS69/002-2	16.10.05	12:26	46° 49,33' N	5° 17,90' W	888	SLS	start deployment
	16.10.05	12:43	46° 49,58' N	5° 17,86' W	890	SLS	end deployment
PS69/002-3	16.10.05	13:00	46° 48,99' N	5° 18,16' W	998	CTD/RO	start cast
	16.10.05	13:06	46° 49,07' N	5° 18,15' W	1013	CTD/RO	at depth: 198m
	16.10.05	13:16	46° 49,18' N	5° 18,12' W	1009	CTD/RO	end cast
PS69/003-1	16.10.05	17:13	46° 24,53' N	5° 55,08' W	4352	CTD/RO	start cast
	16.10.05	18:36	46° 24,33' N	5° 54,84' W	4360	CTD/RO	at depth: 4333m
	16.10.05	19:38	46° 24,30' N	5° 54,67' W	4374	CTD/RO	end cast
PS69/003-2	16.10.05	20:00	46° 24,22' N	5° 54,36' W	4404	SON	start deployment
	16.10.05	22:20	46° 24,15' N	5° 55,09' W		SON	abort test 1
	16.10.05	22:33	46° 24,32' N	5° 55,16' W		SON	start deployment
	16.10.05	22:36	46° 24,34' N	5° 55,15' W		SON	start course track
	17.10.05	09:25	46° 22,76' N	5° 55,08' W	4480	SON	end course track
	17.10.05	19:02	46° 20,70' N	5° 56,54' W		SON	recovery
	17.10.05	19:50	46° 20,14' N	5° 56,19' W	4528	SON	start deployment
	18.10.05	04:44	46° 18,24' N	5° 57,23' W	4556	SON	end deployment
PS69/004-1	18.10.05	11:55	45° 51,06' N	6° 38,63' W	4777	MSDL	start deployment
	18.10.05	12:08	45° 51,12' N	6° 38,52' W	4775	MSDL	at depth: 210m
	18.10.05	12:19	45° 51,16' N	6° 38,44' W	4777	MSDL	end deployment
PS69/004-2	18.10.05	12:22	45° 51,17' N	6° 38,32' W	4775	SLS	start deployment
	18.10.05	12:50	45° 51,66' N	6° 37,65' W	4777	SLS	end deployment
PS69/004-3	18.10.05	12:57	45° 51,75' N	6° 37,55' W	4775	CTD/RO	start cast
	18.10.05	13:05	45° 51,79' N	6° 37,43' W	4766	CTD/RO	at depth: 196m
	18.10.05	13:15	45° 51,76' N	6° 37,31' W	4781	CTD/RO	end cast
PS69/005-1	19.10.05	12:13	46° 12,31' N	4° 6,88' W	167	MSDL	start deployment
	19.10.05	12:22	46° 12,35' N	4° 6,80' W	167	MSDL	at depth: 140m
	19.10.05	12:29	46° 12,39' N	4° 6,74' W	165	MSDL	end deployment
PS69/005-2	19.10.05	12:34	46° 12,41' N	4° 6,64' W	166	SLS	start deployment
	19.10.05	12:58	46° 12,81' N	4° 5,94' W	162	SLS	end deployment
PS69/005-3	19.10.05	13:07	46° 12,97' N	4° 5,76' W	161	CTD/RO	start cast
	19.10.05	13:12	46° 13,01' N	4° 5,67' W	161	CTD/RO	at depth: 151m
	19.10.05	13:19	46° 13,02' N	4° 5,58' W	161	CTD/RO	end cast
PS69/006-1	20.10.05	05:28	45° 44,83' N	5° 31,53' W	4637	GO-FLO	start deployment

Station	Date	Time	Position Lat	Position Lon	Depth [m]	Gear	Action
	20.10.05	05:32	45° 44,83' N	5° 31,53' W	4639	GO-FLO	deployment bottle 1: 20m
	20.10.05	05:34	45° 44,84' N	5° 31,53' W	4638	GO-FLO	deployment bottle 2: 40m
	20.10.05	05:37	45° 44,85' N	5° 31,54' W	4638	GO-FLO	deployment bottle 3: 60m
	20.10.05	05:40	45° 44,85' N	5° 31,55' W	4639	GO-FLO	deployment bottle 4: 80m
	20.10.05	05:43	45° 44,86' N	5° 31,56' W	4638	GO-FLO	at depth: 100m
	20.10.05	05:45	45° 44,86' N	5° 31,57' W	4637	GO-FLO	recovery bottle 4
	20.10.05	05:47	45° 44,86' N	5° 31,59' W	4637	GO-FLO	recovery bottle 3
	20.10.05	05:49	45° 44,86' N	5° 31,60' W	4639	GO-FLO	recovery bottle 2
	20.10.05	05:51	45° 44,86' N	5° 31,61' W	4638	GO-FLO	recovery bottle 1
	20.10.05	05:53	45° 44,86' N	5° 31,63' W	4637	GO-FLO	end deployment
PS69/006-2	20.10.05	06:00	45° 44,86' N	5° 31,65' W	4638	CTD/RO	start cast
	20.10.05	07:26	45° 45,02' N	5° 31,48' W	4620	CTD/RO	at depth: 4623m
	20.10.05	08:30	45° 45,14' N	5° 31,40' W	4620	CTD/RO	end cast
PS69/006-3	20.10.05	08:41	45° 45,16' N	5° 31,36' W	4619	GO-FLO	deployment bottle 1
	20.10.05	08:45	45° 45,16' N	5° 31,35' W	4618	GO-FLO	deployment bottle 2
	20.10.05	08:47	45° 45,16' N	5° 31,35' W	4618	GO-FLO	deployment bottle 3
	20.10.05	08:50	45° 45,16' N	5° 31,33' W	4619	GO-FLO	deployment bottle 4
	20.10.05	08:55	45° 45,16' N	5° 31,30' W	4618	GO-FLO	at depth: 225m
	20.10.05	09:03	45° 45,14' N	5° 31,28' W	4618	GO-FLO	recovery bottle 4
	20.10.05	09:04	45° 45,13' N	5° 31,28' W	4618	GO-FLO	recovery bottle 3
	20.10.05	09:07	45° 45,12' N	5° 31,26' W	4618	GO-FLO	recovery bottle 2
	20.10.05	09:07	45° 45,12' N	5° 31,26' W	4618	GO-FLO	recovery bottle 1
PS69/006-4	20.10.05	09:13	45° 45,10' N	5° 31,24' W	4617	CTD/RO	start cast
	20.10.05	10:25	45° 44,89' N	5° 31,12' W	4616	CTD/RO	at depth: 4614m
	20.10.05	11:33	45° 44,79' N	5° 31,55' W	4618	CTD/RO	end cast
PS69/006-5	20.10.05	11:42	45° 44,74' N	5° 31,50' W	4617	MSDL	start deployment
	20.10.05	11:55	45° 44,69' N	5° 31,56' W	4617	MSDL	at depth: 250m
	20.10.05	12:07	45° 44,64' N	5° 31,54' W	4617	MSDL	end deployment
PS69/006-6	20.10.05	12:12	45° 44,61' N	5° 31,49' W	4618	SLS	start deployment
	20.10.05	12:30	45° 44,28' N	5° 31,33' W	4617	SLS	end deployment
PS69/006-7	20.10.05	12:34	45° 44,23' N	5° 31,29' W	4617	CTD/RO	start cast
	20.10.05	12:42	45° 44,11' N	5° 31,25' W	4616	CTD/RO	at depth: 196m
	20.10.05	12:50	45° 44,00' N	5° 31,26' W	4617	CTD/RO	end cast
PS69/006-8	20.10.05	13:24	45° 44,58' N	5° 31,62' W	4619	CTD/RO	start cast
	20.10.05	13:32	45° 44,47' N	5° 31,57' W	4619	CTD/RO	at depth: 195m
	20.10.05	13:40	45° 44,45' N	5° 31,52' W	4618	CTD/RO	end cast
PS69/007-1	21.10.05	12:19	45° 54,58' N	4° 35,36' W	4063	SLS	start deployment
	21.10.05	12:36	45° 54,87' N	4° 35,34' W	4037	SLS	end deployment
PS69/007-2	21.10.05	12:42	45° 54,79' N	4° 35,35' W	4054	MSDL	start deployment
	21.10.05	12:56	45° 54,87' N	4° 35,47' W	4043	MSDL	at depth: 210m
	21.10.05	13:07	45° 54,95' N	4° 35,47' W	4042	MSDL	end deployment
PS69/007-3	21.10.05	13:14	45° 54,95' N	4° 35,50' W	4045	CTD/RO	start cast
	21.10.05	13:21	45° 55,04' N	4° 35,52' W	4039	CTD/RO	at depth: 196m
	21.10.05	13:32	45° 55,08' N	4° 35,47' W	4037	CTD/RO	end cast

Station	Date	Time	Position Lat	Position Lon	Depth [m]	Gear	Action
PS69/008-1	27.10.05	13:04	33° 33,33' N	14° 30,44' W	4005	MSDL	start deployment
	27.10.05	13:11	33° 33,42' N	14° 30,44' W	3977	MSDL	at depth: 210m
	27.10.05	13:13	33° 33,43' N	14° 30,45' W	3969	MSDL	heave
	27.10.05	13:20	33° 33,45' N	14° 30,44' W	3965	MSDL	end deployment
PS69/008-2	27.10.05	13:23	33° 33,46' N	14° 30,42' W	3965	SLS	start deployment
PS69/008-3	27.10.05	13:32	33° 33,63' N	14° 30,39' W	3927	CTD/RO	start cast
PS69/008-2	27.10.05	13:36	33° 33,69' N	14° 30,37' W	3918	SLS	end deployment
PS69/008-3	27.10.05	13:39	33° 33,73' N	14° 30,36' W	3915	CTD/RO	at depth: 210m
	27.10.05	13:42	33° 33,74' N	14° 30,35' W	3914	CTD/RO	end cast
PS69/009-1	28.10.05	13:02	29° 35,98' N	16° 19,42' W	3673	MSDL	start deployment
	28.10.05	13:11	29° 35,93' N	16° 19,35' W	3673	MSDL	at depth: 210m
	28.10.05	13:12	29° 35,93' N	16° 19,34' W	3673	MSDL	heave
	28.10.05	13:18	29° 35,95' N	16° 19,32' W	3673	MSDL	end deployment
PS69/009-2	28.10.05	13:19	29° 35,95' N	16° 19,32' W	3672	SLS	start deployment
PS69/009-3	28.10.05	13:29	29° 35,98' N	16° 19,20' W	3672	CTD/RO	start cast
	28.10.05	13:36	29° 35,97' N	16° 19,15' W	3673	CTD/RO	at depth: 200m
PS69/009-2	28.10.05	13:44	29° 35,96' N	16° 19,09' W	3673	SLS	end deployment
PS69/009-3	28.10.05	13:44	29° 35,96' N	16° 19,09' W	3673	CTD/RO	end cast
PS69/010-1	29.10.05	13:00	25° 31,82' N	17° 51,88' W	3203	MSDL	start deployment
	29.10.05	13:09	25° 31,81' N	17° 51,83' W	3204	MSDL	at depth: 210m
	29.10.05	13:10	25° 31,81' N	17° 51,83' W	3202	MSDL	heave
	29.10.05	13:17	25° 31,82' N	17° 51,83' W	3204	MSDL	end deployment
PS69/010-2	29.10.05	13:22	25° 31,79' N	17° 51,77' W	3204	SLS	start deployment
PS69/010-3	29.10.05	13:25	25° 31,81' N	17° 51,75' W	3204	CTD/RO	start cast
	29.10.05	13:33	25° 31,83' N	17° 51,67' W	3204	CTD/RO	at depth: 200m
PS69/010-2	29.10.05	13:39	25° 31,85' N	17° 51,61' W	3205	SLS	end deployment
PS69/010-3	29.10.05	13:43	25° 31,85' N	17° 51,57' W	3204	CTD/RO	end cast
PS69/011-1	30.10.05	09:12	22° 30,05' N	20° 29,86' W	4136	GO-FLO	start deployment
	30.10.05	09:16	22° 30,02' N	20° 29,86' W	4137	GO-FLO	deployment bottle 1: 20m
	30.10.05	09:18	22° 30,00' N	20° 29,86' W	4136	GO-FLO	deployment bottle 2: 40m
	30.10.05	09:20	22° 29,98' N	20° 29,87' W	4136	GO-FLO	deployment bottle 3: 60m
	30.10.05	09:21	22° 29,97' N	20° 29,87' W	4136	GO-FLO	deployment bottle 4: 80m
	30.10.05	09:24	22° 29,94' N	20° 29,88' W	4136	GO-FLO	at depth: 105m
	30.10.05	09:27	22° 29,94' N	20° 29,87' W	4136	GO-FLO	recovery bottle 4
	30.10.05	09:29	22° 29,93' N	20° 29,85' W	4136	GO-FLO	recovery bottle 3
	30.10.05	09:31	22° 29,93' N	20° 29,84' W	4135	GO-FLO	recovery bottle 2
	30.10.05	09:33	22° 29,93' N	20° 29,83' W	4135	GO-FLO	recovery bottle 1
	30.10.05	09:34	22° 29,93' N	20° 29,82' W	4135	GO-FLO	end deployment
PS69/011-2	30.10.05	09:40	22° 29,93' N	20° 29,79' W	4135	CTD/RO	start cast
	30.10.05	10:55	22° 29,99' N	20° 29,97' W	4136	CTD/RO	at depth: 4128m
	30.10.05	11:55	22° 29,92' N	20° 30,00' W	4137	CTD/RO	end cast
PS69/011-3	30.10.05	12:00	22° 29,96' N	20° 30,00' W	4136	GO-FLO	start deployment
	30.10.05	12:02	22° 29,97' N	20° 30,00' W	4136	GO-FLO	deployment bottle 1: 20m
	30.10.05	12:03	22° 29,98' N	20° 30,00' W	4136	GO-FLO	deployment bottle 2: 40m
	30.10.05	12:05	22° 29,98' N	20° 30,01' W	4136	GO-FLO	deployment bottle 3: 65m

Station	Date	Time	Position Lat	Position Lon	Depth [m]	Gear	Action
	30.10.05	12:07	22° 29,98' N	20° 30,01' W	4137	GO-FLO	deployment bottle 4: 85m
	30.10.05	12:09	22° 29,98' N	20° 30,01' W	4136	GO-FLO	at depth: 105m
	30.10.05	12:12	22° 29,97' N	20° 30,02' W	4136	GO-FLO	recovery bottle 4
	30.10.05	12:13	22° 29,97' N	20° 30,02' W	4136	GO-FLO	recovery bottle 3
	30.10.05	12:15	22° 29,97' N	20° 30,03' W	4136	GO-FLO	recovery bottle 2
	30.10.05	12:16	22° 29,97' N	20° 30,03' W	4136	GO-FLO	recovery bottle 1
	30.10.05	12:18	22° 29,96' N	20° 30,04' W	4136	GO-FLO	deployment bottle 1: 16m
	30.10.05	12:21	22° 29,96' N	20° 30,04' W	4136	GO-FLO	deployment bottle 2: 65m
	30.10.05	12:22	22° 29,97' N	20° 30,04' W	4136	GO-FLO	deployment bottle 3: 96m
	30.10.05	12:23	22° 29,97' N	20° 30,04' W	4136	GO-FLO	deployment bottle 4: 116m
	30.10.05	12:28	22° 29,98' N	20° 30,03' W	4136	GO-FLO	at depth: 225m
	30.10.05	12:34	22° 29,98' N	20° 30,03' W	4136	GO-FLO	recovery bottle 4
	30.10.05	12:36	22° 29,98' N	20° 30,03' W	4136	GO-FLO	recovery bottle 3
	30.10.05	12:38	22° 29,97' N	20° 30,04' W	4136	GO-FLO	recovery bottle 2
	30.10.05	12:40	22° 29,97' N	20° 30,03' W	4136	GO-FLO	recovery bottle 1
	30.10.05	12:41	22° 29,97' N	20° 30,03' W	4136	GO-FLO	end deployment
PS69/011-4	30.10.05	12:46	22° 29,96' N	20° 30,03' W	4136	SLS	start deployment
PS69/011-5	30.10.05	12:50	22° 29,96' N	20° 30,07' W	4136	CTD/RO	start cast
	30.10.05	13:01	22° 30,01' N	20° 30,18' W	4138	CTD/RO	at depth: 197m
	30.10.05	13:11	22° 30,00' N	20° 30,23' W	4138	CTD/RO	end cast
PS69/011-4	30.10.05	13:13	22° 30,00' N	20° 30,24' W	4138	SLS	end deployment
PS69/011-6	30.10.05	13:21	22° 30,02' N	20° 30,22' W	4138	MSDL	start deployment
	30.10.05	13:30	22° 30,00' N	20° 30,19' W	4138	MSDL	at depth: 210m
	30.10.05	13:32	22° 30,00' N	20° 30,18' W	4138	MSDL	heave
	30.10.05	13:38	22° 30,00' N	20° 30,14' W	4138	MSDL	end deployment
PS69/011-7	30.10.05	13:43	22° 30,00' N	20° 30,10' W	4138	CTD/RO	start cast
	30.10.05	14:00	22° 30,01' N	20° 30,00' W	4135	CTD/RO	at depth: 958m
	30.10.05	14:19	22° 30,02' N	20° 29,97' W	4136	CTD/RO	end cast
PS69/011-8	30.10.05	14:47	22° 30,01' N	20° 30,01' W	4135	CTD/RO	start cast
	30.10.05	14:53	22° 29,99' N	20° 29,99' W	4136	CTD/RO	at depth: 196m
	30.10.05	15:00	22° 29,98' N	20° 29,93' W	4135	CTD/RO	end cast
PS69/011-9	30.10.05	15:14	22° 30,02' N	20° 29,94' W	4135	CTD/RO	start cast
	30.10.05	15:23	22° 30,05' N	20° 29,89' W	4136	CTD/RO	at depth: 154m
	30.10.05	15:31	22° 30,04' N	20° 29,81' W	4136	CTD/RO	end cast
PS69/012-1	31.10.05	13:01	18° 22,35' N	20° 55,31' W	3112	MSDL	start deployment
	31.10.05	13:12	18° 22,37' N	20° 55,38' W	3112	MSDL	at depth: 210m
	31.10.05	13:13	18° 22,38' N	20° 55,38' W	3112	MSDL	heave
	31.10.05	13:19	18° 22,39' N	20° 55,40' W	3112	MSDL	end deployment
PS69/012-2	31.10.05	13:22	18° 22,39' N	20° 55,43' W	3112	SLS	start deployment
PS69/012-3	31.10.05	13:31	18° 22,39' N	20° 55,59' W	3112	CTD/RO	start cast
	31.10.05	13:38	18° 22,44' N	20° 55,65' W	3112	CTD/RO	at depth: 198m
PS69/012-2	31.10.05	13:43	18° 22,47' N	20° 55,71' W	3112	SLS	end deployment
PS69/012-3	31.10.05	13:51	18° 22,45' N	20° 55,78' W	3112	CTD/RO	end cast
PS69/013-1	01.11.05	13:01	13° 54,41' N	20° 48,90' W	4382	MSDL	start deployment
	01.11.05	13:11	13° 54,37' N	20° 48,86' W	4382	MSDL	at depth: 210m
	01.11.05	13:12	13° 54,38' N	20° 48,85' W	4382	MSDL	heave

Station	Date	Time	Position Lat	Position Lon	Depth [m]	Gear	Action
	01.11.05	13:21	13° 54,38' N	20° 48,85' W	4382	MSDL	end deployment
PS69/013-2	01.11.05	13:23	13° 54,36' N	20° 48,86' W	4382	SLS	start deployment
PS69/013-3	01.11.05	13:28	13° 54,33' N	20° 48,88' W	4382	CTD/RO	start cast
	01.11.05	13:36	13° 54,29' N	20° 48,95' W	4382	CTD/RO	at depth: 197m
PS69/013-2	01.11.05	13:46	13° 54,19' N	20° 49,02' W	4384	SLS	end deployment
PS69/013-3	01.11.05	13:47	13° 54,18' N	20° 49,03' W	4384	CTD/RO	end cast
PS69/014-1	02.11.05	07:17	10° 37,46' N	20° 7,74' W	4829	GO-FLO	deployment bottle 1
	02.11.05	07:20	10° 37,46' N	20° 7,74' W	4828	GO-FLO	deployment bottle 2
	02.11.05	07:23	10° 37,45' N	20° 7,74' W	4828	GO-FLO	deployment bottle 3
	02.11.05	07:25	10° 37,45' N	20° 7,74' W	4828	GO-FLO	at depth: 100m
	02.11.05	07:27	10° 37,44' N	20° 7,75' W	4829	GO-FLO	recovery bottle 3
	02.11.05	07:29	10° 37,45' N	20° 7,75' W	4829	GO-FLO	recovery bottle 2
	02.11.05	07:31	10° 37,45' N	20° 7,76' W	4829	GO-FLO	recovery bottle 1
	02.11.05	07:32	10° 37,45' N	20° 7,77' W	4829	GO-FLO	end deployment
PS69/014-2	02.11.05	07:38	10° 37,45' N	20° 7,81' W	4828	CTD/RO	start cast
	02.11.05	09:06	10° 37,39' N	20° 7,87' W	4828	CTD/RO	at depth: 4817m
	02.11.05	10:21	10° 37,31' N	20° 7,80' W	4828	CTD/RO	end cast
PS69/014-3	02.11.05	10:28	10° 37,36' N	20° 7,77' W	4828	GO-FLO	start deployment
	02.11.05	10:30	10° 37,37' N	20° 7,76' W	4829	GO-FLO	deployment bottle 1
	02.11.05	10:33	10° 37,38' N	20° 7,76' W	4829	GO-FLO	deployment bottle 2: 70m
	02.11.05	10:35	10° 37,39' N	20° 7,76' W	4830	GO-FLO	deployment bottle 3: 101m
	02.11.05	10:37	10° 37,40' N	20° 7,75' W	4828	GO-FLO	deployment bottle 4: 135m
	02.11.05	10:40	10° 37,41' N	20° 7,74' W	4828	GO-FLO	at depth: 225m
	02.11.05	10:47	10° 37,45' N	20° 7,75' W	4828	GO-FLO	recovery bottle 4
	02.11.05	10:48	10° 37,46' N	20° 7,75' W	4828	GO-FLO	recovery bottle 3
	02.11.05	10:50	10° 37,48' N	20° 7,76' W	4829	GO-FLO	recovery bottle 2
	02.11.05	10:52	10° 37,49' N	20° 7,77' W	4828	GO-FLO	recovery bottle 1
	02.11.05	10:53	10° 37,49' N	20° 7,77' W	4828	GO-FLO	end deployment
PS69/014-4	02.11.05	10:59	10° 37,51' N	20° 7,76' W	4828	CTD/RO	start cast
	02.11.05	11:05	10° 37,52' N	20° 7,77' W	4828	CTD/RO	at depth: 195m
	02.11.05	11:13	10° 37,52' N	20° 7,76' W	4828	CTD/RO	end cast
PS69/014-5	02.11.05	11:31	10° 37,46' N	20° 7,68' W	4825	CTD/RO	start cast
	02.11.05	11:41	10° 37,43' N	20° 7,67' W	4824	CTD/RO	at depth: 492m
	02.11.05	11:54	10° 37,41' N	20° 7,76' W	4828	CTD/RO	end cast
PS69/014-6	02.11.05	12:03	10° 37,39' N	20° 7,80' W	4829	MSDL	start deployment
	02.11.05	12:14	10° 37,36' N	20° 7,86' W	4827	MSDL	at depth: 210m
	02.11.05	12:15	10° 37,35' N	20° 7,86' W	4827	MSDL	heave
	02.11.05	12:23	10° 37,33' N	20° 7,89' W	4827	MSDL	end deployment
PS69/014-7	02.11.05	12:30	10° 37,30' N	20° 7,91' W	4826	CTD/RO	start cast
PS69/014-8	02.11.05	12:36	10° 37,29' N	20° 7,94' W	4826	SLS	start deployment
PS69/014-7	02.11.05	12:39	10° 37,27' N	20° 7,97' W	4825	CTD/RO	at depth: 200m
	02.11.05	12:49	10° 37,20' N	20° 8,06' W	4825	CTD/RO	end cast
PS69/014-8	02.11.05	13:08	10° 37,03' N	20° 8,11' W	4829	SLS	end deployment
PS69/014-9	02.11.05	13:12	10° 37,01' N	20° 8,10' W	4829	CTD/RO	start cast
	02.11.05	13:19	10° 36,97' N	20° 8,13' W	4833	CTD/RO	at depth: 137m

Station	Date	Time	Position Lat	Position Lon	Depth [m]	Gear	Action
	02.11.05	13:27	10° 36,90' N	20° 8,18' W	4834	CTD/RO	end cast
PS69/015-1	03.11.05	12:58	7° 1,39' N	17° 29,74' W	4859	MSDL	start deployment
	03.11.05	13:08	7° 1,43' N	17° 29,62' W	4859	MSDL	at depth: 210m
	03.11.05	13:09	7° 1,43' N	17° 29,62' W	4859	MSDL	heave
	03.11.05	13:17	7° 1,38' N	17° 29,53' W	4859	MSDL	end deployment
PS69/015-2	03.11.05	13:19	7° 1,37' N	17° 29,49' W	4858	SLS	start deployment
PS69/015-3	03.11.05	13:23	7° 1,38' N	17° 29,39' W	4858	CTD/RO	start cast
	03.11.05	13:30	7° 1,38' N	17° 29,27' W	4859	CTD/RO	at depth: 201m
	03.11.05	13:38	7° 1,37' N	17° 29,16' W	4858	CTD/RO	end cast
PS69/015-2	03.11.05	13:39	7° 1,37' N	17° 29,14' W	4858	SLS	end deployment
PS69/016-1	04.11.05	12:59	3° 42,03' N	14° 43,33' W	4768	MSDL	start deployment
	04.11.05	12:59	3° 42,03' N	14° 43,33' W	4768	MSDL	at depth: 210m
	04.11.05	13:10	3° 41,94' N	14° 43,23' W	4767	MSDL	heave
	04.11.05	13:18	3° 41,92' N	14° 43,18' W	4766	MSDL	end deployment
PS69/016-2	04.11.05	13:23	3° 41,88' N	14° 43,14' W	4766	SLS	start deployment
PS69/016-3	04.11.05	13:25	3° 41,88' N	14° 43,11' W	4766	CTD/RO	start cast
	04.11.05	13:33	3° 41,83' N	14° 43,00' W	4768	CTD/RO	at depth: 197m
	04.11.05	13:43	3° 41,82' N	14° 42,86' W	4766	CTD/RO	end cast
PS69/016-2	04.11.05	13:43	3° 41,82' N	14° 42,86' W	4766	SLS	end deployment
PS69/017-1	05.11.05	12:58	0° 15,88' N	12° 0,72' W	4621	MSDL	start deployment
	05.11.05	13:07	0° 15,91' N	12° 0,75' W	4620	MSDL	at depth: 210m
	05.11.05	13:09	0° 15,91' N	12° 0,74' W	0	MSDL	heave
	05.11.05	13:15	0° 15,91' N	12° 0,70' W	4621	MSDL	end deployment
PS69/017-2	05.11.05	13:18	0° 15,93' N	12° 0,70' W	4620	SLS	start deployment
PS69/017-3	05.11.05	13:23	0° 16,02' N	12° 0,73' W	4618	CTD/RO	start cast
	05.11.05	13:30	0° 16,11' N	12° 0,75' W	4613	CTD/RO	at depth: 205m
PS69/017-2	05.11.05	13:35	0° 16,13' N	12° 0,71' W	4614	SLS	abort deployment
PS69/017-3	05.11.05	13:39	0° 16,16' N	12° 0,67' W	4616	CTD/RO	end cast
PS69/017-2	05.11.05	13:52	0° 16,31' N	12° 0,73' W	4610	SLS	end deployment
PS69/018-1	05.11.05	21:21	0° 41,61' S	11° 16,05' W	3878	GO-FLO	start deployment
	05.11.05	21:22	0° 41,60' S	11° 16,06' W	3878	GO-FLO	deployment bottle 1: 20m
	05.11.05	21:24	0° 41,58' S	11° 16,10' W	3880	GO-FLO	deployment bottle 2: 40m
	05.11.05	21:25	0° 41,58' S	11° 16,12' W	3880	GO-FLO	deployment bottle 3: 60m
	05.11.05	21:27	0° 41,57' S	11° 16,15' W	3878	GO-FLO	deployment bottle 4: 80m
	05.11.05	21:30	0° 41,56' S	11° 16,17' W	3876	GO-FLO	at depth: 99m
	05.11.05	21:31	0° 41,55' S	11° 16,17' W	3876	GO-FLO	recovery bottle 4
	05.11.05	21:32	0° 41,55' S	11° 16,17' W	3879	GO-FLO	recovery bottle 3
	05.11.05	21:33	0° 41,54' S	11° 16,17' W	3875	GO-FLO	recovery bottle 2
	05.11.05	21:34	0° 41,54' S	11° 16,17' W	3877	GO-FLO	recovery bottle 1
	05.11.05	21:36	0° 41,52' S	11° 16,17' W	3874	GO-FLO	end deployment
PS69/018-2	05.11.05	21:40	0° 41,49' S	11° 16,19' W	3874	CTD/RO	start cast
	05.11.05	22:53	0° 41,62' S	11° 15,99' W	3877	CTD/RO	at depth: 3848m
	05.11.05	23:48	0° 41,65' S	11° 15,91' W	3877	CTD/RO	end cast
PS69/018-3	05.11.05	23:54	0° 41,64' S	11° 15,92' W	3877	GO-FLO	start deployment
	05.11.05	23:56	0° 41,64' S	11° 15,92' W	3877	GO-FLO	deployment bottle 1: 21m

Station	Date	Time	Position Lat	Position Lon	Depth [m]	Gear	Action
	05.11.05	23:56	0° 41,64' S	11° 15,92' W	3877	GO-FLO	deployment bottle 2: 70m
	05.11.05	23:58	0° 41,64' S	11° 15,92' W	3876	GO-FLO	deployment bottle 3: 100m
	06.11.05	00:02	0° 41,64' S	11° 15,92' W	3876	GO-FLO	deployment bottle 4: 125m
	06.11.05	00:05	0° 41,64' S	11° 15,91' W	3877	GO-FLO	at depth: 225m
	06.11.05	00:12	0° 41,65' S	11° 15,90' W	3877	GO-FLO	recovery bottle 4
	06.11.05	00:13	0° 41,66' S	11° 15,89' W	3877	GO-FLO	recovery bottle 3
	06.11.05	00:15	0° 41,66' S	11° 15,89' W	3877	GO-FLO	recovery bottle 2
	06.11.05	00:16	0° 41,66' S	11° 15,89' W	3877	GO-FLO	recovery bottle 1
	06.11.05	00:17	0° 41,67' S	11° 15,88' W	3877	GO-FLO	end deployment
PS69/018-4	06.11.05	00:22	0° 41,68' S	11° 15,88' W	3880	CTD/RO	start cast
	06.11.05	00:34	0° 41,70' S	11° 15,87' W	3879	CTD/RO	at depth: 494m
	06.11.05	01:00	0° 41,74' S	11° 15,84' W	3881	CTD/RO	end cast
PS69/018-5	06.11.05	01:06	0° 41,75' S	11° 15,83' W	3881	MSDL	start deployment
	06.11.05	01:17	0° 41,75' S	11° 15,84' W	3881	MSDL	at depth: 210m
	06.11.05	01:19	0° 41,76' S	11° 15,84' W	3881	MSDL	heave
	06.11.05	01:26	0° 41,77' S	11° 15,84' W	3881	MSDL	end deployment
PS69/018-6	06.11.05	01:32	0° 41,75' S	11° 15,86' W	3880	CTD/RO	start cast
	06.11.05	01:40	0° 41,73' S	11° 15,89' W	3880	CTD/RO	at depth: 256m
	06.11.05	01:51	0° 41,75' S	11° 15,87' W	3880	CTD/RO	end cast
PS69/019-1	06.11.05	12:50	2° 9,53' S	10° 7,69' W	3888	MSDL	start deployment
	06.11.05	13:02	2° 9,52' S	10° 7,80' W	3885	MSDL	at depth: 210m
	06.11.05	13:03	2° 9,52' S	10° 7,81' W	3885	MSDL	heave
	06.11.05	13:09	2° 9,51' S	10° 7,85' W	3885	MSDL	end deployment
PS69/019-2	06.11.05	13:14	2° 9,48' S	10° 7,89' W	3885	SLS	start deployment
PS69/019-3	06.11.05	13:17	2° 9,43' S	10° 7,96' W	3877	CTD/RO	start cast
	06.11.05	13:24	2° 9,37' S	10° 8,07' W	3866	CTD/RO	at depth: 199m
PS69/019-2	06.11.05	13:30	2° 9,30' S	10° 8,12' W		SLS	end deployment
PS69/019-4	06.11.05	13:32	2° 9,28' S	10° 8,15' W	3824	SLS	start deployment
PS69/019-3	06.11.05	13:34	2° 9,26' S	10° 8,18' W	3796	CTD/RO	end cast
PS69/019-4	06.11.05	13:46	2° 9,16' S	10° 8,43' W	3797	SLS	end deployment
PS69/020-1	08.11.05	12:34	8° 47.86' S	4° 58.60' W	4269	MSDL	start deployment
	08.11.05	12:46	8° 47.87' S	4° 58.58' W	4270	MSDL	at depth: 210m
	08.11.05	12:48	8° 47.87' S	4° 58.59' W	4269	MSDL	heave
	08.11.05	12:55	8° 47.87' S	4° 58.62' W	4269	MSDL	end deployment
PS69/020-2	08.11.05	13:01	8° 47.84' S	4° 58.65' W	4268	SLS	start deployment
PS69/020-3	08.11.05	13:04	8° 47.81' S	4° 58.68' W	4269	CTD/RO	start cast
	08.11.05	13:11	8° 47.75' S	4° 58.70' W	4274	CTD/RO	at depth: 197m
PS69/020-2	08.11.05	13:18	8° 47.71' S	4° 58.75' W	4274	SLS	end deployment
PS69/020-4	08.11.05	13:19	8° 47.71' S	4° 58.75' W	4273	SLS	start deployment
PS69/020-3	08.11.05	13:21	8° 47.69' S	4° 58.76' W	4274	CTD/RO	end cast
PS69/020-4	08.11.05	13:28	8° 47.62' S	4° 58.78' W	4274	SLS	end deployment
PS69/021-1	09.11.05	11:22	11° 52.33' S	2° 31.00' W	5468	GO-FLO	start deployment
	09.11.05	11:25	11° 52.30' S	2° 30.99' W	5544	GO-FLO	deployment bottle 1: 21m
	09.11.05	11:27	11° 52.28' S	2° 30.99' W	5521	GO-FLO	deployment bottle 2: 40m
	09.11.05	11:28	11° 52.27' S	2° 30.98' W	5598	GO-FLO	deployment bottle 3: 60m

Station	Date	Time	Position Lat	Position Lon	Depth [m]	Gear	Action
	09.11.05	11:30	11° 52.26' S	2° 30.99' W	5576	GO-FLO	deployment bottle 4: 82m
	09.11.05	11:32	11° 52.25' S	2° 30.99' W	5598	GO-FLO	at depth: 106m
	09.11.05	11:33	11° 52.25' S	2° 30.99' W	5574	GO-FLO	recovery bottle 4
	09.11.05	11:35	11° 52.24' S	2° 31.00' W	5575	GO-FLO	recovery bottle 3
	09.11.05	11:36	11° 52.24' S	2° 31.00' W	5589	GO-FLO	recovery bottle 2
	09.11.05	11:37	11° 52.24' S	2° 31.00' W	5552	GO-FLO	recovery bottle 1
	09.11.05	11:38	11° 52.24' S	2° 31.00' W	5537	GO-FLO	end deployment
PS69/021-2	09.11.05	11:43	11° 52.23' S	2° 31.01' W	5575	CTD/RO	start cast
	09.11.05	12:11	11° 52.22' S	2° 30.98' W	5595	CTD/RO	at depth: 1978m
	09.11.05	12:41	11° 52.21' S	2° 30.93' W	5593	CTD/RO	end cast
PS69/021-3	09.11.05	12:46	11° 52.20' S	2° 30.91' W	5586	GO-FLO	start deployment
	09.11.05	12:48	11° 52.20' S	2° 30.91' W	5592	GO-FLO	deployment bottle 1: 21m
	09.11.05	12:50	11° 52.19' S	2° 30.91' W	5588	GO-FLO	deployment bottle 2: 70m
	09.11.05	12:52	11° 52.19' S	2° 30.90' W	5595	GO-FLO	deployment bottle 3: 100m
	09.11.05	12:53	11° 52.19' S	2° 30.90' W	5587	GO-FLO	deployment bottle 4: 120m
	09.11.05	12:57	11° 52.19' S	2° 30.88' W	5588	GO-FLO	at depth: 225m
	09.11.05	13:00	11° 52.19' S	2° 30.86' W	5588	GO-FLO	recovery bottle 4
	09.11.05	13:01	11° 52.19' S	2° 30.85' W	5595	GO-FLO	recovery bottle 3
	09.11.05	13:04	11° 52.20' S	2° 30.83' W	5594	GO-FLO	recovery bottle 2
	09.11.05	13:06	11° 52.20' S	2° 30.81' W	5595	GO-FLO	recovery bottle 1
	09.11.05	13:06	11° 52.20' S	2° 30.81' W	5595	GO-FLO	end deployment
PS69/021-4	09.11.05	13:11	11° 52.14' S	2° 30.78' W	5598	SLS	start deployment
PS69/021-5	09.11.05	13:15	11° 52.07' S	2° 30.79' W	5603	CTD/RO	start cast
	09.11.05	13:21	11° 52.00' S	2° 30.78' W	5716	CTD/RO	at depth: 195m
PS69/021-4	09.11.05	13:26	11° 51.95' S	2° 30.79' W	5695	SLS	end deployment
PS69/021-6	09.11.05	13:29	11° 51.93' S	2° 30.81' W	5748	SLS	start deployment
PS69/021-5	09.11.05	13:30	11° 51.92' S	2° 30.82' W	5748	CTD/RO	end cast
PS69/021-6	09.11.05	13:41	11° 51.79' S	2° 30.81' W	5744	SLS	end deployment
PS69/021-7	09.11.05	13:46	11° 51.79' S	2° 30.81' W	5747	MSDL	start deployment
	09.11.05	13:55	11° 51.80' S	2° 30.75' W	5745	MSDL	at depth: 210m
	09.11.05	13:56	11° 51.80' S	2° 30.75' W	5744	MSDL	heave
	09.11.05	14:02	11° 51.81' S	2° 30.73' W	5743	MSDL	end deployment
PS69/021-8	09.11.05	14:11	11° 51.80' S	2° 30.73' W	5743	CTD/RO	start cast
	09.11.05	14:17	11° 51.78' S	2° 30.72' W	5747	CTD/RO	at depth: 198m
	09.11.05	14:25	11° 51.76' S	2° 30.73' W	5746	CTD/RO	end cast
PS69/021-9	09.11.05	14:40	11° 51.80' S	2° 30.72' W	5748	CTD/RO	start cast
	09.11.05	16:16	11° 51.77' S	2° 30.76' W	5749	CTD/RO	at depth: 5744m
	09.11.05	17:42	11° 51.80' S	2° 30.78' W	5743	CTD/RO	end cast
PS69/021-10	09.11.05	18:04	11° 51.78' S	2° 30.79' W	5746	CTD/RO	start cast
	09.11.05	18:17	11° 51.80' S	2° 30.81' W	5744	CTD/RO	at depth: 788m
	09.11.05	18:34	11° 51.82' S	2° 30.81' W	5746	CTD/RO	end cast
PS69/021-11	09.11.05	18:54	11° 51.79' S	2° 30.83' W	5747	CTD/RO	start cast
	09.11.05	19:20	11° 51.80' S	2° 30.84' W	5746	CTD/RO	at depth: 1966m
PS69/022-1	10.11.05	12:30	14° 16.10' S	0° 35.67' W	5435	MSDL	start deployment
	10.11.05	12:42	14° 16.12' S	0° 35.67' W	5434	MSDL	at depth: 210m
	10.11.05	12:43	14° 16.12' S	0° 35.67' W	5434	MSDL	heave

Station	Date	Time	Position Lat	Position Lon	Depth [m]	Gear	Action
	10.11.05	12:51	14° 16.14' S	0° 35.68' W	5434	MSDL	end deployment
PS69/022-2	10.11.05	12:53	14° 16.12' S	0° 35.68' W	5437	SLS	start deployment
PS69/022-3	10.11.05	12:58	14° 16.06' S	0° 35.72' W	5433	CTD/RO	start cast
	10.11.05	13:05	14° 15.99' S	0° 35.77' W	5429	CTD/RO	at depth: 198m
PS69/022-2	10.11.05	13:09	14° 15.94' S	0° 35.80' W	5426	SLS	end deployment
PS69/022-4	10.11.05	13:12	14° 15.91' S	0° 35.83' W	5423	SLS	start deployment
PS69/022-3	10.11.05	13:17	14° 15.84' S	0° 35.87' W	5415	CTD/RO	end cast
PS69/022-4	10.11.05	13:22	14° 15.81' S	0° 35.92' W	5414	SLS	end deployment
PS69/023-1	11.11.05	13:27	17° 52.23' S	2° 19.28' E	5471	MSDL	start deployment
	11.11.05	13:35	17° 52.20' S	2° 19.27' E	5471	MSDL	at depth: 210m
	11.11.05	13:36	17° 52.20' S	2° 19.27' E	5471	MSDL	heave
	11.11.05	13:43	17° 52.20' S	2° 19.28' E	5470	MSDL	end deployment
PS69/023-2	11.11.05	13:47	17° 52.14' S	2° 19.28' E	5471	SLS	start deployment
PS69/023-3	11.11.05	13:50	17° 52.08' S	2° 19.26' E	5471	CTD/RO	start cast
	11.11.05	13:57	17° 51.99' S	2° 19.25' E	5471	CTD/RO	at depth: 198m
PS69/023-2	11.11.05	14:04	17° 51.90' S	2° 19.24' E	5471	SLS	end deployment
PS69/023-4	11.11.05	14:07	17° 51.87' S	2° 19.24' E	5471	SLS	start deployment
PS69/023-3	11.11.05	14:07	17° 51.87' S	2° 19.24' E	5471	CTD/RO	end cast
PS69/023-4	11.11.05	14:16	17° 51.70' S	2° 19.22' E	5470	SLS	end deployment
PS69/024-1	12.11.05	12:57	21° 6.54' S	4° 59.58' E	2406	MSDL	start deployment
	12.11.05	13:08	21° 6.52' S	4° 59.64' E	2399	MSDL	at depth: 210m
	12.11.05	13:09	21° 6.52' S	4° 59.64' E	2399	MSDL	heave
	12.11.05	13:18	21° 6.49' S	4° 59.67' E	2396	MSDL	end deployment
PS69/024-2	12.11.05	13:21	21° 6.45' S	4° 59.67' E	2398	SLS	start deployment
PS69/024-3	12.11.05	13:24	21° 6.40' S	4° 59.67' E	2402	CTD/RO	start cast
	12.11.05	13:31	21° 6.34' S	4° 59.70' E	2405	CTD/RO	at depth: 196m
PS69/024-2	12.11.05	13:37	21° 6.28' S	4° 59.73' E	2410	SLS	end deployment
PS69/024-4	12.11.05	13:41	21° 6.23' S	4° 59.77' E	2414	SLS	start deployment
PS69/024-3	12.11.05	13:42	21° 6.21' S	4° 59.77' E	2416	CTD/RO	end cast
PS69/024-4	12.11.05	13:49	21° 6.13' S	4° 59.77' E	2433	SLS	end deployment
PS69/025-1	13.11.05	12:59	24° 31,68' S	7° 52,69' E	4717	SLS	start deployment
PS69/025-2	13.11.05	13:01	24° 31,66' S	7° 52,68' E	4717	CTD/RO	start cast
	13.11.05	13:07	24° 31,59' S	7° 52,64' E	4716	CTD/RO	at depth: 198m
PS69/025-1	13.11.05	13:13	24° 31,54' S	7° 52,56' E	4718	SLS	end deployment
PS69/025-2	13.11.05	13:15	24° 31,53' S	7° 52,53' E	4719	CTD/RO	end cast
PS69/025-3	13.11.05	13:17	24° 31,50' S	7° 52,51' E	4719	SLS	start deployment
	13.11.05	13:26	24° 31,39' S	7° 52,37' E	4722	SLS	end deployment
PS69/025-4	13.11.05	13:29	24° 31,40' S	7° 52,31' E	4724	MSDL	start deployment
	13.11.05	13:39	24° 31,37' S	7° 52,21' E	4723	MSDL	at depth: 210m
	13.11.05	13:40	24° 31,37' S	7° 52,20' E	4722	MSDL	heave
	13.11.05	13:47	24° 31,38' S	7° 52,16' E	4722	MSDL	end deployment
PS69/026-1	13.11.05	17:19	25° 0,16' S	8° 16,93' E	4698	GO-FLO	start deployment
	13.11.05	17:20	25° 0,16' S	8° 16,92' E	4697	GO-FLO	deployment bottle 1
	13.11.05	17:23	25° 0,16' S	8° 16,93' E	4698	GO-FLO	deployment bottle 2
	13.11.05	17:25	25° 0,15' S	8° 16,92' E	4698	GO-FLO	deployment bottle 3
	13.11.05	17:25	25° 0,15' S	8° 16,92' E	4698	GO-FLO	deployment bottle 4
	13.11.05	17:27	25° 0,15' S	8° 16,90' E	4698	GO-FLO	at depth: 105m
	13.11.05	17:29	25° 0,14' S	8° 16,88' E	4698	GO-FLO	recovery bottle 4
	13.11.05	17:32	25° 0,13' S	8° 16,87' E	4698	GO-FLO	recovery bottle 3
	13.11.05	17:33	25° 0,13' S	8° 16,86' E	4698	GO-FLO	recovery bottle 2

Station	Date	Time	Position Lat	Position Lon	Depth [m]	Gear	Action
	13.11.05	17:34	25° 0,12' S	8° 16,86' E	4697	GO-FLO	recovery bottle 1
	13.11.05	17:36	25° 0,13' S	8° 16,85' E	4697	GO-FLO	end deployment
PS69/026-2	13.11.05	17:42	25° 0,12' S	8° 16,85' E	4697	CTD/RO	start cast
	13.11.05	19:08	25° 0,06' S	8° 16,88' E	4697	CTD/RO	at depth: 4666m
	13.11.05	20:24	25° 0,08' S	8° 16,98' E	4698	CTD/RO	end cast
PS69/026-3	13.11.05	20:28	25° 0,10' S	8° 16,99' E	4698	GO-FLO	start deployment
	13.11.05	20:30	25° 0,11' S	8° 17,00' E	4698	GO-FLO	deployment bottle 1: 17m
	13.11.05	20:32	25° 0,11' S	8° 17,01' E	4698	GO-FLO	deployment bottle 2: 66m
	13.11.05	20:34	25° 0,12' S	8° 17,01' E	4698	GO-FLO	deployment bottle 3: 96m
	13.11.05	20:36	25° 0,13' S	8° 17,02' E	4698	GO-FLO	deployment bottle 4: 116m
	13.11.05	20:39	25° 0,13' S	8° 17,03' E	4698	GO-FLO	at depth: 225m
	13.11.05	20:44	25° 0,13' S	8° 17,03' E	4698	GO-FLO	recovery bottle 4
	13.11.05	20:45	25° 0,13' S	8° 17,03' E	4698	GO-FLO	recovery bottle 3
	13.11.05	20:46	25° 0,13' S	8° 17,03' E	4698	GO-FLO	recovery bottle 2
	13.11.05	20:48	25° 0,13' S	8° 17,03' E	4698	GO-FLO	recovery bottle 1
	13.11.05	20:49	25° 0,14' S	8° 17,03' E	4698	GO-FLO	end deployment
PS69/026-4	13.11.05	20:55	25° 0,15' S	8° 17,05' E	4698	CTD/RO	start cast
	13.11.05	21:52	25° 0,14' S	8° 17,15' E	4698	CTD/RO	at depth: 4404m
	13.11.05	22:56	25° 0,19' S	8° 17,10' E	4698	CTD/RO	end cast
PS69/026-5	13.11.05	23:24	25° 0,45' S	8° 17,09' E	4699	CTD/RO	start cast
	14.11.05	00:12	25° 0,26' S	8° 17,07' E	4699	CTD/RO	at depth: 3430m
	14.11.05	01:31	25° 0,29' S	8° 17,02' E	4698	CTD/RO	end cast
PS69/026-6	14.11.05	01:43	25° 0,29' S	8° 17,01' E	4698	MSDL	start deployment
	14.11.05	01:57	25° 0,28' S	8° 17,01' E	4698	MSDL	at depth: 280m
	14.11.05	01:58	25° 0,28' S	8° 17,00' E	4698	MSDL	heave
	14.11.05	02:07	25° 0,27' S	8° 17,00' E	4698	MSDL	end deployment
PS69/026-7	14.11.05	02:14	25° 0,29' S	8° 17,01' E	4698	CTD/RO	start cast
	14.11.05	02:29	25° 0,28' S	8° 17,04' E	4698	CTD/RO	at depth: 759m
	14.11.05	02:45	25° 0,25' S	8° 17,07' E	4698	CTD/RO	end cast
PS69/026-8	14.11.05	03:06	25° 0,31' S	8° 17,14' E	4698	CTD/RO	start cast
	14.11.05	03:36	25° 0,31' S	8° 17,07' E	4698	CTD/RO	at depth: 1991m
	14.11.05	04:19	25° 0,21' S	8° 17,14' E	4698	CTD/RO	end cast
PS69/027-1	14.11.05	12:58	25° 57,95' S	9° 21,94' E	4712	MSDL	start deployment
	14.11.05	13:08	25° 57,98' S	9° 21,89' E	4719	MSDL	at depth: 210m
	14.11.05	13:09	25° 57,97' S	9° 21,89' E	4719	MSDL	heave
	14.11.05	13:19	25° 57,94' S	9° 21,84' E	4719	MSDL	end deployment
PS69/027-2	14.11.05	13:22	25° 57,92' S	9° 21,86' E	4719	SLS	start deployment
PS69/027-3	14.11.05	13:25	25° 57,87' S	9° 21,87' E	4719	CTD/RO	start cast
	14.11.05	13:33	25° 57,76' S	9° 21,85' E	4719	CTD/RO	at depth: 197m
PS69/027-2	14.11.05	13:38	25° 57,70' S	9° 21,84' E	4719	SLS	end deployment
PS69/027-4	14.11.05	13:42	25° 57,63' S	9° 21,85' E	4719	SLS	start deployment
PS69/027-3	14.11.05	13:43	25° 57,61' S	9° 21,86' E	4719	CTD/RO	end cast
PS69/027-4	14.11.05	13:56	25° 57,40' S	9° 21,80' E	4720	SLS	end deployment

SON: Sonarboje
MSDL: Multi Sensor Data Logger
SLS: Satlantic Lichtsonde